TECHNICAL REPORT STANDARD TITLE PAGE

1. Report No.	2. Government Accession No.	3. Recipient's Catalog No.
FHWA/TX-81/30+249-1		

4. Title and Subtitle	5. Report Date
IMPROVEMENTS TO THE MATERIALS CHARACTERIZATION AND FATIGUE LIFE PREDICTION METHODS OF THE TEXAS RIGID PAVEMENT OVERLAY DESIGN PROCEDURE	November 1981
	6. Performing Organization Code
7. Author(s)	8. Performing Organization Report No.
Arthur Taute, B. F. McCullough, and W. R. Hudson	Research Report No. 249-1
9. Performing Organization Name and Address	10. Work Unit No.
Center for Transportation Research The University of Texas at Austin Austin, Texas 78712	11. Contract or Grant No. Research Study 3-8-79-249
	13. Type of Report and Period Covered
12. Sponsoring Agency Name and Address	
Texas State Department of Highways and Public Transportation, Transportation Planning Division P.O. Box 5051 Austin, Texas 78763	Interim
	14. Sponsoring Agency Code

15. Supplementary Notes

Study conducted in cooperation with the U.S. Department of Transportation, Federal Highway Administration. Research Study Title: "Implementation of Rigid Pavement Overlay and Design System."

16. Abstract

This report presents certain improvements to the Texas Rigid Pavement Overlay Procedure (RPOD2) with regard to materials characterization and fatigue life predictions. Suggestions are made for characterizing rigid pavement layers from Dynaflect deflections and material tests, and some guidelines for selecting design sections along the length of a road are presented. Finite element analysis is used to quantify the effect of pavement discontinuities on the stresses obtained from layered theory. Further finite element analysis is used in an attempt to relate the critical reflection stresses in an AC overlay to deflection measurements obtained before overlaying. A fatigue equation is derived from AASHO Road Test data on rigid pavements in a mechanistic manner, using few simplifying assumptions. Failure of CRC pavements is defined using condition survey data in terms of a rate of defect (punchout and patch) occurrence, and the predictions of the above fatigue equations are compared to the lives of inservice CRC pavements. The predictions made by RPOD2 of the fatigue lives of asphalt overlaid rigid pavements are compared to existing condition survey data of these pavements, and improvements are suggested.

17. Key Words	18. Distribution Statement
Rigid pavement, continuously reinforced concrete pavement, remaining life, fatigue, materials characterization, deflections, overlays, reflection cracking.	No restrictions. This document is available to the public through the National Technical Information Service, Springfield, Virginia 22161.

19. Security Classif. (of this report)	20. Security Classif. (of this page)	21. No. of Pages	22. Price
Unclassified	Unclassified	328	

Form DOT F 1700.7 (8-69)

IMPROVEMENTS TO THE MATERIALS CHARACTERIZATION AND FATIGUE LIFE PREDICTION METHODS OF THE TEXAS RIGID PAVEMENT OVERLAY DESIGN PROCEDURE

by

Arthur Taute
B. F. McCullough
W. R. Hudson

Research Report Number 249-1

Implementation of Rigid Pavement Overlay and Design System

Research Project 3-8-79-249

conducted for

Texas
State Department of Highways and Public Transportation

in cooperation with the
U. S. Department of Transportation
Federal Highway Administration

by the

CENTER FOR TRANSPORTATION RESEARCH
BUREAU OF ENGINEERING RESEARCH
THE UNIVERSITY OF TEXAS AT AUSTIN

November 1981

The contents of this report reflect the views of the authors, who are responsible for the facts and the accuracy of the data presented herein. The contents do not necessarily reflect the official views or policies of the Federal Highway Administration. This report does not constitute a standard, specification, or regulation.

PREFACE

This report forms part of Project 3-8-79-249, which has as one of its objectives the implementation of the Texas Rigid Pavement Overlay Design Procedure (RPOD2). This procedure was implemented on a number of overlay design projects, which led to some of the recommended improvements to the procedure, as presented in this report.

The text of this report was entered into the DEC System-10 computer at The University of Texas at Austin, which was subsequently used to produce, it is hoped, a typographically error-free report. Thanks are extended to all those who helped in the preparation of this report and in particular to Elaine Hamilton, Eve Falcon, and Sue Tarpley, who entered the text into the computer. Gratitude is expressed to Steve Seeds, Bary Eagleson, David Luhr, and Manuel Gutierrez de Velasco for the many hours of fruitful discussion which led to the majority of findings in this report. In addition, thanks are extended to Gerald Peck and Richard Rogers, at the Texas State Department of Highways and Public Transportation for the many useful comments made during the implementation of the RPOD2 design procedure on Texas highways.

ABSTRACT

This report presents certain improvements to the Texas Rigid Pavement Overlay Procedure (RPOD2) with regard to materials characterization and fatigue life predictions. Suggestions are made for characterizing rigid pavement layers from Dynaflect deflections and material tests, and some guidelines for selecting design sections along the length of a road are presented. Finite element analysis is used to quantify the effect of pavement discontinuities on the stresses obtained from layered theory. Further finite element analysis is used in an attempt to relate the critical reflection stresses in an AC overlay to deflection measurements obtained before overlaying. A fatigue equation is derived from AASHO Road Test data on rigid pavements in a mechanistic manner, using few simplifying assumptions. Failure of CRC pavements is defined using condition survey data in terms of a rate of defect (punch out and patch) occurrence, and the predictions of the fatigue equation are compared to the lives of inservice CRC pavements. The predictions made by RPOD2 of the fatigue lives of asphalt overlaid rigid pavements are compared to existing condition survey data for these pavements, and improvements are suggested.

KEYWORDS: Rigid pavement, continuously reinforced concrete pavement, remaining life, fatigue, materials characterization, deflections, overlays, reflection cracking.

SUMMARY

This report presents certain improvements to the Texas Rigid Pavement Overlay Design Procedure (RPOD2) with regard to materials characterization and fatigue life predictions. These improvements are based on data collected on Texas highways and should result in significant improvements in mechanistic pavement life predictions.

Suggestions are made for the characterization of rigid pavement layers using Dynaflect deflection measurements and laboratory testing. The subgrade is characterized using the Dynaflect sensor 5 deflection, and the upper, bound, pavement layers are characterized using the deflection basin slope or sensor 1 minus sensor 5 deflections. Both these deflection parameters are used in the selection of pavement design sections, as indicated in Fig 2.15, and guidelines are given for this design step.

Finite element analysis is used to relate the effect of pavement discontinuities on the tensile stresses obtained from layered theory to deflection measurements. The analysis indicates that, when deflections at cracks exceed 1.5 times the midspan deflections, the transverse tensile stresses in the pavement exceed the longitudinal stresses, which occur in an uncracked pavement under an axle load. This stress rearrangement due to cracking is illustrated in Fig 3.11.

Additional finite element analysis is used in an attempt to quantify the stresses causing reflection cracking in asphalt overlays on rigid pavements.

As shown in Fig 4.3, the results indicate that severe tensile stresses may exist in the upper surface of an overlay, immediately above cracks in the underlying pavement. Laboratory testing may be required to verify these findings.

Condition survey data of CRC pavements are used to define "failure" of these pavements in terms of a rate of defect (punch outs and patches) occurrence per mile. Economic analysis and observation of the average trend of defect occurrence along Texas CRC pavements indicated that a rate of three defects per year per mile could be used as a criterion for "failure." Once this rate of defect occurrence is reached, further traffic generally results in a significant increase in distress and, correspondingly, maintenance cost. In general this point occurs when the total number of defects per mile in a pavement section equals the pavement age in years.

The data obtained at the AASHO Road Test on Rigid Pavements are analyzed in a mechanistic manner, using as few simplifying assumptions as possible, to obtain a rigid pavement fatigue equation. The predictions of this fatigue equation are compared to the fatigue lives of existing CRC pavements in Texas, using failure criteria and materials characterization as described above and detailed estimates of past traffic. As shown in Fig 5.10, the fatigue equation predictions were found to correlate reasonably well with data obtained from Texas CRC pavements. This equation is thus recommended for further use in design.

The predictions made by RPOD2 regarding the fatigue life of asphalt overlays on CRC pavements are compared to the distress-traffic history of overlay projects of this type in Texas. The design procedure significantly underpredicted the lives of these pavements and recommendations for improving these predictions are made. An additional fatigue equation for use with

overlaid CRC pavements is proposed and an estimate of this equation is made, based on the limited data available. This equation may be improved when "failure" of overlaid CRC pavements is defined and when more condition survey data on this type of structure become available.

For the purposes of rigid overlay designs, severely distressed existing rigid pavements may be characterized using deflection measurements. The PCC layer may be characterized as a material with a modulus such that the deflection basin slope computed using layered theory matches the slope of deflection measurements made at distress locations. In this manner overlay designs will reflect the severity of the distress in the existing pavement, and improved fatigue life predictions may result.

A large number of the above improvements are being incorporated into a Rigid Pavement Rehabilitation Design System which is at present being developed at the Center for Transportation Research. Example designs are presented in the report which may provide a basis for further overlay designs using the improvements to the RPOD2 design procedure as suggested in this report.

IMPLEMENTATION STATEMENT

This report presents a significant number of improvements to the Texas Rigid Pavement Overlay Design Procedure which may result in improved overlay life predictions. Many of these improvements are being incorporated in a Rigid Pavement Rehabilitation Design System which is currently being developed at the Center for Transportation Research.

It is recommended that the suggestions in this report be implemented on future overlay designs and it is hoped they will result in further refinement of the Overlay Design Procedure.

TABLE OF CONTENTS

CHAPTER 1. INTRODUCTION

This report forms part of the SDHPT Research Project 3-8-79-249, and one of the primary objectives of this project is to implement the Texas rigid pavement overlay design procedure. During the implementation phase of the procedure, difficulties and inaccuracies arising from its use need to be overcome, and additional work regarding its application in a pavement design system needs to be done. Some of the present problems center around the estimation of the existing pavement material properties and the estimation of the remaining life of the existing pavement.

The use of material tests and the Dynaflect for the estimation of layer stiffness will be examined. Others have had some success in estimating layer stiffness using the Dynaflect and other deflection devices (Refs 8, 10, 11, 14, 15, 16, and 17). Furthermore, this device has been used with success to estimate the layer stiffness on several, recent SDHPT overlay design projects. Condition surveys have shown that the punch out is the most severe and prevalent form of distress leading toward "failure" of CRC pavements. Finite element analysis of a cracked pavement layer will be used to provide further understanding regarding the development of punch outs in CRC pavements.

Examination of condition survey data should provide information regarding structural failure of a pavement. To date, no distinct definition of failure of a CRC pavement exists. The concept of failure will be examined

and it is envisaged that the structural failure of CRC pavements will be defined in terms of a rate of defect occurrence. Once a rational failure condition has been established, the pavement life predictions of existing fatigue equations can be checked and modified if necessary.

The above should lead to more accurate predictions of CRC pavement fatigue lives. The structural failure of the pavement will be based on condition survey observations, and, therefore, the condition of the pavement at the time of overlay should enable one to make reasonable predictions of the pavement's remaining life. Regular condition surveys of asphalt overlaid CRC pavements have shown that the first signs of distress in the overlay occur immediately above underlying patches and punch outs. For this reason, it is important to examine reflection cracking in more detail, and a finite element analysis will be used to predict the stresses in rigid pavement overlays with varying degrees of load transfer at the cracks. This study should provide more information regarding the mechanism of distress occurrence in rigid pavement overlays and may lead to overlay designs which will reduce reflection cracking.

At all times during the analyses, the stresses within the pavement will be related to surface deflections. In this manner field deflections may provide valuable input regarding the stress distribution in the pavement layers. The findings of the various analyses may be incorporated into future overlay designs and may form an integral part of the Rigid Pavement Rehabilitation Design System which is at present being developed at the Center for Transportation Research (Ref 12).

SCOPE OF REPORT

No single facet of a pavement design procedure can be examined while it is entirely separate from the rest. The design procedure used in RPOD2 may be outlined as shown in Fig 1.1. All the steps are interdependent of one another; the behavioral analysis depends on the materials characterization used in the analysis, and the fatigue life depends on the stresses or strains output from this analysis. In order to improve the fatigue life predictions of RPOD2, this report reexamines each of the steps in the pavement design procedure in the light of developments arising from its implementation.

In Chapter 2, the materials characterization aspect of the design procedure is examined. Some problems which became evident during the implementation phase are indicated, and a number of improvements are presented for use in the future.

Chapter 3 presents the analysis of a cracked pavement slab by finite element analysis. The results from this analysis are related to condition survey data on CRC pavements in Texas.

Chapter 4 presents the analysis of stress in overlays immediately above underlying cracks. Reflection cracking due to differential vertical movements is examined, and here, again, the results are related to condition survey data on overlaid CRC pavements.

In Chapter 5, the fatigue life of existing CRC pavements is examined. A mechanistically derived fatigue equation is presented for use in future designs. Predictions from this equation are checked against condition survey and traffic data.

The "remaining life" of existing CRC pavements has a significant effect on the overlay thickness, designed using the RPOD2 design procedure. In

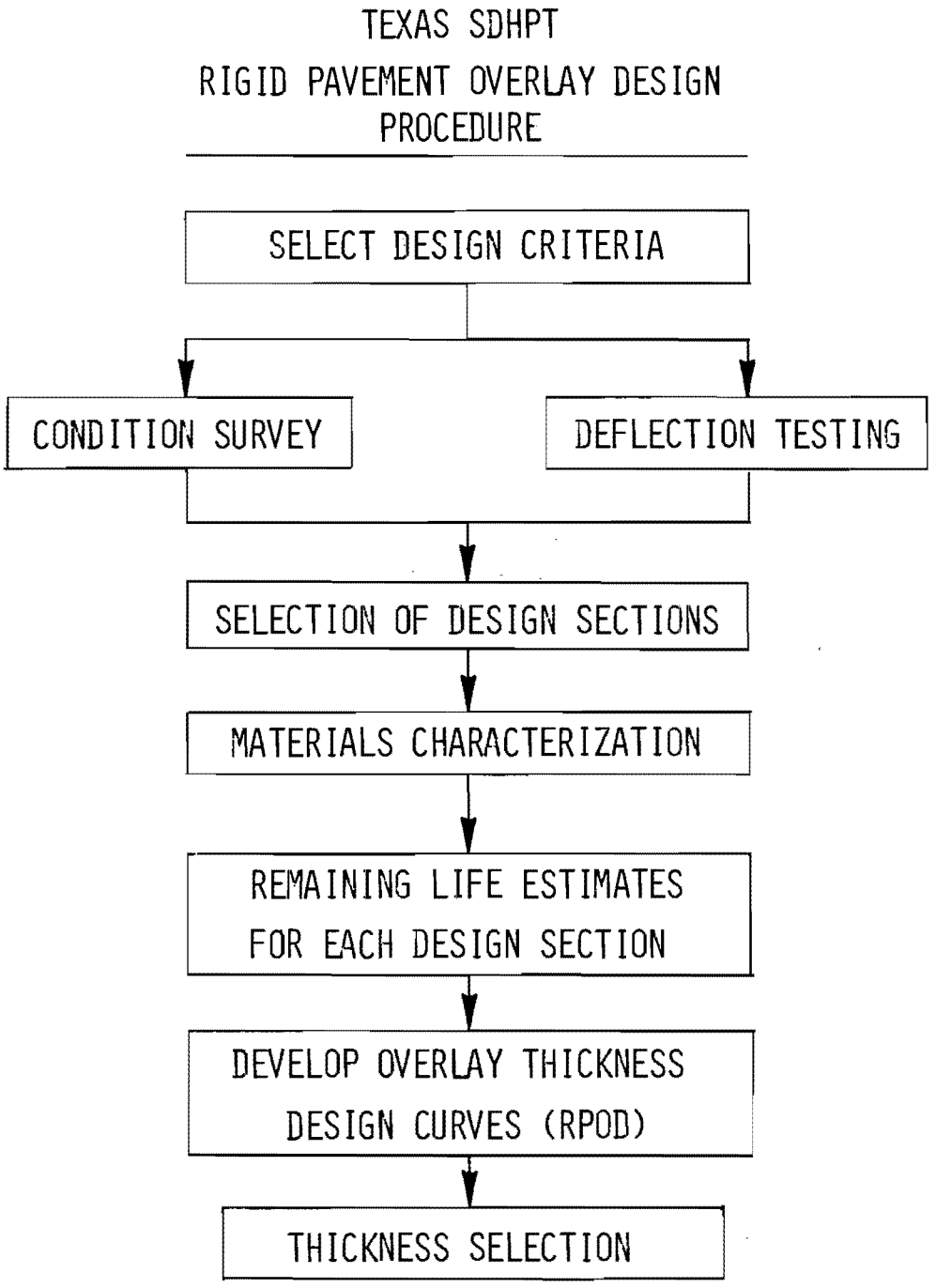

Fig 1.1. Flow diagram of the RPOD2 design procedure (Ref 5).

Chapter 6, some improvements regarding the calculation of remaining life are suggested, and the predictions of overlay lives made by the RPOD2 design procedure are checked against existing condition survey data.

In Chapter 7 recommendations are made for the practical application of the suggestions in this report, while Chapter 8 presents the conclusions and recommendations.

SUMMARY

This report presents a number of improvements to certain facets of the Texas Rigid Pavement Overlay Design Procedure. These improvements should be implemented in future overlay designs and form part of a continual upgrading of the procedure as data become available.

CHAPTER 2. MATERIALS CHARACTERIZATION

Mechanistic design procedures require the use of a suitable theory and model to analyze the behavior of a pavement structure. Plate, layered, and finite element theories have been used for this purpose. Typically, these theories are used to compute the tensile stresses in the upper, bound, pavement layers which are then input into a fatigue equation to predict the life of the pavement. Use of one of these theories requires that the materials making up the pavement be characterized suitably.

Plate theory is often used for rigid pavement design; if so, the concrete layer is represented by a relatively stiff plate and the lower layers are characterized as a bed of linear springs. Elastic layered and finite element theories have also been used with success for rigid pavement design. These last two theories use Young's modulus and Poisson's ratio to characterize the stress strain behavior of the pavement materials.

McCullough (Ref 1) has shown that plate and layered theories predict similar tensile stresses in the bottom of a concrete pavement layer when the supporting structure consists of granular material. The spring constant, k, used in the plate theory calculations is equated to the layer moduli used in layered theory calculations by computing the deflection of the subbase under a plate load with layered theory. This deflection is used to obtain the equivalent k-value of the supporting structure.

Layered theory computer programs that can predict the state of stress, strain, and deflections of pavement structures at minimal cost are freely available. For this reason, layered theory is often used in mechanistic design procedures. Shortcomings of the theory, such as the inability to predict pavement stresses under an edge loading condition, can be overcome by using stress modification factors. These factors can be calculated using plate or finite element theories.

Because layered theory analysis is often used for mechanistic pavement analysis, the material properties most often required for the pavement layers are Young's modulus and Poisson's ratio. Both laboratory and in-situ methods are available for determining these material characteristics. A number of these methods will be described with a view towards their implementation in practice.

LABORATORY TESTING

This involves obtaining representative samples of pavement materials from the field and testing them in the laboratory under simulated field loading and environmental conditions. A number of test methods for determining the elastic parameters of the different pavement materials exist. Only the pros and cons of the laboratory test methods used in the implementation of the Texas Rigid Pavement Overlay Design Procedure, i.e., the Indirect Tensile and Resilient Modulus Tests, will be described.

Indirect Tensile Test

This test method, described in detail in Refs 18 and 19, is used to determine the tensile strength and elastic modulus of the bound pavement layers. The problems associated with this form of testing are

(1) Cost. The test involves the diametral loading of cylindrical discs. These discs can be cut either from cores taken from an existing pavement or from test cylinders of concrete which are to be used for paving. Cores are expensive to cut, and, in CRC pavements, these cores may intersect some reinforcing steel. Coring through reinforcing steel results in rapid bit wear and increased cost.

Modulus testing requires accurate measurement of the load-displacement characteristics of the material. In the indirect tensile test, this involves repeated vertical loading and the measurement of the resulting vertical and horizontal deformation of the specimen. Deformation and recording devices for this are fairly expensive.

(2) Specimen Geometric Accuracy. Coring generally does not result in a smooth cut surface. The circumferential surface of the test discs may thus be fairly rough, resulting in improper seating of the loading strips. This results in inaccurate vertical deformation measurements. A thin layer of suitable material may be applied to these surfaces in order to improve the contact with the loading strips. In order to obtain accurate vertical deformation measurements, this material should have a modulus similar to that of the concrete.

Depending on the quality of the stabilized subbase, coring and subsequent trimming of the sample may result in an extremely irregular specimen which will deform differently in the test than in the field.

(3) Specimen Variation. The moduli of bound pavement layers obtained from the indirect tensile test may vary considerably. This may be due to the heterogeneity of the samples relative to their size. Table A1, Appendix 1, shows the results of indirect tensile tests on cores taken from IH-10 near Beaumont and Columbus, Texas. Similar results are shown in Refs 20 and 21. In the former reference, cores were taken from existing concrete pavements in Texas, and in the latter, cores were taken from a number of airport pavements. In both cases, the coefficient of variation of the tensile strengths of the cores was approximately 13 percent while that of their moduli was approximately 33 percent.

In spite of these negative factors, this test method still remains one of the most economical and most practical methods for determining moduli of stabilized layers. Cores are generally much easier to obtain than beam samples, and, as will be explained later, in the case of a rigid pavement and stabilized subbase, in-situ deflection measurements do not enable the moduli of these bound layers to be distinguished accurately.

This test method has been used with reasonable success in the implementation of RPOD2, and we, therefore, recommend that it be used to provide estimates of moduli of the bound pavement layers.

Resilient Modulus Test

This test, described in detail in Ref 22, is used to estimate the modulus and stress sensitivity of the granular pavement layers and the subgrade. The test involves subjecting a soil sample in a triaxial cell to a range of confining pressures and a range of repeated vertical stresses. The resilient vertical deformation across the middle third of the sample is measured at these stress levels. The sample may range from an "undisturbed" sample of clayey subgrade, obtained with a thin walled tube sampler, to a granular specimen recompacted in the laboratory to field density and moisture content.

As indicated in Fig 2.1, the ratio of principal stress difference (deviator stress) to the resilient strain is called the Resilient Modulus of the material. The Resilient Modulus may vary significantly with the stress level applied to the specimen during testing. In granular materials both the confining pressure and the deviator stress may have a significant effect on the Resilient Modulus whereas in clayey materials the confining pressure may not have a significant effect. The material may be either stress hardening or stress softening, depending on the material type. A stress hardening material will have a higher Resilient Modulus at higher stress levels, whereas a stress softening material will have a lower Resilient Modulus at higher stress levels. This concept is illustrated in Fig 2.1. The relationship of the Resilient Modulus to deviator stress is termed the stress sensitivity of the material.

In order to obtain an indication of the stress sensitivity of the material, values of modulus and principal stress difference are plotted on a log-log scale. At higher stress levels, the points generally lie on a

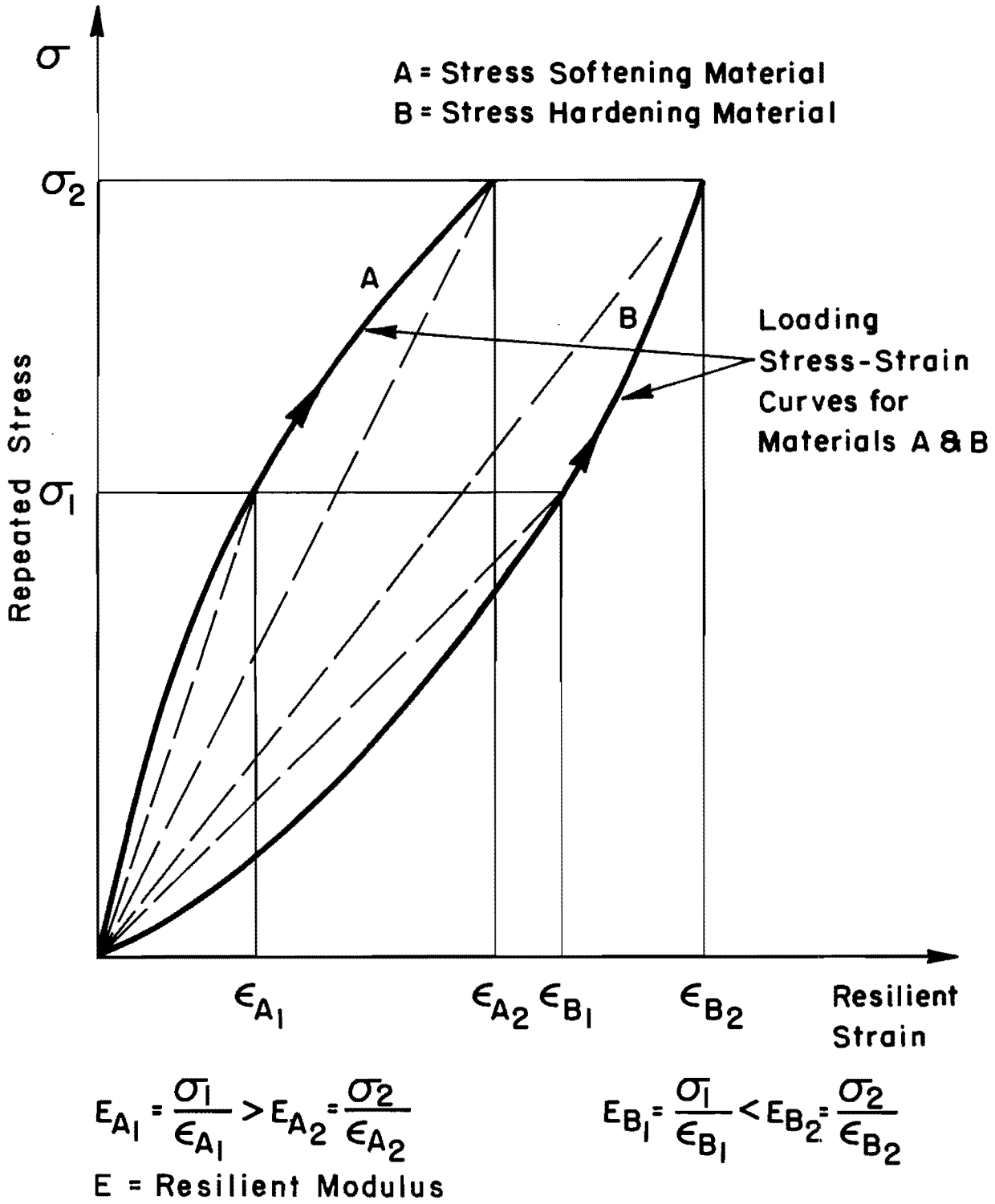

Fig 2.1. Diagram illustrating stress sensitivity.

straight line and the slope (SSG) of this line provides a measure of the stress sensitivity of the material. Some of these plots, obtained from a subgrade clay near Beaumont, are shown in Fig 2.2.

The major problems associated with this type of test are

(1) Cost. Before construction begins subgrade samples are typically obtained from the in-situ soils along the center line of the roadway. Subbase material for testing may be obtained from likely borrow areas in the vicinity of the road. These samples should be representative of the materials which will ultimately form part of the pavement structure and as such may need to be obtained from some depth below the natural ground level. In cut areas, for example, the subgrade of the road may be some distance below the natural ground level. Post construction sampling may be done through a core hole drilled for the purpose of sampling the upper pavement layers. These sampling procedures may be fairly expensive.

As with the indirect tensile test, the laboratory equipment required for conducting the resilient modulus test is relatively inexpensive, but only a few laboratories are equipped to perform the test.

(2) Sample Disturbance. This factor may have a significant effect on both clayey and granular soils. Granular soils can not generally be sampled with a thin walled tube sampler. The material, thus, needs to be recompacted in the laboratory to field moisture content and density. Data from CBR tests have shown that for a particular density, the CBR of soils varies greatly with the compaction method

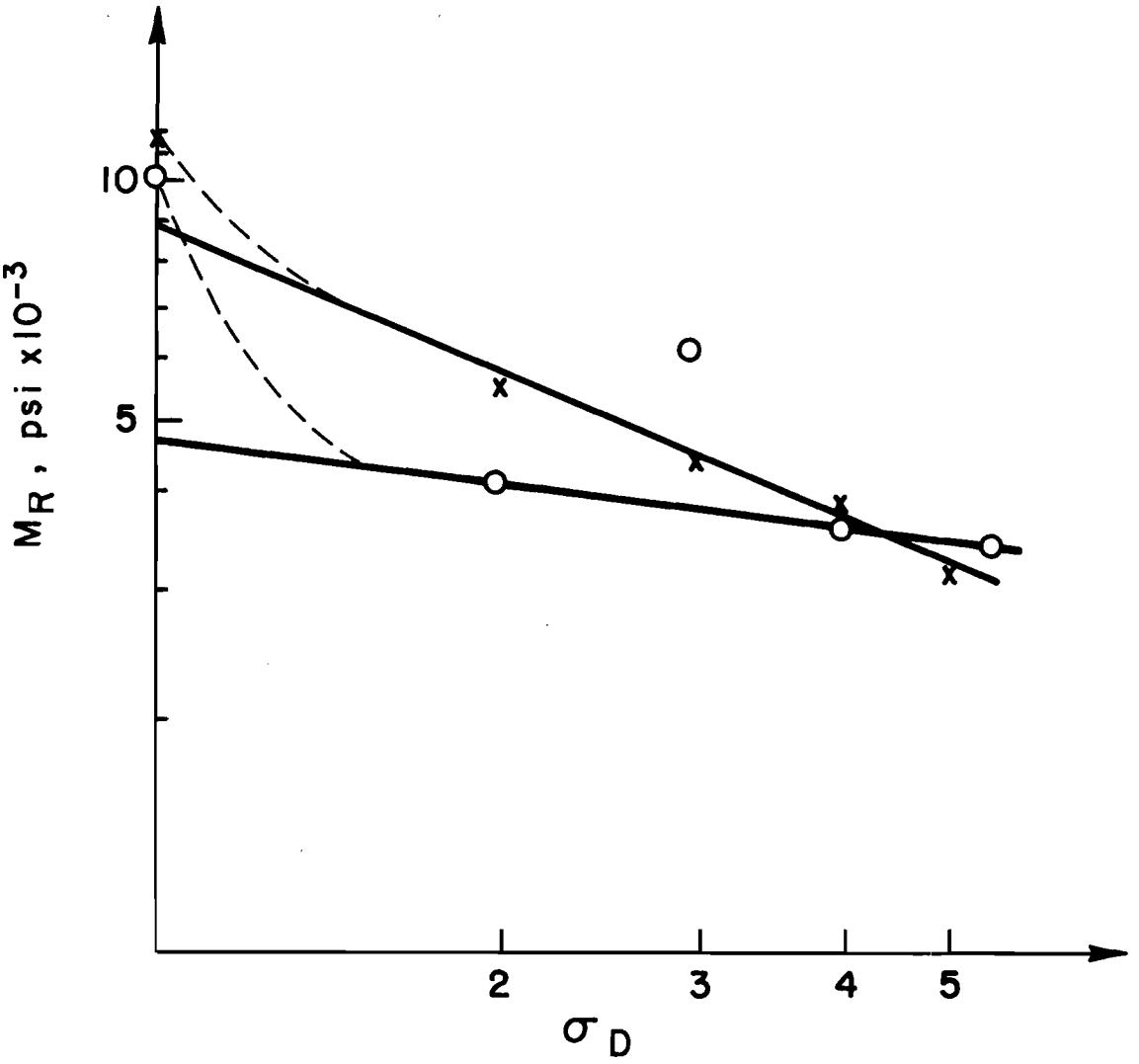

Fig 2.2. Resilient modulus-deviator stress diagram plotted from laboratory results on clay obtained from IH-10, Jefferson County, Texas.

used and with the water content during compaction (Ref 23). This relationship is especially true if the soil contains clay; thus, it can be postulated that the same type of behavior holds true for resilient modulus data.

In the case of a clayey subgrade, sampling may result in significant disturbance. The moisture content and stress history of a clay have a significant effect on the static load deformation relationship of the material. Partially saturated clays, for example, are much stiffer than saturated clays. Similarly, overconsolidated clays are stiffer than normally consolidated clays. These conditions may have similar effects on the resilient load deformation relationship of the material. This effect may be even more pronounced at the low stress levels generally used in the resilient modulus test. Thus, the reduction in effective stress due to sampling and the resulting overconsolidation may be the cause of the very high values of resilient modulus obtained at very low stress levels, as shown in Fig 2.2. Some quantification of the effect of water content on the resilient modulus of a material is provided by Monismith (Ref 24). He presents a figure which shows that at constant dry density the resilient modulus of a fine grained soil decreases appreciably as the water content approaches saturation. Thus, if the material is allowed to dry out upon sampling, significant gains in stiffness may result.

Both these forms of sample disturbance may result in higher test values of resilient modulus, which will result in an unconservative design.

(3) Specimen Variation. As with the indirect tensile test, this test involves the measurement of very small deformations. Any small errors in measurement or any material heterogeneity results in a wide scatter of the test results on samples from a particular soil type. Table A2 shows the results of Resilient Modulus tests on samples of the clayey subgrade along IH-10 near Beaumont. Subgrade soil is seldom homogeneous in the horizontal or vertical direction. Due to the small sample size used in the Resilient Modulus test, minor soil irregularities, such as sand lenses, create significant variation in the test results. This is apparent from studying Table A2.

These paragraphs tend to indicate that laboratory testing may be of questionable value; this is not the case since laboratory testing provides some valuable information which cannot easily be obtained by other means. Subsequent paragraphs will show that laboratory testing in conjunction with deflection measurements may provide a fairly accurate indication of pavement layer stiffnesses and the variation thereof along the length of the road.

DEFLECTION MEASUREMENTS

The use of deflection measurements for the estimation of pavement layer stiffnesses is rapidly gaining popularity and application. Computer programs which model the pavement layers as homogeneous, isotropic, elastic layers provide reasonable estimates of pavement behavior under loading. A Dynaflect is at present used in Texas to obtain pavement deflection measurements.

This device uses two masses rotating in opposite directions to apply a cyclic load to the pavement surface. The cycle frequency used is typically 8 hertz and the peak to peak load applied is 1000 lb. The peak to peak deflections are measured by five geophones, placed as indicated in Fig 2.3. This device thus provides an indication of the displacement and shape of the deflected surface within 4 feet of the load wheels. In the following sections, procedures for estimating material properties from Dynaflect deflections and problems associated with these predictions are discussed.

Estimation of Material Properties from Dynaflect Deflections

The pavement layer stiffnesses can be estimated from Dynaflect deflection measurements using elastic layered theory as follows:

(1) Pavement layer thicknesses, initial estimates of the pavement layer moduli, Poisson's ratio, and the loading and deflection measurement configuration are input into the computer program.

(2) The computed deflections at the five geophone positions can be compared to those actually measured in the field.

(3) The layer moduli used in the computer program can now be adjusted to improve the "fit" of the predicted and actual deflection basins.

(4) This process is repeated until the two deflection basins are virtually the same. The process may have to be repeated several times before a reasonable fit is obtained.

Knowledge of the effects of changes to the various layer moduli on the shape and position of the deflection basin may speed the process considerably.

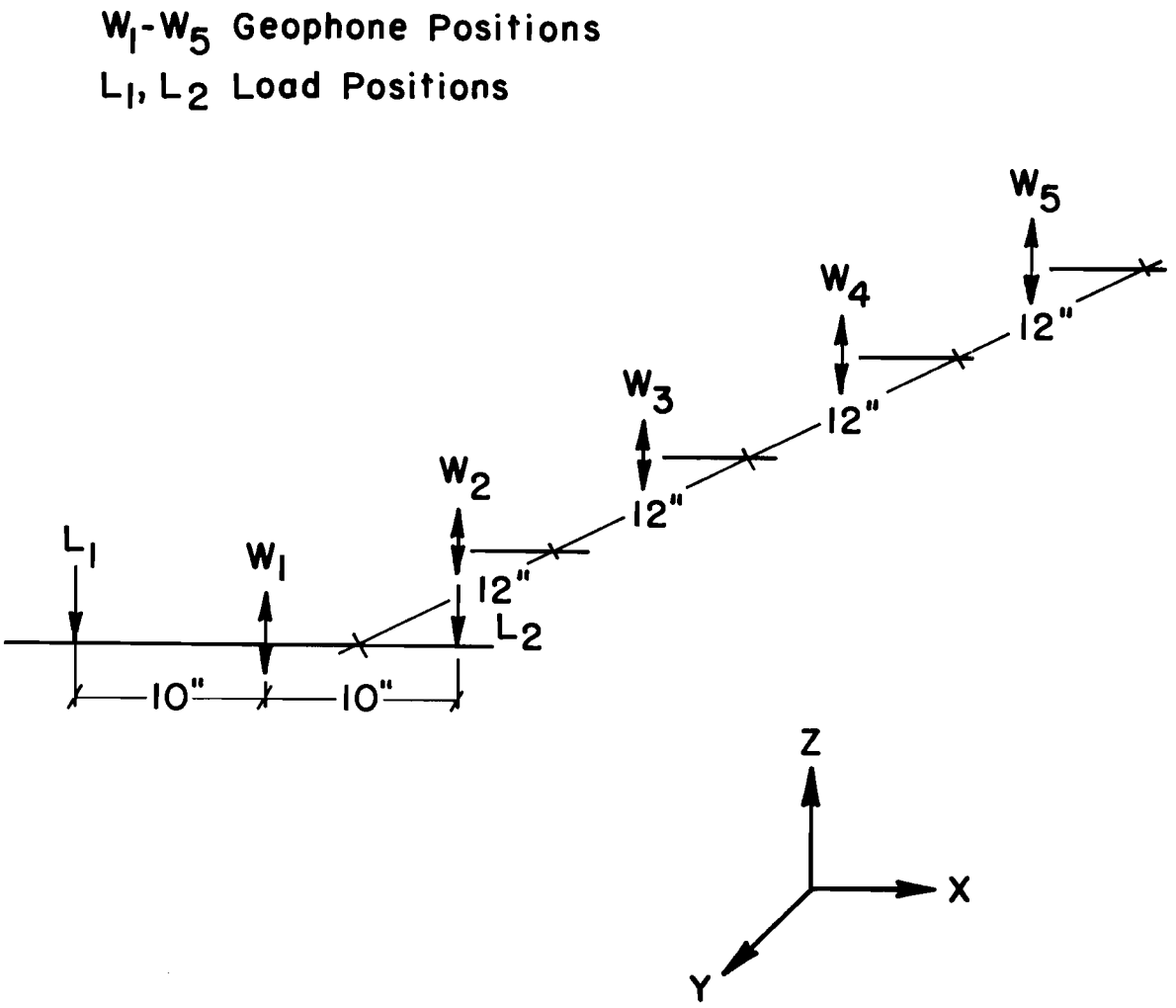

Fig 2.3. Dynaflect loading and deflection measurement layout.

Some of the terms commonly used with Dynaflect deflection basins are

Sensor "i" deflection: Wi

Surface curvature index (SCI): W1-W2

Base curvature index (BCI): W4-W5

Spreadability: (W1 + W2 + W3 + W4 + W5)/5W1

Slope of the deflection basin: W1-W5

These parameters are related to the stiffness of one or more of the pavement layers in varying degrees. This factor is illustrated in Fig 2.4, where deflection basins predicted by layered theory for different layer moduli are presented. Typical CRC pavement structures consist of a concrete pavement layer, a stabilized subbase layer, and a subgrade.

A large number of layered theory computations were made using this type of pavement structure and the following conclusions have been drawn.

(1) As illustrated in Fig 2.4, changes to the surface or stabilized subbase modulus result in significant changes to the sensor 1 deflections and only minor changes to sensor 5 deflections. This corresponds to a change in the deflection basin slope.

(2) Changes to the subgrade moduli result in significant changes to both sensor 1 and sensor 5 deflections. Both these deflection parameters are affected approximately proportionally by changes to the subgrade modulus, which results in little change to the deflection basin slope.

Therefore, it can be hypothesized that the subgrade modulus may be predicted from the deflection at any sensor and that the slope of the basin may be used to predict the surface and subbase modulus. However, the

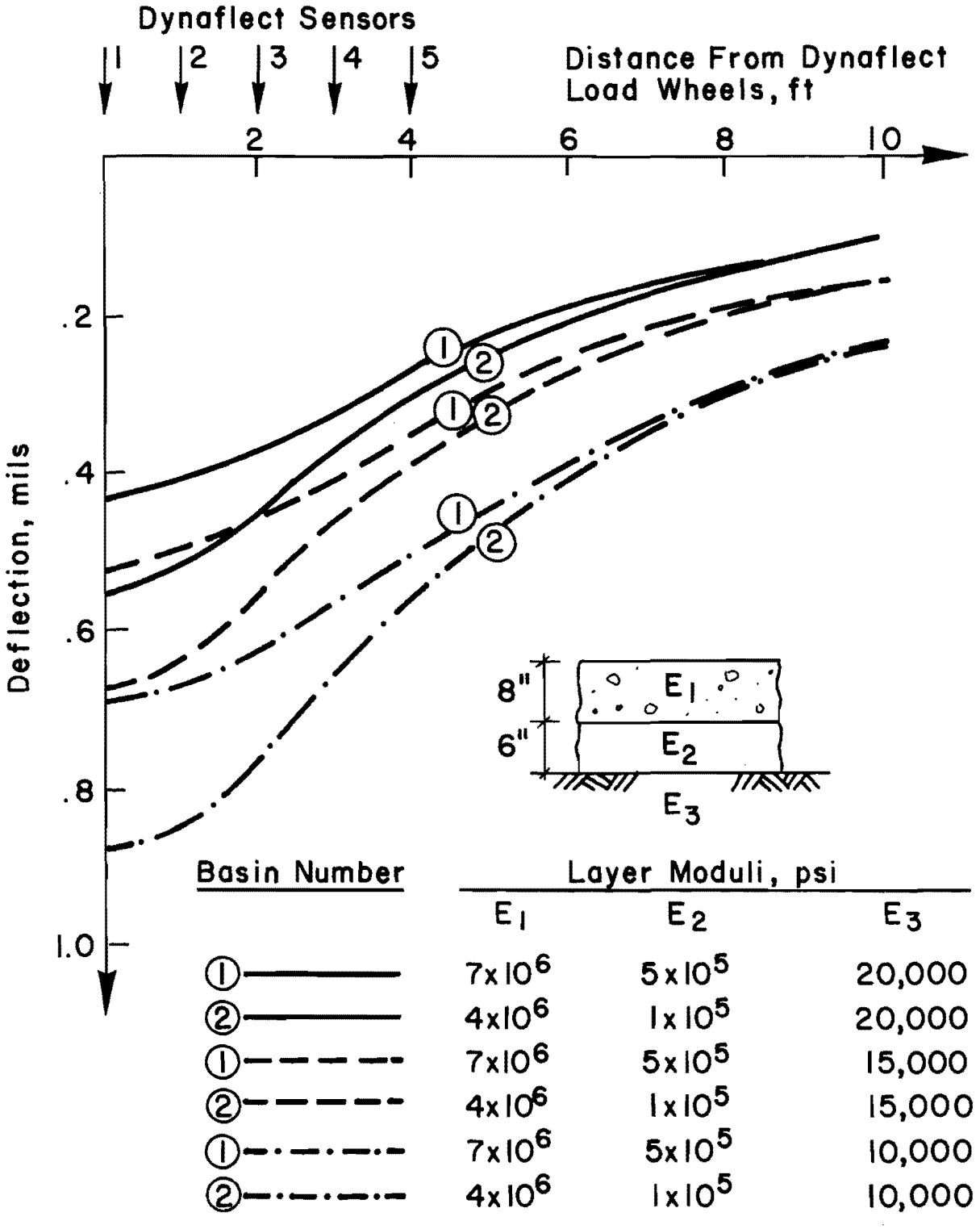

Basin Number	Layer Moduli, psi		
	E_1	E_2	E_3
① ———	7×10^6	5×10^5	20,000
② ———	4×10^6	1×10^5	20,000
① – – – –	7×10^6	5×10^5	15,000
② – – – –	4×10^6	1×10^5	15,000
① –·–·–·–	7×10^6	5×10^5	10,000
② –·–·–·–	4×10^6	1×10^5	10,000

Fig 2.4. The effect of layer moduli on dynaflect deflection basins for a typical rigid pavement structure.

subgrade modulus predicted from the sensor 5 deflection will be fairly accurate for a wide range of surface and subbase moduli, because of the small effect which these moduli have on this deflection parameter. In the case of the basin slope, however, an infinite number of combinations of surface and stabilized subbase modulus exist which, when used in layered theory analysis, will predict approximately the same basin slope.

A number of figures have been prepared to simplify the calculation of layer moduli from Dynaflect deflections. Because the pavement stiffness has a minor effect on the fifth sensor deflection, Fig 2.5 shows the subgrade modulus as a function of sensor 5 deflection and the rigid pavement thickness. Both the layer modulus and the thickness of the layer affect the stiffness of the layer. From the formula for the radius of relative stiffness

$$\ell = \sqrt[4]{\frac{Eh^3}{12k(1-\nu^2)}} \qquad (2.1)$$

where

ℓ = radius of relative stiffness (in.),

E = modulus of elasticity of the slab (psi),

h = thickness of the slab (in.),

ν = Poisson's ratio of the slab, and

k = modulus of subgrade reaction (pci),

it is apparent that the layer thickness has more effect on the radius of relative stiffness than the modulus. For example within the range of modulus and thickness typical of CRC pavements, a 1,000,000 psi change in modulus results in a 5 percent change in ℓ, whereas a one-inch change in thickness

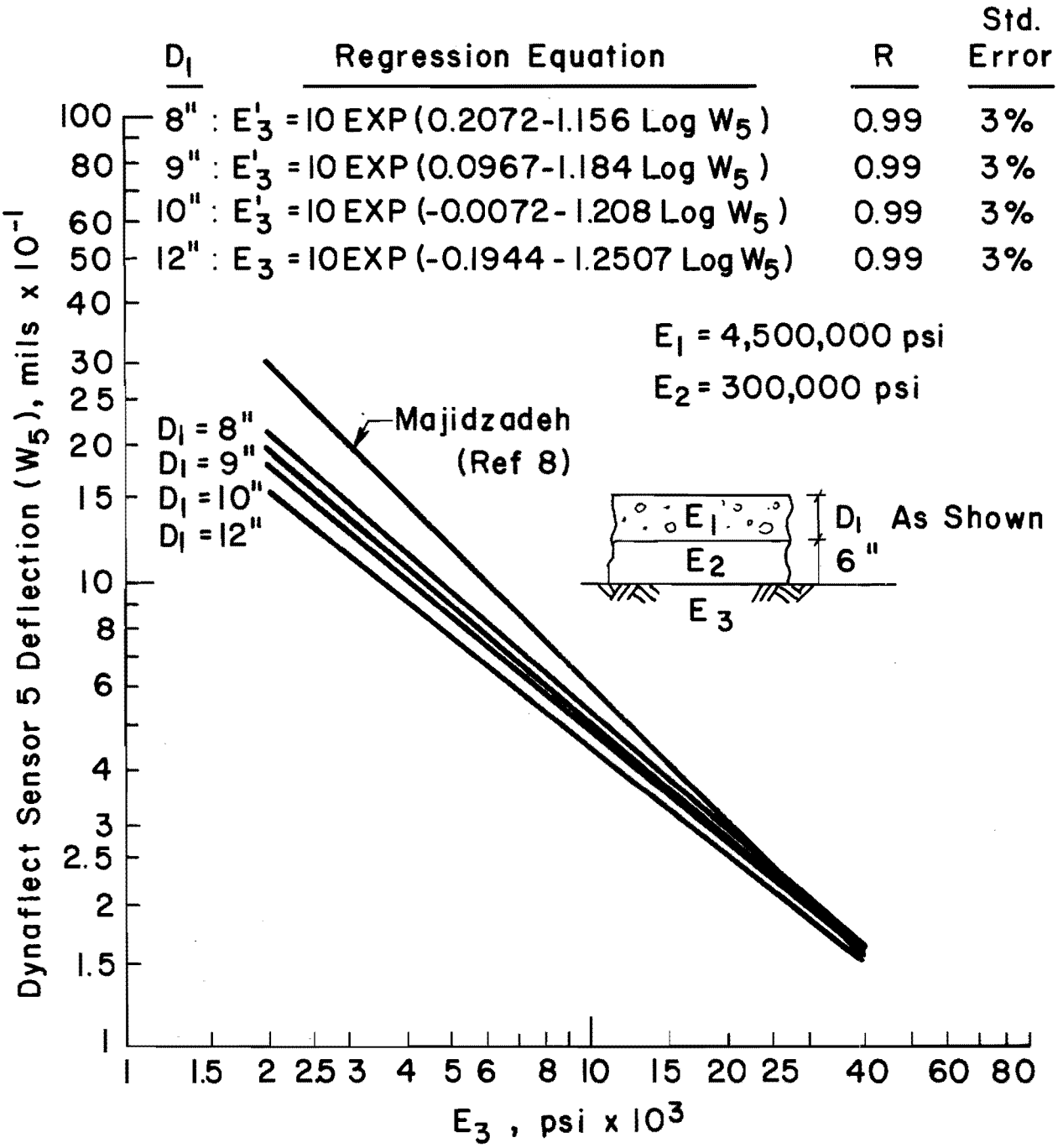

Fig 2.5. Dynaflect sensor 5 - subgrade modulus relationship for different rigid pavement thicknesses.

results in a 10 percent change in ℓ . Furthermore, at the deflection measuring stage, the upper layer thicknesses are generally known, whereas their moduli may not be. Therefore, the subgrade modulus - sensor 5 relationship was also plotted as a function of surface layer thickness.

The relationship in the figure was obtained by regression analysis of data obtained from layered theory computations. In the log-log form presented in the figure and for constant upper layer moduli and thickness the subgrade modulus is very highly correlated to deflection at any point on the pavement surface. The regression equations used in the figure, their correlation coefficients, and standard errors are shown in the figure.

The upper layer moduli-deflection basin slope relationships are presented in Figs 2.6, 2.7 and 2.8 for different subgrade moduli. The data used for plotting these curves were obtained from the results of numerous layered theory computations. The pavement structure used for the computations is indicated on the figures.

A nomograph has also been prepared for trial and error calculations of deflection basin slopes, from layer moduli estimates. The equation used for the development of the nomograph in Fig 2.9 was obtained from regression analysis of layered theory results. The correlation coefficient of this equation is 0.98 and the standard error of the residuals is 8 percent, as shown in Fig 2.9.

The upper layer thicknesses and estimates of the layer moduli are used in the nomograph to obtain a prediction of the deflection basin slope under a Dynaflect load. The selected moduli can be modified until the basin slope obtained in the nomograph coincides with the slope obtained in the field. The numbers above each scale on the nomograph indicate the sequence at which the lines should be crossed, as illustrated in the figure. From the

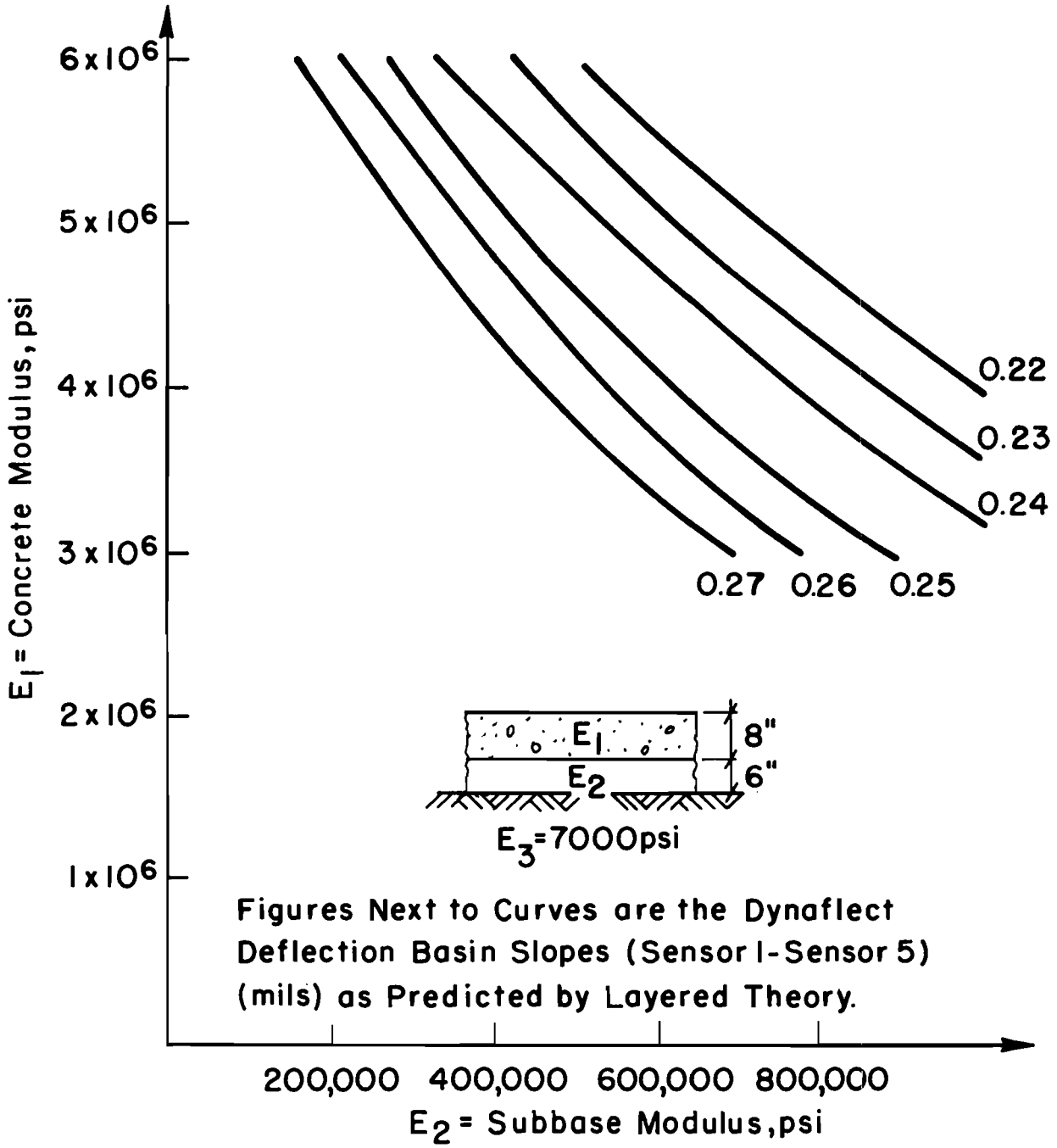

Fig 2.6. Dynaflect deflection basin slopes as a function of layer moduli for a typical rigid pavement structure (subgrade modulus - 7,000 psi).

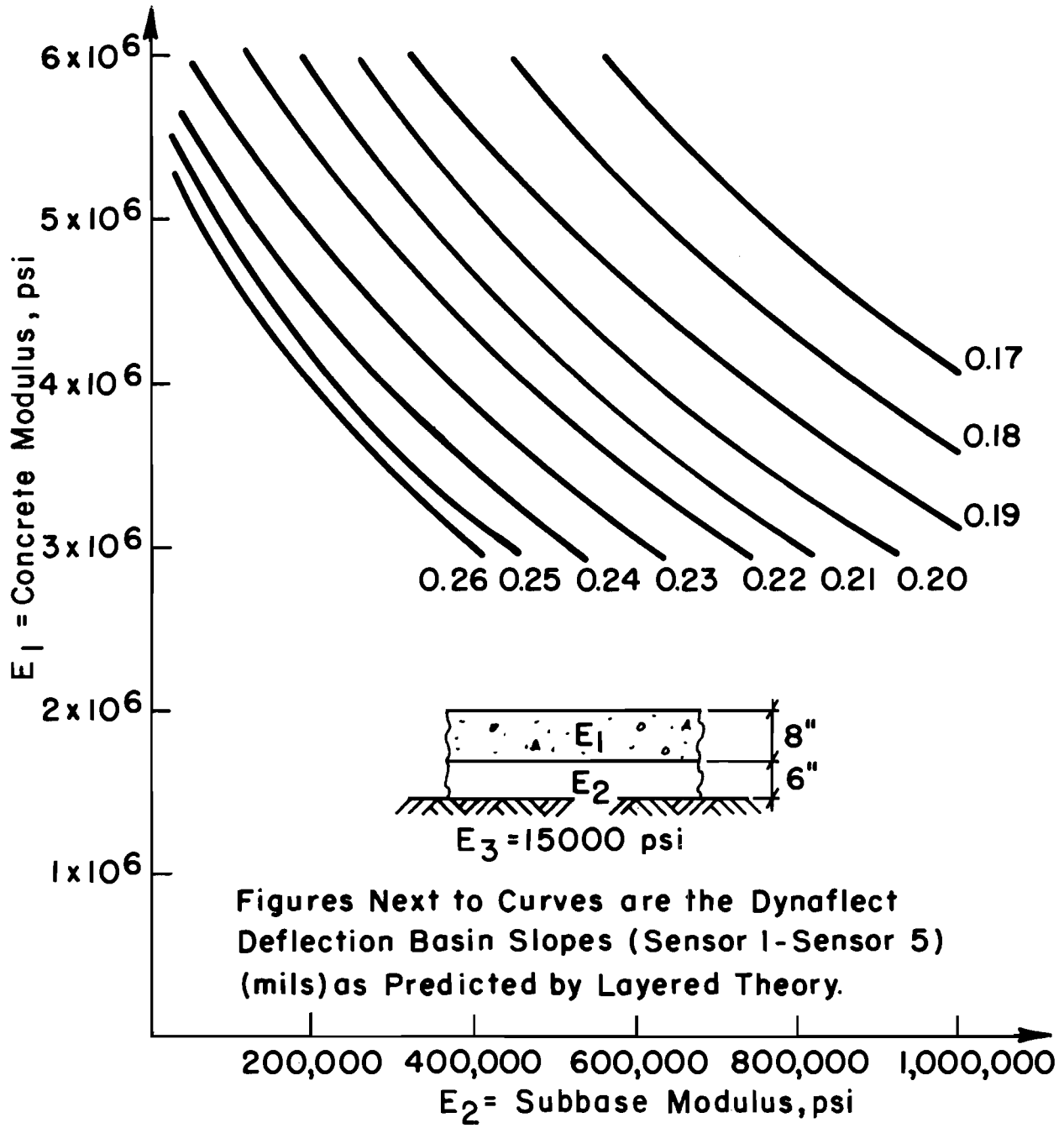

Fig 2.7. Dynaflect deflection basin slopes as a function of the layer moduli for a typical rigid pavement structure (subgrade mudulus = 15,000 psi),

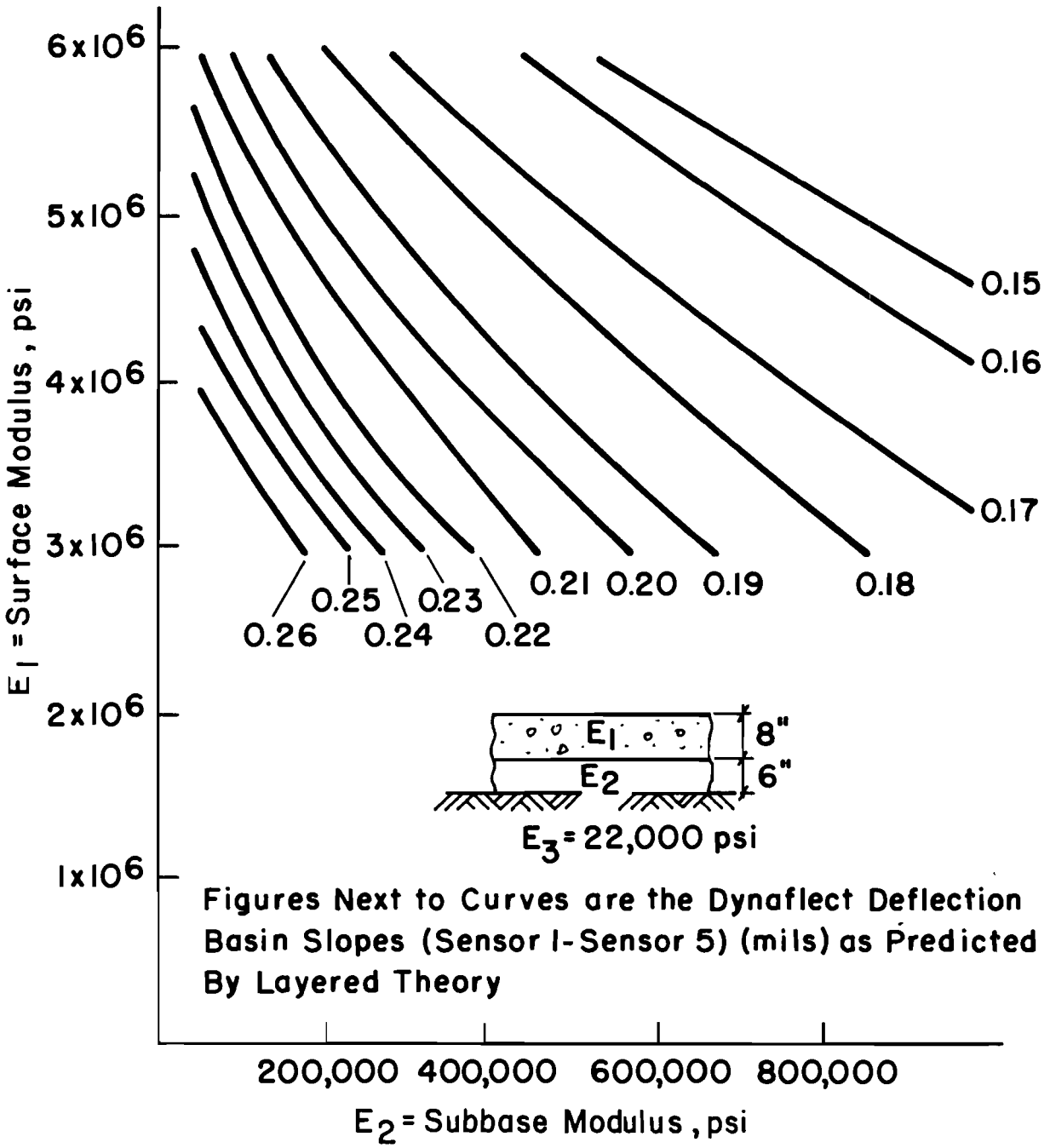

Fig 2.8. Dynaflect deflection basin slopes as a function of layer moduli for a typical rigid pavement strucutre (subgrade modulus = 22,000 psi).

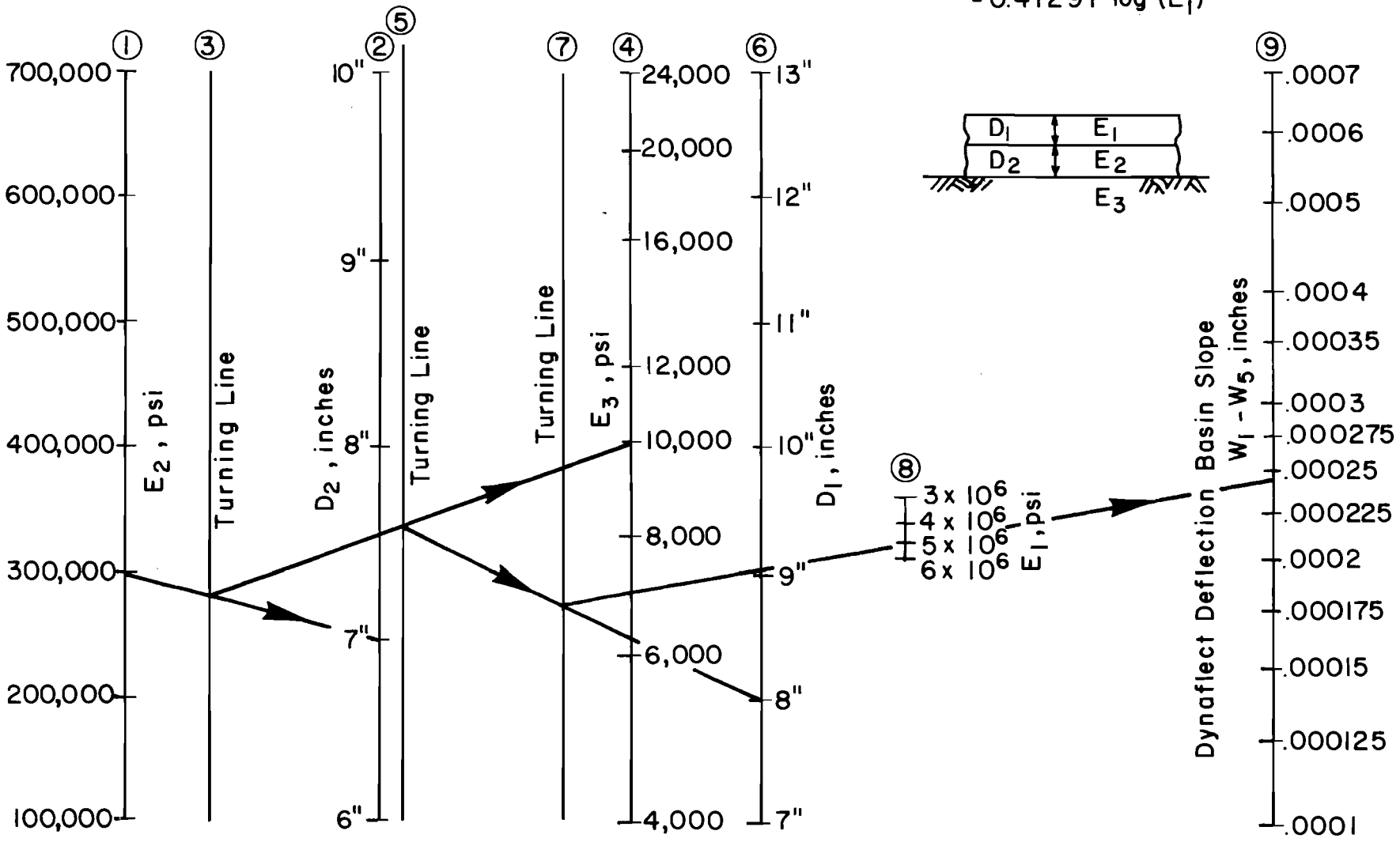

Fig 2.9. Nomograph for predicting the dynaflect deflection basin slope (W_1-W_5) for rigid pavements.

nomograph it is apparent that the basin slope is extremely sensitive to surface and subbase layer thickness and modulus. Thus, whenever possible, laboratory testing should be used to corroborate moduli obtained from this procedure.

In the past, the SCI has often been correlated to layer stiffnesses for asphalt pavements (Ref 10). As shown in Fig 2.4, a typical deflection basin for rigid pavements is very flat with a large radius of curvature. Thus, for rigid pavements the SCI is a very small quantity and any small measurement inaccuracies in the Dynaflect may result in a considerable change in SCI. This may be the cause of the larger average coefficient of variation of the SCI (50 percent) than that of the basin slope (30 percent) in Table A3. For this reason, the slope of the basin (sensor 1 minus sensor 5) has been correlated to the upper layer stiffnesses rather than SCI.

Problems Associated with Deflection-Modulus Predictions

A number of factors exist which may result in inaccurate predictions of moduli from deflection measurements:

(1) stress sensitivity of pavement materials,

(2) variation of subgrade stiffness with depth,

(3) seasonal effects, and

(4) discontinuities in the pavement structure.

All these factors lead to significant changes in the deflection measurements and, consequently, to the moduli predicted from these deflections. If these problems are recognized, deflection measurements, or

calculated moduli, can be adjusted to account for them. In the following paragraphs, methods of accounting for these problems are discussed.

Stress Sensitivity. The fact that pavement materials do not behave in a linear elastic fashion has long been established. In May 1962 at the St Louis conference on the AASHO Road Test (Ref 25), some data were presented which showed that deflections were not proportional to load. In the discussions which followed, Mr. F. N. Hveem stated that deflection-load relationships depended on the nature of the subgrade soil. Subsequent resilient modulus tests of subgrade soils have shown that the stress-strain relationship depends to a large degree on soil type (Refs 19 and 26). Most pavement materials are not linearly elastic and the moduli may vary with stress, as illustrated in Fig 2.1. Clayey soils may be stress softening (i.e., reduced modulus with increased stress), whereas granular materials may be stress hardening (increased modulus with increased stress). The Texas overlay design procedure takes only the stress sensitivity of the subgrade into account by using the slope (SSG) of the Resilient Modulus - principal stress difference line. This parameter was discussed in more detail under the Resilient Modulus test.

Dynaflect deflections do not provide any indication of the stress sensitivity of the pavement material. Deflection devices which are capable of applying different loads to the pavement may provide some indication of the stress sensitivity of the material. At this stage of the implementation of the Texas Rigid Pavement Overlay Design Procedure (RPOD2), an indication of the stress sensitivity of the subgrade is obtained from Resilient Modulus tests.

Variation of Subgrade Stiffness with Depth. Deflection measurements provide an indication of the pavement's response to loading. Layered theory modelling of the pavement structure typically assumes that the subgrade has a semi-infinite depth. Very little of the pavement deflection is due to compression of the surface layers; it is due mostly to compression of the subgrade. For the same subgrade stiffness, loading an infinitely thick subgrade would result in much larger deflections than loading a shallow subgrade supported by a more rigid foundation. This factor is illustrated in Fig 2.10, where a number of deflection basins obtained using the BISAR and ELSYM5 elastic layered theory programs are plotted. The structures used as inputs to the program are indicated in the figure.

This indicates that, if samples of the subgrade from immediately below the subbase layer are tested for modulus, use of this modulus in layered theory computations with an infinite subgrade depth will overpredict the surface deflections. This is illustrated in Fig 2.11, obtained from Ref 1, where computed deflections using moduli from material tests as inputs are compared to field deflections. In reality infinitely thick subgrades and homogeneous subgrades with a well defined depth supported by a rigid foundation seldom exist in the field.

Field conditions will most often be somewhere between these two extremes. A granular subgrade whose stiffness gradually increases with depth or a clayey subgrade which, due to desiccation, may be stiffer at the surface than lower down may be more likely to occur in practice. Furthermore, this condition may change along the length of the road. Cut and fill areas, for example, may have extremely different subgrades. Seismic testing or deep probing may provide some information to the designer in this regard. If no

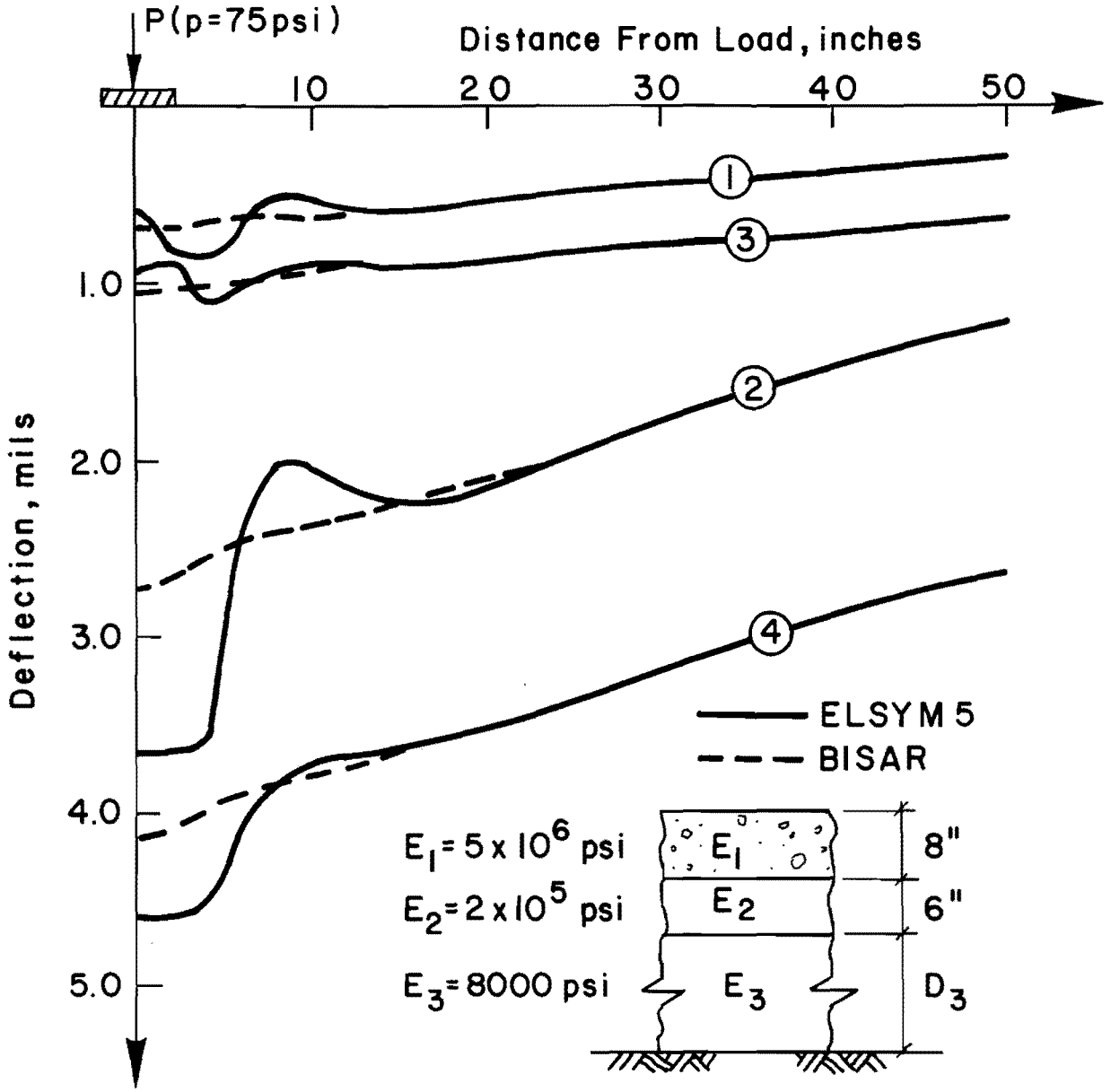

Basin Number	Load-P	Subgrade Thickness- D_3
①	1000 lb	120"
②	1000 lb	∞
③	4000 lb	120"
④	4000 lb	∞

Fig 2.10. Deflection basins obtained from ELSYM5 and BISAR for two different loads and subgrade thicknesses.

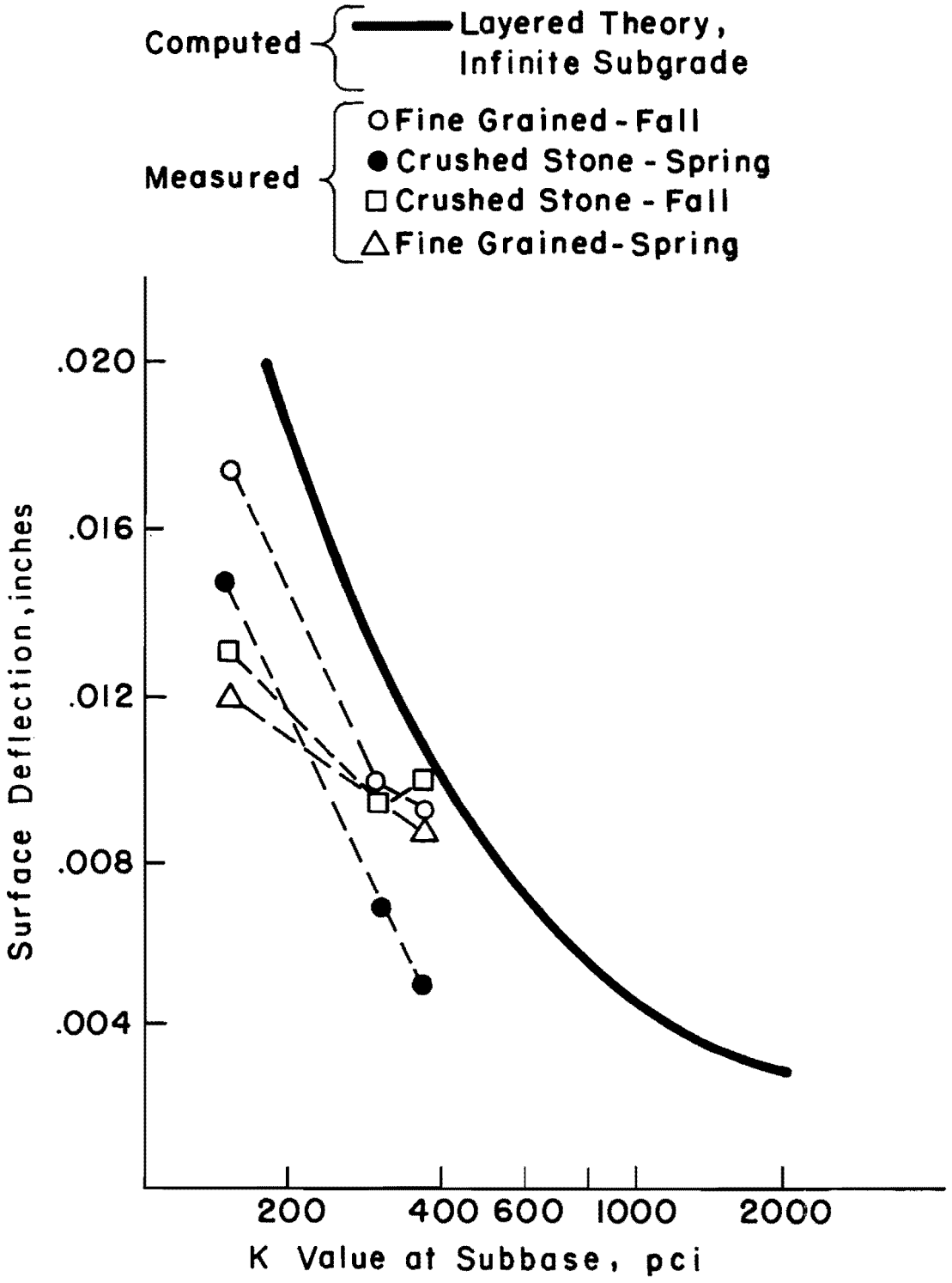

Fig 2.11. Comparison of predicted and measured deflections considering subgrade support (Ref 1).

information is available, "engineering" judgment should be used for an approximation of the change in subgrade stiffness with depth.

Furthermore, from Fig 2.10 it is apparent that layered theory programs, such as ELSYM5, which are based on the CHEVRON 5 program predict unrealistic deflections in the vicinity of the load. For predictions of Dynaflect deflections using ELSYM5 or a similar layered theory program, these discontinuities are significant in the case of a subgrade supported by a rigid foundation because the first sensor is 10 inches away from the loading point and, thus, is above an irregular deflection as predicted by these programs. Therefore, if the deflection measurements are made near the loading point, BISAR should be used to compute "fitted" deflection basins.

These factors need to be considered when predicting subgrade moduli from deflection measurements, and to this end, Fig 2.12 has been prepared. This figure was produced from regression analysis on the results of layered theory computations of the behavior of typical existing pavement structures. It shows the relationship between the subgrade modulus predicted from sensor 5 Dynaflect deflections for a semi-infinite subgrade depth and the subgrade modulus predicted from the same deflection measurement if a rigid foundation exists at some depth.

The figure was obtained as follows:

(1) Numerous layered theory computations of the deflections under the Dynaflect load at the position of the Dynaflect 5th sensor were made. The computations used a pavement structure as indicated in the figure.

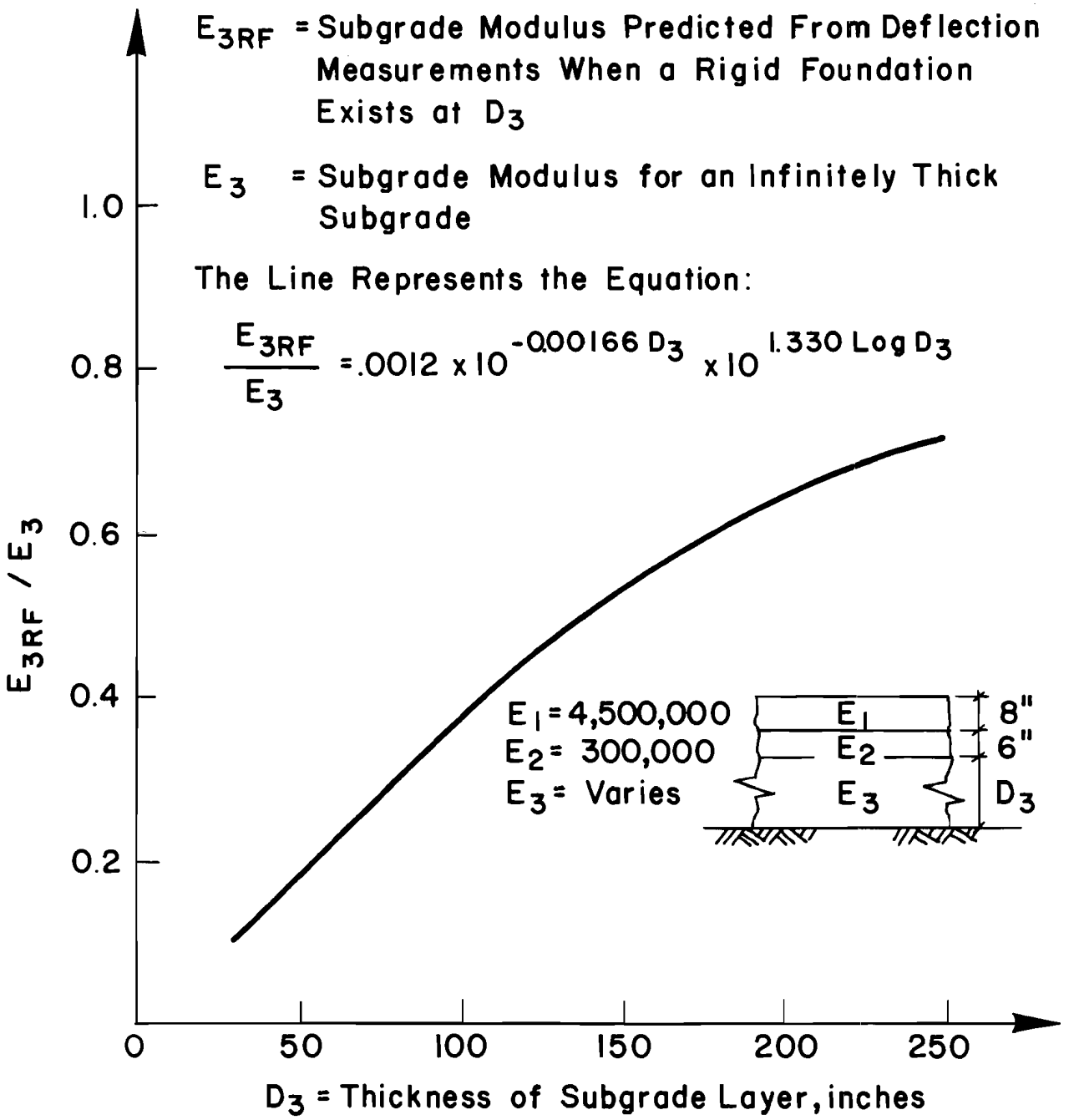

Fig 2.12. The reduction in subgrade modulus predicted using deflection measurements when the subgrade is supported by a rigid foundation at depth D_3.

(2) A regression equation describing the subgrade modulus as a function of the sensor 5 deflection and the depth to the rigid foundation was obtained. This equation is as follows:

$$E_R = 10\exp(-1.3832 - 0.0016584 \cdot D_3 + 0.6394 \cdot \log D_3 - 0.7582 \cdot \log W5 - 0.2034 \cdot \log D_3 \cdot \log W5) \quad (2.2)$$

where

E_R = subgrade modulus as predicted by layered theory from deflections, when a soft subgrade is supported by a rigid foundation;

W5 = sensor 5 Dynaflect deflection;

D_3 = thickness of the soft subgrade layer, inches.

(3) Equation 2.2 was related to the equations presented in Fig 2.5 for the same pavement structure and an infinitely thick subgrade as follows:

$$\frac{E_R}{E} = \frac{10\exp(-1.383 - 0.00166D_3 + 0.6394 \cdot \log D_3 - 0.7582 \cdot \log W5 - 0.2034 \cdot \log D_3 \cdot \log W5)}{10\exp(0.2072 - 1.156 \cdot \log W5} \quad (2.3)$$

which reduces to

$$\frac{E_R}{E} = 10\exp(1.59034 - 0.00166D_3 + 0.6394 \cdot \log D_3 + 0.3978 \cdot \log W5 - 0.20338 \cdot \log D_3 \cdot \log W5) \quad (2.4)$$

Differences in W5 within the range typical of concrete pavements have little effect on this equation, and, therefore, if W5 = 0.004 inches, the equation reduces to

$$\frac{E_R}{E} = 0.0011 \times 10\exp(-0.00166D_3 + 1.33 \cdot \log D_3) \qquad (2.5)$$

From Fig 2.12, it is apparent that this type of analysis may result in substantial reductions to the subgrade modulus depending on the thickness of the soft subgrade layer. The accuracy of Eq 2.5 is reflected by the results presented in Fig 2.13. This graph was developed by making a number of random calculations using layered theory within the ranges of layer thicknesses and moduli shown in Fig 2.12. Although some substantial errors may occur in the moduli predicted using these equations, they are not significant when compared to the uncertainty regarding the actual change of subgrade modulus with depth. Figure 2.12 can, thus, be used to provide an approximate estimate of the reduction to the subgrade modulus calculated from deflections only if a rigid foundation exists. Seismic testing and engineering judgement (provided by test borings for bridge foundations, etc.) should be used to estimate whether any reduction to the subgrade modulus calculated using deflections is required for a particular area.

Seasonal Effects. Deflections measured along the road change due to seasonal changes of moisture and temperature. With CRC pavements, changes in the environment affect the deflection measurements in two ways. Cold temperatures cause the concrete surface layer to shrink, causing an increase of the transverse crack widths. Periods of increased rainfall result in slightly higher moisture contents in the subgrade and a corresponding lower

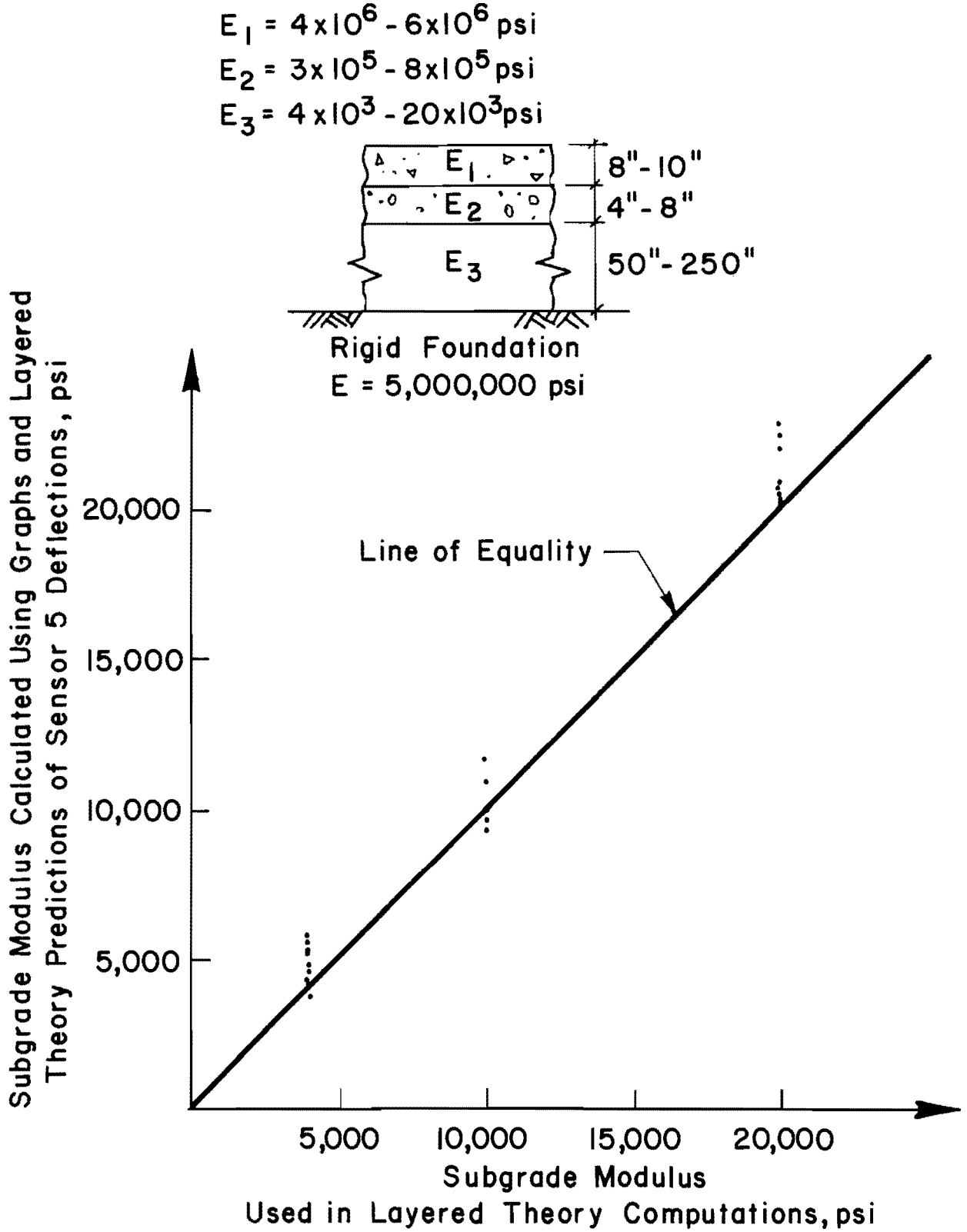

Fig 2.13. Comparison of subgrade modulus used in layered theory analysis and subgrade modulus estimated using graphs from layered theory deflections.

subgrade modulus. The effects of these factors on deflections are illustrated in Ref 27.

First consider the effect of these environmental factors on the Sensor 1 Dynaflect deflections or, in other words, on deflections near the center of the deflection basin. A wet winter will result in an increase in deflection compared to other seasons. This will be due to the wet, soft subgrade and due to the low effective modulus of the surface layer caused by shrinkage and the resulting relatively wide transverse cracks. A dry summer will result in a decrease in this deflection due to the dry stiff subgrade and the high effective surface modulus, caused by expansion and the resulting narrowing of the transverse cracks in the CRC pavement. Wet summers or dry winters may not appreciably change this deflection relative to other seasons, due to the counterbalancing effects of the environment on the different layer moduli.

If, on the other hand, the sensor 5 Dynaflect deflection and the slope of the deflection basin are considered, environmental factors affecting the subgrade and surface may be distinguishable. Moisture effects on the subgrade should affect the sensor 5 deflection and temperature effects on the surface should affect the basin slopes.

Therefore, if laboratory testing can be done to determine the moduli of the surface and subbase layers, deflection measurements should be made during the wettest season of the year to obtain the most critical subgrade modulus from these measurements.

Discontinuities in the Pavement Structure. Cracks in the rigid pavement layer may have an effect on deflections if some loss of load transfer is caused by the cracks. With CRC pavements, the cracks are tightly closed, resulting in very little loss of load transfer. As explained, a drop

in temperature can cause these cracks to open; thus some loss of load transfer may result. This will cause an increase in the sensor 1 deflection with a corresponding change in basin slope and the moduli predicted from this deflection parameter. The effect of these cracks on stresses in the concrete layer is discussed in more detail in Chapter 3 of this report.

VARIATION IN PAVEMENT LAYER STIFFNESSES

Stresses in the upper pavement layers resulting from heavy axle loads will be affected by variation of the pavement layer stiffnesses. The layer stiffnesses are in turn affected by variation in layer thickness and moduli. These material stiffnesses may vary in both the horizontal and vertical planes. Different pavement layers will have different amounts of variation associated with them.

The Effect of Varying Layer Stiffnesses on the Stresses in the Pavement

Before discussing the variations associated with each layer's stiffness, it is useful to know what effect a change in a specific layer stiffness will have on the tensile stresses in the design layers of the pavement. (The design layers of a pavement are defined as those layers which are calculated to last the design life of the pavement, based on fatigue.) This is shown in Fig 2.14 for a typical three-layered pavement structure. The figure was produced from layered theory analysis of the pavement structure while varying the layer moduli. From the figure, it is apparent that decreasing subbase and subgrade moduli results in an increase of the tensile stresses in the surface layer under load. Increasing surface modulus also increases this

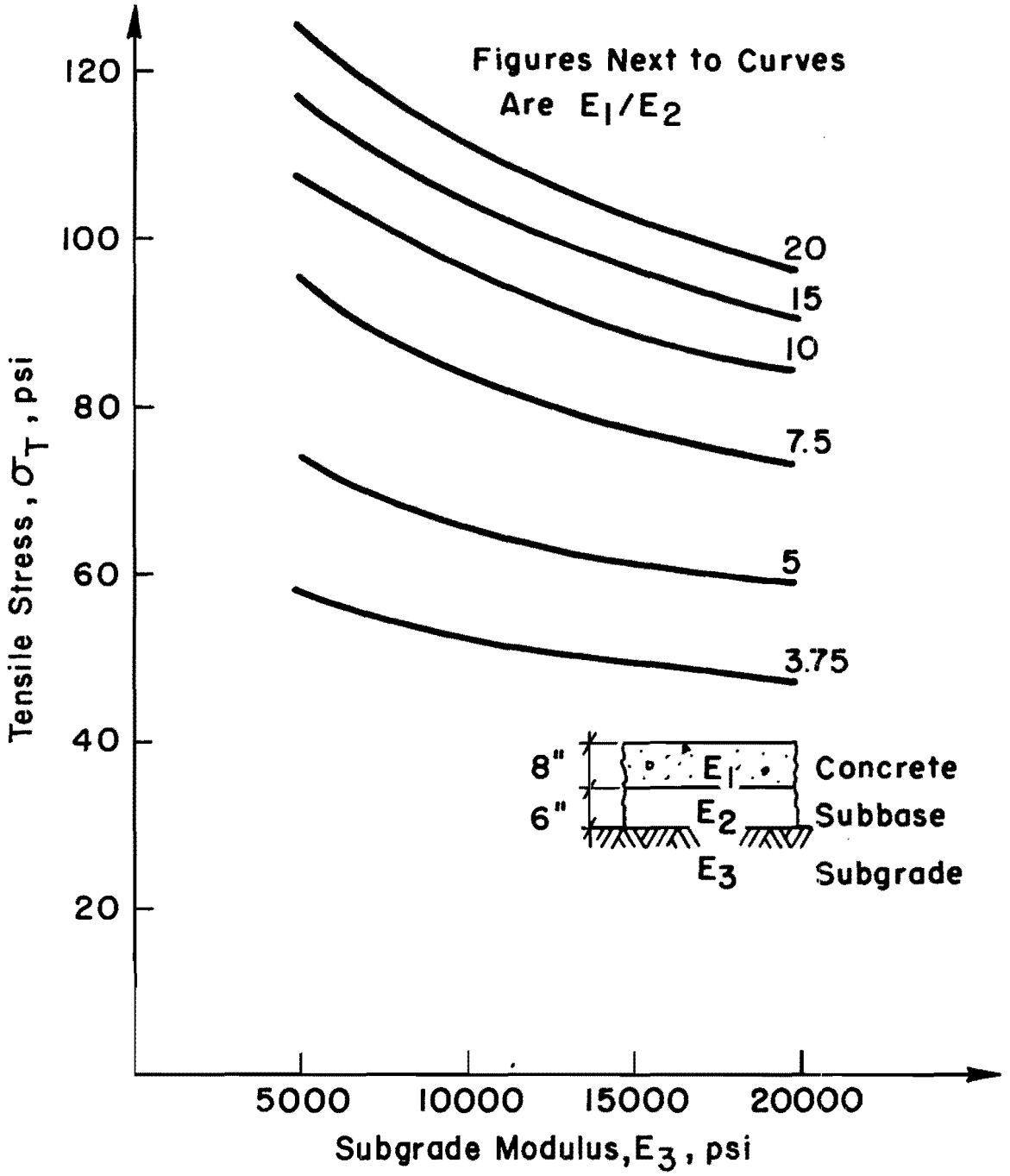

Fig 2.14. The effect of changing layer moduli on the tensile stress in the bottom of a rigid pavement layer.

critical stress. The effect of changing layer thickness on the critical tensile stress in the pavement is difficult to quantify. For example, very thin pavement layers may have no tensile stresses in them under load. It is sufficient to say that, within the range of thicknesses typical of CRC pavements, an increase in layer thickness will decrease the tensile stresses in the rigid pavement layer.

Causes of Variation in Layer Stiffnesses. The causes of variation in each pavement layer's stiffness, for a typical CRC pavement, are discussed separately.

CRC Layer. Due to the construction control exercised over this layer, it normally has only a small variation in thickness from the specified thickness. Similarly, the modulus of the layer may be fairly consistent. Some variation of modulus may be expected in the vertical direction, primarily as a result of placing and curing techniques. This is evident in Ref 20, for which a number of cores were tested for strength and modulus by means of the indirect tensile test. In this report, the coefficient of variation of concrete modulus was approximately 33 percent. Further variation of effective modulus in the horizontal direction may be caused by transverse cracks in the concrete. Additional variation may be caused by the use of different aggregate sources and by different mixing and placing techniques along the length of the road.

Subbase Layer. Here again construction control may limit the variation in layer thickness and modulus. Some variation in modulus may be caused by use of material from different sources in different areas of the project or by use of different quantities of stabilizing agent. The effect of cracking

on the effective modulus of this layer may be similar to the effect on a concrete surface layer, although in this case the loss of load transfer at the cracks is not affected by resistance to movement of the reinforcing steel. A proportion of the variations in the slope of the deflection basins may be attributed to variations in the stiffness of this layer.

Subgrade. The effective stiffness of this portion of the pavement may vary significantly. Variation in material stiffness in both the horizontal and vertical directions may cause significant changes to the effective stiffness "felt" by the upper pavement layers. Similarly, the subgrade may consist of a number of layers of varying thicknesses along the length of the road. For example, pavements in cut and fill areas may have very different subgrades. Similarly, low lying areas with higher water tables may be much softer than freely draining areas. Some of this type of variation has been discussed earlier in this report.

Some of the variation in the subgrade stiffness will be evident from the Dynaflect sensor 5 deflections taken along the length of the road.

Methods of Accounting for the Variations in Layer Stiffnesses

One of the best methods for obtaining an idea of the amount of variation in the layer stiffnesses along the length of a road is with deflection measurements taken at fixed intervals along the road. The measurements are then plotted to provide a visual indication of the variation. This method has the advantages of economy and speed over material sampling and laboratory testing. If stage construction is used, the method can be applied equally well to the compacted subgrade of the pavement under construction.

The variation in layer stiffnesses can be divided into two groups:

(1) random variation and

(2) stratified variation.

Random variation is present in all pavement materials and structures. It is normal and due to the heterogeneous nature of the pavement layers. This variation is often reflected in the deflection measurements by some scatter among the results for a section of roadway. Stratified or assignable variation occurs due to a significant change in factors, such as layer stiffnesses or thicknesses. For example, the subgrade stiffness in a cut or fill area may be significantly different from the adjacent area. If possible the stratified variation should be accounted for by separating design sections with assignable differences. This is not always practical; for example, if an area of a certain weak subgrade type is small it may be included within a larger adjacent section and its variation added to the random variation of the larger section. The random variation may, for example, be accounted for by designing for a deflection based on a certain statistical confidence limit (Refs 3 and 5).

Selection of Design Sections

A visual indication of the deflection and layer stiffness variation is provided when deflection measurements are plotted to scale as a function of distance. The PLOT program, documented in Ref 5, provides a plot of deflections by means of a computer line printer. This plot facilitates dividing the roadway into sections based on stratified variation of deflection data. Previously, deflection sections have been selected based

only on sensor 1 deflections. Now that layer stiffnesses may be predicted from deflection measurements, as described previously, sections may be selected based on the sensor 5 deflections and the slopes of the deflection basins. The sensor 5 deflection is used to select sections with different subgrade stiffnesses and the basin slopes are used to select sections with different effective surface stiffnesses. Sections are selected subjectively, based on a plotted profile of these deflection parameters, as indicated in Fig 2.15.

When design sections are selected, each section representing a change in sensor 5 deflection should also represent a change in the sensor 1 minus sensor 5 deflection parameter, but not vice versa. This is because the subgrade modulus does have a significant effect on the basin slope, but the surface stiffness does not have a significant effect on the sensor 5 deflection.

Furthermore, implementation of the overlay design procedure (RPOD2) has shown that changes in deflection variance are as important as the changes in the mean deflection in the selection of design sections. Areas with similar mean sensor 5 deflections but with significantly different variation thereof should be separated into different design sections. This is illustrated in Fig 2.15 since sections 1 and 2 have similar mean sensor 5 deflections but different variances.

Because sections are selected by considering two deflection parameters and their variances, this process may result in many small sections. In order to keep the number of short sections to a minimum, limits of sections selected from different deflection parameters should be made to coincide wherever possible.

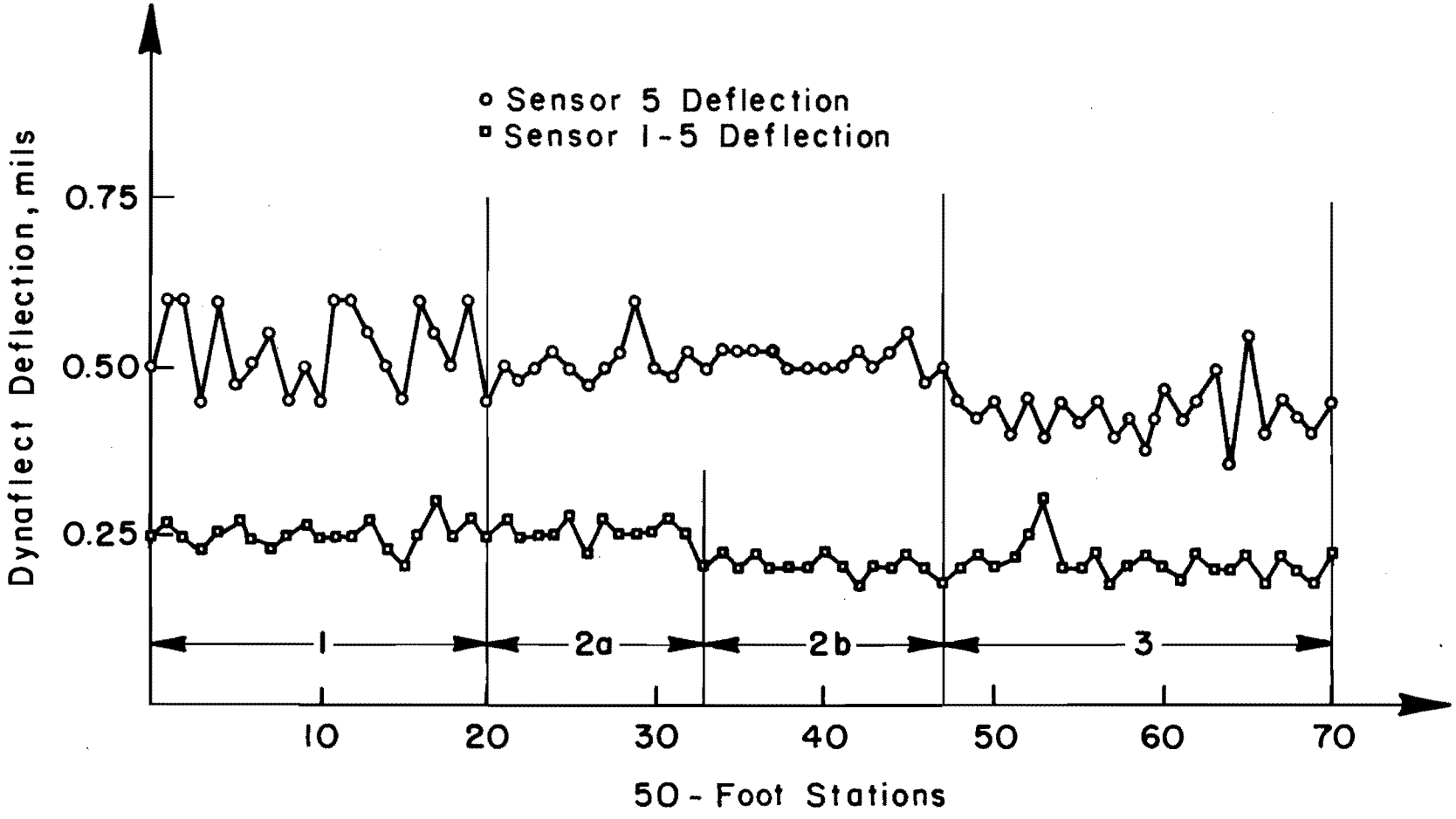

Fig 2.15. Selection of design sections using Dynaflect sensor 1 and sensor 1 minus sensor 5 deflections.

After selection of different design sections, RPOD2 recommends the use of the student's t test to determine whether the section means are significantly different at specific confidence levels. However, one of the shortcomings of this test is that the test assumes that the sections (or data) being tested have similar variances.

As indicated earlier, different sections may have different variances, and, if so, these differences are important factors in the selection of sections. This shortcoming could be overcome by using a statistical test designed for testing differences between sample variances. Before embarking on such a course, the consequences of incorrectly selecting or not selecting a section should be examined.

Section Size

As recommended above, contiguous design sections are selected based on the mean and variance of the Dynaflect sensor 5 deflections and the slope of the deflection basins. The shortest section selected should be long enough so that it is practical and important to construct a distinct set of pavement thicknesses and materials over the length of the section. Implementation of the RPOD2 design procedure has indicated that this length is approximately 1,000 feet.

The section should also be long enough to contain sufficient deflection measurements for the designer to make fairly accurate inferences about the section's overall behavior from this sample of deflections. If the deflection measurements are normally distributed, a statistical formula can be used to determine the sample size. If, for example, the sample mean

should only have a probability, α , of differing from the population mean by more than d percent then the formula is as follows (Ref 28):

$$N = \frac{(tS)^2}{D^2} \qquad (2.6)$$

where

N = sample size,

t = the abscissa of the normal curve which cuts off an area at the tails,

S^2 = variance of the population,

D = d x y where y is the sample mean.

Implementation of the RPOD2 design procedure has shown that a typical value for of the sensor 5 deflection is .10 mil. The sensor 5 deflection depends on the subgrade modulus and typically varies from 0.2 mil to 0.5 mil. A value of 0.3 mil can be used as representative of a fairly good subgrade. Therefore if a = 5 percent and d = 10 percent then

$$N = \frac{(1.96 \times 0.1)^2}{(0.1 \times 0.3)^2} = 24$$

This indicates that, if a section length of 1,000 feet is the shortest practical construction unit length, then, for these constraints on inference accuracy, deflection measurements are required at 50-foot intervals within that section. This inference accuracy becomes important when confidence limits of deflections for the different design sections are predicted.

Design Consequences of Section Selection

A conservative pavement design is one which can withstand high critical tensile stresses in the design pavement layers. As indicated previously, the modulus of each layer has an effect on this tensile stress. These moduli may vary significantly and the combination of layer moduli which results in the highest tensile stress in the design layers under load will result in a conservative design. For example, in the structure indicated in Fig 2.14, high tensile stresses will occur when a high surface modulus coincides with a low subgrade modulus. This situation is, however, not very likely to occur. Because the subgrade modulus generally has a large amount of variation associated with it, the RPOD2 design procedure recommends that the pavement be designed for a certain confidence limit, only with regard to this modulus. Due to the correlation between the subgrade modulus and the Dynaflect sensor 5 (W5) deflection, this may be interpreted as designing for a confidence limit with regard to the W5 deflections. The W5 deflection which corresponds to this confidence limit may be called the design W5 deflection.

This deflection value will depend on the mean and standard deviation of the W5 deflections within the section. Theoretically, this type of design suggests that those portions of the pavement located in areas where the W5 deflection would exceed the design W5 deflection will not last the design life. If the design W5 deflection in two selected design sections is significantly different, then grouping these sections together will result in underdesigning the one section and overdesigning the other. The only consequence of not grouping them together is that an additional design will have to be done.

With the present improvements and simplifications being made to existing design methods, this is not a serious consequence. Furthermore, because design sections are selected based on a number of deflection parameters, it would be difficult to test the sections for any significant differences or similarities with regard to all these deflection parameters. If, however, a design section is short and too few deflection measurements exist within the section to provide reasonable inferences about the actual design sensor 5 deflection, then this deflection may be underestimated. This will result in an underdesigned section of pavement.

Therefore, it should be apparent that simplifications of existing design methods and the complications associated with selecting design sections based on two or more deflection parameters make statistical testing to determine whether sections are significantly different or not superfluous. The designer should use these guidelines and engineering judgement to select as many sections as would be feasible to design.

To assist in the selection of design sections and in the statistical analysis of the deflections within each section, a computer program called MODE has been prepared. A listing of the program appears in Appendix B. The program creates a plot of the frequency and cumulative distributions of the important deflection parameters in each section. As indicated in Figs 2.16 and 2.17, these plots can be used to select the design W5 deflection and the modal deflection values to be used for estimating layer properties.

Trial use of this program for statistical analysis of deflection data obtained along CRC pavements in Texas has shown that deflection parameters are not generally normally distributed. Frequency diagrams of W1, W5, and W1 minus W5 deflections are all generally skewed towards the smaller deflections. This is because deflections which are much higher than the mode

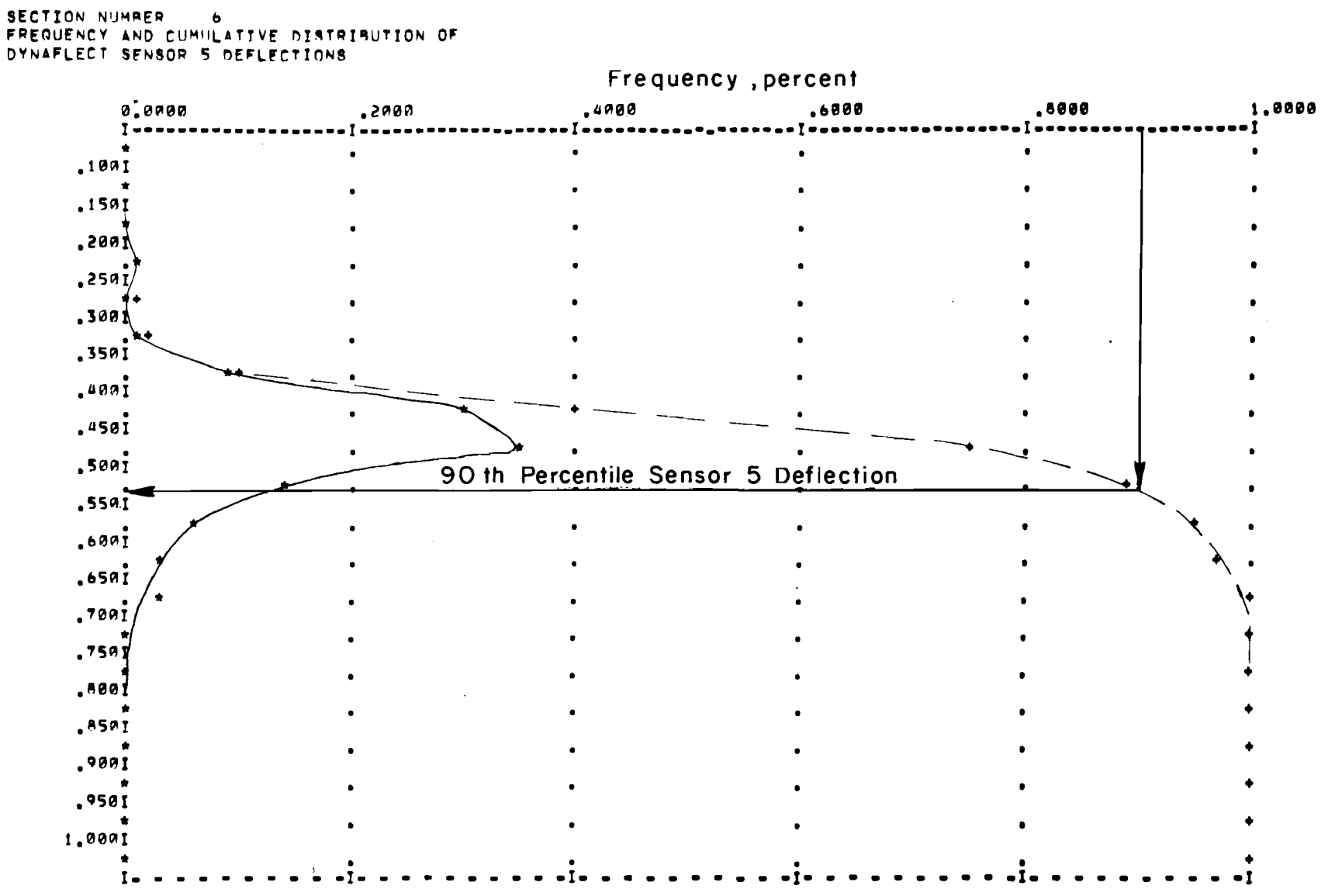

Fig 2.16. Output from Program MODE to select 90th percentile sensor 5 deflection.

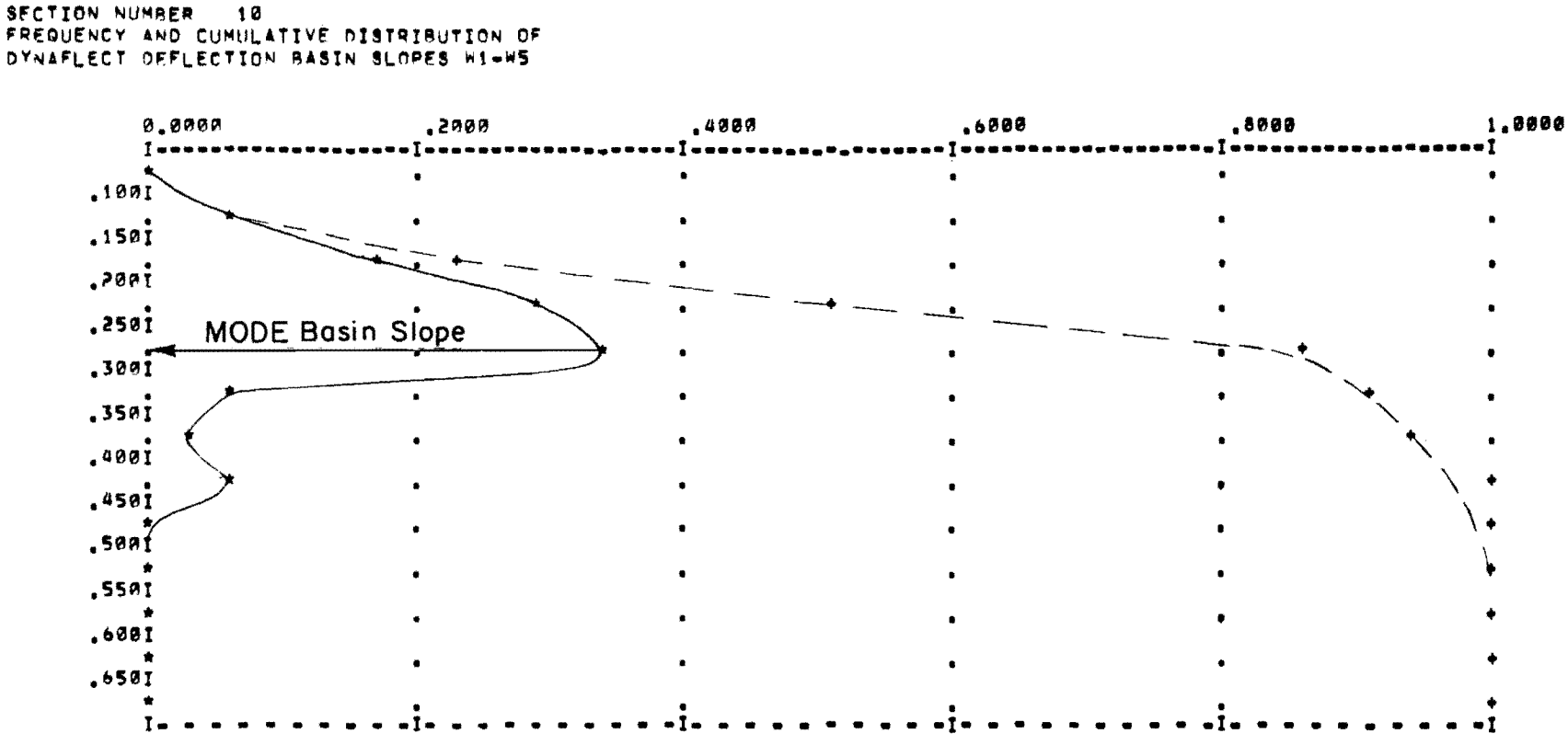

Fig 2.17. Output from Program MODE to select modal deflection basin slope ($W_1 - W_5$).

deflection do occur, whereas deflections much smaller than the mode cannot exist because of the artificial boundary created by zero deflection. The mean deflection is, thus, often slightly higher than the modal deflection. The plot of deflection parameter distributions in a section should be examined and if they are significantly skewed, it is recommended that the mode of the deflection basin slope be used for estimating the surface and subbase moduli. However, when only a few deflections exist in a section, no single mode may exist, and thus, it is recommended that in this case the mean deflection parameters be used to estimate the material stiffnesses. Similarly, when the distribution approaches normality, the means may be used to predict the surface modulus for that section.

It is apparent from Figs 2.6,2.7 and 2.8 that, although changes in the surface layer modulus do not have a significant effect on the Dynaflect W5 deflection and the corresponding subgrade modulus, changes in the subgrade modulus do have a significant effect on the surface modulus selected from basin slope measurements. It may, thus, be reasoned that a large proportion of the variation associated with the basin slope measurements may result from changes in the subgrade modulus. Therefore, it is recommended that the subgrade modulus to be used in the calculation of upper layer moduli from the basin slopes be determined from the same W5 statistic used with the basin slope. Deflection distributions for IH-10 in Hunt county are shown in Appendix B.

SUMMARY

The procedure for characterizing the material properties of a pavement may be summarized as follows:

(1) For a new pavement, used material tests to obtain an indication of the mean and variance of the layer moduli. If stage construction is used, take deflection measurements at every 50 feet along the length of the prepared roadbed. Similar measurements should be taken in the event an existing pavement needs rehabilitation. The measurements should be taken approximately 3 feet in from the outside shoulder.

(2) Run the PLOT4 program using the deflection data as input. This program will plot the profile of the W5 and W1 minus W5 deflections along the length of the road, as illustrated in Fig 2.15.

(3) Select contiguous sections from this plot using the means and variances of both the plotted deflection parameters as selection criteria, with a minimum length of approximately 1,000 feet. To prevent having a number of short sections during the selection process, the limits of sections selected based on W5 deflection and on the basin slope measurements should be made to coincide where possible.

(4) Run the mode program on the deflection data. The program may have to be run once using the sections selected from sensor 5 deflections as input and then again using the sections selected from the basin slope measurements as input.

(5) Use the output from this program as a guideline for selecting sections having similar modal sensor 5 deflections for obtaining core samples.

(6) Obtain 4-inch cores from the bound pavement layers and 3-inch push barrel samples of the subgrade layer. In the event of a granular subgrade, in situ densities and moisture contents should be obtained and the specimens recompacted in the laboratory to simulate field conditions.

(7) Conduct indirect tensile tests on the bound layers and resilient modulus tests on the unbound layers. The moduli obtained from these tests should be used as first estimates of the layer material properties. The slope of the principal stress difference line (SSG) should provide a reasonable estimate of the subgrade stress sensitivity.

(8) Deflection basin fitting techniques are then used to obtain the surface and subbase layer moduli. The modal W5 deflection of a section is used in Fig 2.5 to obtain the modal subgrade modulus for the section. This modulus should be used in conjunction with the moduli estimates for the bound layers obtained from indirect tensile tests, as initial input to a layered theory program. The deflection basin slope of this structure under the Dynaflect load as predicted by layered theory is then compared to the measured modal basin slope of the section. The input moduli for the bound pavement layers may require adjustment and this process is repeated until the basin slope predicted by layered theory corresponds to the modal basin slope. Should a computer not be readily available, Figs 2.5 to 2.9 can be used to provide estimates of these moduli.

(9) This process will provide a set of effective layer moduli which occur most frequently in the section under the Dynaflect load. In order to obtain a reasonably conservative design, a subgrade modulus representative of the weaker spots within a section should be used. The cumulative distribution curve of the sensor 5 Dynaflect deflection for the section plotted by the MODE program may be used for this purpose. Depending on the design reliability required, the W5 deflection corresponding to a required percentile can be selected from the distribution curve to represent the weaker subgrade. This "design deflection" is now used in Fig 2.5 to obtain the design subgrade modulus under the Dynaflect load.

(10) Should the designer have some idea of the nature of the change of subgrade modulus with depth, the design subgrade modulus should be reduced as indicated in Fig 2.12.

(11) The final step in the materials characterization process is to take the stress sensitivity of subgrade into account. The method proposed in RPOD2 uses the slope of the log resilient modulus log deviator stress line obtained from the Resilient Modulus test as an indicator of the stress sensitivity. The method is described in detail in Ref 5.

(12) The materials characterization for the pavement structure used in layered theory analysis is now complete.

This materials characterization is one of the most important steps of a pavement design procedure. The tensile stress in the bound pavement layers, and consequently the fatigue life of the pavement, will depend on the moduli

of the layers used as inputs in layered theory analysis. This aspect of the pavement design process will be referred to throughout this report.

FLOW CHART OF THE PROCEDURE FOR CHARACTERIZING
THE MATERIAL PROPERTIES OF A PAVEMENT

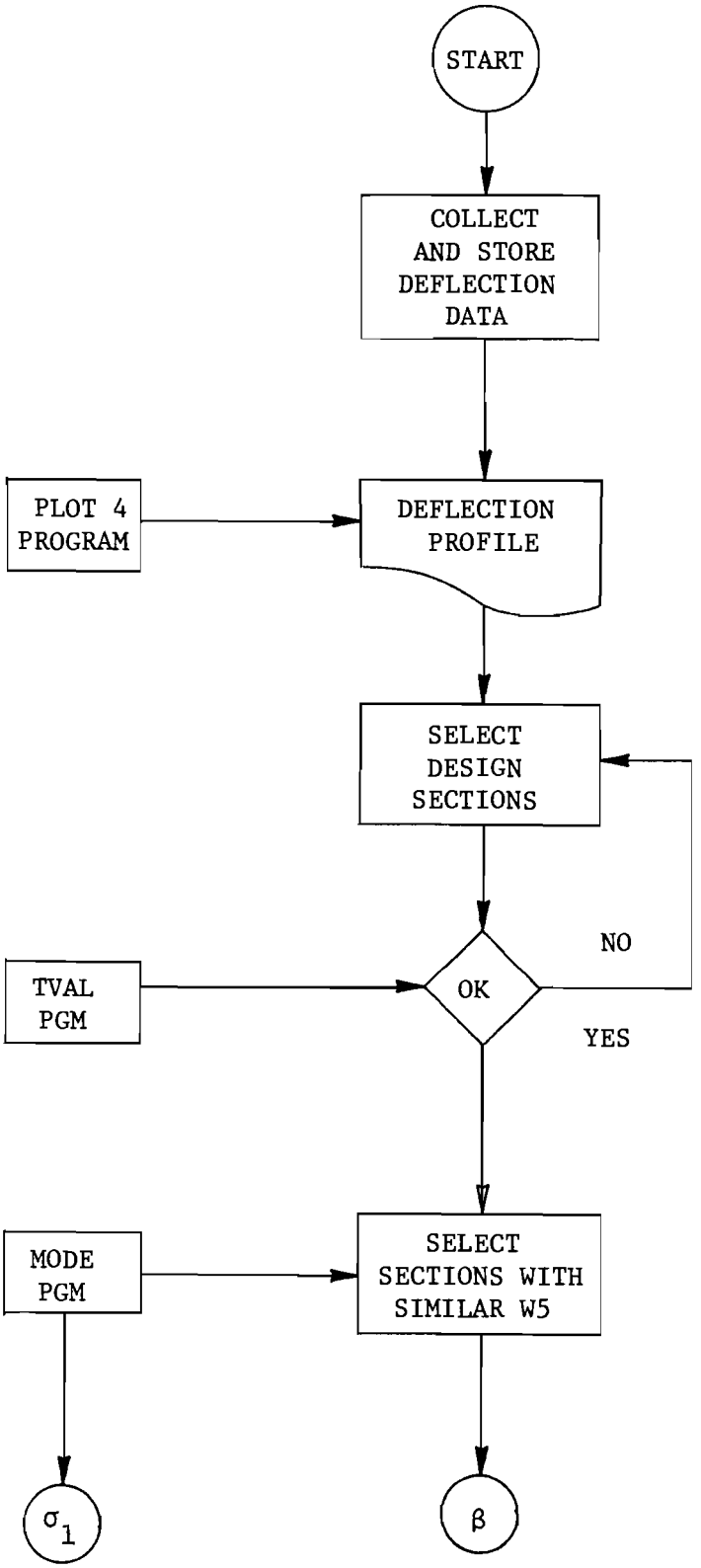

(continued)

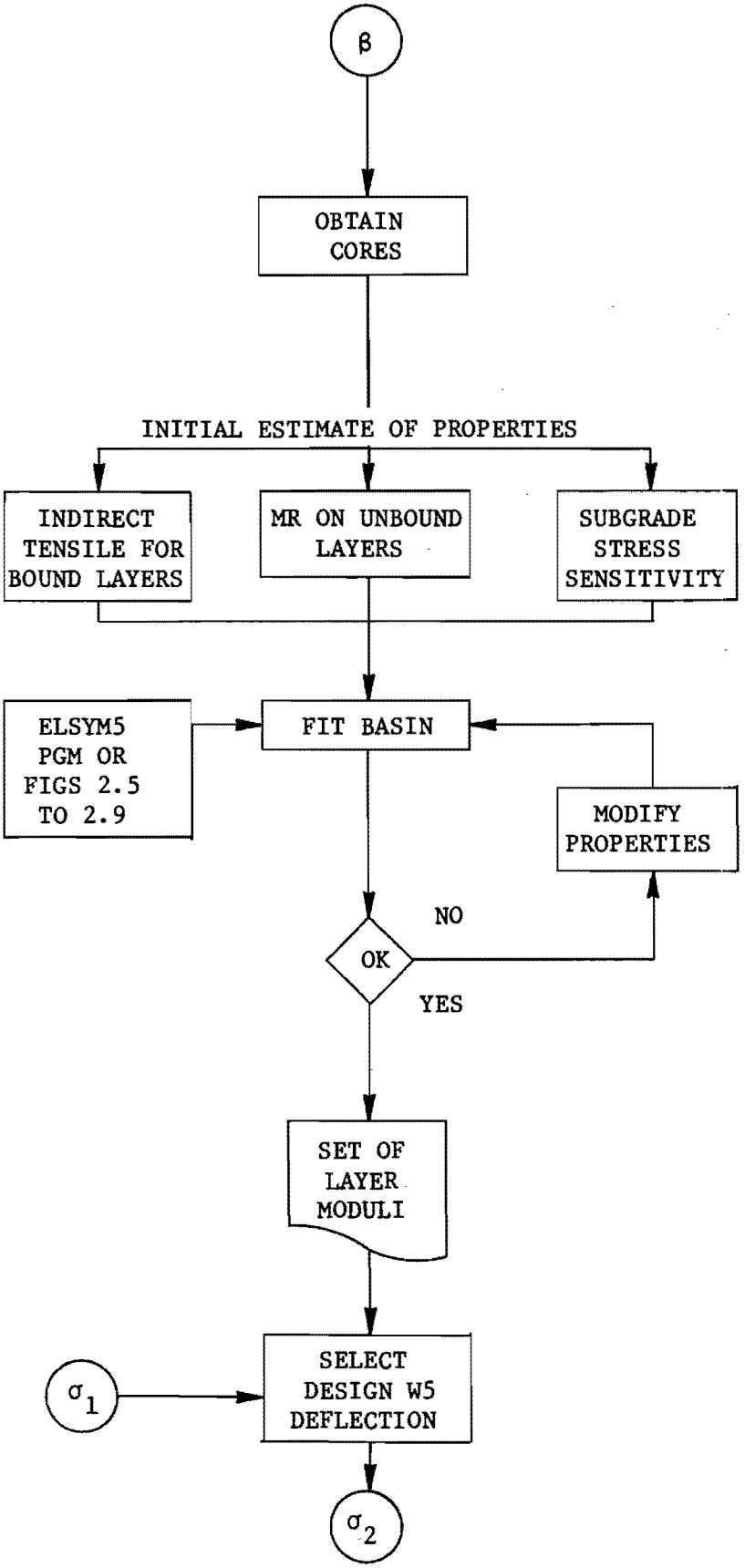
β
OBTAIN CORES
INITIAL ESTIMATE OF PROPERTIES
INDIRECT TENSILE FOR BOUND LAYERS
MR ON UNBOUND LAYERS
SUBGRADE STRESS SENSITIVITY
ELSYM5 PGM OR FIGS 2.5 TO 2.9
FIT BASIN
MODIFY PROPERTIES
NO
OK
YES
SET OF LAYER MODULI
SELECT DESIGN W5 DEFLECTION
σ1
σ2

(continued)

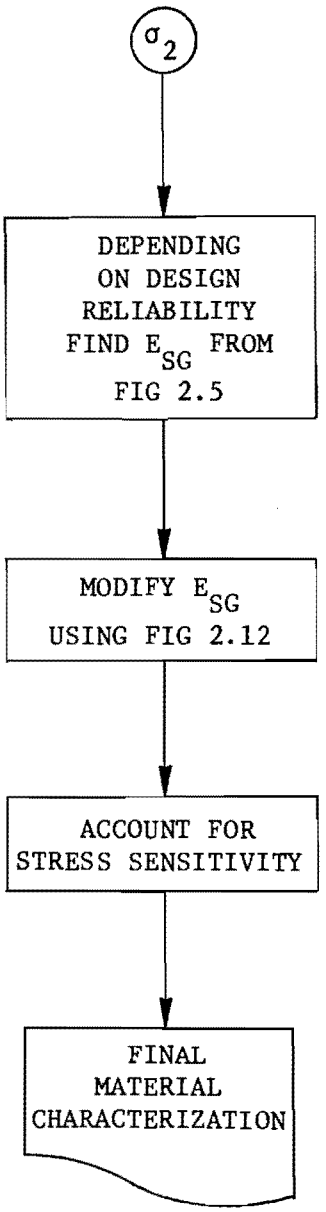
σ_2
DEPENDING ON DESIGN RELIABILITY FIND E_{SG} FROM FIG 2.5
MODIFY E_{SG} USING FIG 2.12
ACCOUNT FOR STRESS SENSITIVITY
FINAL MATERIAL CHARACTERIZATION

CHAPTER 3. THE EFFECT OF PAVEMENT LAYER DISCONTINUITIES ON THE TENSILE STRESSES IN THE PAVEMENT

Mechanistic pavement design procedures use the tensile stresses in the concrete layer in a fatigue equation to predict the pavement life. Discontinuities in the pavement structure may influence the stress distribution significantly and, if higher stresses exist near these discontinuities, they must be accounted for.

As indicated in the previous chapter, layered theory analysis assumes that the pavement layers are elastic, homogeneous, and isotropic, which is seldom the case in practice. In order to consider layer discontinuities in a design procedure, more sophisticated analysis techniques should be used. Discrete and finite element analyses fall into this category. Computer analysis using these methods is time consuming and expensive, relative to layered theory analysis, and, for this reason, these analysis methods will probably be confined to research activities for several years to come by most people.

The results obtained from analysis using these more complex techniques can be applied in standard design procedures which use layered theory. This can be accomplished by modifying either the inputs to or the outputs from layered theory analysis so that the stresses used in the fatigue equation reflect the results obtained from the more complex analysis. The inputs referred to are layer moduli values, and the outputs are tensile stresses.

This chapter will consider only the effects of pavement discontinuities on the stresses in rigid pavement layers. Stresses in overlays caused by underlying pavement discontinuities are discussed in Chapter 4.

ANALYSIS TECHNIQUES

Two of the analysis methods commonly used to examine the stresses occurring in pavements at or near discontinuities are discrete and finite element analyses. The SLAB49 program, developed at the CTR, uses the discrete element type of analysis procedure. This analysis procedure uses plate theory, which models the concrete slab as a stiff plate and the subgrade as a bed of linear springs but allows variation in slab stiffness and subgrade support in all horizontal directions.

The program and analysis procedure are documented in Ref 29. With regard to finite element analysis, many different computer programs have been developed in recent years and, of these, the SAP2 program, developed at the University of California, is currently available at the CTR. This is a generalized, three dimensional, finite element program capable of handling many different structures and using many different element types. One of the elements types used in this program is a three dimensional "brick" element with eight nodes which is well suited to pavement structural analysis.

Both these analysis techniques have been used in the past to analyze the stresses in pavements at discontinuities. The SLAB49 program has been used to predict the increased pavement stresses for edge loading conditions and between cracks, relative to the stresses occurring under an interior loading condition (Refs 30 and 31). Two and three dimensional finite

element analysis has also been used to analyze continuous and jointed concrete pavements and overlaid jointed concrete pavements (Ref 32,33,34.). Pavement behavior as indicated by these analysis techniques, relative to what actually occurs in the field, may be verified by comparing the theoretical and actual deflections of the pavement under load.

Limitations of Discrete and Finite Element Techniques

Discrete element analysis (SLAB49) can consider only a single pavement slab, i.e., one layer supported by a bed of linear springs. This limitation is not severe if the pavement structure beneath the slab consists only of granular layers. McCullough (Ref 1) has shown that this type of analysis and layered theory analysis predict similar tensile stresses in the slab if the supporting structure consists primarily of granular material. However, if the slab supporting structure includes some stabilized layers which can carry load in bending, the spring constant used in the analysis needs to be calculated carefully. The stress deflection relationships predicted by a number of analysis methods are presented in Fig 3.1. The high stresses predicted by SLAB49 occur because the spring constant, k, used in discrete element analysis techniques cannot accurately represent a bound subbase layer carrying some load in bending. The k value is generally obtained from the maximum deflection under a load, without consideration of the shape of the deflection basin. For example, a stiff subbase and soft subgrade may have the same maximum deflection under load as a softer subbase and stiffer subgrade, but the radius of curvature and tensile stresses in the surface layer may differ significantly in the two cases.

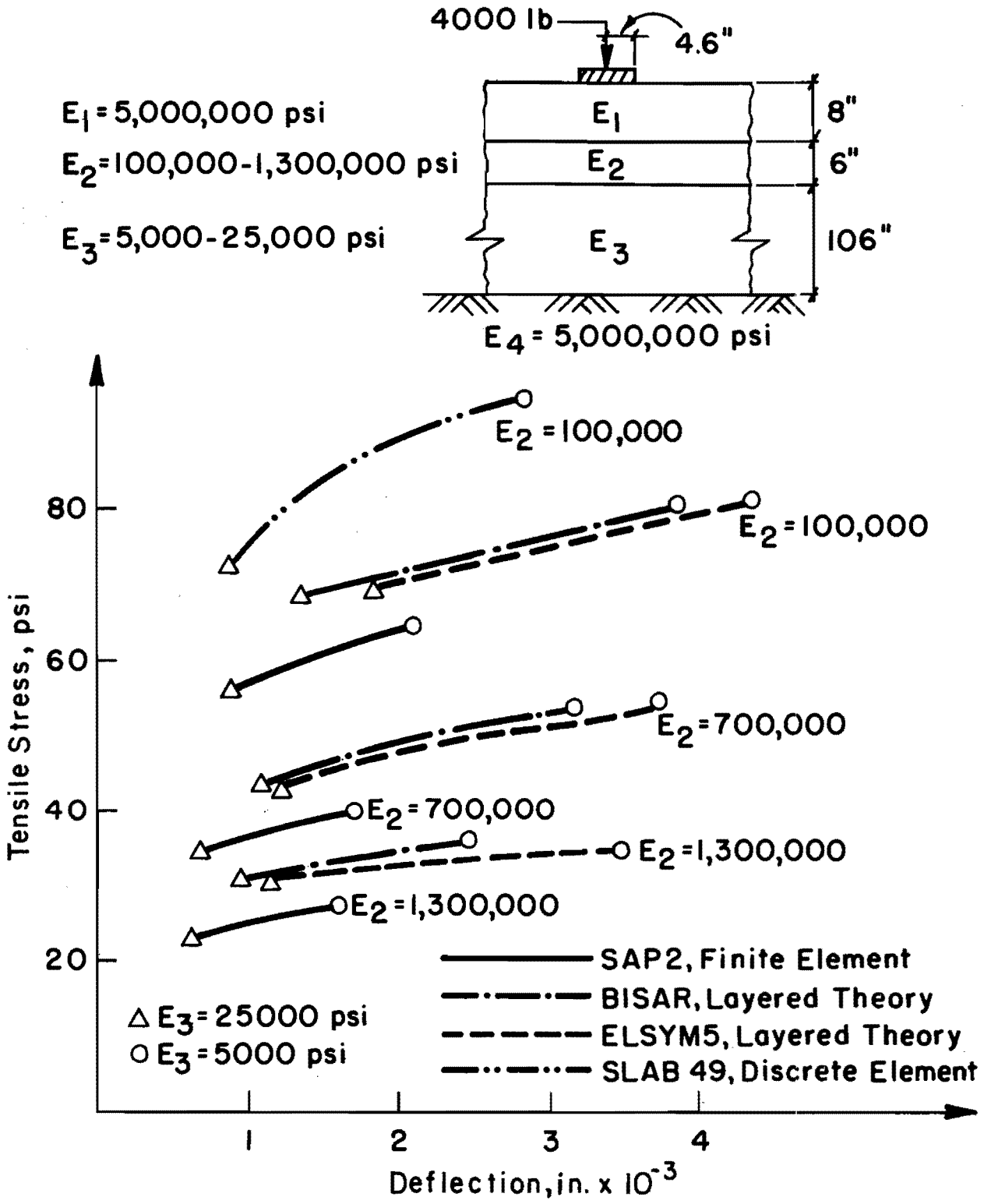

Fig 3.1. Stress as a function of deflection for different analysis techniques.

The SAP2 finite element model can consider a structure consisting of several layers and can, thus, consider an overlay on rigid pavement. Because analysis of the stresses occurring in an overlaid pavement forms part of this report, the SAP2 finite element model was used to analyze cracked pavement structures.

Comparison of Computer Model Predictions

Before making use of different analysis techniques, their relative stress-deformation predictions should be compared. To this end Fig 3.1, has been prepared to compare the relative stress-displacement predictions of the ELSYM5 and BISAR layered theory programs, the SLAB49 discrete element program, and the SAP2 finite element program.

The layered theory and finite element programs use the elastic moduli of the various layers as input. In order to make the elastic moduli used in these programs and the subgrade spring constant, k, used in the SLAB49 program compatible, the structure shown in Fig 3.2 was analyzed using BISAR. The factorial of deformations obtained and the corresponding k values are shown in the figure.

As indicated in Fig 3.1, none of the programs predict the same load-displacement relationships. The two layered theory programs predict the same stresses, but, as indicated in Chapter 2, ELSYM5 does not provide an accurate indication of displacement under the load when a rigid foundation is included in the structure. Although the finite element and layered theory programs do not predict the same stresses or displacements, the relative effect of changes to the subgrade and subbase moduli on these stresses is

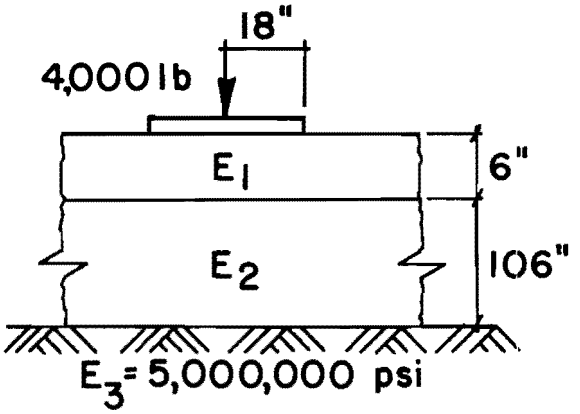

Deflections Calculated From Layered Theory Analysis of the Structure Above, and the Corresponding k Values

		E_1 (psi)			
		100,000	700,000	1,300,000	
E_2 (psi)	5,000	0.0152 259	.00952 413	.00776 506	Deflection (inches) k Value (pci)
	15,000	.00587 669	.00427 920	.00365 1,080	Deflection (inches) k Value (pci)
	25,000	.00373 1,050	.00286 1,370	.00250 1,570	Deflection (inches) k Value (pci)

Fig 3.2. Layered theory analysis (BISAR) to determine k value of a subbase - subgrade structure, for comparison of the stresses predicted in rigid pavements by plate and layered theory.

very similar. On the other hand, the relative effect of these changes on the stresses and displacements predicted by SLAB49 is significantly different.

TYPES OF DISCONTINUITIES ANALYZED

Condition surveys have shown that the most severe and common form of distress in CRC pavements is the punch out. The mechanism of punch out development in CRC pavements is, as of yet, not quite clear. It appears that when the transverse cracks, typical of CRC pavements, are close together, the portion of concrete between two parallel cracks acts as a beam in the transverse direction (Ref 31). The critical stress in the pavement then acts parallel to the cracks, resulting in a longitudinal crack which joins the two transverse cracks. The portion of concrete bounded by the two transverse cracks, the longitudinal crack, and the pavement edge or another longitudinal crack is called a punch out. This is illustrated in Fig 3.3. Following is a discussion of a number of uncertainties regarding this mechanism of punch out occurrence.

(1) Is the longitudinal crack caused by transverse stresses near the bottom of the concrete under the action of an interior wheel load? This situation is illustrated in Fig 3.4. As the load transferred across cracks diminishes, the stress condition at these cracks may approach an edge stress condition with significantly higher stresses than are present for an interior load condition.

(2) Is the longitudinal crack caused by transverse stresses near the surface of the concrete produced by an edge wheel load? This situation is illustrated in Fig 3.5. Although, the majority of

Fig 3.3. Minor and severe punch out in CRC pavement.

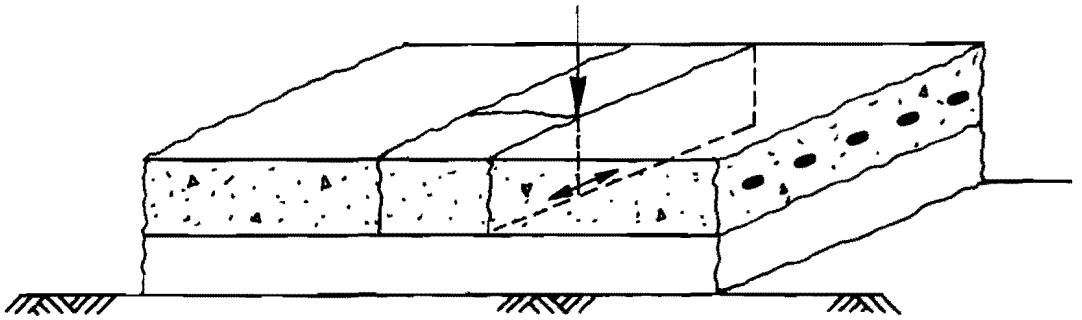

Fig 3.4. Crack caused by an interior load.

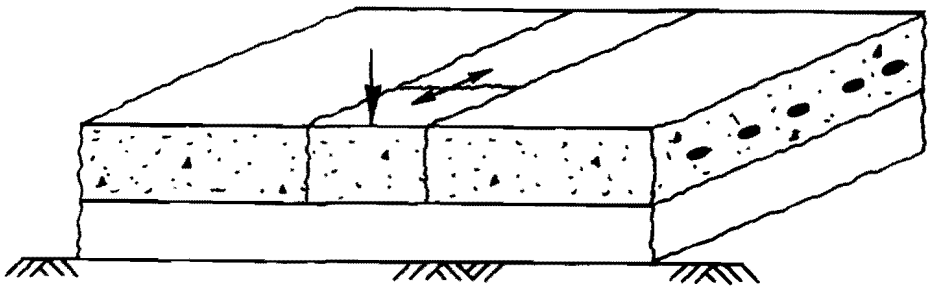

Fig 3.5. Crack caused by an edge load.

wheel loads may pass over the slab at some distance from the shoulder, edge loads result in significantly higher stresses in the slab. These edge loads may also result in high transverse stresses in the surface of the slab due to the cantilever action of the concrete between cracks.

(3) Is the mere occurrence of closely spaced transverse cracks sufficient to cause the occurrence of a punch out, or is significant deterioration of the cracks and loss of load transfer required for a punch out to occur? Static strength of material analyses indicate that cracks create significant reductions to the moment of inertia of a beam, with resulting increased stresses at the cracks. This may also be the case for pavements, which would result in increased stresses near cracks.

Finite element models were used to examine these questions. The results of this analysis, which follow, indicate the stage of crack development at which transverse tensile stresses become the controlling stresses in the pavement and whether significant loss of subgrade support precedes the occurrence of a punch out.

FINITE ELEMENT ANALYSIS

The first step in the analysis procedure was to create finite element structures which are fairly accurate representations of the actual pavement. The eight-node, three-dimensional, "brick" element, which is one of the elements available in the program, was used throughout the analysis.

Using this element, the program has the capability to compute stresses at the element centroid and at any of the six element faces.

In order to ascertain whether the brick element provided accurate results when used across a fairly high stress gradient, the program was used to analyze a simply supported beam. The beam, illustrated in Fig 3.6, consisted of seven elements placed end to end in the horizontal direction and simply supported at each end. The beam was loaded equally at the four center nodes. The stresses and displacements obtained from the finite element analysis coincided almost perfectly with the stresses and displacements obtained from static analysis.

From this analysis, it was concluded that each pavement layer could be represented by a single element in the vertical direction. The brick element will provide accurate results of the stresses in the upper and lower surfaces of the pavement layer in spite of the stress gradient across the depth of the element.

Additional problems were run to determine the effects of the horizontal element generation on the critical tensile stresses in the pavement layers. An interior loading condition on a typical CRC pavement structure was examined in this regard, as shown in Fig 3.7. The results of this analysis are shown in Fig 3.8. This analysis showed that, within the range examined, the size of the element next to the loaded element, relative to the loaded element size, did not have a significant effect on the tensile stresses in the bottom of the loaded element. Computation time can, therefore, be saved by using larger elements adjacent to the loaded element.

The computation time required for finite element analysis increases exponentially with the number of elements in the structure. The most effective way of reducing the number of elements and the computation time is

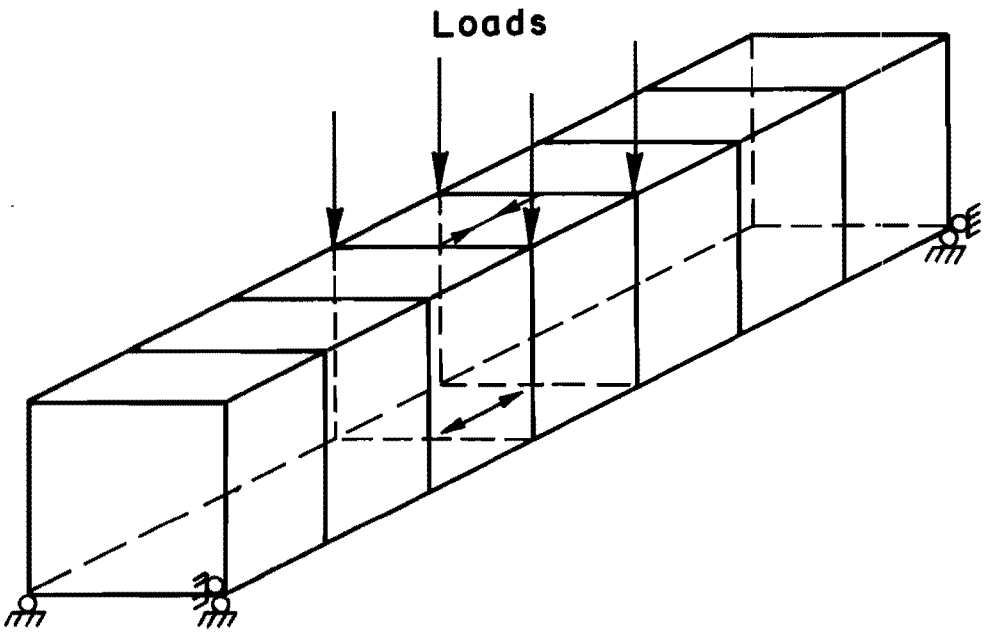

Fig 3.6. Rectangular beam, consisting of seven "brick" elements, used to verify the SAP_2 finite element program for use in pavement design.

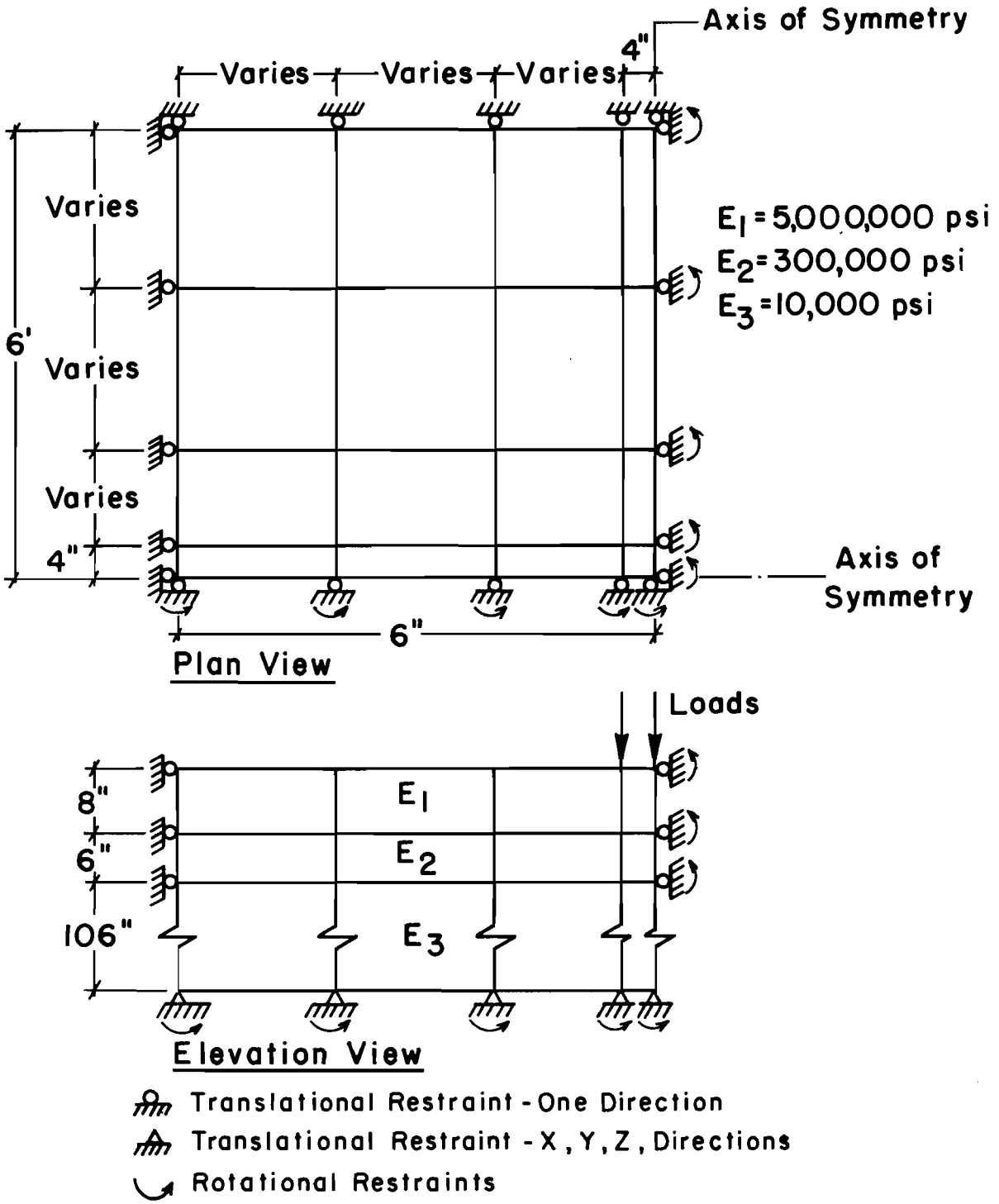

Fig 3.7. Finite element configuration for determining the effect of element mesh generation on the critical tensile stresses at the bottom of rigid pavement layers.

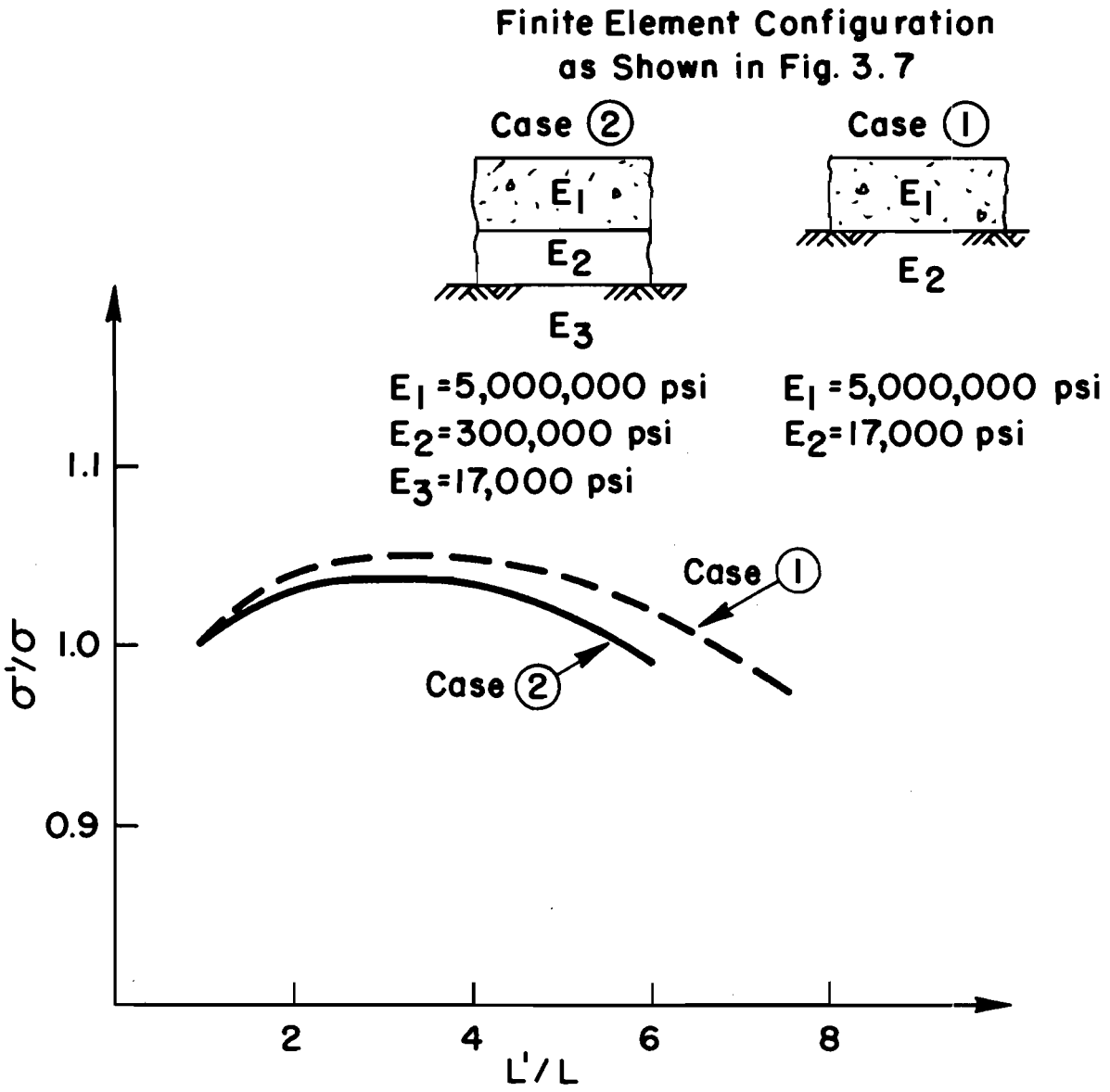

σ' = Tensile Stress in the Bottom of the Loaded Element When Large Elements Surround This Element

σ = Tensile Stress in the Bottom of the Loaded Element When Adjacent Elements are of Similar Size

L' = Length of the Largest Element Adjacent to the Loaded Element

L = Length of the Loaded Element

Fig 3.8. The effect of horizontal element generation on the tensile stresses in the bottom of a concrete pavement layer.

to use symmetry. The element mesh can be split at all axes of symmetry (relative to the load and the element mesh), and rotational and translational constraints can be applied at right angles to the axis to all the nodes along the axis. Thus, wherever possible in the analysis, the finite element mesh representing the pavement structure was split along the axes of symmetry as indicated in Figs 3.7 and 3.9.

Further translational constraints were applied at right angles to all the vertical boundaries. The nodes at the bottom of the structure had rotational and translational constraints in all directions.

ANALYSIS RESULTS

Due to the difference between the stresses predicted using this finite element program relative to stresses obtained from layered theory analysis, the results are presented as stress ratios rather than absolute stress values. The assumption is, therefore, made that, although the stresses obtained from the analysis may not be correct, the relative effect of discontinuities in the pavement on these stresses relative to the uncracked pavement stresses is correct. In order to obtain the actual value of the stresses in the pavement, the stresses obtained from layered theory analysis can be modified in accordance with the results obtained from finite element analysis.

Similarly, the deflections obtained from finite element analysis should be related to those obtained from layered theory and from field measurements. As the load transfer across the crack decreases, the deflection at the crack increases. One definition of load transfer is as follows:

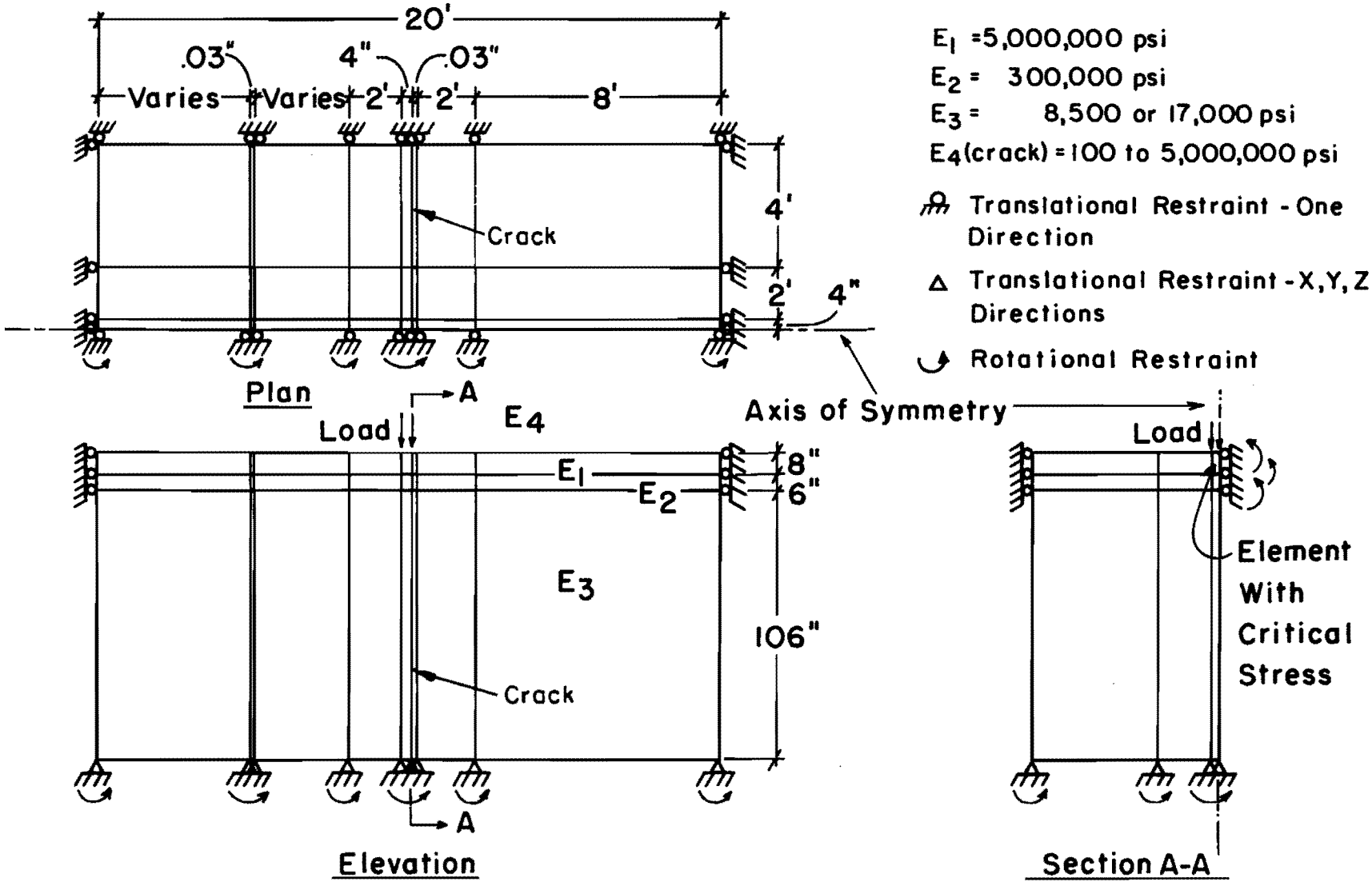

Fig 3.9. Finite element configuration for modeling stresses at the bottom of a cracked concrete pavement layer under an interior loading condition.

$$LT = Wu/Wl \tag{3.1}$$

where

LT = load transfer,

Wu = deflection at the unloaded side of the joint, in.

Wl = deflection at the loaded side of the joint, in. and

$$Wd = Wl - Wu = \text{differential deflection.} \tag{3.2}$$

However, for the purposes of this study, it may be more practical to relate the total deflection at the crack or joint to the interior deflection for an uncracked portion of the pavement. In this manner, field deflections at cracks may be related to interior deflections, and the results of the analysis can be used to determine the stress condition in portions of the pavement with high at-crack deflections. Therefore, decreasing load transfer will be taken into account by analysis of the increased deflections at a crack resulting from a loss of load transfer.

The sensor 1 deflection at the cracks may thus be compared to that between cracks. Furthermore, as indicated previously, because of the relationships between the different deflection parameters and the pavement layer moduli, the effects of changing subgrade modulus may be separated from the effects of reduced load transfer at cracks. For example, if the modal basin slope (representative of surface and subbase moduli) is WMS mils, then any deflection basin slope at a crack significantly exceeding WMS mils may be indicative of a loss of load transfer at the crack. This type of analysis is examined in more detail under the paragraph discussing the analysis results.

Each of the questions raised previously regarding the mechanism of punch out occurrence is addressed separately.

Stresses at Cracks Under an Interior Loading Condition

The structure used in this analysis is shown in Fig 3.9. The effects of changing crack spacing on the tensile stresses in the pavement were analyzed by varying the crack spacing from 1 foot to 10 feet. Changes in load transfer at the cracks were simulated by changing the modulus of the elements representing the crack, e.g., from 5,000,000 psi to 100 psi for the surface layer. The crack width used in the analysis was .03 inch as this was representative of a greater than average crack width as measured in CRC pavements (Ref 35).

The results are indicated in Figs 3.10 and 3.11 for an uncracked and cracked stabilized subbase and in Fig 3.12 for a granular subbase. These results show that initially, for all crack spacings, as the load transfer at the cracks reduces, the tensile stresses in the bottom of the concrete layer also reduce. If the stabilized subbase is not cracked in the same position as the upper concrete layer, then some load is transferred to this layer and the stresses in the concrete layer remain lower than those occurring in an uncracked concrete layer.

However, if the subbase layer has a crack pattern similar to that of the overlying concrete, then the tensile stresses in the concrete layer may increase considerably. For this condition, the maximum tensile stress changes from one acting in the longitudinal direction to one acting in the transverse direction. Depending on the crack spacing, when the surface deflection at the crack exceeds approximately 1.5 times the interior

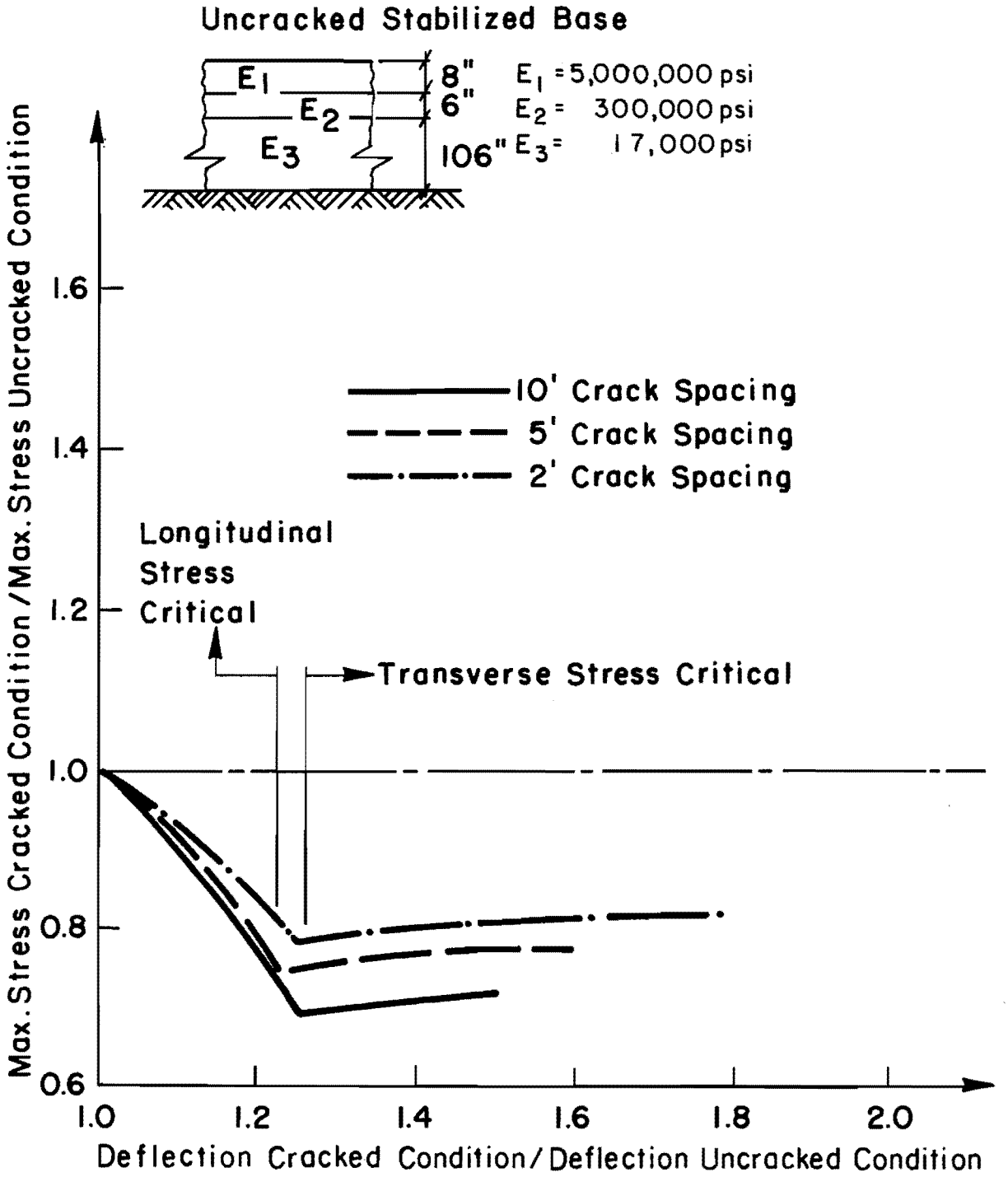

Fig 3.10. The effect of load transfer and crack spacing on the critical tensile stresses in rigid pavement for an interior loading condition. (Subgrade modulus = 17,000 psi)

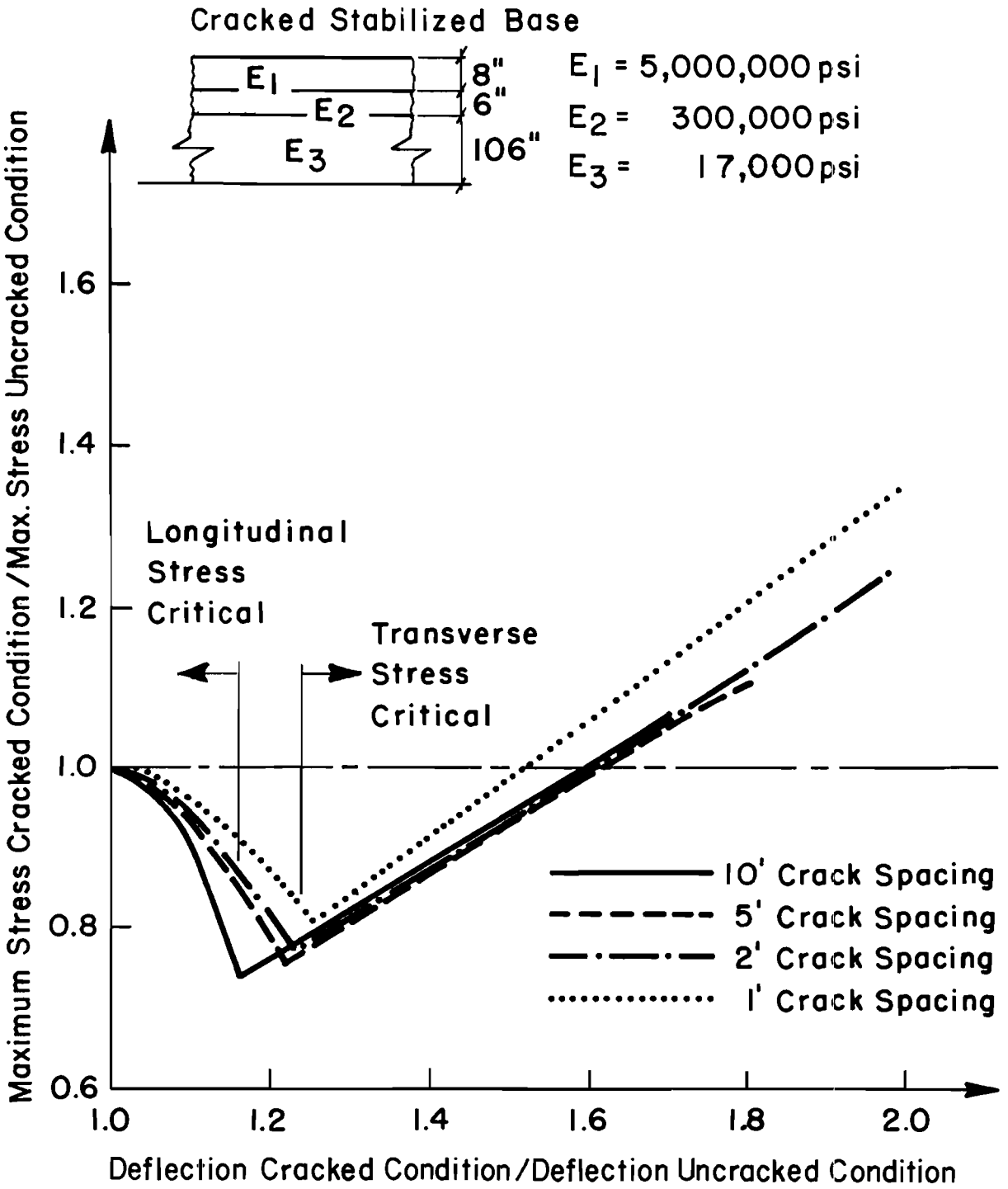

Fig 3.11. The effect of load transfer and crack spacing on the critical tensile stresses in rigid pavement for an interior loading condition. (Subgrade modulus = 17,000 psi)

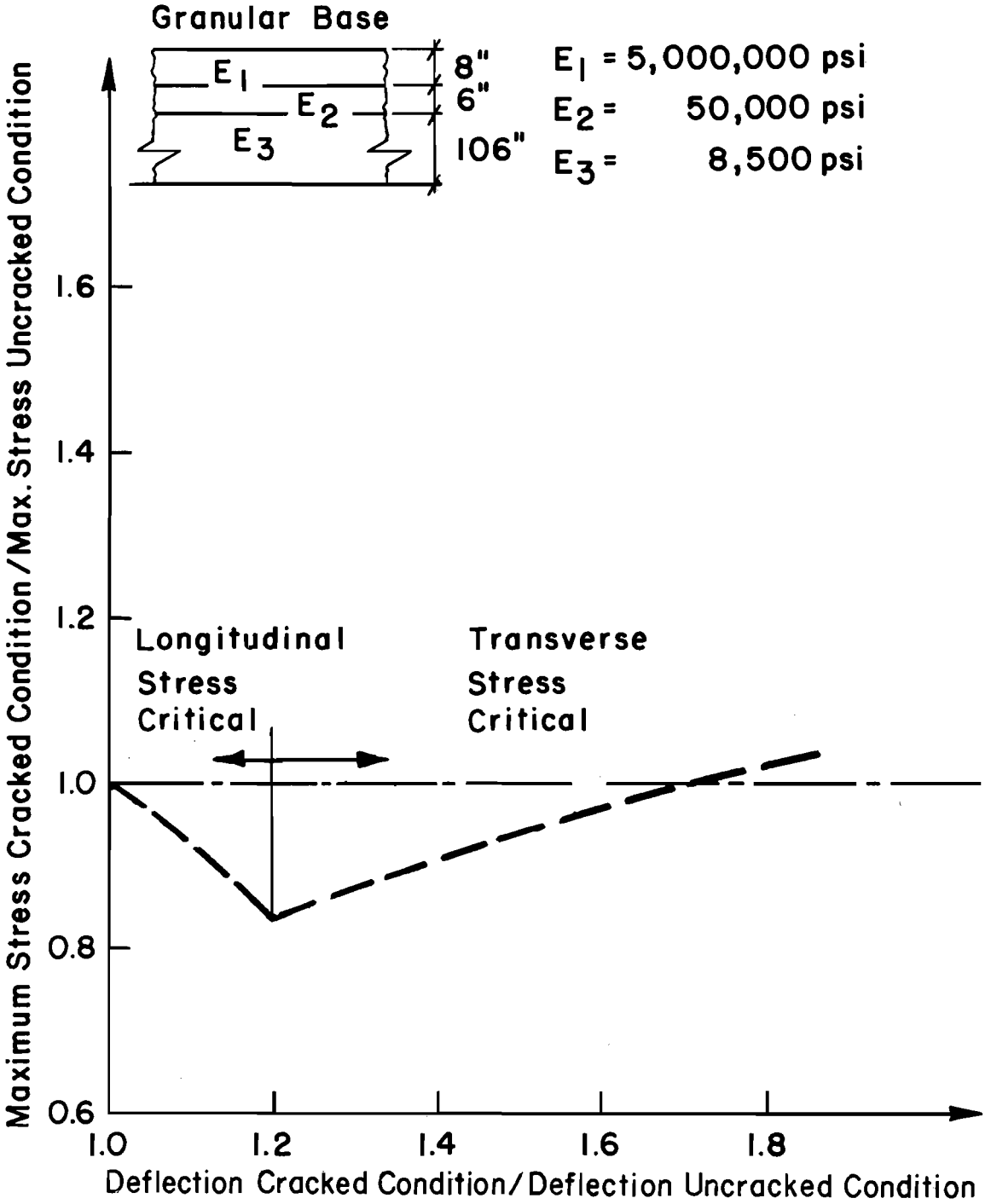

Fig 3.12. The effect of load transfer and crack spacing on the critical tensile stresses in rigid pavement for an interior loading condition. (Subgrade modulus = 8,500 psi)

deflection of an uncracked pavement, the tensile stresses acting parallel to the crack may begin to exceed the tensile stresses in the uncracked pavement. These results also indicate that, as the crack spacing reduces to less than 2 feet, the stresses near the cracks increase more rapidly with loss of load transfer relative to the increase for larger crack spacings.

Stresses Between Closely Spaced Transverse Cracks for an Edge Loading Condition

This type of loading condition has been analyzed using finite element techniques, by La Coursiere, Darter and Smiley (Ref 33). This reference indicates that the portion of concrete between the transverse cracks acts as a cantilever with resulting tensile stresses in the surface of the concrete. The transverse surface tensile stresses in this reference exceed edge stresses calculated using influence charts when the crack spacing is less than one foot and when no load transfer exists across the cracks. This maximum tensile stress occurs approximately 3 feet from the pavement edge. Furthermore, erosion of the subgrade support was shown to cause further significant increases in these stresses. The stress-deflection relationship of such a loading condition was examined using the SAP2 finite element program.

The finite element configuration used in the analysis is indicated in Fig 3.13. The axis of symmetry splits the concrete segment between two transverse cracks. Material properties similar to those used in the previous analysis are used again in this analysis.

The results of this analysis are shown in Figs 3.14 and 3.15 for two different crack spacings and subgrade moduli. The results indicate that, for

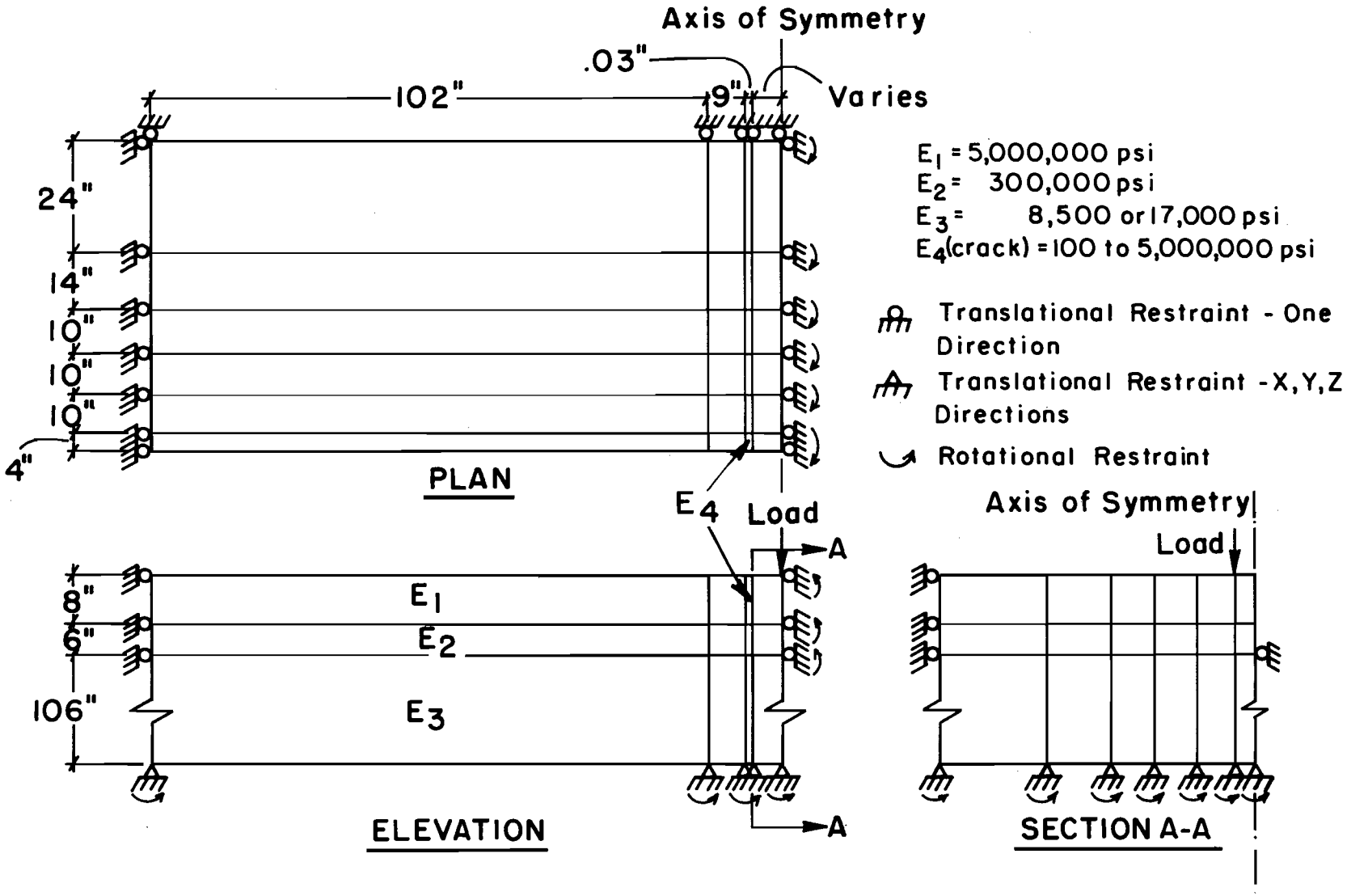

Fig 3.13. Finite element configuration to determine the effect of edge loads on the stresses in a cracked pavement layer.

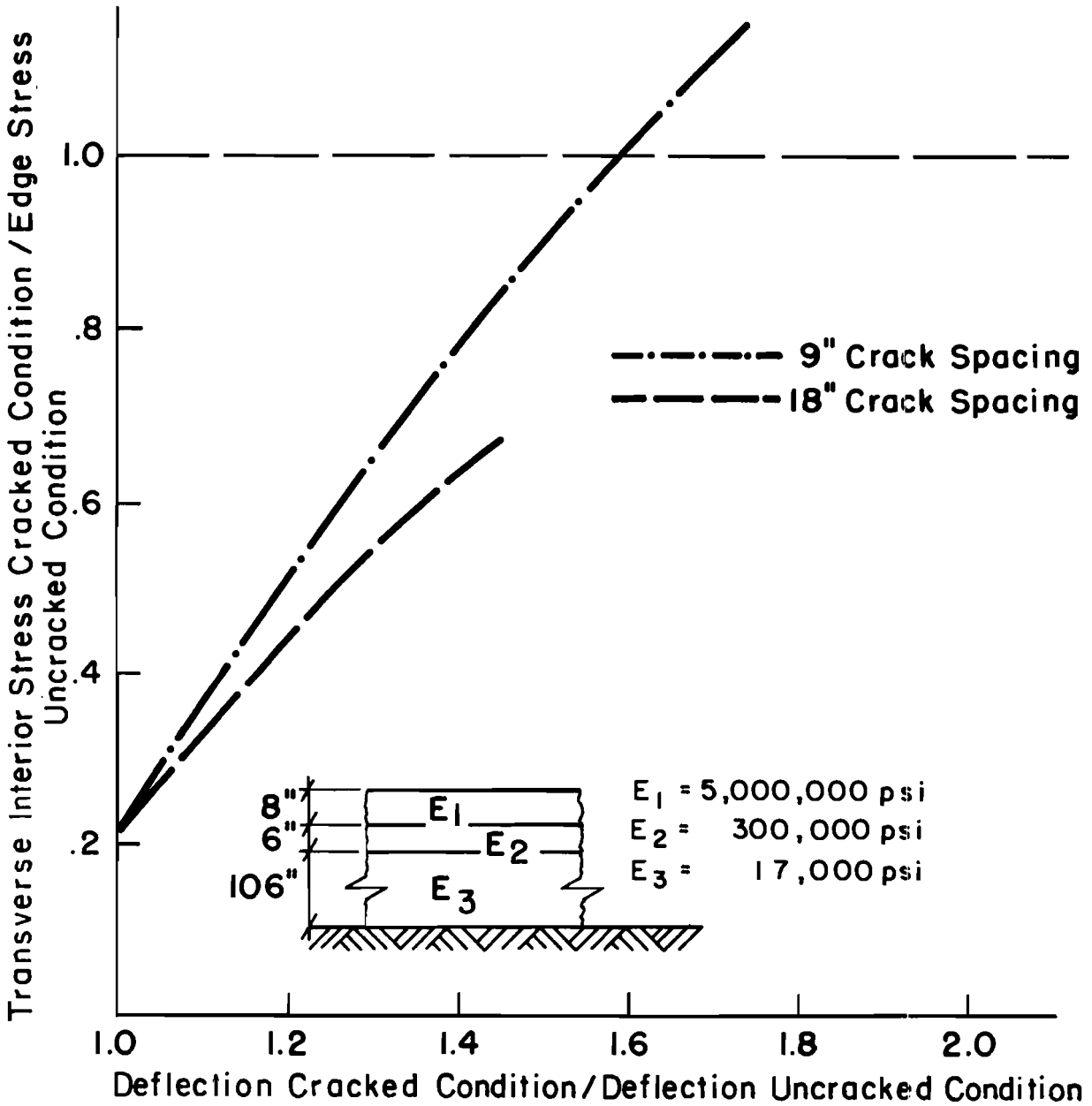

Fig 3.14. The effect of load transfer and crack spacing on the critical tensile stresses in rigid pavement for an edge loading condition (Subgrade modulus = 17,000 psi).

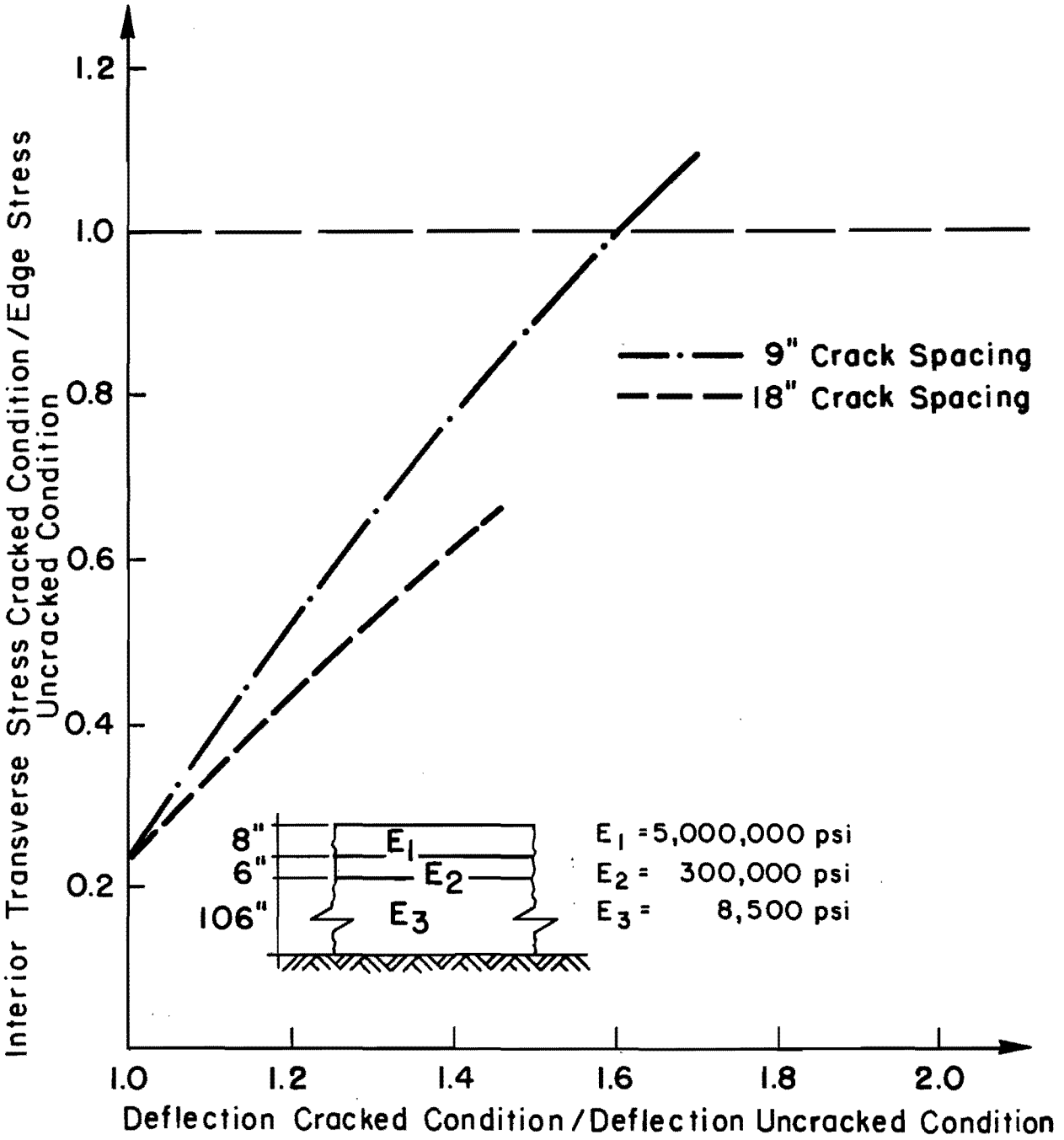

Fig 3.15. The effect of load transfer and crack spacing on the critical tensile stresses in rigid pavement for an edge loading condition (Subgrade modulus = 8,500 psi).

a 9-inch crack spacing, the deflection at the edge should exceed approximately 1.6 times the uncracked edge deflection for the interior transverse stress to exceed the uncracked edge stress. Crack spacing has a significant influence on the stress-deflection relationship for this loading configuration. This is to be expected when considering the cantilever-type structure of the portion of concrete between the two parallel transverse cracks.

Influence of Loss of Subgrade Support on Stresses

As indicated in the previous two paragraphs, the deflections at cracks must be significantly greater than the deflections at midspan before the transverse stresses, which cause punch outs, exceed longitudinal stresses. In the finite element model, the modulus of the elements representing the cracks had to be reduced to approximately 100 psi to obtain these deflections. In CRC pavements the cracks are normally fairly tight and at-crack and midspan deflections seldom differ significantly. This is shown in Fig. 3.16 and 3.17, where plots of at-crack and adjacent midspan Dynaflect sensor 1 deflections are presented for in-service pavements.

It may, therefore, be hypothesized that some loss of subgrade support is required for significant differential movements at the cracks to occur. These movements will, in time, abrade the concrete at the cracks and reduce the load transfer. The reduced load transfer will result in higher deflections and finally a punch out.

The analysis may, therefore, indicate that the mere occurrance of closely spaced cracks in a pavement is insufficient to cause punch out development. However, should some loss of subgrade support occur, punch outs

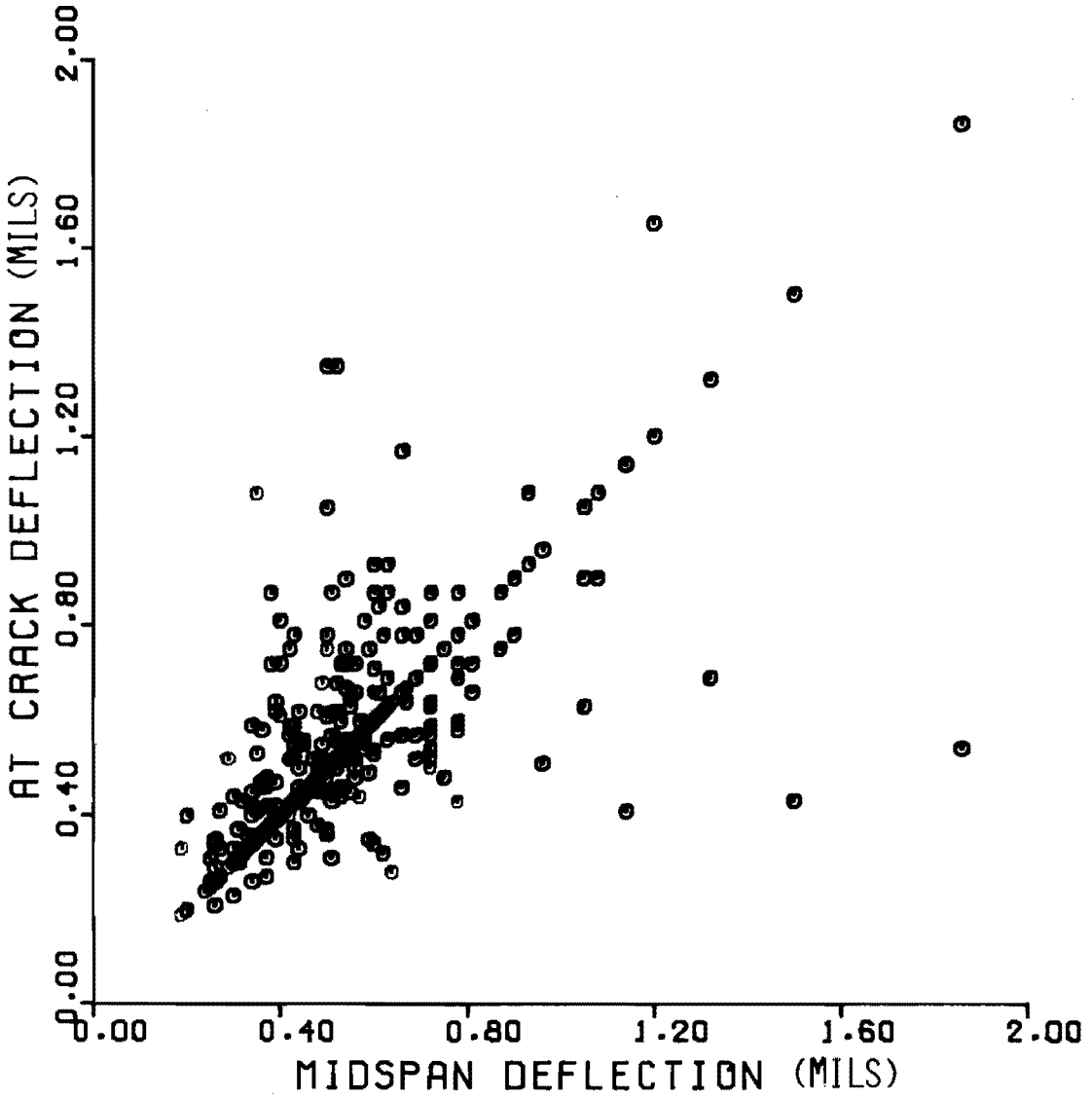

Fig 3.16. Comparison of at-crack and midspan Dynaflect deflections along IH-10, District 17, Texas.

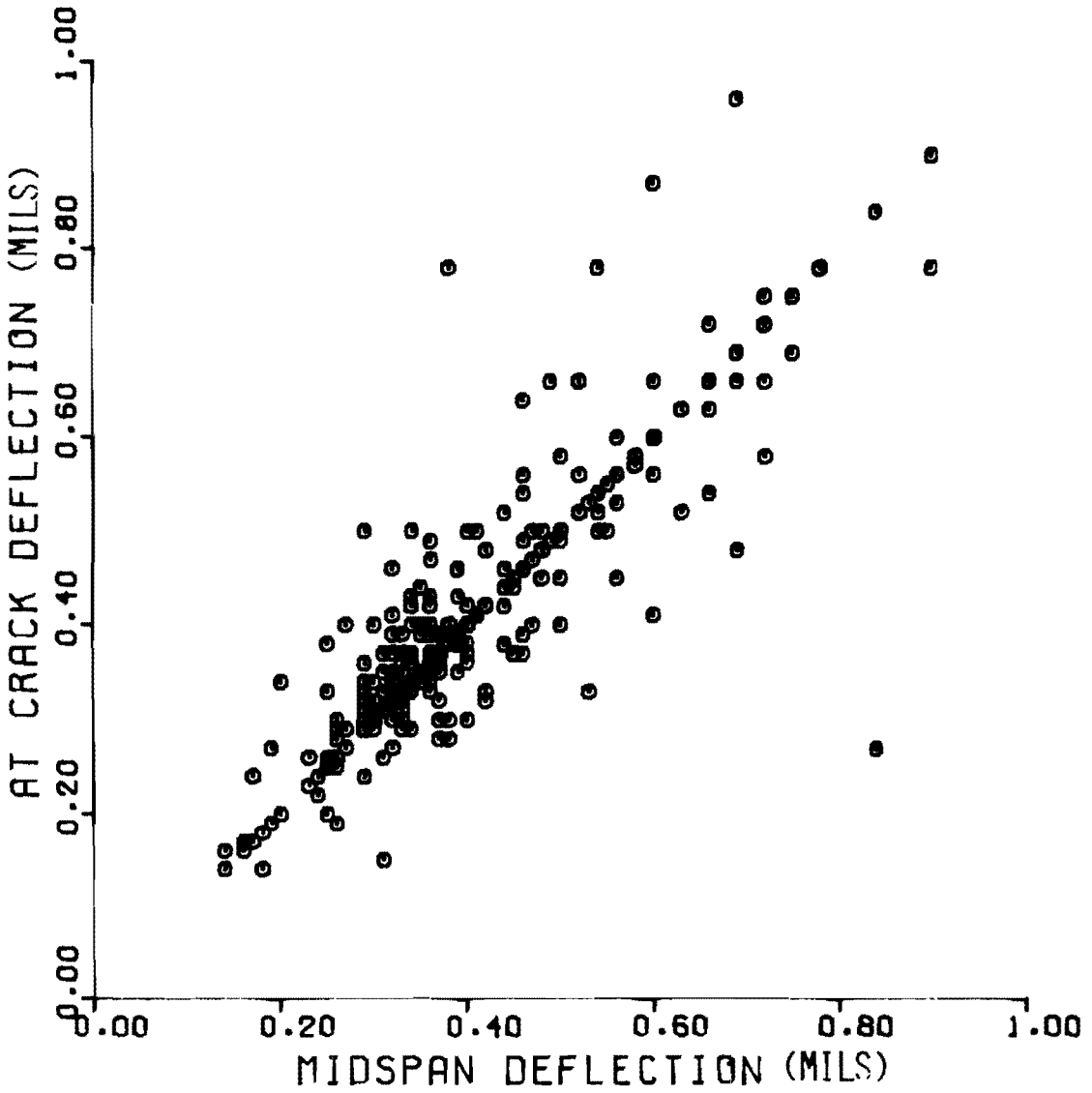

Fig 3.17. Comparison of at-crack and midspan Dynaflect deflections along IH-10, District 13, Texas.

are more likely to form in areas with small crack spacings than in areas with large crack spacings.

DISCUSSION OF RESULTS

Any increase in tensile stress in the design pavement layer should be accounted for in design procedures. As indicated in this chapter, cracks in a pavement layer initially result in a decrease of the tensile stresses in that layer. The excess stresses are then redistributed among the lower layers. A similar stress redistribution between the subbase and subgrade may occur upon cracking of a stablilized subbase layer.

Therefore, in the early stages of a pavement's life, the critical stresses occur in the uncracked portions of the pavement. For both interior and edge loading conditions these stresses occur immediately under the wheel load in a longitudinal direction.

However, once the concrete pavement layer and subbase layer have cracked and the load transfer has been reduced considerably, the critical stresses shift to the transverse direction. For an interior load these stresses occur immediately below the load, whereas, for an edge loading condition, the cantilever effect causes these stresses to be located at some distance from the load.

For both the interior and edge loading conditions, the transverse stresses in the cracked pavement exceed the longitudinal stresses for the uncracked pavement condition when the deflections under the load exceed roughly 1.5 times the deflection for the uncracked condition. These findings

findings need to be examined in the light of condition survey and deflection data obtained from CRC pavements in Texas.

Condition Survey Data

Most punch outs which occur in practice are approximately one foot long. For example, in the 1974 condition survey of CRC pavements along IH-20 and IH-30 in District 19, 38 severe punch outs were counted, of which 28 were in the 1 to 4 foot long category. This may indicate that higher stresses occur in areas with close spaced cracks, which is corroborated by this analysis.

Furthermore, in some localized areas, very small crack spacings (6 inches) exist without the occurrence of punch outs. This is consistent with the hypothesis that the prime causative factor for punch outs involves loss of load transfer and/or subgrade support and not simply crack spacing.

Deflection Data

As indicated in Table A3, not many sensor 1 deflections exceed the modal sensor 1 deflections by more than 50 percent within a section. The coefficient of variation of the sensor 1 deflections for the majority of sections in the table is around 30 percent. A significant amount of this variation may be caused by variation in the subgrade.

These results may also be compared to a deflection study of punch outs, patches, and pumping which was conducted in District 9. For the section studied, the modal Dynaflect sensor 5 deflection was 0.25 mil and the modal basin slope (sensor 1 - sensor 5) was 0.18 mil. The average basin slope for all the deflections taken at minor punch outs was 0.45 mil. Therefore, in

order to eliminate the effects of differing subgrade support on the sensor 1 deflection, this punch out deflection should be written as

$$0.25 + 0.45 = 0.70 \text{ mil},$$

and the modal sensor 1 deflection for the sections is equal to

$$0.25 + 0.18 = 0.43 \text{ mil}.$$

The increased deflection at the punch out, due only to the effect of the cracks surrounding the punch out, is, therefore,

$$0.7/0.43 = 1.63 \text{ times the modal sensor 1 deflections for the section.}$$

Admittedly, the longitudinal crack forming a part of the punch out may have a significant effect on the deflection, but this serves to illustrate a method for calculating a deflection value above which punch outs may readily occur, that is,

$$\text{if} \quad M5 + S > 1.5^{*}(M5 + MS)$$

$$\text{or} \quad S > 0.5^{*}M5 + 1.5^{*}MS$$

where

MS = modal basin slope (W1-W5) for the section,

S = critical basin slope, and

M5 = modal sensor 5 deflection for the section.

This is illustrated further in the frequency diagram presented in Fig 2.17. This diagram, produced by the MODE program, shows the at-joint, sensor 1 - sensor 5 deflections for a section of IH-30 near Greenville, Texas. The pavement is a 10-inch concrete pavement with joints every 15 feet. From the diagram, it is apparent that 20 percent of the joints have a deflection basin slope greater than the critical slope as calculated above. Therefore, longitudinal cracks or corner breaks can be expected as one of the first signs of distress at these points.

SUMMARY

The finite element analysis of concrete pavements indicates that the stresses as calculated by layered theory need only be modified to account for the stresses resulting from an edge loading condition. Cracks in CRC pavements result in an initial reduction of stresses in the concrete layer and a redistribution of these stresses among the lower layers. The highest stresses in the pavement layers will occur under an edge load.

Softening of the lower layers near the edge due to moisture ingress may result in some differential vertical movement of the concrete layer at the cracks. This will result in abrasion of the vertical concrete at the crack faces, with a corresponding reduction in load transfer at the cracks. Once the load transfer has been reduced to such an extent that the deflections at

the cracks exceed the uncracked pavement deflections by more than 50 percent, punch outs may occur in areas with crack spacings of approximately one foot.

From a construction point of view, this analysis may lend support to the use of PCC shoulders with PCC pavements. These shoulders will not only reduce high edge stresses but may also reduce the probability of moisture ingress at the shoulders. Asphalt concrete shoulders often rut adjacent to the PCC pavement to form a hollow in which water can pond, and it is also difficult to keep the longitudinal joint between the asphalt shoulder and the pavement sealed.

CHAPTER 4. STRESSES WHICH CAUSE REFLECTION CRACKING IN OVERLAYS ON CONCRETE PAVEMENTS

The stress condition in an overlaid concrete pavement is complex and the critical stresses with regard to failure of the overlaid pavement need to be determined. These critical stresses may either be tensile stresses in the existing pavement, tensile stresses in the overlay, or stresses causing reflection of cracks in the old pavement. Reflection of underlying cracks in the overlay may be caused by either horizontal movements or differential vertical movements of the underlying pavement. In the latter case, the stresses are a complex combination of compressive, tensile, and shear stresses. In this chapter, reflection cracking, specifically in asphalt overlays, due to vertical differential movements will be examined using finite element techniques.

Continuously reinforced concrete pavement has numerous closely spaced cracks. The dimensions of these narrow cracks, unlike the joints in jointed concrete pavements, do not change significantly due to changing temperatures. Furthermore, reflection cracking caused by horizontal temperature movements in overlays of jointed concrete pavements may be controlled effectively by bond breakers and cushion courses (Ref 3). For these reasons, only reflection cracking due to differential vertical movements will be examined in this chapter. Fatigue cracking of concrete overlays, which may not be related to reflection cracking, will be examined in a later chapter.

CONDITION SURVEY RESULTS

Condition surveys of overlaid concrete pavements have shown that reflection cracking is a serious problem (Refs 36,and 37). Reflection cracking due to differential vertical movements may not be controlled effectively by bond breakers or cushion courses. In CRC pavements, the first types of underlying distress to reflect through the overlay are punch outs and patches in the original pavement.

This is reflected in Table 4.1 where results obtained in Ref 37 are presented. In this reference, a study of the distress in an overlaid section of IH-45 was conducted. Because the original pavement was constructed as an experimental pavement, detailed condition surveys of distress were conducted throughout its life (Ref 38). Thus the pavement was an ideal study project. In this study, distress manifestations in the original pavement were sketched on a large scale-plan. Subsequent to overlaying, further distress in the overlay was sketched on the same plan.

During the more recent condition surveys, the locations of the various distress manifestations were determined by equipping the survey vehicle with an electronic distance measuring instrument. This instrument was calibrated to measure distances, repeatably, to within 5 feet per mile. Prior to the overlaying, the distance measuring instrument was not available, and thus the position of the underlying distress could not be determined as accurately as indicated above. However, when the resulting plan was studied it became apparent that some cracks in the overlay could be related to underlying distress because of the shape and size of these distress manifestations. The locations of the pre-overlay distress could, thus, be adjusted on the plan.

TABLE 4.1. PERCENTAGE OF UNDERLYING DEFECTS IN CRCP WHICH HAVE REFLECTED THROUGH THE EXISTING ASPHALT OVERLAY - IH-45, WALKER COUNTY, TEXAS.

Lane	Overlay Thickness (inches)	Percent Reflected Defects
SB	2.5	95
SB	4.0	71
SB	6.0	54*
NB	2.5	64
NB	5.0	21
NB	6.0	2

* This section had several unrepaired punchouts in the CRC pavement.

Traffic since overlay - 5 x 10^6 18-kip ESAL'S

In this manner the distress in the overlay could be related to distress in the underlying pavement with reasonable accuracy.

The results of this study indicate that reflection cracking due to differential vertical movement in the underlying pavement is a problem in overlaid CRC pavements. The high degree of reflection cracking in the case of a 6 inch overlay was probably due to the severe nature of the underlying distress. In this area, the severe punch-outs were not patched prior to overlaying and virtually all of them reflected through the overlay.

In an attempt to provide mechanistic design information regarding the occurrence of reflection cracks, this type of distress was examined using the SAP2 finite element program.

FINITE ELEMENT MODEL

A section of the pavement including a portion of the subgrade was modelled with finite elements as shown in Fig 4.1. The finite element configuration used to represent the overlaid cracked pavement is shown in Fig 4.2. This configuration is the result of numerous trial computations, which were made to determine the most realistic configuration requiring the least amount of computer time.

Because condition surveys showed that the first signs of reflection cracks occurred along the edge of the pavement, an edge loading condition was examined. In the analysis the crack width in the original pavement was changed from 0.04 inch to 0.24 inch, which was considered to be representative of a crack surrounding a minor punch out to a severe punch

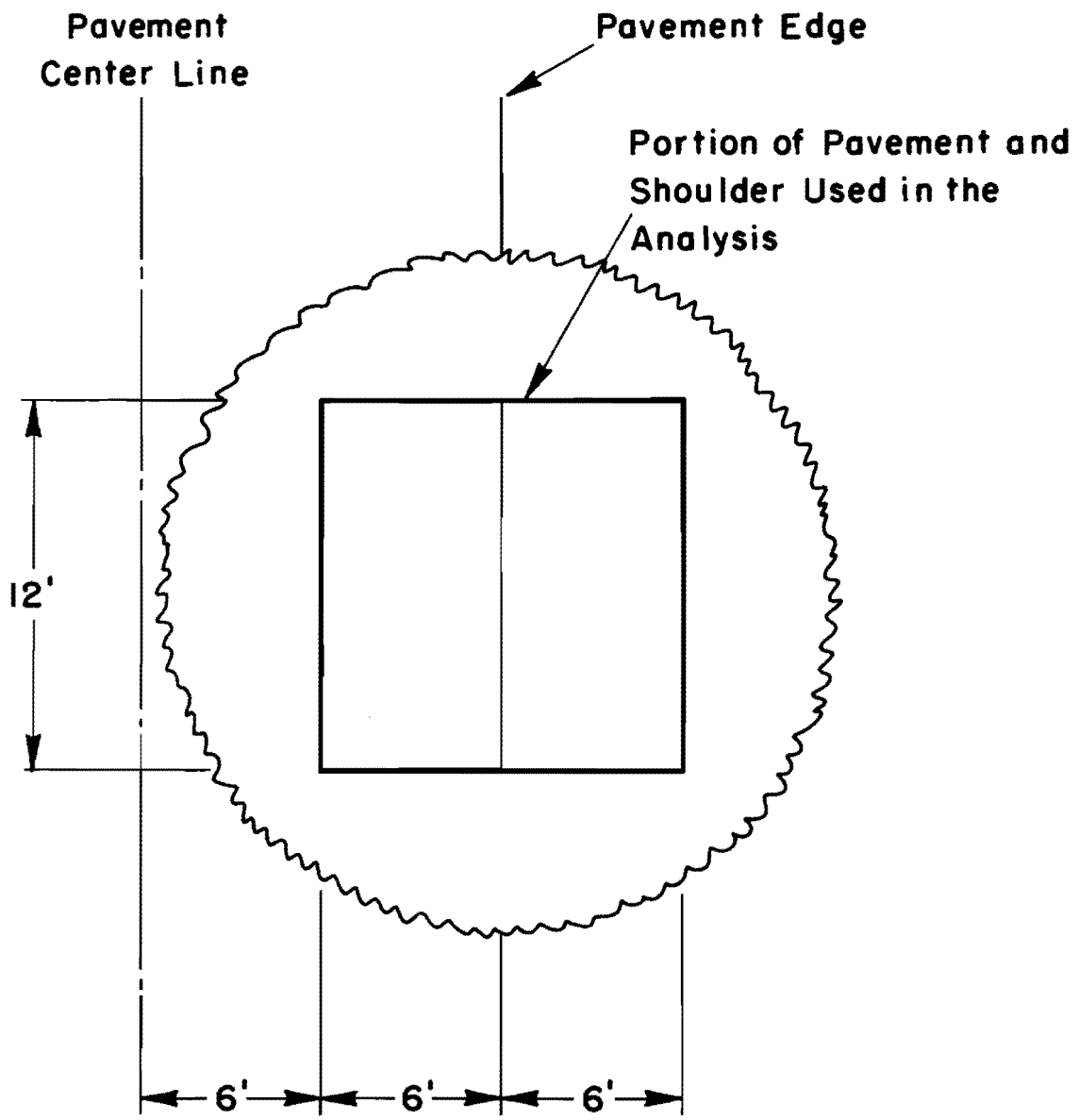

Fig 4.1. Portion of the pavement and shoulder used in the analysis.

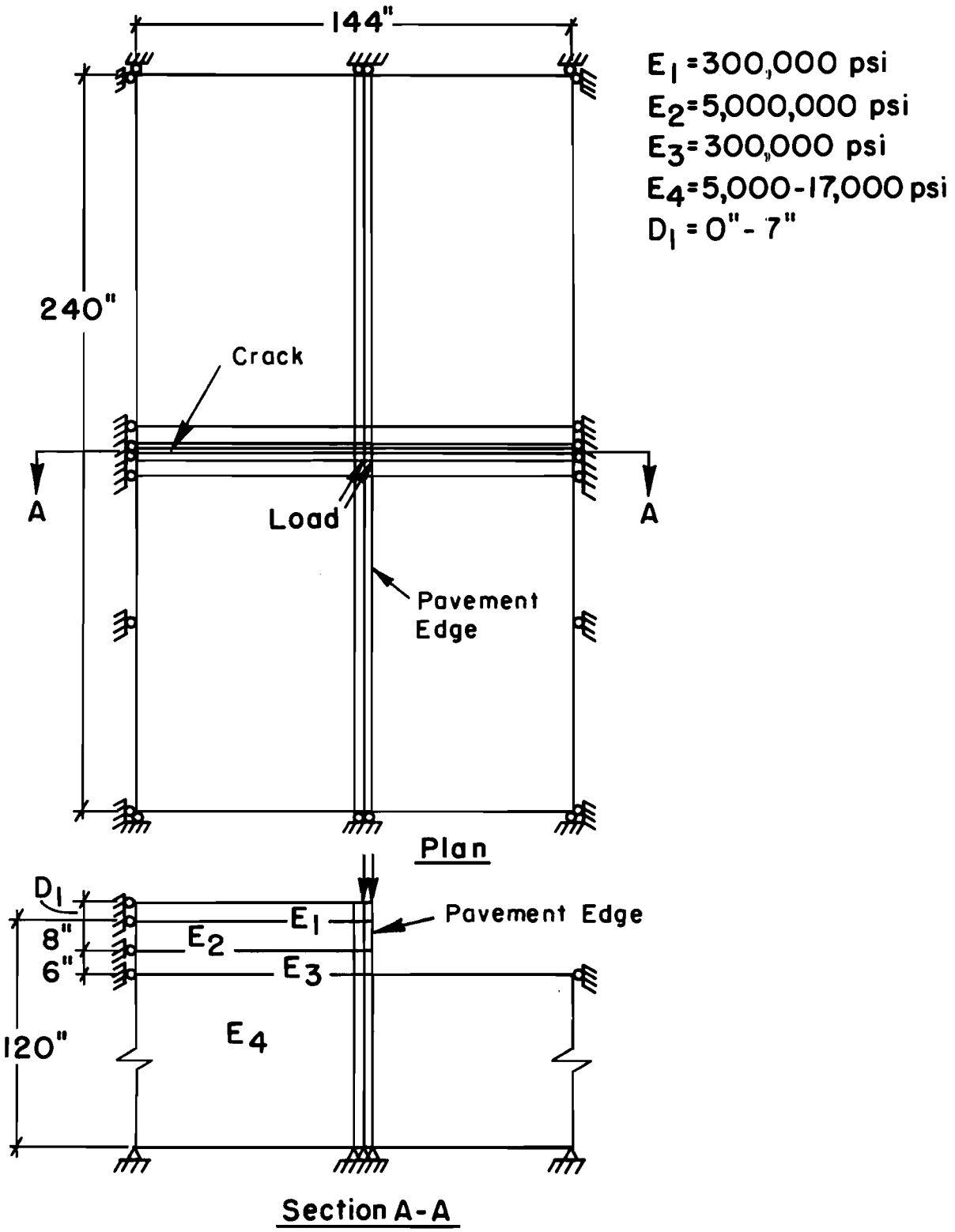

Fig 4.2. Finite element configuration for computing reflection stresses in an asphalt overlay on rigid pavement.

out. The modulus of the elements representing the crack was varied from 1 psi to 10,000 psi.

In order to relate the stresses obtained in the overlay to before-overlay deflection measurements, the deflections of the non-overlaid pavements were calculated for the same levels of load transfer as were later used in the overlay study. This was done using the finite element configuration shown in Fig 4.2. The modulus of the elements forming the crack in the concrete pavement was varied and the ratio of the edge deflection with a "soft" crack relative to the edge deflection of the uncracked pavement was noted. These results appear in Table 4.2 for changing crack width and modulus, and subgrade modulus.

RESULTS FO FINITE ELEMENT ANALYSIS

The analysis showed that the most critical stresses in the overlay are the shear stresses immediately above the cracks in the underlying pavement, and the tensile stresses in the surface of the overlay. These stresses are plotted for a specific load transfer against overlay thickness in Fig 4.3. The tensile stresses in the surface of the overlay are plotted against the degree of relative deflection at the non-overlaid crack in Fig 4.4.

These results show that, high tensile stresses may exist in the overlay surface. Furthermore, very little loss of load transfer at cracks is required for these high stresses to occur. Results from indirect tensile tests of inservice asphalt-treated materials (Ref 46) show that the static tensile strength of asphalt concrete may be about 100 psi. Figure 4.3 shows that the tensile stresses resulting from finite element analysis may exceed

TABLE 4.2a. RESULTS FROM FINITE ELEMENT ANALYSIS OF DEFLECTIONS AT CRACKS BEFORE OVERLAYING

Crack Width (inch)	E_4 (10^3 psi)	E_5 (crack) (psi)	W_1 (10^{-3} inch)	W_2 (10^{-3} inch)
0.04	17	5,000,000	2.9	2.5
		10,000	3.5	2.6
		100	5.3	2.4
0.04	5	5,000,000	5.6	5.0
		100,000	5.7	5.1
		10,000	6.4	5.4
		100	9.7	5.7
		10	9.9	5.7
0.24	5	10,000	7.8	5.8
		100	10.1	5.6

Finite element configuration indicated in Fig 4.2 without overlay layer

Load = 4000 lb

D_1 = 0.0

E_2 = 5,000,000 psi

E_3 = 300,000 psi

E_4, E_5 = As shown

W_1 = deflection under the load next to the crack

W_2 = deflection at the opposite side of the crack

TABLE 4.2b. RESULTS FROM FINITE ELEMENT ANALYSIS OF OVERLAYED PAVEMENTS

Crack Width (inch)	E_4 (10^3 psi)	E_5 (crack) (psi)	D_1 (inches)	σ (psi)	τ (psi)
0.04	17	10,000	1	283	220
		100	1	330	225
		100	4	93	90
		100	7	42	40
0.04	5	5,000,000	1	45	2
		100,000	1	135	100
		10,000	1	360	255
		100	1	392	270
		10	1	389	265
		10,000	4	116	105
		100	3	150	135
		1,000	7	55	50
		100	7	42	35
0.24	5	100	1	220	150
		100	4	68	65
		100	7	40	30

Finite element configuration indicated in Fig 4.2.

Load = 4,000 lb

D_1 - As shown

E_1 - 300,000 psi

E_2 - 5,000,000 psi

E_3 - 300,000 psi

E_4, E_5 - As shown

σ = tensile stress in the surface of the overaly above underlying cracks

τ = shear stress in the bottom of the overlay above underlying cracks

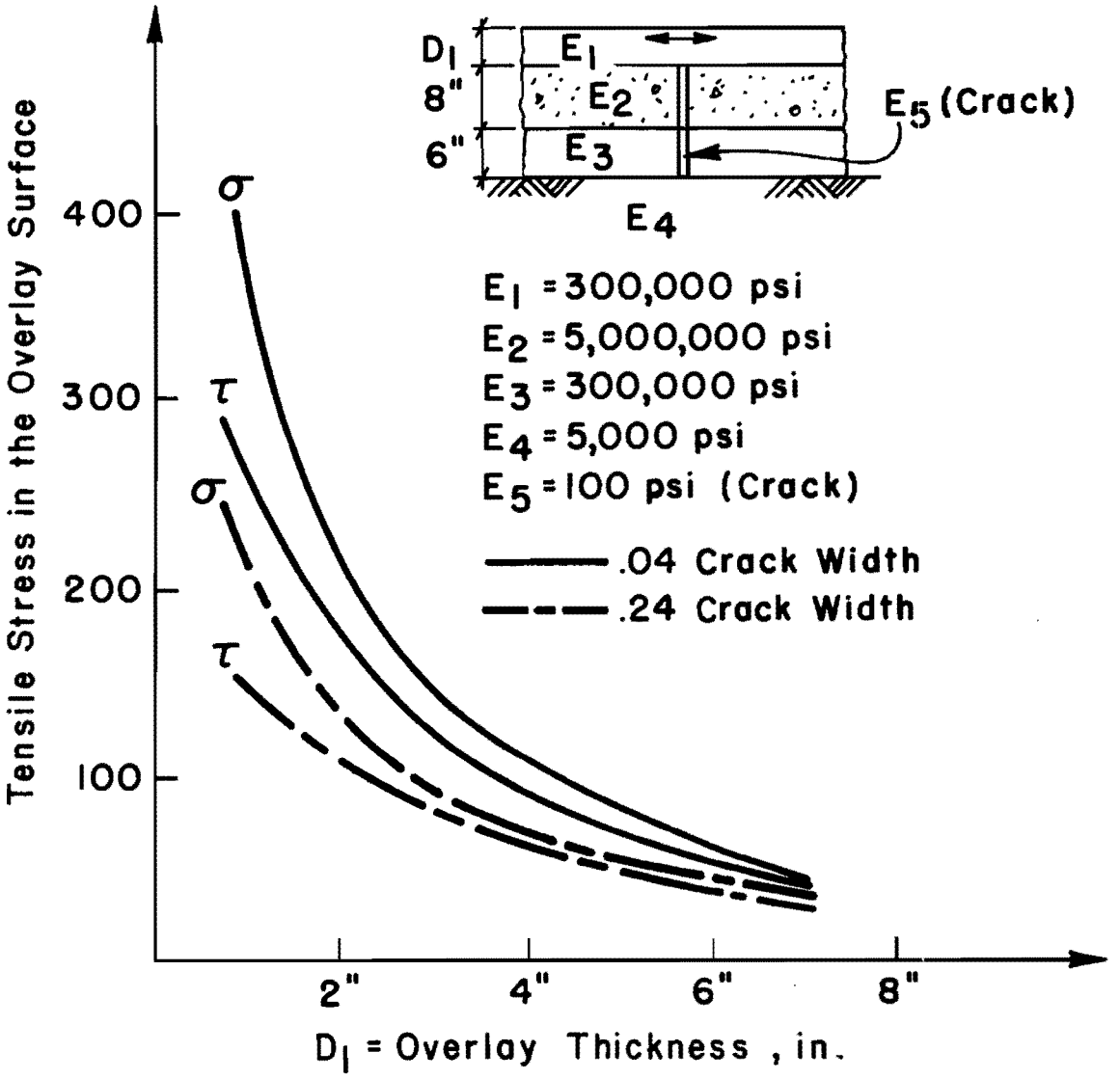

Fig 4.3. The effect of crack width and overlay thickness on the shear and tensile stresses in an asphalt overlay on a cracked rigid pavement.

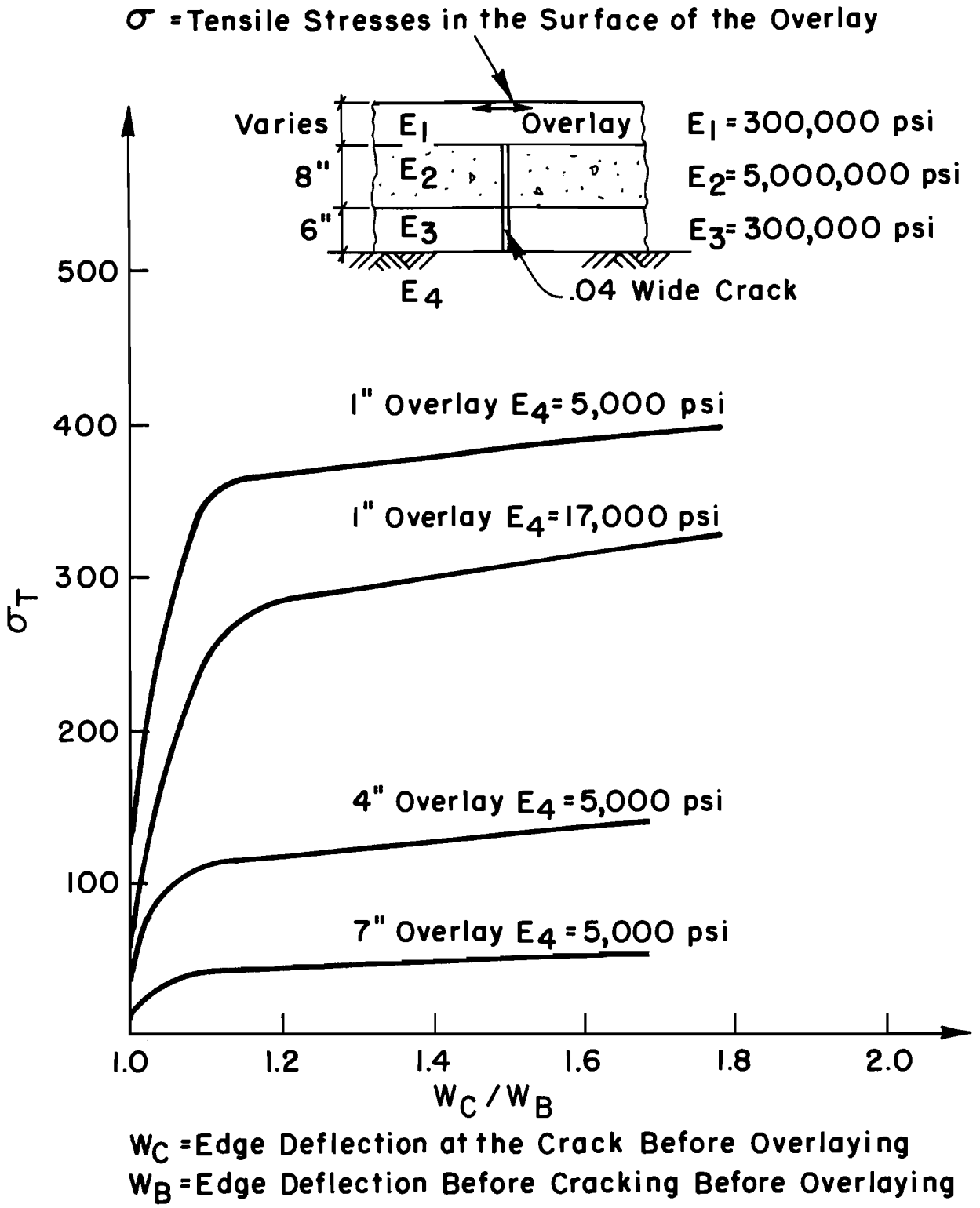

Fig 4.4. The effect of load transfer on the tensile stresses in the upper surface of an asphalt overlay on rigid pavement.

the static tensile strength of asphalt for overlays less than 4 inches thick. Furthermore, the results indicate that within the range of crack widths and degrees of load transfer analyzed, these tensile and shear stresses decrease with increasing crack widths.

Condition surveys show that reflection cracking is a severe problem in overlaid jointed concrete pavements. The results of the finite element analysis , however, seem to indicate that the tensile and shear stresses decrease with increasing crack width. This apparent contradiction may occur because no loss of subgrade support was considered in the analysis. Erosion of subbase and subgrade material in the vicinity of pavement joints may result in extremely high differential deflection at the joint, resulting in reflection cracks in the overlay. The condition survey results shown in Table 4.1 do not indicate an extremely high degree of reflection cracking in areas with a 2.5-inch-thick overlay. On-site investigation of the existing reflection cracks showed that most were small and, at this stage, insignificant. It can therefore be concluded that

(1) The analysis results may not be very realistic. A significant modelling error may be that the finite element model cannot represent any movement at the overlay and PCC interface. Laboratory model testing along the lines of that performed in Ref 34 may be required to obtain more information in this regard.

(2) The underlying CRC pavement provides a firm base, which assists in the self healing process of the asphalt concrete. During hot, summer days, the asphalt softens and is subjected to compressive stresses between the wheel load and the concrete, resulting in the apparent healing of the cracks.

(3) A period of time is required for the cracks to propagate through the overlay. The cracks, therefore, are inconsequential for an extensive time period.

SUMMARY

The analysis indicated that the major stresses causing reflection cracking in asphalt overlays of CRC pavements were the tensile stresses in the surface and the shear stresses in the bottom of the overlay. Due to the complex nature of the stresses occurring in the overlay immediately above cracks in the underlying pavement, it is recommended that this type of distress occurrence be modelled by laboratory testing. In this manner, the parameters affecting reflection cracking may be studied in detail.

Condition surveys along IH-45 in Walker county have shown that, provided reasonable repairs are made prior to overlaying, fairly thin overlays on CRC pavements do not deteriorate rapidly. The CRC pavement along this highway was poorly vibrated during construction and the bottom of this layer was poorly compacted (Ref 1). At the time of overlaying a more severe distress condition existed along this pavement than is typical of CRC pavements being overlaid presently. It may, therefore, be reasonable to assume that asphalt overlays on CRC pavements which are not as severely distressed as this section may outperform this overlay.

CHAPTER 5. FATIGUE LIFE OF RIGID PAVEMENTS

Pavements gradually wear out with time due to the repeated stresses induced in the pavement by traffic and environment. This pavement wear-out and the corresponding prediction of a pavement life are major aspects of any design procedure.

THE CONCEPT OF FAILURE

Before pavement life can be determined, or predicted, the pavement condition which constitutes "failure" needs to be determined. This was recognized at the AASHO Road Test and led to the introduction of the Present Serviceability Index (PSI). This concept is based on the pavement's ability to serve the user. As the pavement roughness increases, the level of service decreases until the roughness reaches a predetermined level, at which the pavement is said to have failed. This type of pavement failure can be termed "functional failure."

This concept may, however, be extended so that the pavement function may be defined as the ability of the pavement to serve the user as economically as possible. Economics can be applied to pavements only if reasonable estimates of total pavement costs can be made. These costs include construction, maintenance, rehabilitation, and user costs. Estimates of the

first three components depend to a large extent on the pavement's structural life, whereas user costs depend largely on the pavement's performance, or serviceability-time history. Reasonable estimates of pavement structural life and performance are, thus, required before a comparative economic analysis can be made.

In addition, condition survey and serviceability studies conducted along CRC pavements in Texas have shown that maintenance can keep pavement serviceability reasonably high, even if a severe distress condition exists along the pavement. For example, although the 1978 CRCP condition survey showed a significant increase in distress, no corresponding decrease in serviceability was measured.

Both pavement performance and functional life depend on the occurrence of distress in the pavement structure. The exact relationship between structural distress and functional performance is difficult to determine and may vary significantly, depending on the amount of maintenance applied. Furthermore, mechanistic pavement design procedures generally predict the pavement life only to a point of distress which may be termed "structural failure."

The exact level of distress which constitutes structural failure may vary greatly, depending on pavement type, environment, and the required level of service. In addition, distress may occur more rapidly in some areas than in others. Pavements in areas with wet climates and clayey subgrades may deteriorate faster than those in drier regions, even if the tensile stresses predicted using layered theory are similar. Distress prediction models based on condition survey data (Ref 35) illustrate the different factors which may have an effect on distress occurrence. However, a fatigue equation is

is usually used to predict structural failure in pavement design procedures (Refs 1, 3, 5, 21, 23, and 24).

For concrete pavements, the fatigue equation is generally of the form

$$N = A(f/\sigma)B \tag{5.1}$$

where

N = number of applications to a terminal distress condition,

f = flexural strength of the concrete,

σ = tensile stress in the concrete under load.

A and B are constants and vary with the different fatigue equations, as shown in Fig 5.1.

The fatigue equation generally represents some terminal condition, depending on the data used in the development. For example, if the equation was derived from laboratory testing, it would most probably represent the number of applications required in order to initiate fatigue macro-cracking. However, not only do fatigue curves derived from laboratory testing and those derived from field data differ considerably, but it may also be impractical to use this form of terminal situation in a design procedure.

Differences Between Laboratory and Field Fatigue Equations

A number of curves which illustrate the difference between equations developed from laboratory and field data are shown in Fig 5.1. At the higher

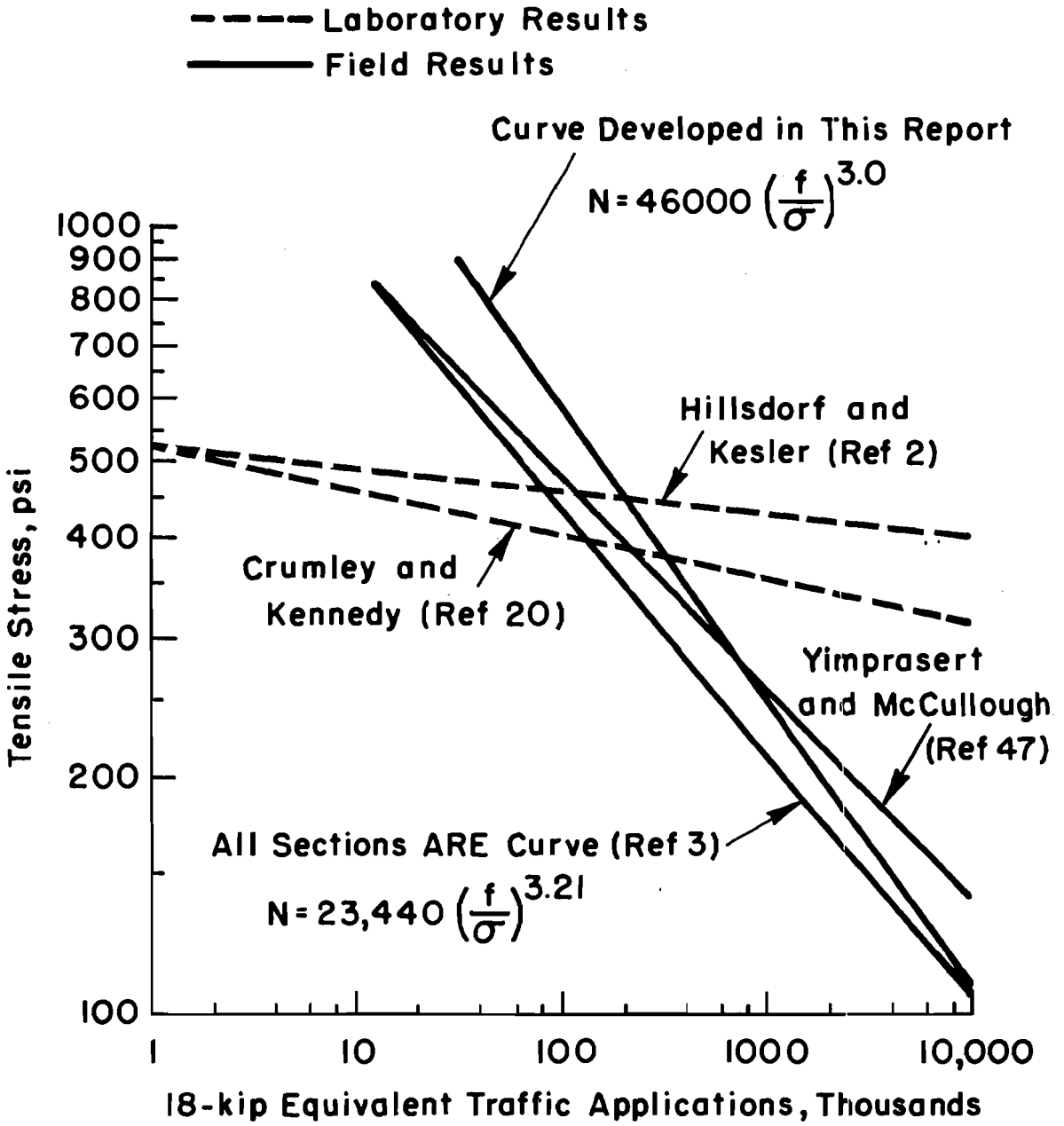

Fig 5.1. Comparison of fatigue curves developed from field and laboratory data.

stress levels, the "laboratory curves" predict fewer applications to failure than the "field curves," and at lower stress levels the opposite is the case. This may be due to a number of reasons:

(1) Crack Propagation. At the higher stress levels, the cracks in in-service pavements may take a while to propagate to the surface of the pavement. In contrast, as soon as a macro-crack develops in a laboratory test, the specimen fails and the fatigue life has been reached.

(2) Variation in Material Properties. Variations in subgrade and pavement layer stiffnesses may cause significantly higher stresses in the pavement layer than predicted by layered theory from load only. This may result in earlier cracking at lower stress levels.

(3) Environmental Effects. Moisture and temperature effects may result in significantly higher stresses in the pavement than predicted by layered theory. Moisture may enter the subgrade support and cause significant softening, which in turn will cause a considerable increase in stresses (Ref 3) in the pavement. A further moisture effect may be the creation of voids due to pumping. Voids beneath the rigid pavement layer may create significantly higher stresses in this layer than those predicted by layered theory (Ref 3). The magnitude of the stress may vary depending on the size and shape of the void.

Temperature may effect the tensile stresses in pavement in two ways. Thermal contraction may cause tensile stresses in the pavement which should be added to the tensile stresses caused by traffic loading. In addition, vertical temperature differentials

across the depth of the slab may cause warping stresses in the top or bottom of the concrete layer. For example, corner deflection measurements taken at the AASHO Road Test in the early morning were significantly higher than those taken later in the day. This was found to be due to warping of the slab and, depending on the direction of the warp, would result in tensile stresses in one of the slab surfaces.

(4) Dynamic Loading. Vehicles moving at high speeds may create significant dynamic loads in the pavement at discontinuities. In this regard, it is interesting to note that the relative damage of tandem to single axles as measured by the equivalencies developed from the AASHO Road Test is greater on rigid pavements than on flexible pavements. This may be partially due to dynamic loading at the slab joints and cracks.

(5) Redistribution of Stresses. As indicated in Chapter 3, cracking in a concrete pavement layer results in reduced stressed in this layer and some redistribution of the stresses amongst the lower layers. Increased stresses in the lower layers may result in significant deformation of these layers with a resultant increase of the stresses in the concrete layer.

These factors may be responsible for some of the differences between the laboratory and field fatigue equations and may serve to illustrate the complexity of developing a predictive equation for pavement life.

The Terminal Condition Represented by a Fatigue Equation

Fatigue equations developed from field data are semi-empirical in nature and therefore, if possible, the fatigue equation should be made to predict a terminal condition at which further traffic would result in a rapid increase in distress. This would serve two purposes:

(1) The distress occurring prior to this condition may result from construction deficiencies and the extremes in the variation of pavement material properties. For example, it may represent cracking of all the areas with a subgrade stiffness less than the 90th percentile subgrade modulus. This concept is illustrated in Fig 5.2, which shows the frequency and cumulative distribution of the fatigue life of a section of pavement.

In the preparation of this figure, it was assumed that the only factor which had a significant effect on the variation of the fatigue life was the variation in the subgrade modulus as determined from the Dynaflect sensor 5 deflection. The figure was prepared from statistical data output by the program MODE, which has the capability to transform Dynaflect sensor 5 deflections into subgrade moduli by using the regression equations in Fig 2.5. If the pavement surface and subbase moduli and stress sensitivity are input into the program, the regression equations presented in Appendix G are used to predict the deviator stress at the subgrade-subbase interface under the Dynaflect and an 18-kip axle load. These deviator stresses are used, as shown in the Appendix, to calculate the subgrade modulus corresponding to a range of

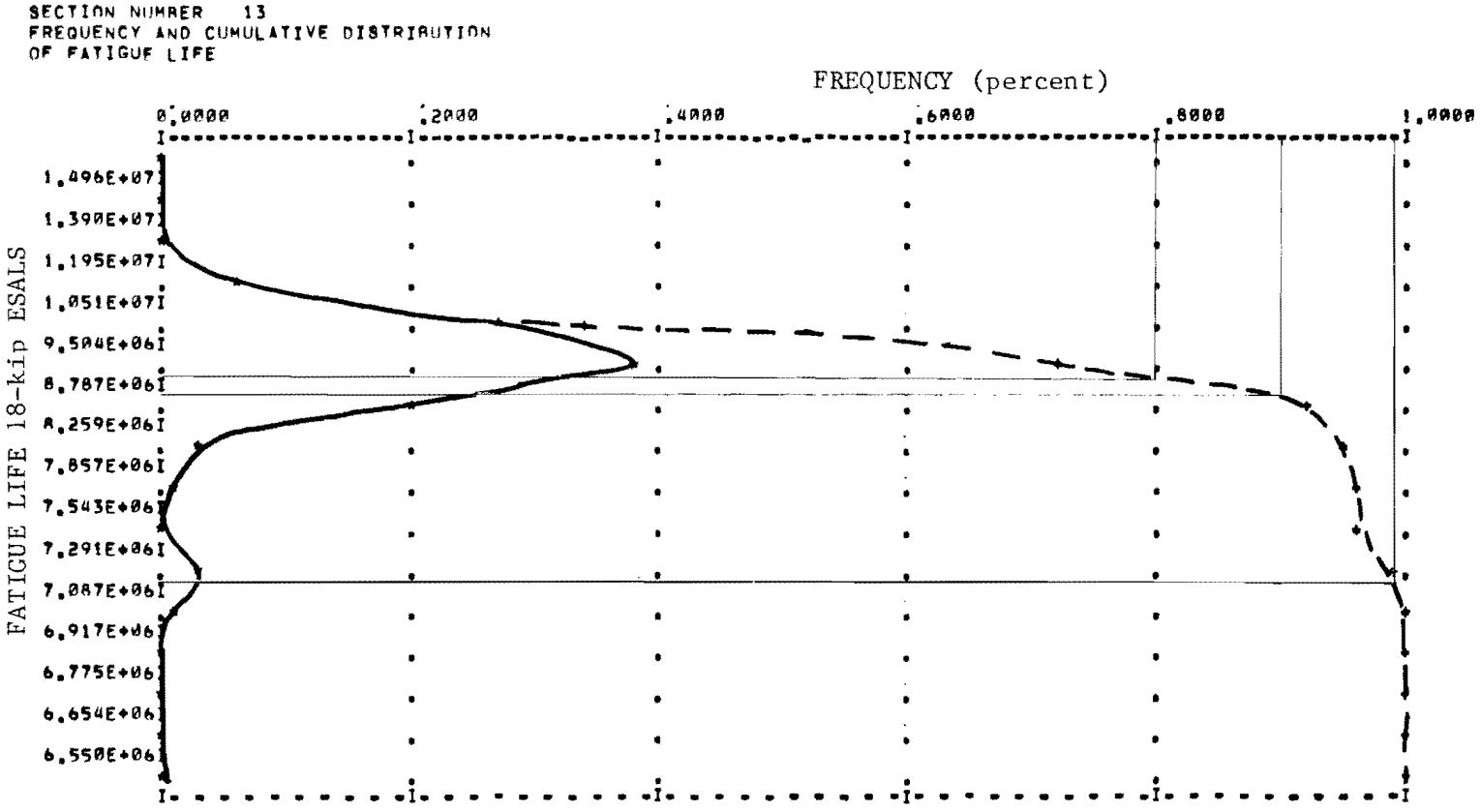

Fig 5.2. Frequency diagram and cumulative distribution of pavement fatigue life.

sensor 5 deflections under an 18-kip axle load. Another regression equation, obtained from Ref 48, is then used to predict the stress in the bottom of the pavement under an 18-kip axle load for the same range of sensor 5 deflections. If a stress modification factor for edge loading is input into the program, these stresses will be modified to reflect this loading condition. These stresses are then used in the fatigue equation to predict the pavement life for a range of sensor 5 deflections. This program thus provides a means of comparing the effects of different levels of sensor 5 deflections on the pavement fatigue life.

The cumulative distribution of the fatigue life is thus assumed to correspond to that of the subgrade modulus for the section. Furthermore, it may be reasonable to assume that the vertical axis of the cumulative distribution diagram corresponds to the length of the pavement section. Thus, at the 90th percentile of the fatigue life, or approximately 7.0 million 18-kip ESAL applications, as indicated in Fig 5.2, one percent of the pavement may show distress. A further 1.5 million applications are required for 10 percent of the pavement to show distress. Once the 90th percentile of fatigue life (and subgrade modulus) has been reached, it requires a only further 0.3 million applications for an additional 10 percent of stressed area. From a large number of such diagrams, it was found that, at the 90th percentile of the subgrade modulus (and the fatigue life), the distribution diagram becomes a reasonably straight line and each further traffic application may result in a proportional amount of distress.

Thus, by letting the fatigue equation represent a condition at which further traffic would result in rapidly increasing distress, extreme material property variation and construction deficiencies are implicitly allowed for. Minor maintenance over the life of the pavement may be all that is required to maintain a reasonable riding quality up to this point in the pavement's life.

(2) Further traffic would result in a rapid increase of distress, and thus the terminal condition defined by the fatigue equation may coincide fairly closely with the stage at which rehabilitation becomes more economical than maintenance. This may be termed "economic failure" of the pavement.

This concept is illustrated further in Appendix E. In this appendix, costs are assigned to various pavement maintenance and rehabilitation procedures. The CRC pavement condition survey data are then examined in order to determined at which point rehabilitation becomes more economical than continued maintenance.

From Appendix E, it is apparent that the critical rate of defect occurrence, after which an overlay may be more economical than continued maintenance, is approximately three defects per mile per year. Different traffic densities may cause differences in the critical, and subsequent, rates of defect occurrence. However, in this event both the rehabilitation and the maintenance costs may increase, resulting in approximately the same ratio of maintenance to rehabilitation cost.

It is therefore recommended that the terminal condition, or "structural failure" of CRC pavements, as represented by a fatigue equation, be defined as that condition where the number of defects per mile equals the pavement age in years. This terminal condition is founded on comparative cost analysis and the variation in material properties. The stress used in the fatigue equation should correspond to the 90th percentile subgrade modulus, because, as indicated previously, at this point further traffic applications may result in a rapid increase in distress.

DEVELOPEMENT OF A FATIGUE EQUATION

In the previous paragraphs, the differences between fatigue curves developed from laboratory data and those developed from field data were examined. From this, the need for developing fatigue equations from field data is apparent.

The most significant problems associated with this type of approach are the lack of accurate traffic data and the narrow range of stresses within which working pavements operate. Condition surveys have shown that, although most CRC pavements in Texas are 8 inches thick, the occurrence of distress varies significantly. Furthermore, condition surveys have shown the defects in pavements to be directionalized, which may be due to a corresponding traffic distribution.

However, the AASHO Road Test has provided useful data for fatigue analysis and the resulting fatigue equation may be corroborated or modified using local data. The fatigue equation used in the RPOD2 design procedure

was developed from the AASHO Road Test data and thus will be reevaluated using some of the principles described in this report.

REEVALUATION OF THE AASHO ROAD TEST DATA IN THE DEVELOPMENT OF A FATIGUE EQUATION

The RPOD2 design procedure uses a fatigue equation developed from the AASHO Road Test data to make predictions of the pavement life (Refs 3 and 5). During the development of this equation, several simplifying assumptions were made which should be reexamined in the light of recent developments:

(1) Constant values of pavement layer moduli were used throughout.

(2) The terminal condition of the pavement was considered to be the initiation of Class 3 and 4 cracking (Class 3 cracking is defined as significantly spalled cracks which are approximately 1/4 inch wide and Class 4 is any crack which has been sealed).

(3) The AASHO equivalency factors, which related the number of axle loads of different types and weights to the number of 18-kip single axles required to reach a terminal serviceability condition, were assumed to be valid.

The AASHO Road Test data were reexamined using a basic mechanistic procedure with fewer simplifying assumptions. Some of the developments listed earlier in this report were also used in the analysis. The analysis was done in steps as follows:

(1) Materials Characterization. The rigid pavements tested at the AASHO Road Test were jointed concrete pavement supported by a clay subgrade

with or without a granular subbase. Two slab types, 15-foot unreinforced and 40-foot reinforced, were used in the experiment. The slab and subbase thicknesses were varied among the test sections.

The moduli of the concrete and subbase layers as obtained in Ref 3 were assumed to be correct and were kept constant throughout the analysis. The modulus of the subgrade was determined using the deflection measurements taken during the Road Test. The assumption was, therefore, made that all the variation in the deflection measurements was due to changes in the subgrade modulus. The deflections taken during the winter and summer months varied significantly at the Road Test and this variation corresponded to the seasonal variation in the occurrence of cracked sections as shown in Fig 5.3(b). It was thus decided to model the subgrade separately for the winter and summer months. An average edge deflection taken during each season was used to represent the subgrade modulus for these periods. The periods during which the different subgrade modulus values were used are indicated in Fig 5.3 (a).

The subgrade modulus for use ½l the analysis was determinel by fitting layered theory 'efl'ction ½compu½½pinns to phEdeFlebtins mEasured at the Road Test. Thus, the edge deflections measured at the Road Test had to be converted to interior deflections. This was done using the curves shown in Fig 5.4, obtained using the SAP2 finite element model. The finite element representation of an edge load condition is shown in Fig 5.5.

The subgrade modulus was then calculated from the interior deflections using layered theory. This was done as indicated in Appendix C for each section at the Road Test. The subgrade modulus calculated in this manner would be a mean effective modulus under the wheel load used on each section.

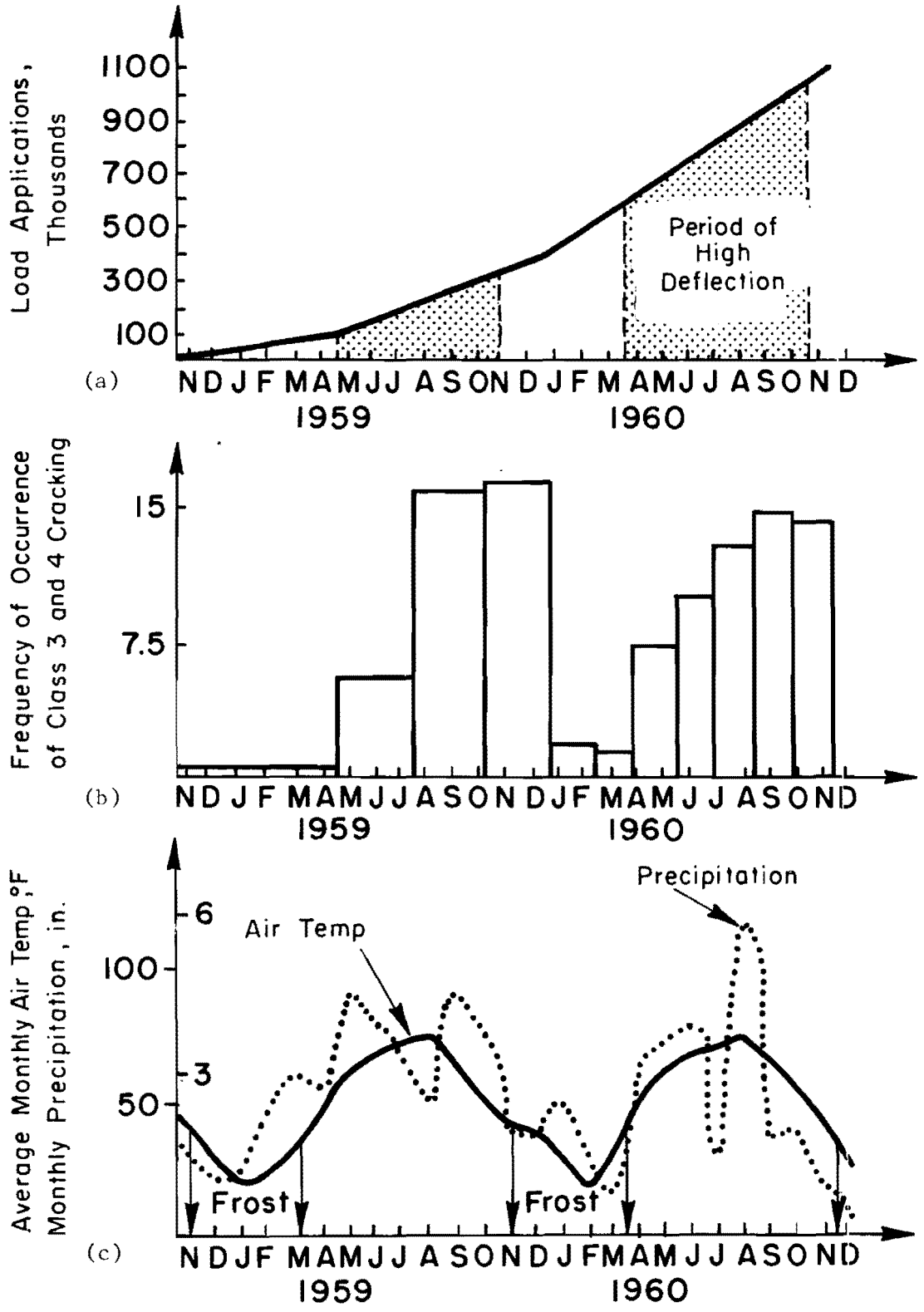

Fig 5.3. The relationship of distress occurrence and environmental and traffic variables at the AASHO road test.

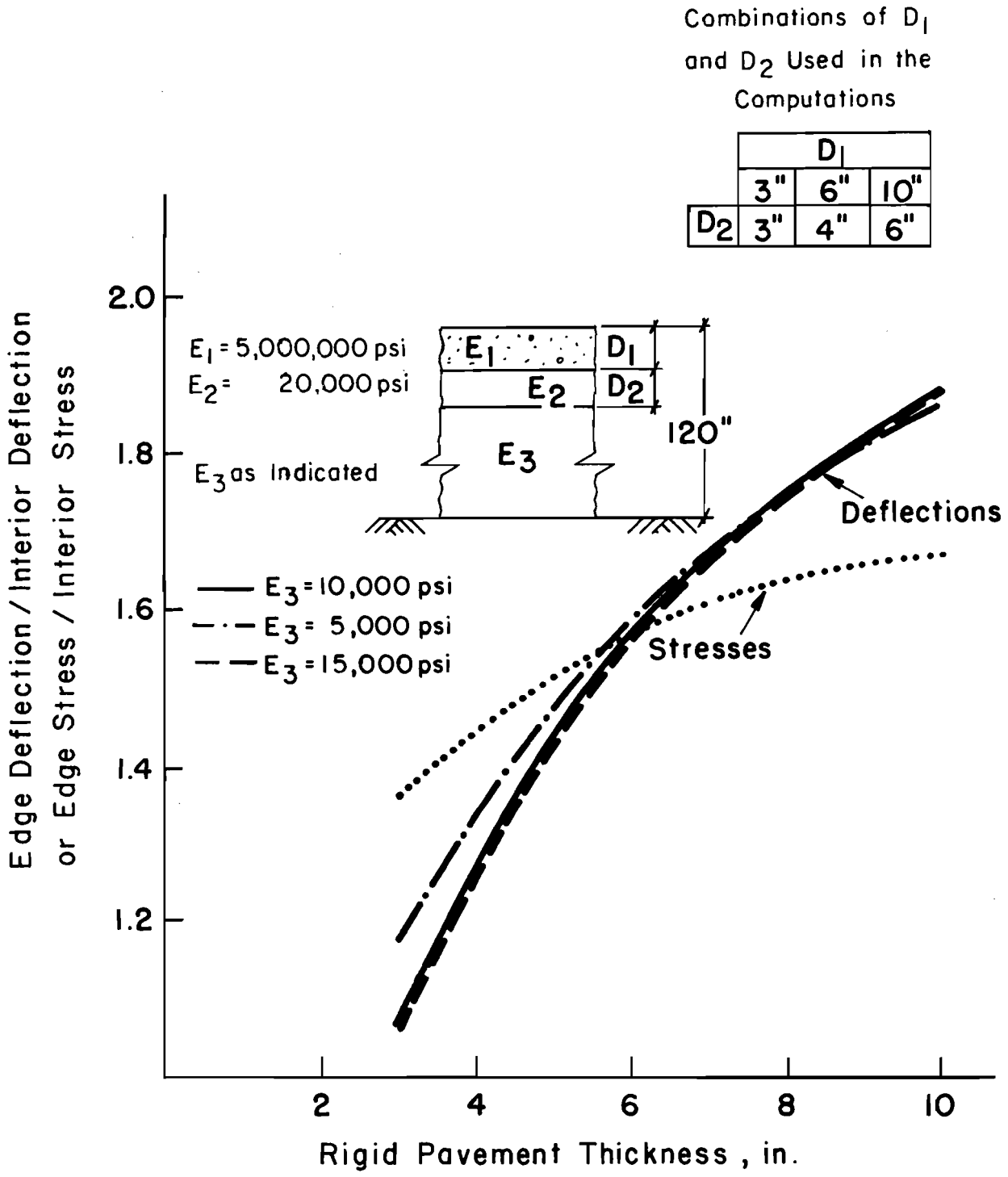

Fig 5.4. Edge to interior stress and deflection relationships for different rigid pavement thicknesses as determined by the SAP2 finite element program.

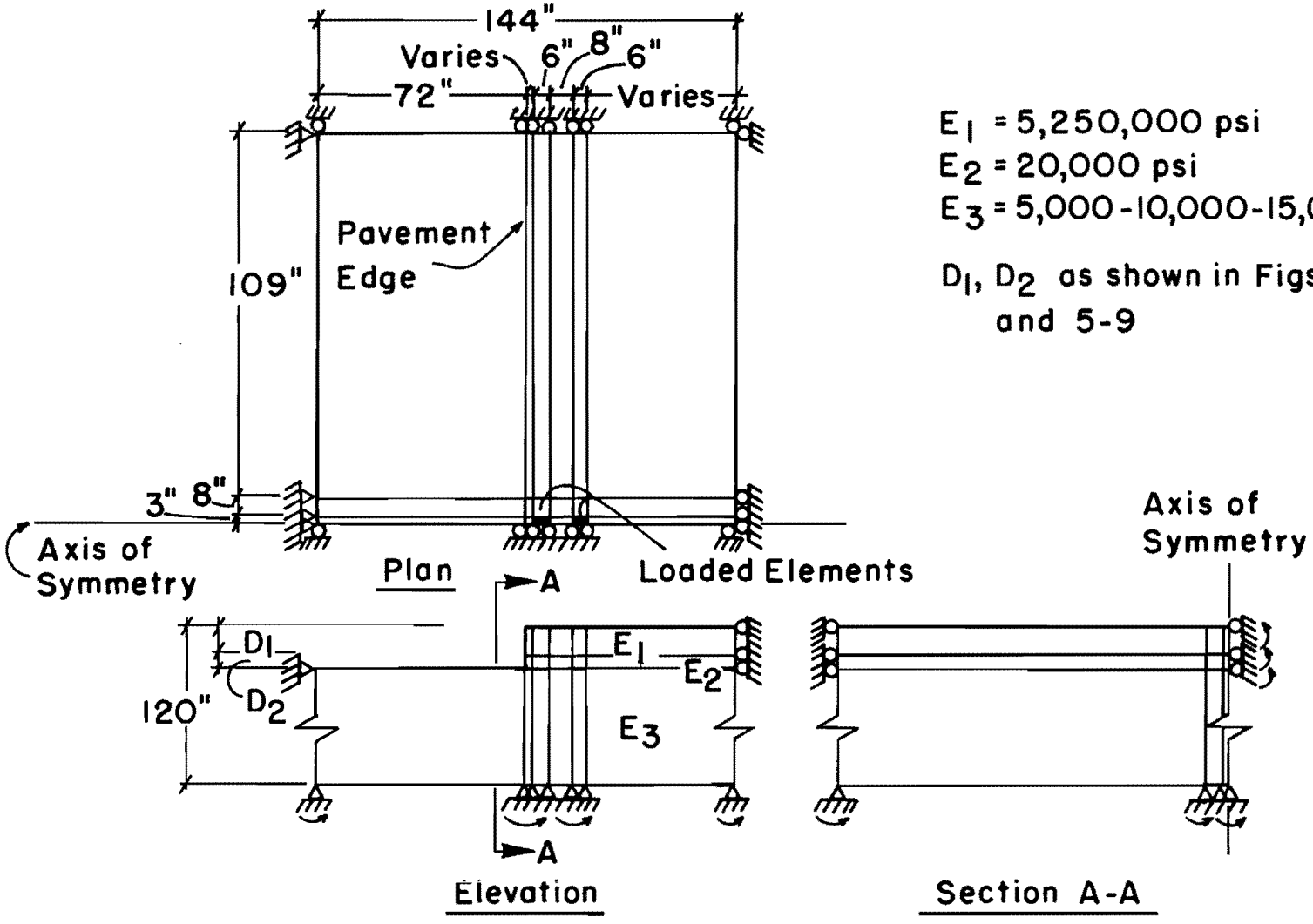

Fig 5.5. Finite element configuration to determine the ratio of edge to interior deflections and stresses at the AASHO road test.

These calculations resulted in a wide range of subgrade moduli; however, a regression analysis performed on the results showed that much of this variation could be explained by changes in the surface layer thickness, the principal stress difference in the top of the subgrade, and the different wheel loads. The remaining unexplained variation was assumed to be due to the natural variation of the material. Thus, to obtain a subgrade modulus for the different seasons for each section which would be representative of the weaker effective moduli within that section, the moduli predicted by this regression equation were reduced proportionally to the standard errors of the equations. This was done as shown below, to obtain a modulus representative of the weakest 10 percent of the subgrade within each section:

$$E = E^{*} - SE \times E^{*} \times 1.3$$

where

E = Subgrade moduli used in fatigue equation calculations,

E^{*} = Subgrade moduli predicted by the regression equations,

SE = Standard error of the regression equations.

It is interesting to note that for both seasons, the regression equations explained approximately 80 percent of the variation in the calculated subgrade moduli. Furthermore, increasing principal stress differences, as predicted by layered theory, corresponded to increasing subgrade moduli, as predicted from the deflection measurements. This is contrary to the results obtained from Resilient Modulus tests on this material (Refs 43 and 44). However, in Ref 25, results from a study by

A. C. Benkelman indicate that for increased load, the deflections increased less than proportionally, indicating a stress hardening pavement structure. This may explain the above apparent contradictions and may indicate the need for additional investigation.

(2) Stress Calculations. Having calculated a subgrade modulus representative of the weaker subgrade within a section for each season, the tensile stresses occurring in the bottom of the concrete layer under the applied load were calculated using layered theory. However, the wheel loads applied at the Road Test were distributed as shown in Fig 5.6 (Ref 40) and, thus, some indication of the increase in stresses for an edge loading condition was required. The SAP2 finite element configuration shown in Fig 5.5 was adjusted and used for this purpose. The results are shown in Fig 5.6.

(3) Terminal Condition. Bearing some of the earlier comment regarding pavement terminal condition in mind, a terminal distress condition had to be selected for use in the fatigue equation. Examination of the Road Test data showed that, as the cracking index approached 50 feet per 1000 square feet, further loading resulted in a rapid increase in distress and the pavement was soon removed from the measurement program. This figure was thus chosen as representative of a failed jointed concrete pavement. (The cracking index was defined as the length of the crack projections on, or perpendicular to, the center line of the pavement, whichever was the longest.) The number of axle loads applied prior to this terminal condition was used in the development of a fatigue equation.

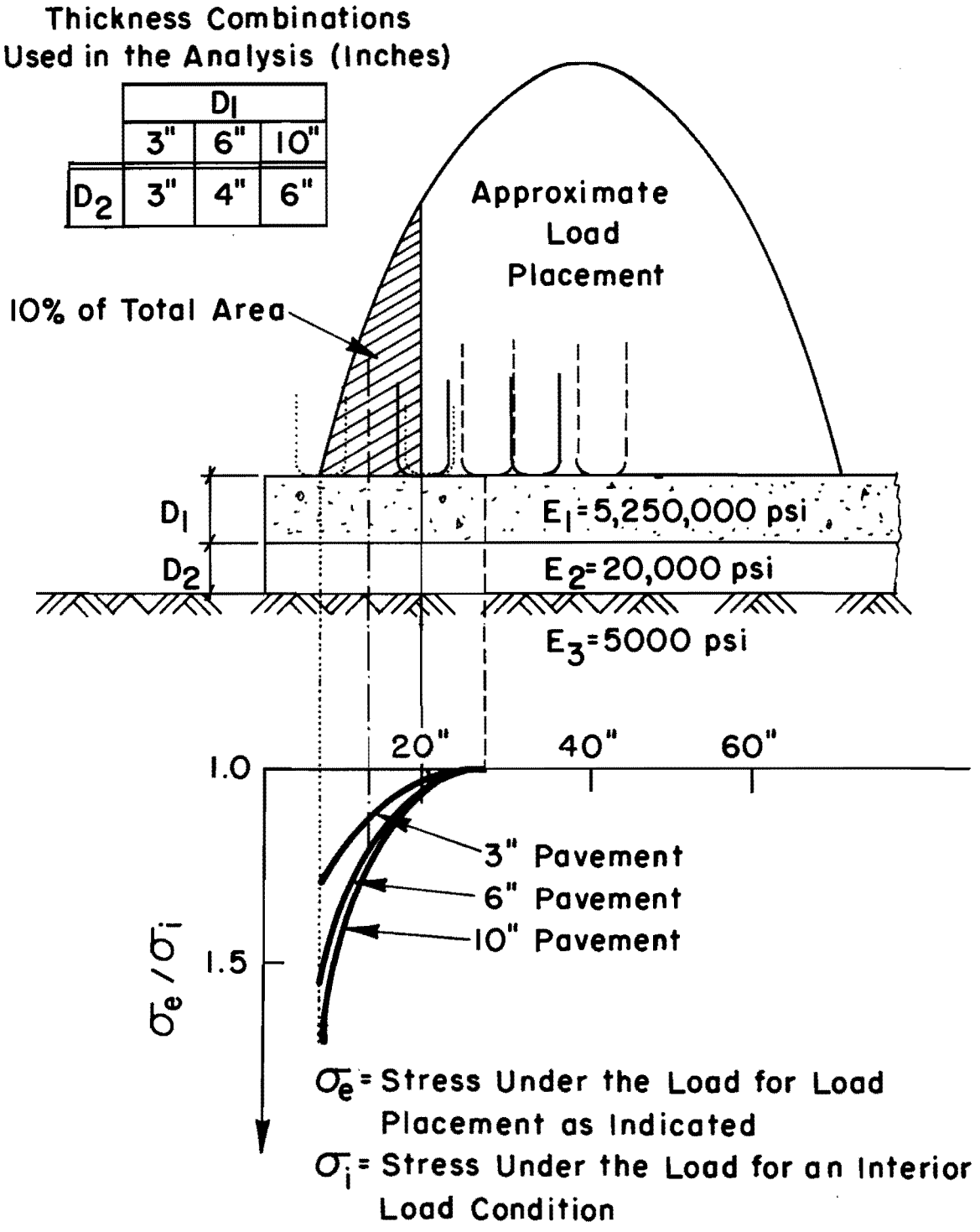

Fig 5.6. Planned load placement at the AASHO road test and the corresponding ratio of the stress under the load relative to the interior stress for different rigid pavement thicknesses.

(4) Development of a Fatigue Equation. The fatigue equation was developed by regression analysis of the log of the number of axle applications to failure against the log of the tensile stress in the pavement surface layer under load. Four different stress levels were used in the analysis:

(1) summer interior stresses,

(2) summer edge stresses under the 10 percent of the traffic loads which are near the edge, as shown in Fig 5.6,

(3) winter interior stresses, and

(4) winter edge stresses as for summer edge stresses.

Because four different stress levels and the corresponding number of applications at each stress level were used to develop the fatigue equation the concept of equivalent stress was used.

This concept is illustrated in Appendix D. The equivalent stress is that stress at which a number of applications will result in the same damage to the structure as when a similar number of applications are distributed among a number of stress levels. For each combination of stresses and applications, different fatigue equations will result in a different effective stress. Thus a trial and error procedure was used to develop the fatigue equation.

The fatigue equation presently used in the RPOD2 design procedure was used as a starting point for the development. Three iterations were generally sufficient to result in an accurate equation.

A significant outcome of this analysis was the difference between the number of tandem and the number of single axles applied before failure. This is illustrated in Fig 5.7, which shows the regression equation and scatter

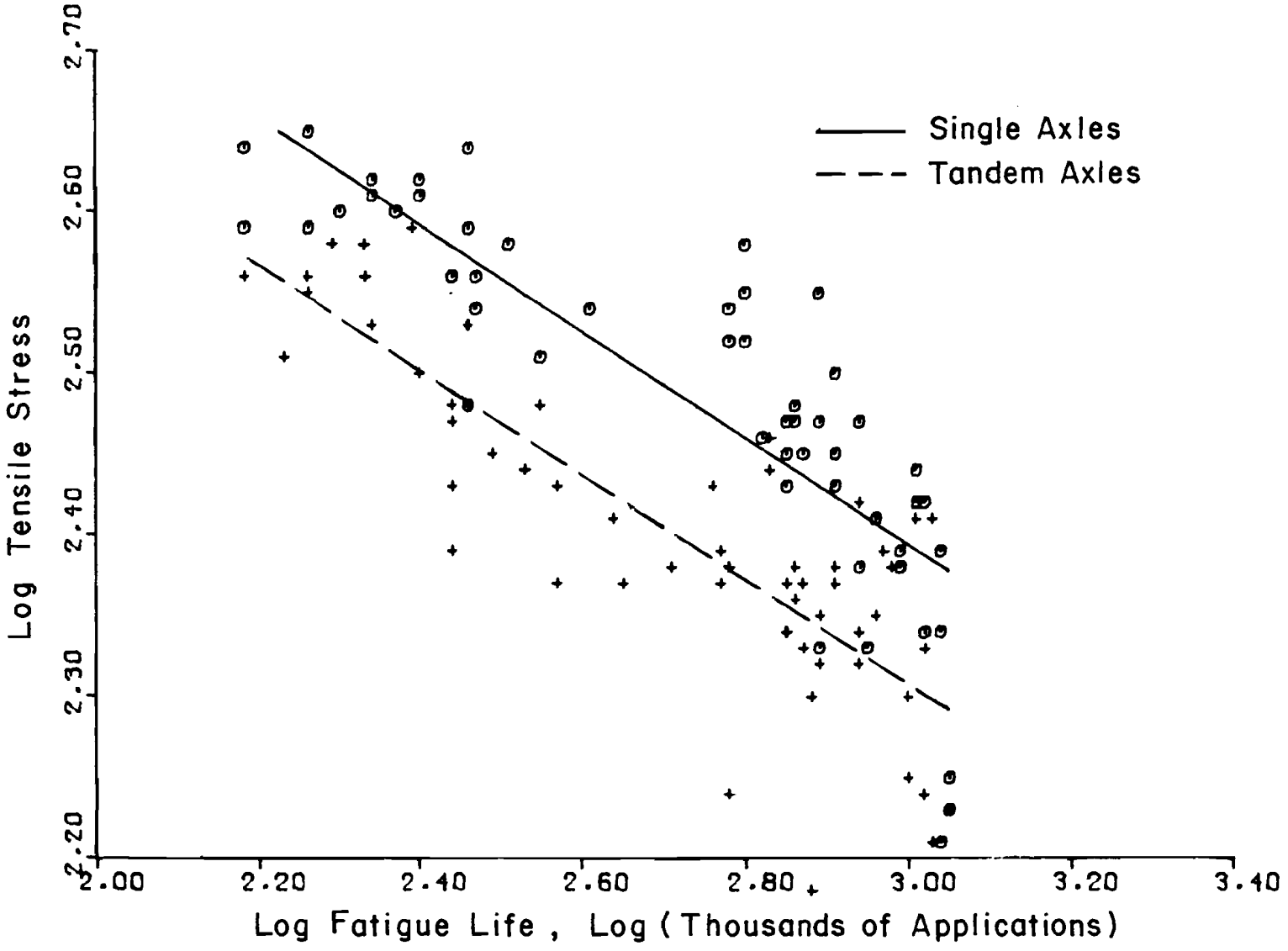

Fig 5.7. Stress-fatigue relationship for rigid pavements obtained from single and tandem axle loadings at the AASHO road test.

diagrams for both the single and tandem axle loads. The number of tandem axle applications was increased until the two regression lines virtually coincided, as shown in Fig 5.8. The final regression equation is shown in Fig 5.9. The number of tandem axle applications had to be increased by 1.9 for the two lines to coincide. This value may be compared to the AASHO equivalencies for a single and a tandem axle, which produce approximately the same tensile stresses in the bottom of the pavement layer. In the case of an 18-kip single axle and a 36-kip tandem axle the equivalencies differ by a factor of approximately 2.35 (layered theory computations indicate that these two axle loadings produce approximately the same tensile stresses for an 8-inch pavement).

The final fatigue equation,

$$N = 46000\ (f/\sigma)3.0 \qquad (5.2)$$

was developed with few assumptions and this may make valid its application in conditions unlike those at the Road Test. Some of the conditions at the Road Test should, however, be kept in mind when this equation is used in other situations.

(1) The rigid pavements had granular subbases which often exhibited extreme amounts of pumping.

(2) The spring thaw at the Road Test was severe and this may often not be the case, especially in Texas.

(3) The Road Test pavements had granular shoulders, which are not common along Interstate Highways at this time.

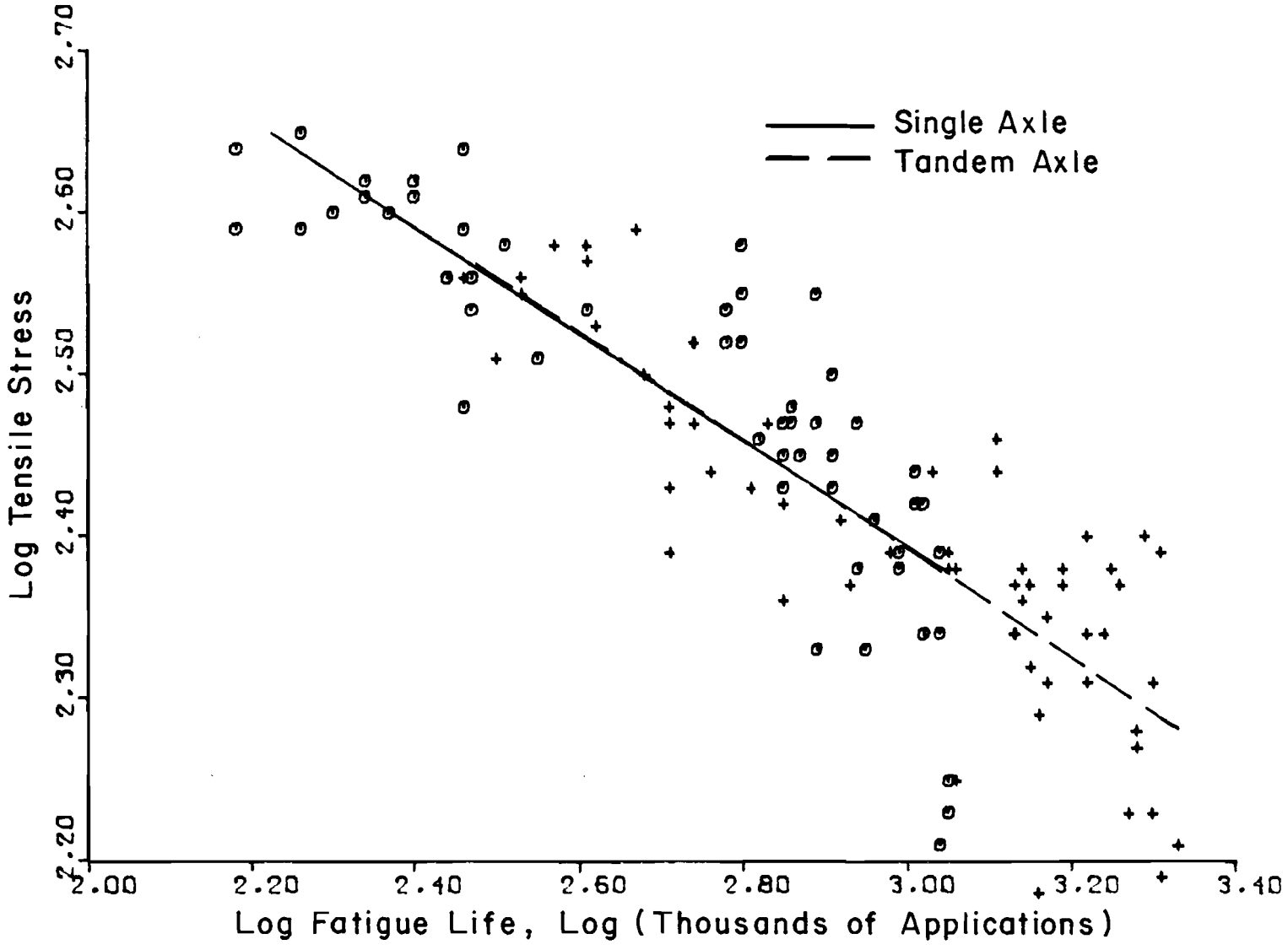

Fig 5.8. Stress-fatigue relationship for rigid pavements obtained from single and tandem axle loadings at the AASHO road test.

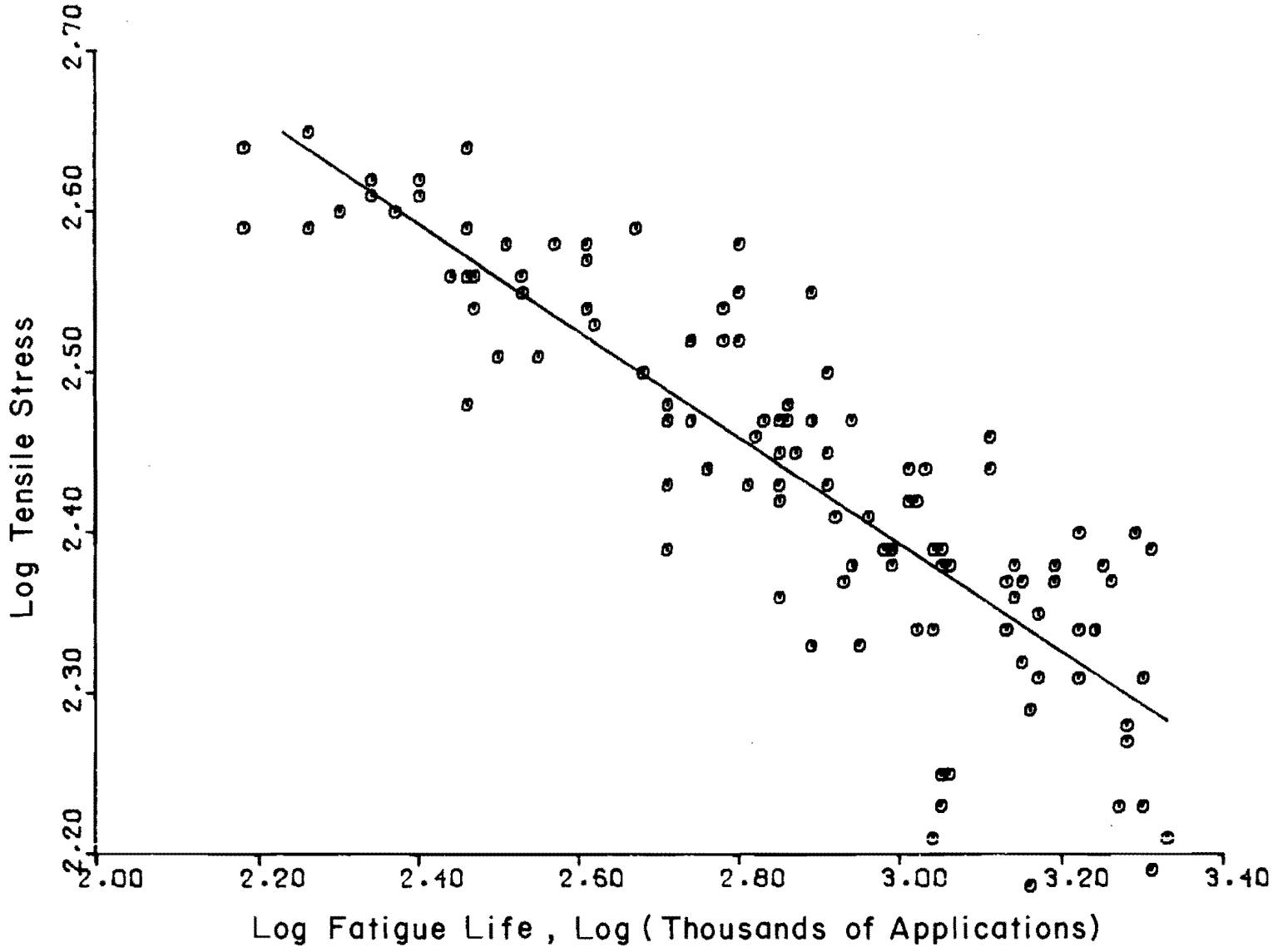

Fig 5.9. Final stress-fatigue relationship for rigid pavements using data from the AASHO road test.

(4) Very little of the Road Test traffic encroached on the pavement edge, which may not be the case along existing highways.

These factors should be kept in mind whenever an extrapolation of the fatigue curve is used to predict pavement lives.

CORRELATION OF THE FATIGUE EQUATION TO CONDITION SURVEY AND TRAFFIC DATA

Some CRC pavements in Texas are presently at the terminal distress condition as described earlier. It is therefore possible to check the fatigue life predictions from the equation derived from the Road Test data with the fatigue lives of the Texas pavements. This may be determined by plotting the number of 18-kip ESALs which have passed over the pavement prior to the terminal distress condition against the stress-strength ratio, as indicated in Fig 5.10. The plotted points may be compared to the extrapolation of the fatigue equation derived from Road Test data.

There are a number of assumptions associated with this procedure which should be mentioned.

(1) Traffic data. The uncertainties regarding the transverse and directional traffic distributions have been mentioned in a previous paragraph. The Texas SDHPT has a large number of counting and weighing stations in use; they provided the data for traffic analysis. The approach adopted for calculating the number of 18-kip ESAL's applied is as follows:

(a) Obtain the average annual daily traffic (AADT) on each section of road for each year of its life.

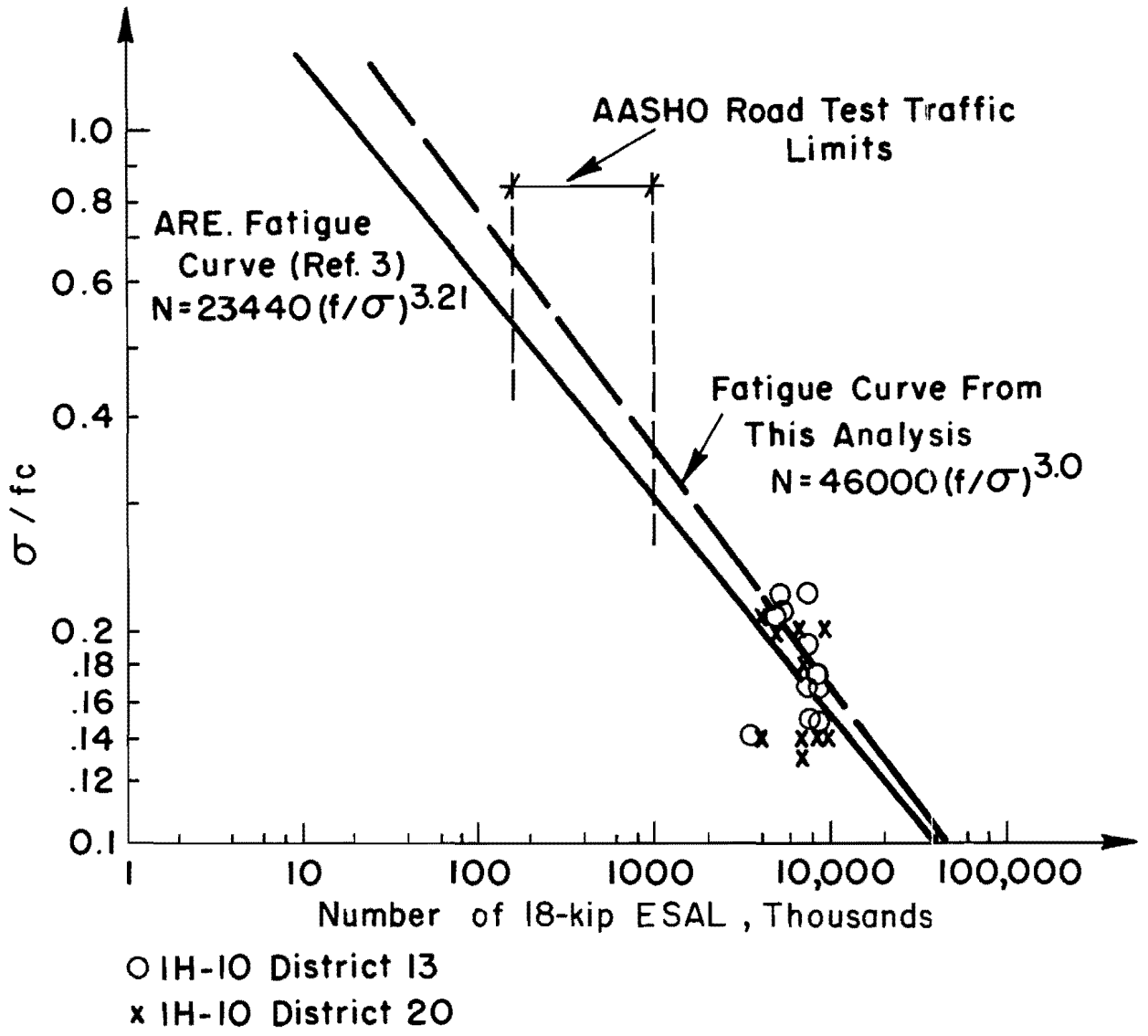

Fig 5.10. Correlation between fatigue curves developed from AASHO road test data and data from CRC pavements in Districts 13 and 20, Texas.

(b) Use the nearest or most applicable manual count station to obtain an indication of the percentage of trucks in the traffic mix, excluding pick-ups.

(c) Obtain the number of 18-kip ESAL's per truck by using the data included in W-4 Tables. These tables are produced from weighing station data and they provide an indication of the truck and axle weight distributions. The tables showing the average distributions for all the rural weighing stations were used in the analysis. The total number of 18-kip ESAL's counted at the weighing stations was divided by the total number of trucks counted, excluding pick-ups, to obtain the average number of 18-kip ESAL's per truck. The results are shown in Fig 5.11.

Between 1974 and 1976, the Texas SDHPT changed its weighing methods from static vehicle weight measurements to a dynamic, weighing-in-motion system. At the same time, the legal axle weight limit was changed from 18 to 20 kips. As indicated in Fig 5.11, a large increase in the calculated number of 18-kip ESAL's per truck occurred during these years. In this analysis the assumption was made that this increase was due entirely to the different weighing systems and the concomitant differences associated therewith. The 1976 and 1978 data were thus assumed to be correct. The extrapolation line indicated in Fig 5.11, which has a slope similar to that of the earlier data points, was used in the analysis to represent the number of 18-kip ESAL's per truck.

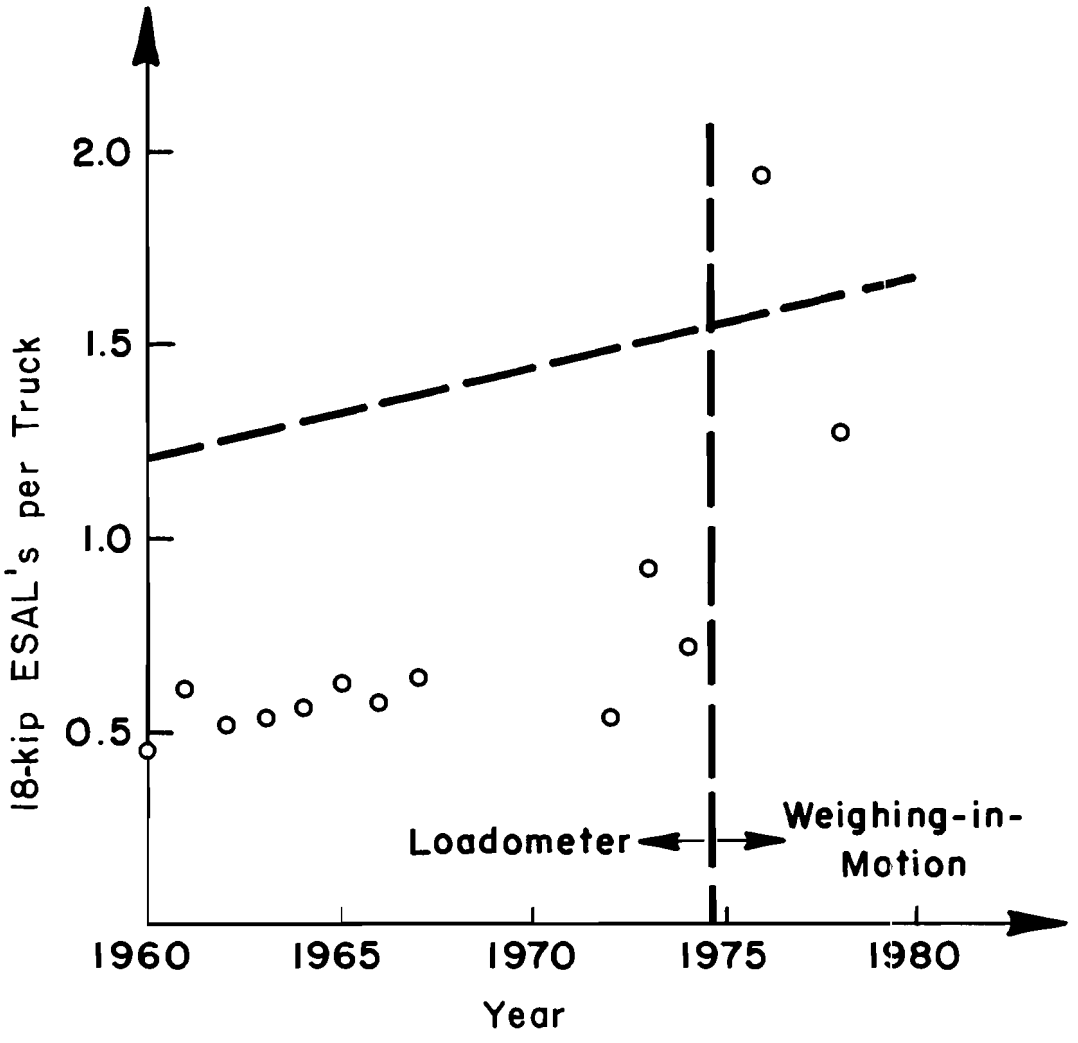

Fig 5.11. Number of 18-kip ESAL's per truck as obtained from W-4 tables for Texas highways (all rural weighing stations).

(d) Once the number of 18-kip ESAL's per day in both directions had been obtained in this manner, the total 18-kip ESAL's over the life of the pavement were obtained by addition of the daily number of equivalent axles over the life of the pavement. This calculation is shown in Appendix F for a number of pavement sections.

(e) No lane distribution factor was applied.

(f) A transverse distribution which may be closer to the pavement edge than the distribution of loads at the AASHO Road Test was taken into account by multiplying the stresses in the pavement, as obtained from layered theory, by a factor of 1.2.

(g) The traffic data used do not reflect any seasonal or weekly variation in axle weights. This factor may be fairly significant, as indicated in Ref 48.

(2) Stress Data. The stresses in the upper pavement layer were obtained using layered theory and layer moduli derived from deflection measurements. No seasonal deflection variation was considered in the analysis. In addition, no variation in the surface and subbase modulus was considered. The assumption was made that the only layer stiffness variation which had an effect on the pavement fatigue life was that of the subgrade. This aspect of the pavement design procedure may warrant further investigation. The stresses calculated in the rigid pavement layer overlying the 90th percentile subgrade modulus were used throughout the analysis.

(3) Pavement Failure Condition. The pavement failure condition as defined earlier in this chapter was used in the analysis. In many instances the distress condition at the time of condition surveying

was significantly higher than the terminal distress condition. In these instances, the traffic at the terminal condition had to be estimated using the data in the tables in Appendix A.

The data plotted in Fig 5.10 were obtained from Tables 5.1 and 5.2, which present the condition survey and stress data for different sections of highway in Districts 13 and 17 in Texas. A concrete flexural strength of 690 psi was used to plot the fatigue equations derived from AASHO Road Test data. This was the average 21-day flexural strength of this concrete (Ref 41). In this figure, a flexural strength of 650 psi was used to plot the data obtained from the Texas highways.

SUMMARY

The terminal condition of CRC pavements has been defined in a rational manner, based on comparative cost analysis and a rate of distress development. Pavements with a number of defects per mile equal to the pavement age in years are expected to deteriorate more and more rapidly in future years.

A fatigue equation has been derived from AASHO Road Test data in a mechanistic manner. The equation differs slightly from the equation developed in Ref 3. An attempt has been made to check the accuracy of this equation when applied to CRC pavements in Texas, by making use of condition survey, traffic, and deflection data. In general, the fatigue equation predictions correlate reasonably well with the observed pavement lives when the variation of the environment and material stiffnesses and the inaccuracies in the traffic data are considered.

TABLE 5.1. CONDITION SURVEY DATA AND TENSILE STRESSES AT THE BOTTOM OF THE RIGID PAVEMENT LAYER

Sub Section	Limits (Stations)	Defects Per Mile and 18-kip ESAL's to Date Indicated						Tensile Stress (psi)
		1974		1978		1979		
		Defects/ Mile	TRAF, millions	Defects/ Mile	TRAF, millions	Defects/ Mile	TRAF millions	
EB 1	750 - 761	0	4	0	7	0	8	135
EB 2	- 773	15	4	20	7	22	8	88
EB 3	- 884	3	4	7	7	16	8	113
EB 4	- 930	1	4	3	7	20	8	113
EB 5	- 1001	2	4	9	7	9	8	113
EB 6	- 1003	2	4	3	7	3	8	140
EB 7	- 1121	0	4	2	7	4	8	113
EB 8	26 - 37	10	5	15	10	41	11	140
EB 9	- 85	1	5	1	10	1	11	113
EB 10	- 149	7	5	13	10	37	11	135
Avg		4	4.3	7.3	7.9	15.3	8.9	
WB 1	149 - 112	5	5	14	10	36	11	135
WB 2	- 88	O/LAY						
WB 3	- 26	0	5	8	10	10	11	113
WB 4	1121 - 1109	3	4	23	7	69	8	99
WB 5	- 1065	9	4	1	7	18	8	140
WB 6	- 926	9	4	4	7	14	8	123
WB 7	- 880	9	4	5	7	16	8	113
WB 8	- 750	1	4	9	7	17	8	99

TABLE 5.2. CONDITION SURVEY DATA AND TENSILE STRESSES AT THE BOTTOM OF THE RIGID PAVEMENT LAYER

Sub Section	Limits (Stations)	Defects Per Mile and 18-kip ESAL's to Date Indicated				Tensile Stress (psi)
		1974		1978		
		Defects/ Mile	TRAF, millions	Defects/ Mile	TRAF, millions	
WB 1	838.6 - 838.0	58	5.0	207	9.0	92
WB 2	- 837.5	24	5.0	90	9.0	137
WB 3	- 837.0	0	5.0	0	9.0	97
WB 4	- 836.6	8	5.0	25	9.0	93
WB 5	- 835.9	6	5.0	100	9.0	82
WB 6	- 833.2	4	5.0	41	9.0	92
WB 7	- 832.9	0	5.0	12	9.0	94
EB 8	833.3 - 833.6	0	5.0	0	9.0	94
EB 9	- 834.1	4	5.0	57	9.0	93
EB 10	- 835.0	2	5.0	13	9.0	93
EB 11	- 835.8	4	5.0	35	9.0	145
EB 12	- 836.1	0	5.0	0	9.0	93
EB 13	- 836.5	30	5.0	65	9.0	144
EB 14	- 838.5	1	5.0	7	9.0	133
EB 15	- 839.2	3	5.0	33	9.0	128

CHAPTER 6. FATIGUE OF OVERLAID RIGID PAVEMENTS

Mechanistic design procedures predict a pavement's life based on the amount of fatigue damage done to some of the bound pavement layers. Prior to overlaying, the fatigue damage done to the concrete surface layer by repeated traffic applications should be considered whereas, after the pavement has been overlaid, the fatigue damage done to both the overlay and to the underlying, old pavement should be considered.

The fatigue damage occurs due to repeated tensile stresses in the pavement layers which arise from bending of these layers under load. In addition to these tensile stresses, an overlay may be subjected to additional stresses caused by movement of the underlying pavement at discontinuities. These discontinuities may, thus, reflect through the overlay as cracks.

All the various modes of pavement fatigue need to be considered in a design procedure, and the method by which this is done in the RPOD2 design procedure will be described.

FATIGUE LIFE OF OVERLAID RIGID PAVEMENTS AS DETERMINED BY RPOD2

The RPOD2 design procedure predicts the fatigue life of an overlaid rigid pavement in a number of ways, depending on the traffic history, deflections, condition survey data, and the pavement structure:

(1) The first step in the design procedure is to estimate the pavement layer stiffnesses from deflection data and material tests. The tensile stresses in the rigid pavement layer are then calculated using layered theory and an 18-kip single axle load. These stresses and the past number of 18-kip ESAL's are used in conjunction with a fatigue equation to calculate the fatigue damage done to the existing pavement. This is done as follows:

$$D = \Sigma \frac{n}{N} \tag{6.1}$$

where

D = damage,

n = past number of 18-kip ESAL applications,

N = total allowable number of 18-kip ESAL applications.

The remaining life of the pavement is equal to one minus damage and is usually expressed as a percentage. If the pavement has Class 3 and 4 cracking, the assumption is made that no remaining life is left in the pavement.

(2) If the original pavement layer has more than 25 percent remaining life, then the tensile stresses in this layer are computed, after overlaying, under an 18-kip axle load. This stress is used in the fatigue equation mentioned earlier to calculate a total allowable number of 18-kip ESAL applications for the overlaid pavement. This number is multiplied by the remaining life to obtain the number of future applications allowed on the pavement.

(3) If the pavement has little or no remaining life, then the design model uses different approaches, depending on the overlay type. If a concrete overlay is used, the original surface modulus is reduced to 500,000 psi, which is a representative value obtained from deflection studies of cracked pavements at the AASHO Road Test (Ref 3). The tensile stresses in the bottom of the overlay are then computed using layered theory, and these stresses are used in the fatigue equation to predict the life of the overlaid pavement.

If an asphalt overlay is used, the pavement is represented by a single subgrade layer with a modulus which results in a deflection under an 18-kip ESAL equal to the deflection of the cracked (E1=500,000 psi) pavement structure, as computed using layered theory. Layered theory is then used to compute the tensile strains in the asphalt overlay placed on this subgrade, and they are used in a fatigue equation to predict the overlay life.

(4) The equations used in the procedure to calculate the fatigue lives of the PCC and AC layers were developed from AASHO Road Test data in Ref 3.

(5) Reflection cracking is analyzed separately from fatigue cracking by utilizing measurements of horizontal and vertical differential movements.

This procedure will now be examined with regard to fatigue of overlaid pavements, in the light of developments mentioned in earlier chapters of this report.

SUGGESTED MODIFICATIONS TO THE RPOD2 PROCEDURE REGARGIND ASPHALT OVERLAYS ON CRC PAVEMENTS

Condition surveys of CRC pavements in Texas overlaid with asphalt concrete have provided data which may be used to improve the overlay life predictions from the RPOD2 design procedure. These overlaid pavements are outperforming the predictions of this design procedure, and the procedure should thus be updated to reflect these data.

The Remaining Life of an Existing CRC Pavement

In Chapter 5 the "failure" condition of CRC pavements was defined using sound engineering principles. In that chapter, it was indicated that, once the rate of defect occurrence in a CRC pavement reached 3 defects per mile per year, further load applications would result in a rapid increase in distress. This rate of defect occurrence generally corresponded to the pavement condition at which the number of defects per mile equaled the pavement age in years. Thus, it may be hypothesized that, at this stage of the unoverlaid pavement's life, it has no remaining life.

However, condition surveys of overlaid pavements indicate that relatively thin overlays may significantly extend the pavement's life. For example, in Walker County, an asphalt overlay ranging in thickness from 2.5 to 6.0 inches was placed on a section of IH-45 which had approximately 13 defects per mile. The overlay was placed on the existing 8-inch CRC pavement in 1974, at which time the pavement was 14 years old and had carried approximately 8 million 18-kip ESAL's. The condition of this pavement, thus, approximately corresponded to the failure condition described in Chapter 5.

Since that time, the pavement has carried approximately 5 million 18-kip ESAL's without any significant distress. During a 1979 condition survey of the overlaid pavement, 13 defects per mile were counted when the defects were averaged over the length of the project. These defects include patches and reflection cracks, with each patch given a weight of one and each reflection crack given a weight of 0.5. These defects are far less severe than the defects occurring in an unoverlaid rigid pavement because of the insignificant nature of the reflection cracks and the ease with which an asphalt overlay may be patched.

Approximately 50 percent (Ref 37) of the defects in the overlay could be related to defects such as patches and punch outs in the underlying pavement, which existed prior to overlaying. The remaining 50 percent may result from the reflection of old cracks in the underlying concrete or from the reflection of newer cracks which have occurred since overlaying or may be due to a loss of bond between the overlay and the underlying concrete. The exact proportions of these distress mechanisms are difficult to determine; however, careful examination of the distressed areas and "engineering judgment" suggest that most of the defects have occurred due to the reflection of cracks which existed in the underlying pavement prior to overlaying.

A further example is provided by an overlaid section of IH-10 near Beaumont, Texas. This section of road was overlaid with 3 1/4 inches of asphalt in 1975, at which time the pavement had carried approximately 5 million 18-kip ESAL's during its 13 year life. In a 1974 condition survey, the pavement had approximately 11 defects per mile, which indicated very little life remaining.

From 1975 to 1979 the pavement carried approximately 3 million 18-kip ESAL's and, in a condition survey conducted along the overlaid pavement in

1979, an average of six defects per mile were counted. Thus, the life of this pavement has also been extended significantly with an overlay which provides very little additional structural support.

These data indicate that, although the remaining life of an unoverlaid pavement may be negligible, the application of an overlay may provide a significant increase in the pavement life.

Causes of Increased Pavement Life

The increase in rigid pavement life caused by overlaying may be explained by examining the differences between the fatigue curves developed from laboratory and field data. These differences are examined for non-overlaid pavements in Chapter 5 and may be reexamined for overlaid CRC pavements.

At low stress levels the difference between the fatigue curves is primarily due to the stress concentration factors which exist in the field. Many of these factors may be reduced significantly by overlaying.

(1) An overlay may provide an effective seal against moisture incursion and the resulting erosion of subgrade support.

(2) An overlay may reduce warping stresses because of the reduced vertical temperature differentials expected at some depth below the surface.

(3) An asphaltic overlay may be relatively soft at high temperatures resulting in the resealing of reflection cracks and a reduction in dynamic loads which may occur at pavement discontinuities.

These factors should be taken into account in a pavement design procedure because ignoring them may lead to extremely conservative design. For example, use of RPOD2 for analysis of the section of IH-45 in Walker County mentioned previously resulted in an asphalt concrete overlay thickness of approximately 10 inches to carry the 5 million 18-kip ESAL applications already applied since overlaying. This is far in excess of the 2 1/2 to 6 inch overlay which is performing successfully on this pavement to date.

This excessive overlay thickness results from the analysis because the procedure models the old pavement as a single subgrade layer when it has a negligible amount of remaining life. The condition survey data of overlaid pavements relative to the RPOD2 design predictions and the reduction in stress concentration factors mentioned earlier indicate the need for an additional fatigue curve for use with overlaid pavements.

Estimation of a Fatigue Curve for Use with Overlaid Rigid Pavements

The reduction in the stress concentration factors due to overlaying indicates that a fatigue curve for use with overlaid pavements should lie between existing laboratory and field fatigue curves. Unfortunately no data exist regarding the type and quantity of distress which constitutes "failure" of overlaid rigid pavements and, thus, a fatigue relationship cannot be developed from field data. However, such a fatigue curve may be estimated based on existing experience with overlaid pavements and the curve may be improved as additional data become available from ongoing condition surveys.

As an upper bound for the fatigue equation, it appears reasonable that a CRC pavement overlaid with asphalt concrete should not last as long as a new CRC pavement with an initial thickness equal to the total pavement plus

overlay thickness. For example, a 14-inch CRC pavement should last longer than an 8-inch CRC pavement overlaid with 6 inches of asphalt concrete. The tensile stresses in the CRC layer for both these cases, and the fatigue life of the full depth CRC pavement are plotted on Fig 6.1 for a number of thickness combinations. From the data plotted in this figure, a fatigue line was drawn below the upper bound as defined above so that it would provide reasonable predictions of the future lives of existing asphalt overlaid CRC pavements. The predictions of the fatigue equation are checked against the data obtained from the two overlaid projects mentioned previously, in Appendix A. The equation of this line is

$$N = 43000(f/\sigma)^{3.2} \qquad (6.2)$$

The inclusion of an additional fatigue equation in the design procedure does not complicate the procedure excessively and should provide accurate predictions of the fatigue lives of overlaid CRC pavements.

Use of an Additional Fatigue Equation in the Overlay Design Procedure

If an additional fatigue equation is to be used in the RPOD2 design procedure, some modifications will be required. The steps in an asphalt overlay design for a CRC pavement will now progress as follows:

(1) The use of a failure condition as defined in Chapter 5 and the results of the CRCP condition surveys conducted in Texas provide a rational method for estimating pavement remaining life. The use of condition survey data in the estimation of remaining life ensures

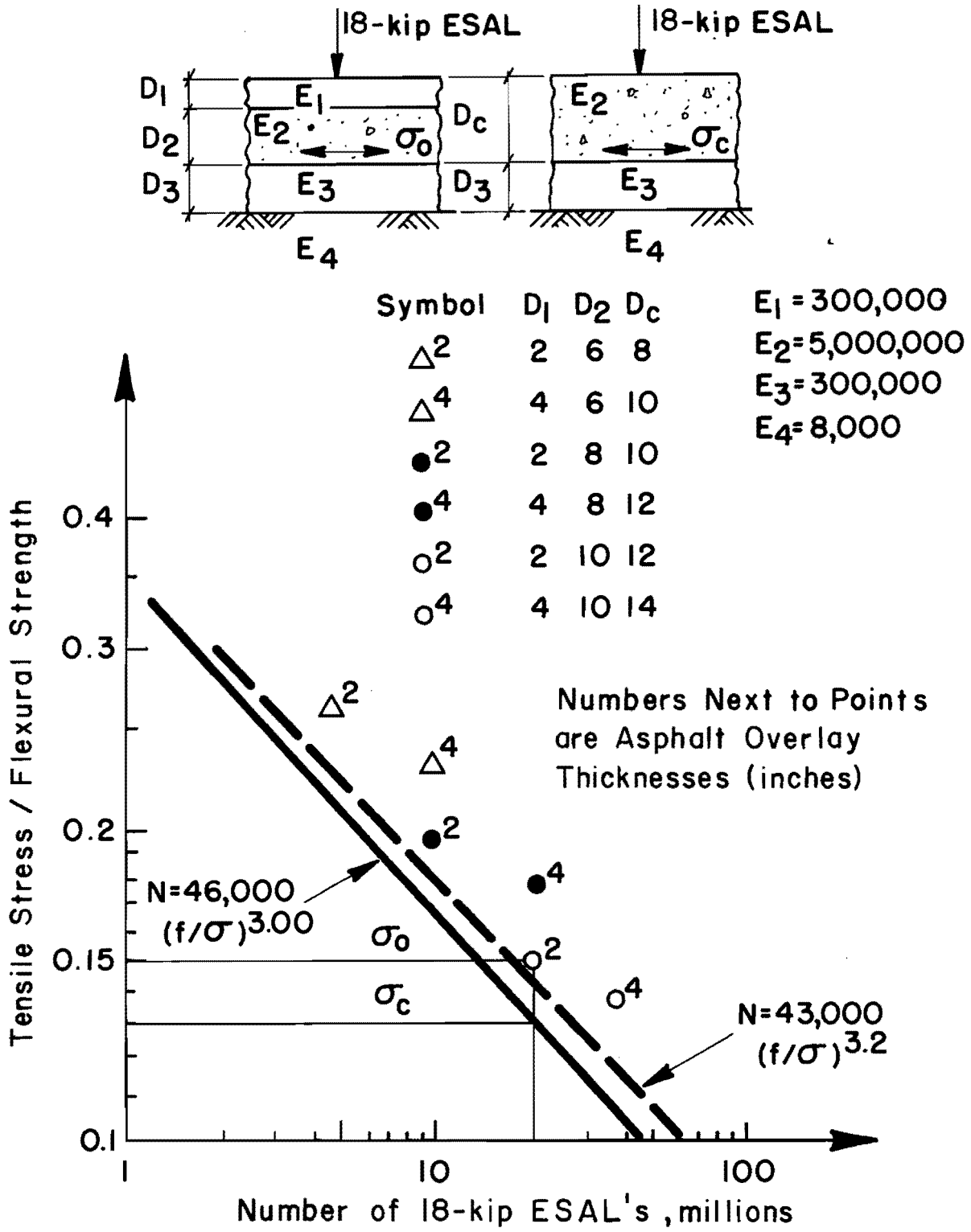

Fig 6.1. Figure showing the non-overlaid and overlaid rigid pavement fatigue curves and calculated points which provide the upper rounds for the position of the overlaid fatigue curve.

that many of the inaccuracies associated with fatigue life prediction are eliminated from this procedure. A number of calculations may now be used to arrive at the final estimate of the pavement remaining life.

(2) The first calculation uses condition survey data in order to ascertain whether the unoverlaid pavement has zero remaining life or is approaching or has gone beyond this point. When the number of defects per mile equals the pavement age in years or when the rate of defect occurrence is equal to three per year, then the unoverlaid pavement has no remaining life.

(3) The second calculation uses the tensile stresses in the pavement layer under an 18-kip ESAL as computed by layered theory and the number of past 18-kip ESAL's in the rigid pavement fatigue equation to determine the pavement's remaining life. If the remaining life calculated using this approach is significantly different from that estimated from condition survey data, then the layer stiffnesses and past traffic applications should be checked and modified to insure that this calculation provides results similar to those obtained from the condition survey data. For example, a traffic directional distribution factor may be applied or the estimates of surface and subbase layer moduli may be changed but still retain the same basin slope to bring the remaining life calculations closer to the condition survey estimates.

(4) The third calculation involves the use of the overlaid pavement fatigue equation and the final stresses and number of 18-kip ESAL's as obtained above, to obtain estimates of the remaining life of the overlaid pavement.

An example of these calculations is as follows:

Date: 1980.

Pavement age: 16 years.

Defects per mile: 1974 - 7, 1978 - 20.

Therefore, the remaining life of the unoverlaid pavement is §0.

Tensile stress in the bottom of the rigid pavement layer (using the first estimate of layer moduli): 90 psi.

Past traffic: 10 million 18-kip ESAL's in one direction.

Therefore, using a flexural strength of 650 psi and Eq 5.1, the remaining life of the unoverlaid pavement is found to be 0.

Now adjust the surface and subbase moduli to increase the stresses in the surface layer to 100 psi and, based on the directional distribution of failures in the roadway, adjust the past traffic to 13 million 18-kip ESAL's.

Now, from Eq 5.2, the unoverlaid pavement's remaining life is approaching zero. Use these final values of stress and number of applications in the fatigue equation for overlaid CRC pavements (Eq 6.2) to calculate the remaining life of the overlaid pavement. From this calculation the remaining life is 26 percent.

This procedure should provide predictions of overlay life based on present pavement condition and, provided the overlay is thick enough to withstand reflection cracking, these calculations should provide reasonable estimates of pavement life. Further calculations are shown in Appendix A for some of the overlay projects mentioned previously. It is recommended that this type of overlay design procedure be used for all overlays on CRC pavements which will significantly improve the moisture environment of the overlaid pavement. All overlays constructed to a width which significantly exceeds that of the main lanes fall into this category. This procedure should not be used for overlays on jointed concrete pavement, because of the severe reflection cracking problem which exists along these pavements.

SUGGESTED MODIFICATIONS TO THE RPOD2 DESIGN PROCEDURE REGARDING PCC OVERLAYS ON RIGID PAVEMENTS

The implementation of the RPOD2 design procedure on a project along IH-30 in Hunt County, Texas, resulted in some suggested improvements to the procedure for rigid overlay design. These suggestions are mainly centered around the modulus to be used for the old rigid pavement layer with no remaining life.

The Effective Stiffness of a Cracked Pavement Layer

The RPOD2 design procedure assigns a modulus of 500,000 psi to a rigid pavement layer when no remaining life is left in that layer. This figure was obtained by fitting computed and measured deflections for cracked pavement layers at the AASHO Road Test. The variety of rigid pavement types and the

availability of Dynaflect deflection data in Texas suggest that this type of deflection fitting be done on each project before overlaying. For example, the reinforcing steel in CRC pavements may reduce the deflection of this pavement type near discontinuities, relative to the pavements at the AASHO Road Test, whereas severely spalled joints with little load transfer may result in higher deflections in jointed concrete pavements than those obtained at the Road Test.

The most severe stresses in the overlay will occur immediately above discontinuities in the underlying pavement. For this reason, it may be advisable to characterize a pavement with no remaining life by fitting layered theory deflection basins to those obtained in the field at pavement discontinuities.

At present, other than the deflection data obtained on the project along IH-30 in Hunt County, no significant amount of deflection data at pavement discontinuities exists in Texas. However, this type of analysis may warrant further investigation and, to this end, the analysis procedure used on the above project will be presented.

Analysis of Jointed Concrete Pavement in Hunt County, Texas

A 15-mile section of 15-foot jointed concrete pavement along IH-30 in Hunt County required an overlay to withstand approximately 30 million 18-kip ESAL's during the next 20 years. The "wrinkled tin" joints had severely spalled and the pavement riding quality was such that an overlay was required. The past traffic was approximately 12 million 18-kip ESAL's.

Dynaflect deflections were taken at joint and midspan every 100 feet and the joint and midspan deflections were later separated into groups for

independent analysis. In this regard the deflection measurements were separated using as a switch a computer program which used the comments regarding each deflection measurement. This type of separation could be accomplished easily provided standardized comments are used to indicate deflections measured at the different pavement discontinuities.

Estimation of material properties using the midspan deflection data and subsequent fatigue analysis indicated that the pavement had no remaining life. Condition surveys of the pavement also showed that approximately 10 percent of the slabs were cracked, which further reinforced this observation. Some of the most severe stresses in the overlay would occur immediately above the joints and, thus, the joint deflection basin slopes were used to separate the project into sections. An unbonded CRC overlay was considered to be optimum for resisting reflection cracking and for carrying the large number of 18-kip equivalencies expected in the future.

A separate analysis was conducted to determine the effect of the subgrade on the stresses in the overlay and, as indicated in Fig 6.2, the subgrade modulus had a negligible effect on these stresses. A subgrade modulus of 6000 psi was thus chosen to represent the clays in the area.

A basin fitting technique was used to estimate the effective layer moduli, which resulted in the same basin slope as computed using layered theory as the higher deflection basin slopes measured on the project. As indicated in Chapter 2, a number of combinations of surface and subbase modulus would result in the same basin slopes, and, thus, engineering judgment was used to obtain the layer moduli for various basin slopes, as indicated in Table A.14.

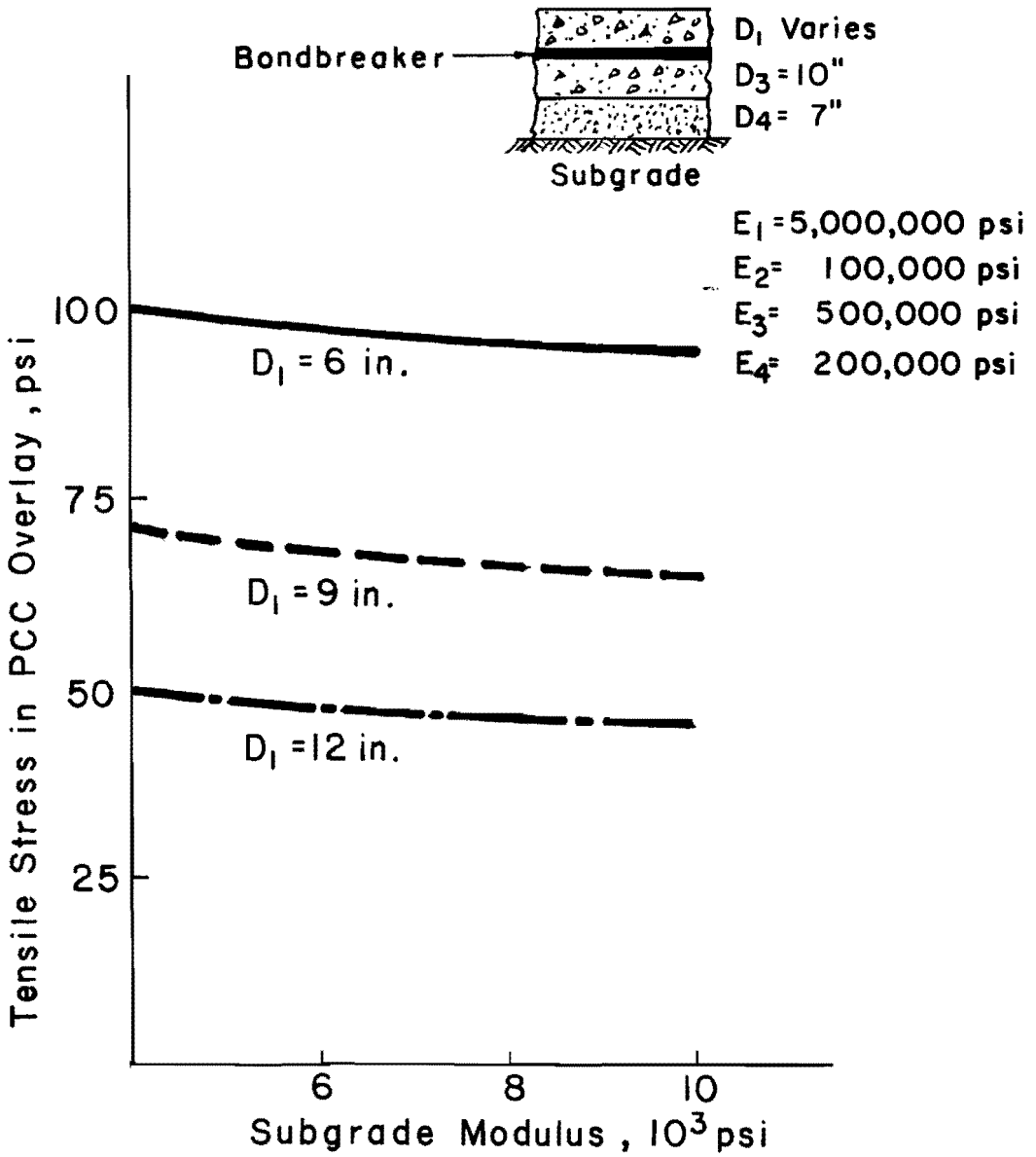

Fig 6.2. The effect of varying subgrade modulus on the tensile stresses in the bottom of an unbonded PCC overlay.

The modulus of the existing rigid pavement had the most severe effect on the tensile stresses in the overlay and, thus, a different surface modulus was used to correspond to each basin slope.

The cumulative distributions of the deflection basin slopes as produced by the program MODE were used to estimate the number of joints which had a deflection basin slope greater than the design slope and might thus require repair.

SUMMARY

These suggestions regarding modifications to the RPOD2 design procedure should make overlay designs more mechanistic and make more use of deflections and condition survey data than has been done in the past. Asphaltic overlays and full width PCC overlays of CRC pavements are designed by making use of condition survey data to predict the remaining life of the pavement and by then increasing the remaining life of the pavement to account for the overlaid condition. Rigid overlays on rigid pavements are designed using an effective modulus for the existing rigid pavement determined from deflection measurements when no remaining life is left in the layer.

CHAPTER 7. COMPILATION OF STUDY RESULTS INTO AN OVERLAY DESIGN PROCEDURE

This report presents some improvements to the RPOD2 design procedure which have arisen from its trial use on some Texas highways. Extensive use is made of Dynaflect deflections and condition survey data obtained along CRC pavements in Texas. This chapter summarizes the more important findings of the report and makes recommendations regarding the implementation thereof.

MATERIALS CHARACTERIZATION

The existing pavement materials are characterized by making use of deflection measurements and laboratory testing. The Indirect Tensile test is used to obtain initial estimates of the moduli of the bound pavement layers and the Resilient Modulus test is used to obtain an indication of the stress sensitivity of the subgrade. Dynaflect deflections are used to improve these estimates of the bound layer moduli and are also used to calculate the effective subgrade modulus under the Dynaflect load. This is made possible because, as indicated in Fig 2.4, the surface and subbase moduli have very little effect on the Dynaflect sensor 5 deflection. This deflection is thus indicative of the subgrade modulus. Figure 2.5 has been prepared from layered theory analysis to determine the subgrade modulus under the Dynaflect load from the sensor 5 deflection.

The Dynaflect deflection basin slope, or sensor 1 minus sensor 5, is indicative of the moduli of the upper, bound, pavement layers. However, a number of combinations of layer moduli exist which will produce the same deflection basin slope and, thus, laboratory testing is required to obtain initial estimates of these moduli. Figures 2.6 to 2.9 have been prepared from layered theory analysis to determine the upper layer moduli given a subgrade modulus and deflection basin slope.

The subgrade thickness has a significant effect on the deflections computed using layered theory. Thus, Fig 2.12 has been prepared from regression analysis of layered theory results to indicate the reduction required in the subgrade modulus, calculated from the sensor 5 deflection, if a rigid foundation exists at some depth.

Deflection Measurements

Because of the increased reliance on deflection measurements for the materials characterization phase of the design procedure, it is recommended that deflections be taken at every 50 feet for CRC pavements and at the joint and midspan at every 100 feet along jointed concrete pavements. Wherever possible, approximately every second deflection measurement made along CRC pavements should be taken at a pavement discontinuity, such as a punch out or patch. This will facilitate the estimation of an effective pavement modulus for the CRC pavement layer with no remaining life and will give some indication of the measures to be taken to avoid reflective cracking in a subsequent overlay.

The deflection measurements made at the different pavement discontinuities may be distinguished by the inclusion of a standard

abbreviation in the first three columns of the space reserved for comments on the deflection data field sheet. Suggested abbreviations such as have been used before in Texas are

MPO - minor punch out

SPO - severe punch out

PCP - Portland cement concrete patch

ACP - asphalt concrete patch

MID - midspan deflection

JNT - joint deflection

CRK - deflection at a crack

The data can then be sorted to determine the effects of the various distress manifestations on the deflections, and the program MODE can be used to obtain the deflection distributions associated with each distress type.

Selection of Pavement Design Sections

The pavement should then be divided into sections based on deflection measurements and condition survey data, and each section should be analyzed separately to provide the optimum overlay thickness. The deflection measurements used for this purpose depend on the condition of the existing pavement and on the type of overlay envisaged. If a pavement has some remaining life, or if an asphalt overlay is envisaged, the roadway is divided into sections based on the deflections taken at a midspan-type position.

Both the Dynaflect sensor 5 deflections and the deflection basin slopes are used to determine the section limits. These deflection parameters are plotted against the length of the road, using the PLOT4 program, which is an

improved version of the PLOT program documented in Ref 5. Every section limit based on the sensor 5 deflection should also coincide with a section limit of the deflection basin slopes because of the effect which the sensor 5 deflection has on this parameter.

Because the deflections are not normally distributed, the modal deflection parameters in each section are used to determine the layer moduli for that section, as indicated earlier. To this end program MODE, which will provide statistical information about the different deflection parameters, has been prepared.

After having characterized the upper layer moduli using the modal deflection parameters, the subgrade modulus should be reduced for design to that modulus which corresponds to the 90th percentile sensor 5 deflection within a section. The stress sensitivity of the subgrade modulus should then be taken into account, as indicated in Ref 5, by using the results of Resilient Modulus testing.

If the pavement has no remaining life and if a PCC overlay is envisaged, then the deflections taken at distress manifestations or at pavement discontinuities should be used to determine the section limits. The most severe stresses in the overlay will occur at these positions, and, thus, the existing pavement may be characterized as having an effective modulus, which would result in the same basin slope as obtained at these positions when analyzed using layered theory. Basin fitting techniques may thus be used to calculate these effective moduli.

If the deflection basin slopes at some of the distress manifestations or pavement discontinuities are far greater than the design slopes used, then it may be advisable to seek out these areas with deflection measuring equipment and to repair them before overlaying.

This material characterization procedure should result in pavement layer moduli which are representative of the actual field conditions. However, in order to obtain an estimate of the seasonal variation and the long-term behavior of the different deflection parameters, it is recommended that some long-term deflection measurements be made at some selected locations. These sections should encompass the various distress manifestations and pavement discontinuities mentioned earlier.

STRESSES AT PAVEMENT DISCONTINUITIES

A finite element analysis was conducted to determine whether the tensile stresses in pavements at cracks exceeded the interior stresses as obtained from layered theory. This analysis showed that only when the load transfer at the crack had reduced to the extent that the deflection at the crack exceeded 1.5 times the uncracked deflection did the tensile stresses parallel to the crack exceed the interior stresses. The stress deflection relationship obtained from this analysis is shown in Fig 3.10.

A similar analysis was conducted to determine the effects of cracks on the stresses in the pavement for an edge loading condition. This analysis also indicated that, once the edge deflection exceeded approximately 1.5 times the uncracked edge deflection, the tensile stresses in the surface of the pavement would exceed the uncracked edge stresses in the bottom of the rigid pavement layer. These results are shown in Figs 3.14 and 3.15 for different subgrade stiffnesses.

From this analysis, it is recommended that, if a significant proportion of the sensor 1 deflection measured within a section of road exceeds 1.5

times the modal sensor 1 deflection, the stresses in the pavement calculated using layered theory be increased in accordance with the figures.

STRESSES IN OVERLAYS ABOVE UNDERLYING DISCONTINUITIES

In an attempt to analyze reflection cracking, a finite element analysis was conducted on asphalt overlaid rigid pavements. The results from this analysis were not entirely conclusive because of some difficulties in accurately modelling this structure. It is therefore, strongly recommended that an experimental analysis of reflection cracking be undertaken.

FATIGUE OF EXISTING CONCRETE PAVEMENTS

Failure of rigid pavements was defined as that condition where additional heavy traffic applications would result in a rapid increase in distress. Examination of the AASHO Road Test data indicated that, for jointed pavements, this distress condition was reached when the cracking index was 50 feet per 1,000 square feet. Examination of condition survey data obtained from Texas CRC pavements indicated that this distress condition corresponded approximately to a rate of defect (punch outs and patches) occurrence of three defects per mile per year. Economic analysis confirmed that it was generally more economical to overlay before this rate of defect occurrence was exceeded.

Furthermore, this rate generally occurred when the number of defects per mile in the pavement equaled the pavement age in years. It is, therefore,

recommended that this latter criterion be used to determine whether a pavement section has significant remaining life.

The fatigue equation developed from the AASHO Road Test data in Ref 3 was reevaluated using fewer simplifying assumptions. Deflection measurements were used to characterize the subgrade for the sections for different seasons, and the corresponding tensile stresses in the bottom of the rigid pavement layer were calculated using layered theory. The transverse axle load distribution at the Road Test and finite element analysis were used to approximate the number of applications applied at an increased stress due to traffic loadings close to the pavement edge. The seasonal interior and edge stresses were then converted to an equivalent stress, which would do the same amount of damage to the pavement with a number of applications equal to the total number of applications of the other stress levels. This was done using the fatigue equation developed in Ref 3.

Separate regression analyses were performed using the number of axles to failure (as defined earlier) against the equivalent tensile stresses in rigid pavement layer for single and tandem axles. From this it became apparent that the number of tandem axle applications had to be increased by 1.9 to obtain the same stress-applications-to-failure relationship as obtained with single axles. It is, therefore, recommended that this factor be used whenever Miner's hypothesis is used to compute the damage done to rigid pavements by tandem axle applications.

This process was repeated until the fatigue equation used to compute the equivalent stress was similar to the fatigue equation developed from the regression analysis. The final fatigue equation, which is recommended for use in rigid pavement, is in Fig 5.10.

This fatigue equation correlates reasonably with failure of some selected CRC pavements in Texas, as shown in Fig 5.10, and can thus be used with reasonable confidence in further pavement designs.

FATIGUE OF OVERLAID RIGID PAVEMENTS

The analytical modelling of existing pavements by the RPOD2 design procedure was examined in the light of condition survey results of asphalt overlaid CRC pavements and a recent PCC overlay design carried out on a jointed concrete pavement in Texas.

Condition surveys of asphalt overlaid CRC pavements indicate that relatively thin overlays (3 to 6 inches) may significantly extend the pavement's life. For example, CRC pavements which had already failed according to the condition survey criterion mentioned previously would carry traffic significantly in excess of the pavement life predictions made by RPOD2. This occurs primarily because RPOD2 models the existing pavement with no remaining life as an equivalent subgrade layer, based on the Dynaflect sensor 1 deflections.

This modelling is probably more severe than the field condition and hence the discrepancy. The recommended alternative to this form of modelling is to increase the remaining life of the overlaid pavement. This increase in remaining life can be explained by examining the differences between the fatigue curves developed from laboratory and field data. At low stress levels the laboratory data predict far more allowable applications than the field data. These differences may be ascribed to stress concentrating factors which are present in the field. Many of these factors, such as

moisture incursion and the resulting erosion of subgrade support, and warping stresses caused by vertical temperature differentials, are reduced considerably by overlaying.

A tentative fatigue equation for use with overlaid rigid pavements is thus presented in Fig 6.1. This curve has been estimated using the existing condition survey data on asphalt overlaid pavements and the subjective judgement that a new PCC pavement equal in thickness to the total overlaid pavement thickness will last longer than the overlaid pavement.

The RPOD2 design procedure assigns a modulus of 500,000 psi to a cracked rigid pavement layer with no remaining life. This value was obtained by analyzing the maximum deflections obtained on cracked pavements at the AASHO Road Test using plate theory. It is recommended that this modulus of the cracked pavement layer rather be obtained from deflection basin fitting procedures. The deflection basin slopes at pavement distress manifestations and pavement discontinuities may be compared to those obtained from layered theory analysis. The surface and subbase moduli used in the analysis may then be varied until the measured and computed basin slopes are equal.

In order to avoid reflection cracking, PCC overlays are very often unbonded, and in this case the subgrade modulus has very little effect on the stresses in the overlay, as indicated in Fig 6.2. Thus an estimated value of subgrade modulus may be used throughout this analysis. Results of some basin fitting techniques applied to a 10-mile jointed pavement with severely spalled joints are shown in Table A.14.

The above improvements to the RPOD2 design procedure are being incorporated in the RPRDS program, which is currently being developed at The University of Texas (Ref 12). This program analyzes various alternate pavement rehabilitation strategies, using mechanistic procedures, in order to

obtain an optimum strategy with regard to total costs. Continued collection of condition survey data and deflections, coupled with further implementation of the above procedures, should serve to provide continuous improvements to these procedures.

CHAPTER 8. CONCLUSIONS AND RECOMMENDATIONS

This report suggests improvements to a number of facets of the RPOD2 design procedure and it is recommended that these improvements be implemented in future design. The findings in the report may be listed as follows:

(1) Pavement materials are characterized using material tests and deflection data so that the predicted fatigue life of the existing pavement corresponds to condition survey results.

(2) Cracks in an existing rigid pavement do not create stresses in the rigid pavement layer which exceed those predicted by layered theory until the deflections at cracks significantly exceed those measured at an uncracked interior or edge condition.

(3) Reflection stresses in an asphalt overlay on rigid pavements are difficult to model analytically and laboratory testing is recommended for this purpose.

(4) A fatigue equation derived from AASHO Road Test data provides reasonable estimates of pavement life and is recommended for future use.

(5) The RPOD2 design procedure significantly underpredicts the lives of overlaid CRC pavements when little remaining life is left in the original pavement. An exogenous fatigue equation, which improves the correlation of the design predictions to condition survey data,

is recommended for use until additional data become available from condition surveys of these pavements.

(6) The effective moduli of overlaid rigid pavements may be determined from deflection measurements, thus eliminating the use of a standard effective modulus for all pavement types and distress conditions.

The majority of the improvements recommended in this report resulted from the implementation of existing procedures. Future application of these recommendations may result in additional improvements as more data become available.

REFERENCES

1. McCullough, B. F., "A Pavement Overlay Design System Considering Wheel Loads, Temperature Changes, and Performance," Institute of Transportation and Traffic Engineering Graduate Report, University of California, Berkeley, July 1969.

2. Hilsdorf, H. K., and C. E. Kesler, "Fatigue Strength of Concrete Under Varying Flexural Stresses," Proceedings, Vol 63, American Concrete Institute, October 1966, pp 1059-1075.

3. Treybig, Harvey J., B. F. McCullough, Phil Smith, and Harold von Quintus, "Overlay Design and Reflection Cracking Analysis for Rigid Pavements, Volume 1 - Development of New Design Criteria," Research Report FHWA-RD-77-66, Federal Highway Administration, Washington, D.C., August 1977.

4. Treybig, Harvey J., B. F. McCullough, Phil Smith, and Harold von Quintus, "Overlay Design and Reflection Cracking Analysis for Rigid Pavements, Volume 2 - Design Procedures," Research Report FHWA-RD-77-67, Federal Highway Administration, Washington, D.C., August 1977.

5. Schnitter, Otto, W. R. Hudson, and B. F. McCullough, "A Rigid Pavement Overlay Design Procedure for Texas SDHPT," Research Report 177-13, Center for Highway Research, The University of Texas at Austin, May 1978.

6. Gutierrez de Velasco, M., and B. F. McCullough, "Summary Report for 1978 CRCP Condition Survey in Texas," Research Report 177-20, Center for Highway Research, The University of Texas at Austin, March 1980.

7. Noble, C. S., and B. F. McCullough, "Distress Prediction Models for CRCP," Research Report 177-21, Center for Transportation Research, The University of Texas at Austin, December 1979.

8. Majidzadeh, Kamran, "Pavement Condition Evaluation Utilizing Dynamic Deflection Measurements," Research Report No. OHIO-DOT-13-77 Federal Highway Administration, Washington, D.C., June 1977.

9. Barksdale, R. D., and R.G. Hicks, "Material Characterization and Layered Theory for Use in Fatigue Analysis," Highway Research Board, Special Report No. 140, Washington, D.C., 1973.

10. Scrivner, F. H., and C. H. Michalak, "Linear Elastic Layer Theory as a Model of Displacement Measured within and Beneath Flexible Pavement Structures Loaded by the Dynaflect," Research Report No. 123-25, THD, CFHR, TTI, College Station, Texas August 1974.

11. Murdock, J. W., and C. E. Kesler, "Effect of Range of Stress on Fatigue Strength of Plain Concrete Beams," Proceedings, Vol 55, American Concrete Institute, August 1958, pp 222-231.

12. Seeds, S. B., "A Design System for Rigid Pavement Rehabilitation," Master's Thesis, The University of Texas at Austin, May 1980.

13. Seeds, S. B., B. F. McCullough, M. Gutierrez de Velasco, and W. R. Hudson, "Implementation of the New Texas SDHPT Overlay and Reinforcement Design Procedures," a paper presented at the Transportation Research Board Annual Meeting, Washington D. C., January 1980.

14. Ullditz, P., "Overlay and Stage by Stage Design," Volume 1, Fourther International Conference on the Structural Design of Asphalt Pavements, Ann Arbor, Michigan, January 1977.

15. Koole, R. C., "Overlay Design Based on Falling Weight Deflections Measurements," Research Record 700, Transportation Research Board, Washington, D. C., 1979.

16. Paterson, W. D. O., "Behavior of Pavements Containing a Cement-Treated Crushed Stone Base under Heavy Vehicle Simulator Testing," National Institute for Transportation and Road Research, CSIR, South Africa, July 1977.

17. Michalak, C. H., D. Y. Lu, and G. W. Truman, "Determining Stiffness Coefficients and Elastic Moduli of Pavement Materials From Dynamic Deflections," Research Report 207-1, Texas Transportation Institute, Texas A and M University, College Station, Texas, November 1976.

18. Anagnos, J. N., and T. W. Kennedy, "Practical Method of Conducting the Indirect Tensile Test," Research Report 98-10, Center for Highway Research, The University of Texas at Austin, August 1972.

19. Hudson, W. Ronald, and Thomas W. Kennedy, "An Indirect Tensile Test for Stabilized Materials," Research Report 98-1, Center for Highway Research, The University of Texas at Austin, January 1968.

20. Crumley, J. A., and T. W. Kennedy, "Fatigue and Repeated-Load Elastic Characteristics of Inservice Portland Cement Concrete," Research Report 183-9, Center for Highway Research, The University of Texas at Austin, June 1977.

21. Treybig, Harvey J., B. Frank McCullough, and W. Ronald Hudson, "Continuously Reinforced Concrete Airfield Pavement - Volume 1, Tests on Existing Pavement and Synthesis of Design Methods," Report No. FAA-RD-73-33-1, Prepared for Air Force Weapons Laboratory, U.S. Army Engineers Waterways Experiment Station and Federal Aviation Administration, May 1974.

22. "Test Procedures for Characterizing Dynamic Stress - Strain Properties of Pavement Materials," Transportation Research Board, Special Report, No. 162, Washington, D. C., 1975.

23. Yoder, E. J., and M. W. Witczak, Principles of Pavement Design, 2nd edition, John Wiley and Sons, New York, 1975.

24. Monismith, C. L., "Pavement Design: The Fatigue Subsystem," Highway Research Board, Special Report 140, January 1973.

25. "The AASHO Road Test, Proceedings of a Conference held May 16-18, 1962, St. Louis, Mo.," Special Report 73, Highway Research Board, Washington, D. C., 1962.

26. Nair, K., and Chang, C-Y, "Flexible Pavement Design and Management - Materials Characterization," NCHRP 140, 1973.

27. McCullough, B. F., and H. J. Treybig, "A Statewide Deflection Study of Continuously Reinforced Concrete Pavement in Texas," Technical Report No. 46-5, Texas Highway Department, August 1966.

28. Cochran, W. G., Sampling Techniques, John Wiley and Sons, Inc., 1963.

29. Hudson, W. R., and Hudson Matlock, "Discontinuous Orthotropic Plates and Pavement Slabs," Research Report 56-6, Center for Highway Research, The University of Texas, Austin, May 1966.

30. Treybig, Harvey J., W. R. Hudson, and Adnan Abou-Ayyash, "Application of Slab Analysis Methods to Rigid Pavement Problems," Research Report 56-26, Center for Highway Research, The University of Texas at Austin, May 1972.

31. McCullough, B. F., J. C. M. Ma, and C. S. Noble, "Limiting Criteria for the Design of CRCP," Research Report 177-17, Center for Highway Research, The University of Texas at Austin, August 1979.

32. Coetzee, N. F., and C. L. Monismith, "Analytical Study of Minimization of Reflection Cracking in Asphalt Concrete Overlays by Use of a Rubber - Asphalt Interlayer," Research Record 700, Transportation Research Board, Washington D.C., 1979.

33. La Coursiere, S. A., M. I. Darter, and S. A. Smiley, "Performance of Continuously Reinforced Concrete Pavement in Illinois," Report No. FHWA-IL-UI-172, Federal Highway Administration, Washington, D. C., December 1978.

34. Luther, Michael S., Kamran Majidzadeh, and Che-Wei Chang, "Mechanistic Investigation of Reflection Cracking of Asphalt Overlays," Transportation Research Record No. 572, Transportation Research Board, 1976.

35. Strauss, P. J., B. F. McCullough, and W. R. Hudson, "Continuously Reinforced Concrete Pavement: Structural Performance and Design/Construction Variables," Research Report 177-7, Center for Highway Research, The University of Texas at Austin, May 1977.

36. McGhee, K. H., "Attempts to Reduce Reflection Cracking of Bituminous Concrete Overlays on Portland Cement Concrete Pavements," Research Record 700, Transportation Research Board, Washington, D. C., 1979.

37. Jackson, T. J., "Analysis of the Performance of Asphaltic Concrete Pavement Overlays for Maintenance Purposes," Term Paper CE377K, The University of Texas at Austin, December 1979.

38. McCullough, B. F., and Thomas P. Chesney, "Sixteenth Year Progress Report on Experimental Continuously Reinforced Concrete Pavement in Walker County," Report 177-6, Center for Highway Research, The University of Texas at Austin, April 1976.

39. "The AASHO Road Test," Special Report 61A, "History and Description of Project," Highway Research Board, 1961.

40. "The AASHO Road Test, Report 3, Traffic Operation and Pavement Maintenance," Special Report 61C, Highway Research Board, Washington, D. C., 1962.

41. "The AASHO Road Test, Report 5, Pavement Research," Special Report 61E, Highway Research Board, 1962.

42. "The AASHO Road Test," Data Systems of the AASHO Road Test No. DS-4292 R - History Plots for Rigid Pavement Test Sections, Highway Research Board,

43. Austin Research Engineers, Inc., "Asphalt Concrete Overlays of Flexible Pavements - Volume 1, Development of New Design Criteria," Research Report No. FHWA-RD-75-75, Federal Highway Administration, Washington, D. C., June 1975.

44. Austin Research Engineers, Inc., "Asphalt Concrete Overlays of Flexible Pavements, Volume 2 - Design Procedures," Report FHWA-RD-75-76, August 1975.

45. Porter, Byron P., and Thomas W. Kennedy, "Comparison of Fatigue Test Methods for Asphaltic Materials," Research Report 183-4, Center for Highway Research, The University of Texas at Austin, April 1975.

46. Navarro, D., and Thomas W. Kennedy, "Fatigue and Repeated-Load Elastic Characteristics of In-Service Asphalt-Treated Materials," Research Report 183-2, Center for Highway Research, The University of Texas at Austin, January 1975.

47. Yimprasert P., and B. F. McCullough, "Fatigue and Stress Analysis Concepts for Modifying the Rigid Pavement Design System," Research Report 123-16, Center for Highway Research, The University of Texas at Austin, January 1973.

48. Machemehl, R. B., Clyde E. Lee, and C. M. Walton, "Truck Weight Surveys by In-Motion-Weighing," Research Report 181-1F, Center for Highway Research, The University of Texas at Austin, September 1975.

49. Vesic, A. S., and S. K. Saxena, "Analysis of Structural Behavior of AASHO Road Test Rigid Pavements," National Cooperative Highway Research Program, Report 97, 1970.

APPENDIX A

EXAMPLES OF OVERLAY DESIGNS

EXAMPLES OF OVERLAY DESIGNS

Overlays designed and existing fatigue lives checked according to the recommendations of this report:

1. IH-10 Near Beaumont, Jefferson County
2. IH-10 Near Columbus, Colorado County
3. IH-10 Near Beaumont, Jefferson County
4. IH-45 Near Huntsville, Walker County
5. IH-30 Near Greenville, Hunt County

CONCRETE PAVEMENT OVERLAY DESIGN

I. PROJECT IDENTIFICATION INFORMATION

DISTRICT	COUNTY	HIGHWAY	CONTROL	SEC	JOB	CFHR No
20	Jefferson	IH-10	739	2		2009

From Mile Post 833.3 at the Hamshire exit to Mile Post 838.6 near Fannett.

SCOPE

Design an AC overlay for a 10-year design life.

II. PAVEMENT STRUCTURES

EXISTING

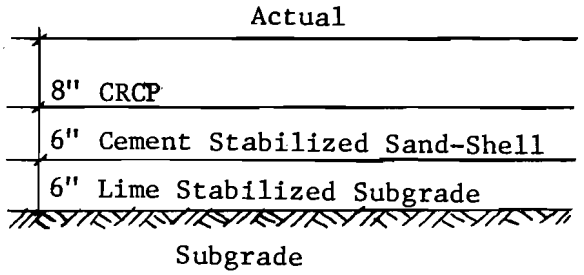

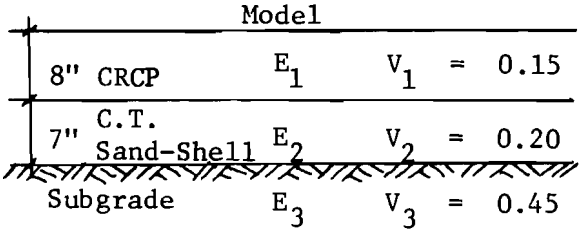

PROPOSED OVERLAID STRUCTURE

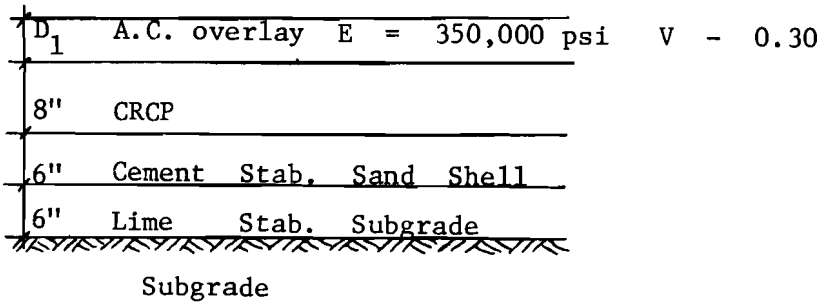

III. TRAFFIC

Age	Traffic in 18-kip ESAL'S.	
Years	Past to 1978	1980-1990
17	9×10^6	10×10^6

IV. DESIGN THICKNESSES

Section		Limits (Mile posts)	Design Thickness
WB	1	838.6 - 838.0	6.0"
	2	- 837.5	6.0"
	3	- 837.0	3.0"
	4	- 836.6	4.0"
	5	- 835.9	3.0"
	6	- 833.3	6.0"
	7	- 832.9	6.0"
EB	8	833.3 - 833.6	3.0"
	9	- 834.1	6.0"
	10	- 835.0	6.0"
	11	- 835.8	6.0"
	12	- 836.1	3.0"
	13	- 836.4	6.0"
	14	- 838.6	5.0"
	15	- 839.2	6.0"

V. DESIGN INFORMATION

A. MATERIALS CHARACTERIZATION

1. General Comments

Condition Survey Data

1974 and 1978 Data available.

Remaining Life From Condition Survey Data

Zero remaining life at $\pm$ 13 defects per mile.

Deflections Used For Section Selection (Depending on remaining life of existing pavement, pavement type and overlay type.)

Sensors and sensor 1 minus sensor 5.

Laboratory Testing (Tests done or assumptions made. M_r S_{sg} f_c)

Repeated indirect tensile tests for concrete and subbase moduli.

Resilient Modulus tests for subgrade modulus and stress sensitivity.

Assume f_c = 650 psi for fatigue calculations.

2. Layer Stiffnesses

Table from MODE.
Lab test results.
Table for calculating layer moduli based on deflection basin slopes, condition survey data and fatigue life.
90^{th} percentile subgrade modulus.
Moduli from deflection basin slopes at pavement joints or defects if no remaining life.

Table A.1 - Indirect tensile test results

Table A.2 - M_R results - Average S_{SG} = - 0.7

Table A.3 - Dynaflect deflection statistics for each section and modal subgrade modulus under the Dynaflect load.

Table A.4 - Calculation of pavement remaining life from condition survey data and correlation of material properties to these results using deflection basin slopes pavement stresses and a fatigue equation.

TABLE A.1

RESULTS OF INDIRECT TENSILE TESTS ON CONCRETE SURFACE AND CEMENT STABILIZED, OYSTER SHELL SUBBASE FROM IH-10 NEAR BEAUMONT (CONTROL 739-2, MP833-839)

CONCRETE SPECIMENS

SAMPLE No.	LOCATION	LOAD (pounds)	E (psi, millions)
2B SURFACE	WB MP837	1000	3.27
		2000	3.18
2B BOTTOM		1000	3.65
		2000	3.29
5C	WB MP835	1000	8.07
		2000	4.65
6A SURFACE	WB MP833.5	1000	4.20
		2000	3.05
6A MIDDLE		1000	6.58
		2000	4.50
10D SURFACE	EB MP835	1000	2.59
10D MIDDLE		1000	7.33
		2000	4.32
10D BOTTOM		1000	3.32
		2000	3.09
13E MIDDLE	EB MP838	1000	4.15
		2000	4.52
14F SURFACE	EB MP839	1000	4.98
		2000	3.60
14F MIDDLE		1000	2.92
		2000	2.98

AVERAGE ELASTIC MODULUS AT 1000 lb LOAD = 4.64

COEFFICIENT OF VARIATION C_V = 40%

AVERAGE ELASTIC MODULUS AT 2000 lb LOAD = 3.60

COEFFICIENT OF VARIATION C_V = 21%

Continued

TABLE A.1(CONTINUED)

STABILIZED SUBBASE

SAMPLE No.	LOCATION	LOAD (pounds)	E (psi, millions)
2B SURFACE	WB MP837	400	2.21
		600	2.31
2B MIDDLE		400	1.84
		600	1.31
5C MIDDLE	WB MP835	400	0.99
		600	1.77
6A MIDDLE	WB MP833.5	400	0.49
		600	0.47
6A BOTTOM		400	2.14
		600	1.66
14F MIDDLE	EB MP839	400	1.74
		600	1.58

AVERAGE ELASTIC MODULUS AT 400 lb LOAD = 1.57

COEFFICIENT OF VARIATION = 44%

AVERAGE ELASTIC MODULUS AT 600 lb LOAD = 1.52

COEFFICIENT OF VARIATION = 40%

TABLE A.2

RESULTS OF RESILIENT MODULUS TESTS ON SUBGRADE SAMPLES FROM IH-10 NEAR BEAUMONT (CONTROL 739-2)

SAMPLE No.	LOCATION	σ_3 (psi)	$\sigma_1 - \sigma_3$ (psi)	M_R (psi)	S_{SG}
2B TOP	WB MP837	2	1	3350	0.0
			2	1340	
			3	1245	
			4	1390	
			5	1375	
2B BOTTOM		1	1	9830	-0.11
			2	3350	
			3	3350	
			4	3040	
			5	3000	
		2	1	11630	-0.65
			2	5530	
			3	4550	
			4	3800	
			5	3130	
5C MIDDLE	WB MP835	1	1	20360	-0.34
			2	11400	
			3	9720	
			4	8910	
			5	8285	
		2	1	20360	-0.31
			2	11400	
			3	10360	
			4	9270	
			5	8380	
5C BOTTOM	WB MP835	1	1	14250	-0.45
			2	7810	
			3	6350	
			4	5880	
			5	5000	

Continued

TABLE A.2 (CONTINUED)

SAMPLE No.	LOCATION	σ_3 (psi)	$\sigma_1 - \sigma_3$ (psi)	M_R (psi)	S_{SG}
5C BOTTOM	WB MP835	2	1	15000	-0.34
			2	8510	
			3	6350	
			4	5800	
			5	5090	
6A MIDDLE	WB MP833.5	1	1	9500	0.0
			2	3800	
			3	3000	
			4	3670	
			5	3904	
		2	1	11875	-0.18
			2	5290	
			3	4915	
			4	4600	
			5	4670	
10D TOP	EB MP835	1	1	24000	-0.36
			2	12100	
			3	10300	
			4	9600	
			5	9100	
		2	1	25030	-0.36
			2	12600	
			3	11000	
			4	10300	
			5	9050	
10D MIDDLE	EB MP835	1	1	5700	-0.42
			2	3260	
			3	3000	
			4	2960	
			5	3100	
		2	1	10180	-0.65
			2	4250	
			3	(6840)	
			4	3620	
			5	3560	

Continued

TABLE A.2 (CONTINUED)

SAMPLE No.	LOCATION	σ_3 (psi)	$\sigma_1 - \sigma_3$ (psi)	M_R (psi)	S_{SG}
13E TOP	EB MP838	1	1	28500	-0.23
			2	15620	
			3	13900	
			4	13100	
			5	12390	
		2	1	28500	-0.31
			2	16050	
			3	13900	
			4	12740	
			5	12076	
14F TOP	EB MP839	1	1	35000	-0.31
			2	25900	
			3	20900	
			4	19700	
			5	19000	
		2	1	35600	-0.31
			2	23800	
			3	21900	
			4	20000	
			5	18000	
14F MIDDLE	EB MP839	1	1	28500	-0.32
			2	15833	
			3	13154	
			4	11753	
			5	10878	
		2	1	25900	-0.32
			2	21111	
			3	14740	
			4	12530	
			5	11310	
14F BOTTOM		1	1	11400	-0.51
			2	6260	
			3	5210	
			4	4670	
			5	4070	
		2	1	11400	-0.51
			2	6200	
			3	5340	
			4	4750	
			5	4320	

TABLE A.3

TABLE OF DEFLECTION PARAMETER STATISTICS
SLOPE = SENSOR 1 - SENSOR 5
SCI = SENSOR 1 - SENSOR 2
BCI = SENSOR 4 - SENSOR 5
SPREADABILITY = (SENSOR 1+2+3+4+5)/(5 TIMES SENSOR 1)
AVE = AVERAGE MD = MODE STD = STANDARD DEVIATION CV = COEFFICIENT OF VARIATION
NSEC = NUMBER OF DEFLECTIONS IN SECTION

SECTION		SENSOR 1				SENSOR 5				SLOPE				SPREADABILITY			SCI			BCI		
N	NSEC	AVE	MD	STD	CV	AVE	MD	STD	CV	AVE	MD	STD	CV	AVE	STD	CV	AVE	STD	CV	AVE	STD	CV
1	28	.65	.65	.08	.13	.46	.43	.06	.14	.18	.1A	.04	.21	.87	.02	.03	.82	.01	.41	.84	.01	.29
2	21	.60	.55	.09	.14	.37	.35	.05	.14	.22	.2s	.07	.31	.82	.04	.05	.84	.02	.48	.85	.02	.38
3	21	.47	.45	.07	.14	.29	.30	.05	.17	.18	.1s	.06	.35	.81	.06	.07	.84	.02	.68	.84	.01	.38
4	17	.55	.55	.06	.12	.37	.38	.03	.08	.18	.1A	.04	.22	.84	.03	.03	.83	.01	.37	.84	.01	.21
5	31	.44	.45	.10	.22	.29	.30	.05	.18	.15	.1s	.05	.36	.93	.33	.36	.82	.01	.41	.27	.91	3.37
6	115	.66	.65	.13	.20	.48	.48	.07	.15	.18	.1A	.08	.41	.87	.03	.04	.83	.04	1.17	.84	.02	.54
7	24	.56	.55	.07	.13	.37	.38	.05	.14	.19	.1A	.05	.24	.84	.03	.04	.83	.01	.47	.85	.02	.36
8	23	.67	.65	.12	.18	.48	.50	.10	.21	.19	.1s	.05	.23	.87	.03	.03	.82	.01	.49	.86	.02	.29
9	48	.60	.65	.14	.20	.48	.45	.09	.19	.19	.1s	.07	.34	.88	.03	.04	.82	.01	.51	.86	.03	.46
10	35	.84	.85	.14	.16	.59	.60	.08	.14	.26	.2A	.07	.27	.86	.02	.03	.85	.03	.58	.88	.03	.33
11	13	.63	.65	.10	.29	.43	.60	.11	.26	.19	.2s	.09	.45	.85	.04	.04	.86	.03	.48	.87	.03	.44
12	14	.88	.85	.16	.19	.54	.60	.11	.20	.27	.2A	.07	.24	.85	.02	.03	.86	.02	.35	.89	.03	.33
13	95	.56	.55	.11	.20	.36	.35	.07	.20	.20	.2s	.07	.32	.86	.20	.24	.85	.02	.45	.13	.91	3.68
14	27	.74	.85	.12	.16	.51	.45	.09	.17	.23	.2A	.07	.20	.85	.03	.04	.87	.02	.35	.87	.03	.43

SUBGRADE MODULUS UNDER THE DYNAFLECT LOAD

SECTION	MODAL SUBGRADE MODULUS
1	12720.
2	15962.
3	18941.
4	14785.
5	18941.
6	11373.
7	14785.
8	18743.
9	12876.
10	8775.
11	8775.
12	8775.
13	15962.
14	12876.

TABLE A.4

TABLE FOR CALCULATING REMAINING LIFE

IH-10 DISTRICT 20
CFHR 2009

SECTIONS		CONDITION SURVEY		NON-OVERLAYED REMAINING LIFE ESITIMATES								OVERLAID REM. LIFE			
				FIRST ESTIMATE				FINAL ESTIMATE							
SEC-TION	LIMITS (Mile Posts)	DEF-ECTS PER MILE	RL_1	E_1 psi $x10^6$	E_2 psi $x10^5$	N_{90} 18 kip $x10^6$	RL_2 %	E_1 psi $x10^6$	E_2 psi $x10^5$	N_{90} 18 kip $x10^6$	RL_2 %	σ_{90} psi	n 18 kip $x10^6$	N_{all} 18 kip $x10^6$	RL_3 %
		74 78											9.0		
WB 1		58 207	<<0	4.5	8.0	16.0	44	5.0	4.0	5.5	<0	132		7.0	0
2		24 90	<0	4.5	3.0	5.0	<0	4.5	3.0	5.0	<0	137		6.3	0
3		0 0	>0	4.5	6.0	13.0	36	4.5	6.0	13.0	31	97		19.0	53
4		8 25	<0	4.5	7.0	16.0	44	5.0	6.0	10.5	14	106		14.2	37
5		6 43	<0	4.5	10.0	23.0	61	5.0	7.0	13.2					
6		4 41	<0	4.5	8.0	16.0	44	5.0	6.0	9.0	0	113		11.6	22
7		0 10	>0	4.5	7.0	15.0	40	5.0	6.0	10.0	10	108		13.4	33
EB 8		0 0	>0	4.5	7.0	15.0	40	4.5	7.0	15.0	40	92		22.4	60
9		4 57	<0	4.5	8.0	16.0	44	5.0	6.0	8.5	0	113		11.6	22
10		2 13	0	4.5	8.0	15.0	40	5.0	7.0	10.5	14	107		13.8	35
11		4 35	<0	4.5	3.0	4.0	<<0	4.0	4.0	7.0	0	122		9.1	35
12		0 0	>0	4.5	8.0	16.0	44	4.5	8.0	16.0	44	91		23.1	61
13		30 65	<0	4.5	3.0	4.0	<<0	4.0	4.0	7.0	0	121		9.3	3
14		1 7	>0	4.5	3.0	5.5	<0	4.0	4.0	9.0	0	113		11.6	22
15		3 33	<0	4.5	4.0	6.0	<0	4.0	4.0	7.5	0	120		9.6	6

RL_1 Remaining Life from condition survey data. RL_2 Remaining Life for non-overlaid pavement.
N_{90} Fatigue Life corresponding to 90th percentile Sensor 5 Deflection. N_{all} Allowable applications.

B. FATIGUE LIFE PREDICTION

1. General Comments

Fatigue of Existing Pavements

Fatigue life predictions correlated to condition survey results in Table A.4

Overlay Fatigue

In cases of no remaining life, an overlay thickness of 6 inches is recommended to last the design life.

Reflection Cracking

Minimum overlay thickness of 3 inches is recommended to resist reflection cracking and bond failures.

2. Fatigue Life

Table showing fatigue lives of different pavement layers.

Table A.5 shows the remaining fatigue life of the existing concrete pavement with varying asphalt overlay thicknesses.

TABLE A.5. PREDICTION OF FATIGUE LIFE FOR DISTRICT 20 PROJECT

IH-10 DISTRICT 20
CFHR 2009

RIGID PAVEMENT OVERLAY DESIGN									EXISTING OVERLAYS			
SECTIONS	EXISTING MTL. PROPS.			REMAINING LIFE	FUTURE FAT. LIFE WITH O/L THICK				TRAFFIC ESTIMATES 10^6 18kip			
	E_1 10^6 psi	E_2 10^5 psi	E_3 10^3 psi		3"	6"	9"	12"	O/L THICK	PAST TRAFFIC	DEFECTS PER MILE	TOTAL TRAFFIC
WB 1	5.0	4.0	4.0	0								
2	4.5	3.0	4.8	0								
3	4.5	6.0	6.6	53	15.0	25.3	43.3	73.3				
4	5.0	6.0	6.0	37	7.9	13.2	22.4	37.8				
5	5.0	7.0	6.5	49	13.9	23.0	39.0	46.0				
6	5.0	6.0	3.6	22	3.6	5.9	10.0	17.1				
7	5.0	6.0	5.1	33	6.4	10.6	18.1	30.8				
EB 8	4.5	7.0	5.1	60	19.1	31.6	53.1	88.7				
9	5.0	6.0	3.5	22	3.5	5.8	10.0	16.9				
10	5.0	7.0	3.0	35	6.7	10.8	18.1	30.6				
11	4.0	4.0	2.9	1								
12	4.5	8.0	3.2	61	19.8	32.0	53.0	9.0				
13	4.0	4.0	3.3	3								
14	4.0	4.0	5.6	22	4.1	7.2	12.8	22.5				
15	4.0	4.0	3.3	6								

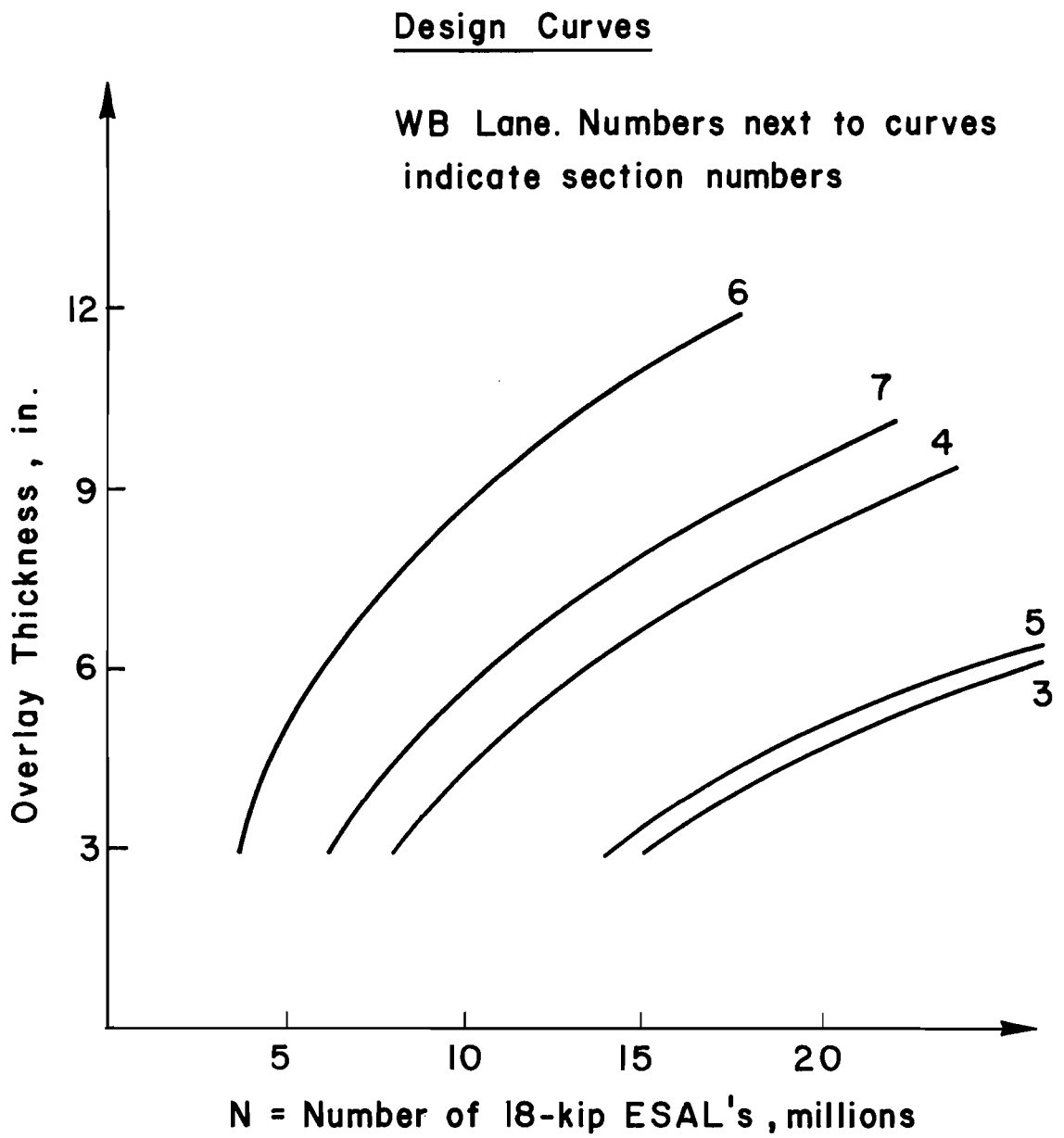

Fig A.1. Design chart for westbound lane of IH-10 - in District 20.

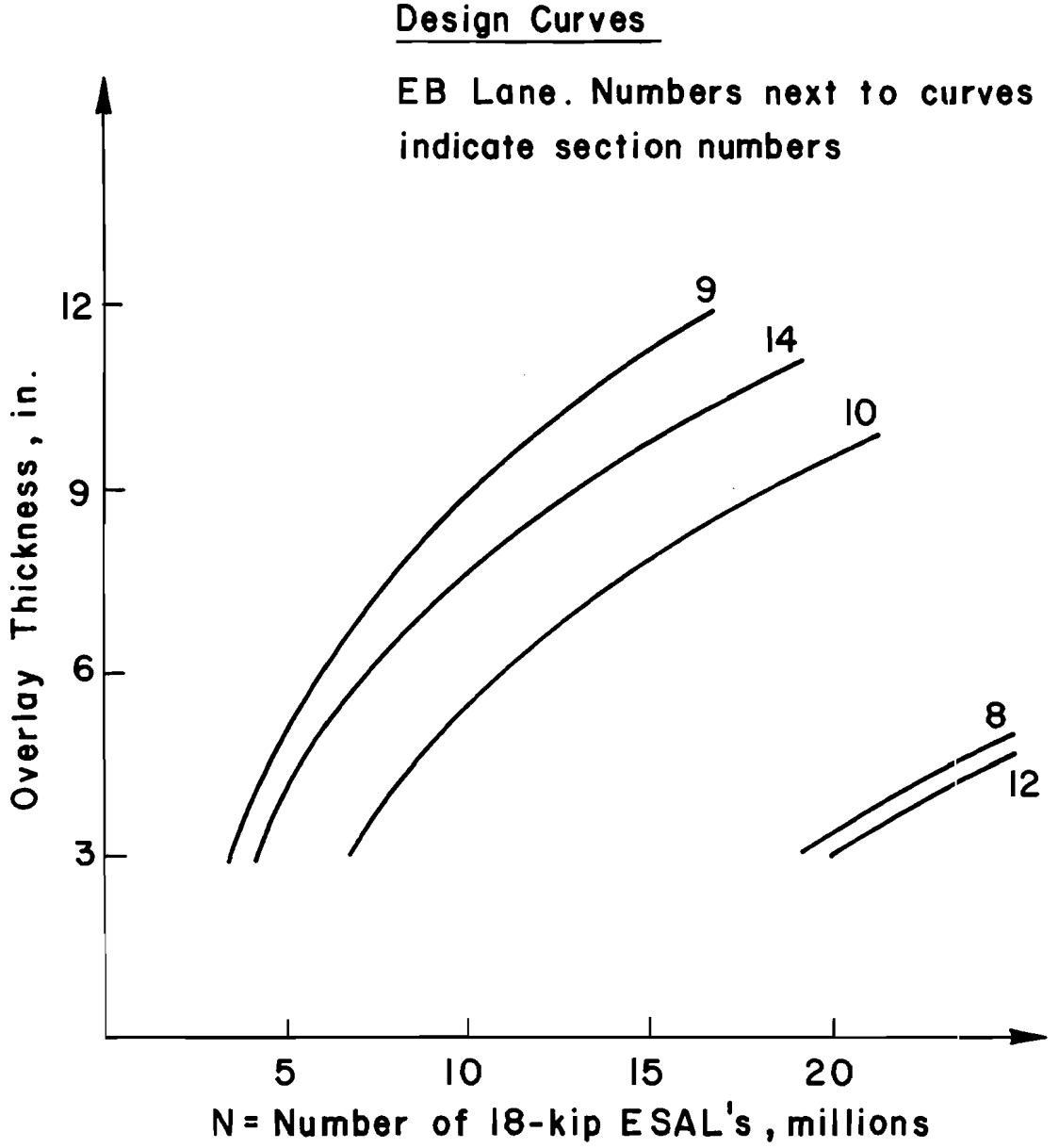

Fig A.2. Design chart for eastbound lane of IH-10 - in District 20.

CONCRETE PAVEMENT OVERLAY DESIGN

I. PROJECT IDENTIFICATION INFORMATION

DISTRICT	COUNTY	HIGHWAY	CONTROL	SEC	JOB	CFHR No
13	Colorado	IH-10	535	8	4	1301
and 13	Fayette	IH-10	271	1	8	1302

SCOPE

Design on AC overlay to last 10 years along IH-10 from Station 750 (Mile Post 689.6) to station 1121 (Mile Post 696.7) in Fayette County and from Station 26 (Mile Post 697) to Station 149 (Mile Post 699.4) in Colorado County.

II. PAVEMENT STRUCTURES

EXISTING

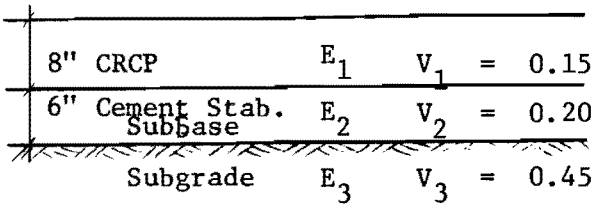

PROPOSED OVERLAID STRUCTURE

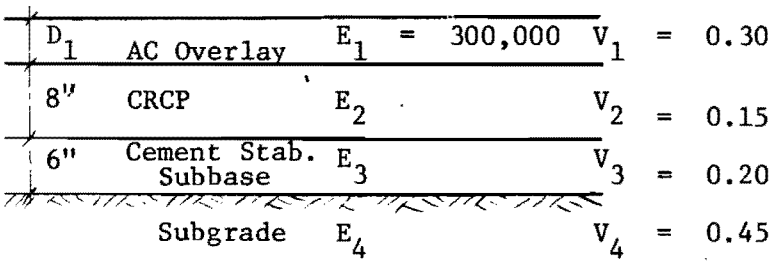

III. TRAFFIC

CFHR	Age	Traffic in 18-kip ESAL'S.	
		Past to 1978	1980-1990
1301	18	9.7×10^6	25×10^6
1302	16	6.9×10^6	17×10^6

IV. DESIGN THICKNESSES

SECTION		LIMITS (STATIONS)	DESIGN THICKNESSES (INCHES)
CFHR EB	1	750-761	5
	2	761-773	12*
	3	773-884	8*
	4	884-930	6
	5	930-1001	5
	6	1001-1033	4
	7	1033-1121	4
CFHR 1301	8	26-37	10*
	9	37-85	4
	10	85-149	11*
WB	1	149-112	6.
	2	112-88	11*
	3	88-26	6
CFHR 1302	4	1121-1109	9*
	5	1109-1065	6
	6	1065-926	5
	7	926-880	5
	8	880-748	5

*No fatigue of the overlay was considered. RPRDS (Ref 12) can consider this fatigue and may result in reduced thicknesses for these cases.

V. DESIGN INFORMATION

1. MATERIALS CHARACTERIZATION

A. General Comments

Condition Survey Data

1974, 1978, and 1979 data available.

Remaining Life From Condition Survey Data

Zero remaining life at approximately 15 defects per mile.

Deflections Used For Section Selection (Depending on remaining life of existing pavement, pavement type and overlay type.)

Pavement undersealing was undertaken along this section of road. Before grouting, sensor 1 deflections were taken at every 100 feet. After grouting further selected deflections were taken at cracks. All these deflections were used for selecting sections.

Laboratory Testing (Tests done or assumptions made. M_r S_{sg} f_c)

Indirect tensile tests for tensile strength and modulus of surface layer. (Table A.5) For fatigue calculations use a 95 percentile flexural strength of (620x1.6) - 1.6 (620x1.6x.17) = 722 psi [flexural strength $\approx$ 1.6 x tensile strength (Ref 5)].

B. Layer Stiffnesses

Table from MODE.
Lab test results.
Table for calculating layer moduli based on deflection basin slopes, condition survey data and fatigue life.
90^{th} percentile subgrade modulus.
Moduli from deflection basin slopes at pavement joints or defects if no remaining life.

TABLE A.5 Indirect tensile test results.

TABLE A.6 Calculation of pavement remaining life from condition survey data and correlation of material properties to these results using deflection basin slopes, pavement stresses and a fatigue equation.

TABLE A.5

RESULTS OF INDIRECT TENSILE TESTS ON CONCRETE SURFACE LAYER FROM IH-10 NEAR COLUMBUS (CONTROL 535-8-4 AND 271-1-8)

SAMPLE	LOCATION (STA.)	LOAD (POUNDS)	E (10^6PSI)	TENSILE STRESS AT BREAK (PSI)
1	793 + 67	1000	2.4	600
		2000	2.4	
2	794 + 80	1000	3.9	450
		2000	4.4	
3	795 + 57			515
4	795 + 57	1000	4.6	588
		2000	4.0	
5	797 + 38	1000	3.1	505
		2000	3.3	
6	127 + 99	1000	2.6	717
		2000	3.3	
7	129 + 07	1000	(16.3)	631
		2000	3.3	
8	139 + 48	1000	2.2	645
		2000	2.2	
9	149 + 28			747
10	819 + 29	1000	1.3	614
		2000	1.7	
11	838 + 54			809

AVERAGE CONCRETE MODULUS = 2.98×10^6 psi

COEFFICIENT OF VARIATION = 33%

AVERAGE TENSILE STRENGTH = 620 psi

COEFFICIENT OF VARIATION = 17%

TABLE A.6

TABLE FOR CALCULATING REMAINING LIFE

IH-10 DISTRICT 13
CFHR 1301, 1302

SECTIONS		CONDITION SURVEY		NON-OVERLAYED REMAINING LIFE ESITIMATES								OVERLAYED REM. LIFE			
				FIRST ESTIMATE				FINAL ESTIMATE							
SEC-TION	LIMITS	DEF-ECTS PER MILE 178 179	RL_1	E_1 psi $x10^6$	E_2 psi $x10^5$	N_{90} 18 kip $x10^6$	RL_2	E_1 psi $x10^6$	E_2 psi $x10^5$	N_{90} 18 kip $x10^6$	RL_2	90 psi	N_{90} 18 kip $x10^6$	N_{all} 18 kip $x10^6$	RL_3
EB 1	750-761	178 179	>0	2.5	0.5	5.9	0	1.8	2.0	0.3	>0	111	8.0	12.3	35
2	-773	20 22	<0	4.0	6.0	24.7	68	4.5	5.0	6.9	<0	122	8.0	9.1	12
3	-884	7 16	0	3.0	2.0	11.2	29	2.5	2.5	7.7	0	118	8.0	10.1	21
4	-930	3 20	0	3.0	2.0	16.2	51	2.5	2.5	7.7	0	118	8.0	10.1	21
5	-1001	9 9	>0	3.0	2.0	11.2	29	2.7	2.5	10.3	>0	107	8.0	13.8	42
6	-1033	3 2	>0	3.0	1.0	8.8	9	2.2	2.0	9.4	>0	110	8.0	12.7	37
7	-1121	2 4	>0	3.0	2.0	13.4	40	2.5	2.5	9.6	>0	110	8.0	12.7	37
8	26-37	15 41	<0	3.0	1.0	7.7	0	2.0	2.0	9.6	<0	110	11.0	12.7	13
9	-85	1 1	>0	3.0	2.0	13.8	20	2.0	2.3	13.0	>0	99	11.0	17.7	38
10	-149	13 37	<0	2.5	0.5	5.9	0	1.8	2.0	9.3	<0	111	11.0	12.3	11
WB 1	149-112	14 36	<0	2.5	0.5	8.1	0	2.0	2.0	10.9	0	105	11.0	14.7	25
2	-88	O/LAY											11.0		
3	-26	10 6	>0	3.0	2.0	12.8	20	2.5	3.0	11.6	>0	103	11.0	15.6	30
4	1121-1109	23 69	<0	3.0	3.0	17.3	54	3.0	3.0	7.4	<0	119	8.0	9.8	18
5	-1065	1 18	0	3.0	1.0	9.5	16	2.5	2.0	8.4	0	114	8.0	11.3	29
6	-926	4 14	0	2.5	1.0	10.6	25	2.2	1.8	8.7	0	113	8.0	11.6	31
7	-880	5 16	0	3.0	2.0	13.8	42	2.2	1.8	8.7	0	113	8.0	11.6	31
8	-748	9 17	0	3.0	3.0	17.3	54	2.2	1.8	8.7	0	113	8.0	11.6	31

RL_1 remaining life from condition survey data. RL_2 remaining life for non-overlayed pavement.

N_{90} fatigue life corresponding to 90th percentile sensor 5 deflection. N_{all} allowable applications.

2. FATIGUE LIFE PREDICTION

A. General Comments

Fatigue of Existing Pavements

Fatigue life predictions correlated to condition survey results in Table A.6.

Overlay Fatigue

Only fatigue of the existing pavement is considered, no overlay fatigue is considered.

Reflection Cracking

A minimum thickness of 3 inches is recommended to resist reflection cracking.

B. Fatigue Life

Table showing fatigue lives of different pavement layers.

Table A.7 shows the remaining fatigue life of the existing concrete pavement with varying asphalt overlay thicknesses.

CONCRETE PAVEMENT OVERLAY DESIGN

I. PROJECT IDENTIFICATION INFORMATION

DISTRICT	COUNTY	HIGHWAY	CONTROL	SEC	JOB	CFHR No
20	Jefferson	IH-10	739	2	56	2004

From Walden Road in Beaumont to 0.6 miles N.E. of FM 365.

SCOPE

Compare the overlay life predictions of the design procedure to the condition of an existing asphalt overlay and engineering estimates of the future life of the overlay.

II. PAVEMENT STRUCTURES

EXISTING

ACTUAL

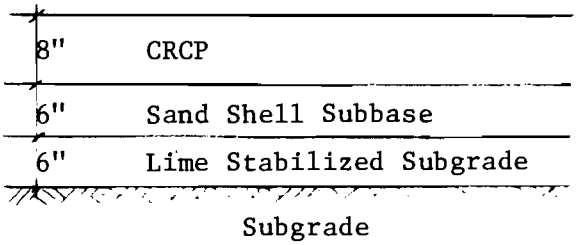

MODEL

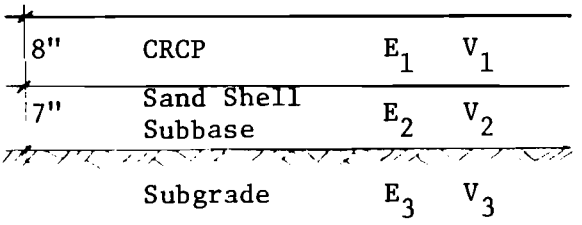

PROPOSED OVERLAID STRUCTURE

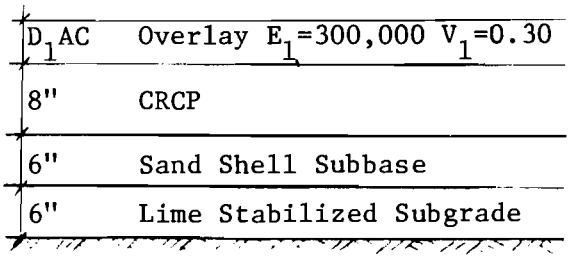

III. TRAFFIC

AGE [Years]	TRAFFIC IN 18-kip ESAL's PAST TO OVERLAY Construction in 1974	1974-1978
18	6×10^6	3×10^6

IV. DESIGN THICKNESSES

The CRC pavement was overlaid during 1974 and 1975 with an average thickness of 3 1/4 inches of asphalt concrete.

Section 5 in the west bound lane already had a 3" thick overlay at this time and was thus overlayed with an additional 1 1/2" of aspahlt concrete.

V. DESIGN INFORMATION

1. MATERIALS CHARACTERIZATION

A. General Comments

Condition Survey Data

1974 Condition survey before overlaying

1979 Condition survey after overlaying

Remaining Life From Condition Survey Data

Zero remaining life at approximately 15 defects per mile.

Deflections Used For Section Selection (Depending on remaining life of existing pavement, pavement type and overlay type.)

No defelction measurements were obtained.

Laboratory Testing (Tests done or assumptions made. M_r S_{sg} f_c)

No laboratory testing was done. Material properties similar to those obtained along an adjacent section of road (CFHR 2009), were used as initial estimates.

B. Layer Stiffnesses

Table from MODE.
Lab test results.
Table for calculating layer moduli based on deflection basin slopes, condition survey data and fatigue life.
90^{th} percentile subgrade modulus.
Moduli from deflection basin slopes at pavement joints or defects if no remaining life.

Table A.8 Calculation of pavement remaining life using condition survey data and estimates of layer moduli.

TABLE A.8

TABLE FOR CALCULATING REMAINING LIFE

IH-10 DISTRICT 20
CFHR 2004

SECTIONS		CONDITION SURVEY		NON-OVERLAID REMAINING LIFE ESTIMATES								OVERLAID REM. LIFE			
				FIRST ESTIMATE				FINAL ESTIMATE							
SECTION	LIMITS [MILES]	DEFECTS PER MILE	RL_1	E_1 psi $x10^6$	E_2 psi $x10^5$	N_{90} 18 kip	RL_2	E_1 psi	E_2 psi	N_{90} 18 kip	RL_2	σ_{90} psi	n 18 kip $x10^6$	N_{all} 18 kip $x10^6$	RL_3
		1974		NO DEFLECTIONS											
EB 1	8- 8.9	40	<0	3.0	2.5	5.4						132	6.0	7.1	16
2	- 9.8	11	0	3.0	3.0	6.7						124		8.6	30
3	-10.8	26	<0	3.0	2.5	5.4						132		7.1	16
4	-11.6	40	<0	3.0	2.5	5.4						132		7.1	16
5	-12.8	O/LAY	<0												
6	-13.7	10	0	3.0	3.0	6.7						124		8.6	30
7	-14.6	7	>0	3.0	3.0	6.7						124		8.6	30
8	-15.6	8	>0	3.0	3.0	6.7						124		8.6	30
9	-16.5	9	>0	3.0	3.0	6.7						124		8.6	30
10	-17.5	5	>0	3.0	3.0	6.7						124		8.6	30

RL_1 remaining life from condition survey data. RL_2 remaining life for non-overlaid pavement.
N_{90} fatigue life corresponding to 90th percentile sensor 5 deflection. N_{all} allowable applications.

TABLE A.8 Continued

TABLE FOR CALCULATING REMAINING LIFE

IH-10 DISTRICT 20
CFHR 2004

SECTIONS		CONDITION SURVEY		NON-OVERLAID REMAINING LIFE ESTIMATES								OVERLAID REM. LIFE			
				FIRST ESTIMATE				FINAL ESTIMATE							
SECTION	LIMITS	DEFECTS PER MILE	RL_1	E_1 psi $x10^6$	E_2 psi $x10^5$	N_{90} 18 kip	RL_2	E_1 psi	E_2 psi	N_{90} 18 kip	RL_2	σ_{90} psi	n 18 kip $x10^6$	N_{all} 18 kip $x10^6$	RL_3
		1974		NO DEFLECTIONS									6.0		
WB 1	17.5-16.4	3	>0	3.0	3.0	6.7						124		8.6	30
2	-15.5	10	0	3.0	3.0	6.7						124		8.6	30
3	-14.2	2	>0	3.0	3.0	6.7						124		8.6	30
4	-13.0	5	>0	3.0	3.0	6.7						124		8.6	30
5	-12.1	0	>0	3.0	2.5	5.4						132		7.1	16
6	-11.6	2	>0	3.0	3.0	6.7						124		8.6	30
7	-10.6	12	0	3.0	3.0	6.7						124		8.6	30
8	- 9.7	3	>0	3.0	3.0	6.7						124		8.6	30
9	- 8.8	7	>0	3.0	3.0	6.7						124		8.6	30
10	- 8.0	3	>0	3.0	3.0	6.7						124		8.6	30

RL_1 remaining life from condition survey data. RL_2 remaining life for non-overlaid pavements.
N_{90} fatigue life corresponding to 90^{th} percentile sensor 5 deflection. N_{all} allowable applications.

2. FATIGUE LIFE PREDICTION

A. General Comments

Fatigue of Existing Pavements

Fatigue life predictions correlated to condition survey results in Table A.8.

Overlay Fatigue

Only fatigue in the existing pavement is considered.

Reflection Cracking

No reflection cracking analysis was done.

B. Fatigue Life

Table showing fatigue lives of different pavement layers.

Table A.9 shows the remaining fatigue life of the existing pavement compared to engineering estimates of the total traffic which will pass over the overlayed pavement before failure will occur.

TABLE A.9

IH-10 DISTRICT 20
CFHR 2004

RIGID PAVEMENT OVERLAY DESIGN									EXISTING OVERLAYS			
SECT-IONS	EXISTING MTL. PROPS.			REM-AINING LIFE	FUTURE FAT. LIFE WITH O/L THICK				TRAFFIC ESTIMATES 10^6 18kip			
	E_1 10^6 psi	E_2 10^5 psi	E_3 10^3 psi		3"	6"	9"	12"	O/L THICK	PAST TRAFFIC	DEFECTS PER MILE	TOTAL TRAFFIC
EB 1	3.0	2.5	5.0	16	2.2	4.3	8.3	15.4	3.0	3.0	63.0	5.0
2	3.0	3.0		30	6.4	12.0	22.0	40.0	3.0	3.0	3.0	7.0
3	3.0	2.5		16	2.2	4.3	8.3	15.4	3.0	3.0	9.0	7.0
4	3.0	2.5		16	2.2	4.3	8.3	15.4	3.0	3.0	23.0	6.0
5	3.0	2.5		16	2.2	4.3	8.3	15.4	4.5	4.0	54.0	5.0
6	3.0	3.0		30	6.4	12.0	22.0	40.0	3.0	3.0	7.0	7.0
7	3.0	3.0		30	6.4	12.0	22.0	40.0	3.0	3.0	25.3	6.0
8	3.0	3.0		30	6.4	12.0	22.0	40.0	3.0	3.0	5.0	7.0
9	3.0	3.0		30	6.4	12.0	22.0	40.0	3.0	3.0	1.0	7.0
10	3.0	3.0		30	6.4	12.0	22.0	40.0	3.0	3.0	2.0	7.0

TABLE A.9 Continued

IH-10 DISTRICT 20
CFHR 2004

RIGID PAVEMENT OVERLAY DESIGN									EXISTING OVERLAYS			
SECT-IONS	EXISTING MTL. PROPS.			REM-AINING LIFE	FUTURE FAT. LIFE WITH O/L THICK				TRAFFIC ESTIMATES 10^6 18kip			
	E_1 10^6 psi	E_2 10^5 psi	E_3 10^3 psi		3"	6"	9"	12"	O/L THICK	PAST TRAFFIC	DEFECTS PER MILE	TOTAL TRAFFIC
WB 1	3.0	3.0	5.0	30	6.4	11.9	22.0	40.0	3.0	3.0	4.0	7.0
2	3.0	3.0		30	6.4	12.0	22.0	40.0	3.0	3.0	8.0	7.0
3	3.0	3.0		30	6.4	12.0	22.0	40.0	3.0	3.0	2.0	7.0
4	3.0	3.0		30	6.4	12.0	22.0	40.0	3.0	3.0	0.0	7.0
5	3.0	2.5		16	2.2	4.3	8.3	15.4	3.0	3.0	0.0	7.0
6	3.0	3.0		30	6.4	12.0	22.0	40.0	3.0	3.0	1.0	7.0
7	3.0	3.0		30	6.4	12.0	22.0	40.0	3.0	3.0	2.0	7.0
8	3.0	3.0		30	6.4	12.0	22.0	40.0	3.0	3.0	3.0	7.0
9	3.0	3.0		30	6.4	12.0	22.0	40.0	3.0	3.0	0.0	7.0
10	3.0	3.0		30	6.4	12.0	22.0	40.0	3.0	3.0	0.0	7.0

CONCRETE PAVEMENT OVERLAY DESIGN

I. PROJECT IDENTIFICATION INFORMATION

DISTRICT	COUNTY	HIGHWAY	CONTROL	SEC	JOB	CFHR No
17	Walker	IH-45				1701

From Montgomery County Line to South of Huntsville.

SCOPE

Compare the overlay life predictions of the design procedure to the condition of an existing asphalt overlay and engineering estimates of the future life of the overlay.

II. PAVEMENT STRUCTURES

EXISTING

ACTUAL

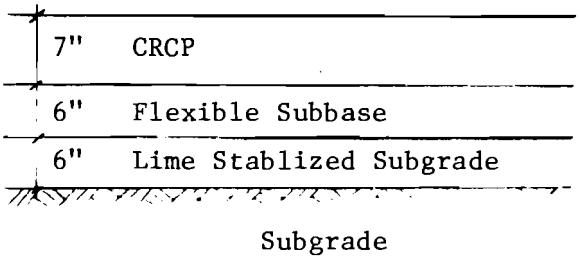

MODEL

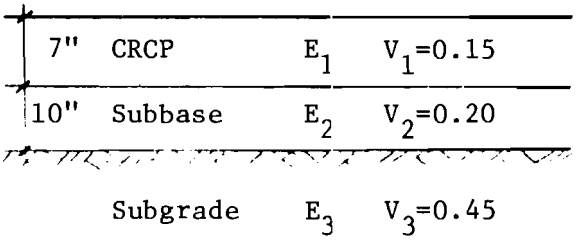

PROPOSED OVERLAID STRUCTURE

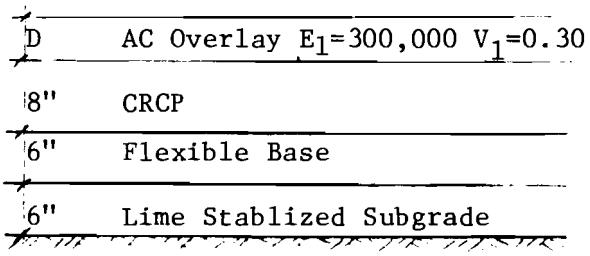

III. TRAFFIC

AGE [Years]	TRAFFIC IN 18-kip ESAL's	
	PAST TO OVERLAY Construction in 1974	1974-1978
19	8×10^6	5×10^6

IV. DESIGN THICKNESSES

The pavement was overlayed during 1974 and 1975 with an asphalt overlay varying in thickness from 2 1/2 inches to 6 inches.

V. DESIGN INFORMATION

1. MATERIALS CHARACTERIZATION

A. General Comments

Condition Survey Data

1974 Condition survey before overlaying
1979 Condition survey after overlaying

Remaining Life From Condition Survey Data

Zero remaining life at approximately 14 defects per mile.

Deflections Used For Section Selection (Depending on remaining life of existing pavement, pavement type and overlay type.)

Deflection measurements taken at every 500 feel prior to overlaying.

Laboratory Testing (Tests done or assumptions made. M_r S_{sg} f_c)

Some laboratory testing of pavement materials was done before overlay and is documented in Ref 1.

B. Layer Stiffnesses

Table from MODE.
Lab test results.
Table for calculating layer moduli based on deflection basin slopes, condition survey data and fatigue life.
90^{th} percentile subgrade modulus.
Moduli from deflection basin slopes at pavement joints or defects if no remaining life.

Table A.10 Dynaflect deflection statistics for each section and model subgrade modulus under the Dynaflect load.

Table A.11 Calculation of pavement remaining life using condition survey data and correlation of material properties to these results using deflection basin slopes, pavement stresses and a fatigue equation.

TABLE A.10

TABLE OF DEFLECTION PARAMETER STATISTICS
SLOPE = SENSOR 1 - SENSOR 5
SCI = SENSOR 1 - SENSOR 2
SCI = SENSOR 4 - SENSOR 5
SPREADABILITY = (SENSOR 1+2+3+4+5)/(5 TIMES SENSOR 1)
AVE = AVERAGE MD = MODE STD = STANDARD DEVIATION CV = COEFFICIENT OF VARIATION
NSEC = NUMBER OF DEFLECTIONS IN SECTION

N/A

SECTION		SENSOR 1				SENSOR 5				SLOPE				SPREADABILITY			SCI			SCI		
N	NSEC	AVE	MD	STD	CV	AVE	MD	STD	CV	AVE	MD	STD	CV	AVE	STD	CV	AVE	STD	CV	AVE	STD	CV
1	49	.74	.75	.14	.18	.33	.35	.07	.22	.41	.3A	.13	.30	.29	.02	.06	.74	.14	.18	-.33	.07	-.22
2	29	.74	.65	.14	.19	.33	.30	.09	.27	.41	.4S	.11	.28	.29	.02	.06	.74	.14	.19	-.33	.09	-.27
3	16	.60	.55	.13	.22	.29	.25	.07	.25	.31	.2S	.07	.23	.30	.01	.03	.60	.13	.22	-.29	.07	-.25
4	9	.68	.65	.15	.22	.25	.28	.06	.23	.43	.3A	.13	.31	.27	.02	.06	.68	.15	.22	-.25	.06	-.23
5	28	.75	.65	.20	.27	.28	.30	.07	.23	.47	.3B	.21	.45	.28	.02	.08	.75	.20	.27	-.28	.07	-.23
6	16	.91	.75	.18	.19	.36	.35	.10	.28	.56	.5A	.15	.28	.28	.02	.06	.91	.18	.19	-.36	.10	-.28
7	18	.97	.75	.57	.58	.30	.25	.05	.16	.67	.5S	.54	.81	.27	.02	.06	.97	.57	.58	-.30	.05	-.16
8	25	.84	.85	.29	.34	.34	.38	.07	.21	.51	.4S	.25	.50	.28	.01	.05	.84	.29	.34	-.34	.07	-.21
9	18	.70	.65	.07	.10	.36	.33	.05	.14	.34	.3S	.08	.11	.30	.01	.05	.70	.07	.10	-.36	.05	-.14
10	10	.75	.75	.05	.07	.38	.33	.06	.16	.37	.3S	.04	.11	.30	.01	.04	.75	.05	.07	-.38	.06	-.16
11	7	.75	.75	.17	.23	.41	.38	.08	.19	.33	.3S	.11	.32	.31	.01	.04	.75	.17	.23	-.41	.08	-.19
12	32	.75	.65	.17	.22	.26	.28	.08	.30	.49	.4A	.14	.28	.27	.02	.08	.75	.17	.22	-.26	.08	-.30

SUBGRADE MODULUS UNDER THE DYNAFLECT LOAD

SECTION	MODAL SUBGRADE MODULUS
1	15962.
2	18941.
3	23189.
4	28861.
5	18941.
6	15962.
7	23189.
8	18941.
9	17330.
10	17330.
11	14785.
12	28861.

TABLE A.11

TABLE FOR CALCULATING REMAINING LIFE

IH-45 DISTRICT 17
CFHR 1701

SECTIONS		CONDITION SURVEY		NON-OVERLAID REMAINING LIFE ESTIMATES								OVERLAID REM. LIFE			
				FIRST ESTIMATE				FINAL ESTIMATE							
SECTION	LIMITS [MILES]	DEFECTS PER MILE	RL_1	E_1	E_2	N_{90}	RL_2	E_1	E_2	N_{90}	RL_2	σ_{90}	n	N_{all}	RL_3
				psi	psi	18 kip		psi	psi	18 kip		psi	18 kip	18 kip	
				$x10^6$	$x10^5$	$x10^6$	%	$x10^6$	$x10^5$	$x10^6$	%		$x10^6$	$x10^6$	%
		1974											8.0		
NB 1	0- 4.9	13	0	2.5	1.0	5.0	<0	2.3	1.4	8.1	0	116		10.7	25
2	4.9- 7.8	39	<0	2.0	1.0	6.6	<0	1.9	1.0	7.1	<0	121		9.3	14
3	8.8-10.3	47	<0	3.2[8"]	1.0	5.9	<0	3.0	1.2	7.4	<0	120		9.6	16
4	10.3-11.2	96	<0	2.0	1.0	6.8	<0	2.0	1.0	6.8	<0	123		8.9	10
5B 5	0- 2.5	16	0	2.0	1.0	7.2	<0	1.9	1.1	8.7	0	113		11.6	31
6	3.6- 5.1	16	0	2.0	0.5	3.5	<0	1.5	0.7	6.6	<0	124		8.6	7
7	5.1- 6.1	5	>0	2.0	0.5	3.5	<0	1.5	0.7	7.4	<0	119		9.8	29
8	6.1- 8.7	14	0	2.0	1.0	6.8	<0	1.9	1.1	8.2	0	115		11.0	27
9	8.7- 9.6	7	>0	2.5	1.0	5.0	<0	2.2	1.5	9.5	>0	110		12.7	37
10	9.6-10.6	6	>0	2.5	1.0	4.8	<0	2.2	1.5	9.3	>0	111		12.3	35
11	10.6-11.3	9	>0	2.5	1.0	4.8	<0	2.2	1.5	9.3	>0	111		12.3	35

RL_1 remaining life from condition survey data. RL_2 remaining life for non-overlaid pavements.
N_{90} fatigue life corresponding to 90th percentile sensor 5 deflection. N_{all} allowable applications.

2. FATIGUE LIFE PREDICTION

A. General Comments

Fatigue of Existing Pavements

Fatigue life correlated to condition survey results in Table A.11.

Overlay Fatigue

Only fatigue in the existing pavement is considered.

Reflection Cracking

No reflection cracking analysis was done.

B. Fatigue Life

Table showing fatigue lives of different pavement layers.

Table A.12 shows the design predictions of the remaining fatigue life of the existing pavement compared to engineering estimates of the total traffic which will pass over the overlaid pavement before failure will occur.

TABLE A.12

IH-45 DISTRICT 17
CFHR 1701

SECTIONS	RIGID PAVEMENT OVERLAY DESIGN								EXISTING OVERLAYS			
	EXISTING MTL. PROPS.			REMAINING LIFE	FUTURE FAT. LIFE WITH O/L THICK				TRAFFIC ESTIMATES 10^6 18kip			
	E_1 10^6 psi	E_2 10^5 psi	E_3 10^3 psi		3"	6"	9"	12"	O/L THICK	PAST TRAFFIC	DEFECTS PER MILE	TOTAL TRAFFIC
NB 1	2.3	1.4	9.0	25	5.4	12.0	25.0	48.0	2.5	5.0	44.0	8.0
2	1.9	1.0	9.0	14	2.9	6.9	15.0	30.0	6.0	5.0	1.0	10.0
3	3.0	1.2	10.0	16	2.9	6.0	11.8	22.2	5.0	5.0	13.0	10.0
4	2.0	1.0	14.0	10	2.4	5.6	12.5	22.4	2.5	5.0	33.0	8.0
5B 5	1.9	1.1	12.0	31	8.3	19.5	42.7	85.3	2.5	5.0	24.0	9.0
6	1.5	0.7	7.5	7	1.4	3.6	8.0	16.4	6.0	5.0	18.0	9.0
7	1.5	0.7	11.0	29	7.1	18.1	41.5	85.7	2.5	5.0	14.0	10.0
8	1.9	1.1	10.0	27	6.6	15.5	33.5	66.5	4.0	5.0	26.0	10.0
9	2.2	1.5	9.5	37	9.8	21.6	45.0	87.0	2.5	5.0	31.0	8.0
10	2.2	1.5	9.5	35	9.3	20.4	42.5	82.0	4.0	5.0	16.0	10.0
11	2.2	1.5	7.5	35	8.3	18.1	37.2	71.1	2.5	5.0	34.3	8.0

CONCRETE PAVEMENT OVERLAY DESIGN

I. PROJECT IDENTIFICATION INFORMATION

DISTRICT	COUNTY	HIGHWAY	CONTROL	SEC	JOB	CFHR No
1	Hunt	IH-30	9	13		

From Rockwall county line to South West of Loop 315. Approximately 15.1 miles in each direction.

SCOPE

Design a CRC overlay to last 20 years.

II. PAVEMENT STRUCTURES

EXISTING

ACTUAL

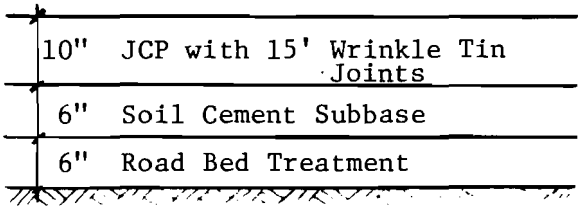

MODEL

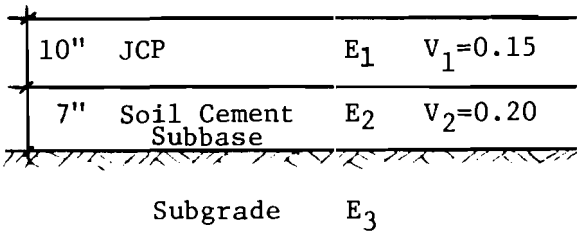

PROPOSED OVERLAID STRUCTURE

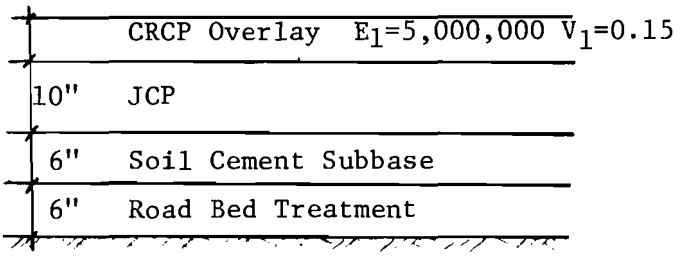

III. TRAFFIC

AGE	TRAFFIC IN 18-kip ESAL's	
[Years]	PAST TO 1979	1980 - 2000
± 18	12×10^6	35×10^6

IV. DESIGN THICKNESSES

SECTIONS		LIMITS (MILE POSTS)	OVERLAY THICKNESS	NUMBER OF JOINT REPAIRS
WB	A	94.2-93.6	9.5	19
	B	-93.2	8.0	0
	C	-92.9	9.5	0
	D	-91.5	8.0	34
	E	-90.1	10.0	5
	F	-87.9	8.0	54
	G	-87.7	9.5	7
	H	-84.7	8.0	74
	I	-82.7	9.0	70
	J	-81.1	10.0	101
	K	-78.8	10.0	32
EB	A	79.0-82.2	10.0	23
	B	-83.1	11.0	38
	C	-84.6	9.5	32
	D	-85.1	10.0	56
	E	-85.8	8.5	12
	F	-86.1	10.0	0
	G	-87.1	8.5	7
	H	-88.6	9.5	26
	I	-89.4	8.0	14
	J	-89.8	10.0	7
	K	-92.9	8.5	15
	L	-92.3	9.5	11
	M	-93.1	8.0	14
	N	-94.1	9.5	7
	O	-94.4	8.5	2

V. DESIGN INFORMATION

1. MATERIALS CHARACTERIZATION

A. General Comments

Condition Survey Data

Condition survey done in 1979 prior to overlay.

Remaining Life From Condition Survey Data

Condition survey indicated approximately 10% class III and IV cracking. Zero remaining life assumed.

Deflections Used For Section Selection (Depending on remaining life of existing pavement, pavement type and overlay type.)

Deflection basin slopes at the pavement joints.

Laboratory Testing (Tests done or assumptions made. M_r S_{sg} f_c)

No laboratory testing.

B. Layer Stiffnesses

Table from MODE.
Lab test results.
Table for calculating layer moduli based on deflection basin slopes, condition survey data and fatigue life.
90^{th} percentile subgrade modulus.
Moduli from deflection basin slopes at pavement joints or defects if no remaining life.

Table A.13 Defelction statistics of the at-joint deflections.

Table A.14 Deflection basin slopes corresponding to estimated layer moduli.

TABLE OF DEFLECTION PARAMETER STATISTICS
SLOPE = SENSOR 1 - SENSOR 5
SCI = SENSOR 1 - SENSOR 2
BCI = SENSOR 4 - SENSOR 5
SPREADABILITY = (SENSOR 1+2+3+4+5)/(5 TIMES SENSOR 1)
AVE = AVERAGE MD = MODE STD = STANDARD DEVIATION CV = COEFFICIENT OF VARIATION
NSEC = NUMBER OF DEFLECTIONS IN SECTION

SECTION		SENSOR 1				SENSOR 5				SLOPE				SPREADABILITY			SCI			BCI		
N	NSEC	AVE	MD	STD	CV	AVE	MD	STD	CV	AVE	MD	STD	CV	AVE	STD	CV	AVE	STD	CV	AVE	STD	CV
1	152	1.07	1.15	.37	.34	.61	.60	.19	.31	.46	.38	.27	.58	.82	.29	.35	.12	.16	1.38	.14	.21	1.45
2	41	1.62	1.15	.78	.48	.84	.83	.31	.37	.77	.68	.49	.63	.75	.05	.06	.25	.16	.64	.14	.11	.80
3	51	1.10	1.05	.26	.23	.59	.60	.12	.20	.51	.43	.18	.35	.77	.06	.08	.14	.07	.51	.12	.08	.64
4	31	1.69	1.15	.94	.56	.70	.80	.26	.32	.90	.58	.72	.79	.74	.07	.09	.26	.19	.70	.17	.20	1.17
5	35	.87	.75	.21	.24	.52	.50	.10	.19	.35	.28	.14	.41	.81	.04	.06	.07	.06	.85	.07	.04	.55
6	18	1.01	.75	.49	.48	.56	.35	.21	.38	.45	.33	.30	.65	.79	.07	.08	.11	.09	.83	.09	.06	.67
7	31	.88	.75	.18	.23	.48	.45	.09	.18	.32	.28	.12	.36	.81	.04	.05	.06	.04	.62	.07	.04	.55
8	62	1.03	1.05	.33	.32	.57	.50	.14	.25	.47	.43	.21	.46	.77	.05	.07	.13	.08	.59	.09	.06	.70
9	32	.84	.75	.20	.24	.59	.50	.27	.45	.25	.23	.28	1.13	.83	.07	.08	.08	.06	.74	.01	.25	28.41
10	20	1.43	.75	.47	.33	.76	.85	.16	.21	.68	.53	.34	.50	.75	.04	.05	.21	.10	.46	.12	.06	.48
11	93	.81	.65	.23	.28	.47	.43	.08	.18	.35	.23	.18	.51	.80	.05	.06	.09	.05	.56	.09	.07	.80
12	25	1.16	1.15	.27	.24	.73	.70	.21	.28	.44	.58	.26	.60	.79	.05	.07	.16	.09	.59	.05	.19	3.80
13	38	.78	.65	.17	.21	.45	.43	.08	.19	.33	.28	.12	.35	.79	.04	.05	.08	.05	.58	.08	.03	.42
14	40	1.01	.85	.22	.22	.51	.45	.10	.19	.50	.43	.15	.30	.76	.04	.05	.13	.05	.42	.13	.05	.37
15	18	.83	.65	.16	.19	.48	.40	.10	.21	.34	.28	.11	.33	.80	.05	.06	.10	.04	.41	.10	.05	.48

SUBGRADE MODULUS UNDER THE DYNAFLECT LOAD

SECTION	MODAL SUBGRADE MODULUS
1	6653.
2	6162.
3	8775.
4	6376.
5	10743.
6	15962.
7	12876.
8	10743.
9	10743.
10	5961.
11	12867.
12	7395.
13	12867.
14	12876.
15	13763.

TABLE OF DEFLECTION PARAMETER STATISTICS
SLOPE = SENSOR 1 - SENSOR 5
SCI = SENSOR 1 - SENSOR 2
BCI = SENSOR 4 - SENSOR 5
SPREADABILITY = (SENSOR 1+2+3+4+5)/(5 TIMES SENSOR 1)
AVE = AVERAGE MD = MODE STD = STANDARD DEVIATION CV = COEFFICIENT OF VARIATION
NSEC = NUMBER OF DEFLECTIONS IN SECTION

SECTION		SENSOR 1				SENSOR 5				SLOPE				SPREADABILITY			SCI			BCI		
N	NSEC	AVE	MD	STD	CV	AVE	MD	STD	CV	AVE	MD	STD	CV	AVE	STD	CV	AVE	STD	CV	AVE	STD	CV
1	23	1.22	.75	.50	.41	.59	.68	.14	.23	.63	.28	.52	.83	.74	.06	.09	.18	.10	.54	.11	.16	1.49
2	16	.81	.65	.21	.26	.54	.43	.18	.34	.27	.28	.07	.27	.83	.04	.04	.06	.03	.49	.04	.03	.69
3	15	1.12	.95	.28	.25	.62	.78	.14	.22	.50	.43	.16	.32	.77	.04	.05	.15	.07	.46	.10	.09	.91
4	38	.77	.65	.23	.29	.49	.43	.12	.25	.28	.23	.13	.47	.82	.04	.05	.07	.05	.74	.06	.04	.65
5	72	1.02	.85	.34	.33	.54	.68	.14	.27	.48	.33	.24	.50	.77	.06	.08	.13	.10	.77	.10	.06	.55
6	84	.88	.85	.24	.27	.54	.68	.13	.24	.34	.23	.18	.51	.82	.05	.06	.08	.05	.68	.11	.12	1.12
7	10	1.07	.65	.46	.43	.55	.38	.23	.42	.52	.43	.26	.50	.75	.05	.07	.19	.11	.57	.11	.05	.47
8	97	.88	.45	.22	.25	.56	.48	.13	.23	.33	.23	.15	.46	.83	.05	.07	.09	.06	.74	.09	.06	.65
9	85	1.01	.95	.32	.32	.59	.60	.13	.22	.42	.28	.23	.54	.79	.05	.07	.12	.09	.75	.09	.06	.68
10	83	1.51	.75	.75	.50	.77	.58	.24	.31	.74	.38	.55	.74	.76	.07	.09	.24	.17	.71	.16	.16	1.02
11	119	1.22	.85	.40	.33	.65	.60	.15	.23	.56	.43	.28	.50	.78	.13	.16	.18	.11	.58	.14	.08	.55

SUBGRADE MODULUS UNDER THE DYNAFLECT LOAD

SECTION	MODAL SUBGRADE MODULUS
1	6653,
2	12867,
3	7395,
4	12867,
5	8775,
6	8775,
7	14785,
8	12876,
9	8775,
10	9200,
11	8775,

TABLE A.14 DEFLECTION BASIN SLOPES CORRESPONDING TO LAYER MODULI FOR 10 INCH JCP.

DEFLECTION BASIN SLOPE DYNAFLECT SENSOR 1 MINUS SENSOR 5	E_1 $x10^6$psi	E_2 $x10^5$psi	E_3 $x10^3$psi
0.5	5	2	6
0.7	4	2	6
0.8	3.5	1	6
1.0	3	0.5	6
1.2	1.75	0.5	6

2. FATIGUE LIFE PREDICTION

A. General Comments

Fatigue of Existing Pavements

Existing pavement assumed to have no remaining life. It is recommended that all joints which have a basin slope exceeding the design basin slope, be repaired.

Overlay Fatigue

Overlay fatigue considered by modelling the existing pavement in accordance with the steep basin slope obtained at the pavement joints.

Reflection Cracking

Reflection cracking implicitly allowed for by the above modelling procedure.

B. Fatigue Life

Table showing fatigue lives of different pavement layers.

Table A.15 Overlay thicknesses and number of joints requiring repair for a range of joint basin slopes.

TABLE A.15

PERCENT JOINTS/NO. OF JOINTS REQUIRING REPAIR FOR THE JOINT BASIN SLOPE/OVERLAY THICKNESS, INDICATED												
SECT-IONS	W_1-W_5	D_{o1}	W_1-W_5	D_{o1}	W_1-W_5	D_{o1}	W_1-W_5	D_{o1}	W_1-W_5	D_{o1}	W_1-W_5	D_{o1}
	0.5	8.0	0.6	8.5	0.7	9.0	0.8	9.5	1.0	10.0	1.2	11.0
WB A	55	116	30	64	15	32	9	19	9	19	4	8
B	0	0	0	0	0	0	0	0	0	0	0	0
C	35	31	25	22	10	9	0	0	0	0	0	0
D	7	34	3	15	1	5	0	0	0	0	0	0
E	35	172	25	173	15	74	8	39	1	5	0	0
F	7	54	3	23	2	15	1	8	1	8	1	8
G	45	32	25	18	15	11	10	7	10	7	0	0
H	7	74	4	42	2	21	2	21	0	0	0	0
I	20	141	15	106	10	70	6	42	4	28	1	7
J	55	310	50	282	40	225	31	174	18	101	12	68
K	45	364	25	202	17	138	12	97	4	32	1	8

TABLE A.15 CONTINUED

PERCENT JOINTS/NO. OF JOINTS REQUIRING REPAIR FOR THE JOINT BASIN SLOPE/OVERLAY THICKNESS, INDICATED												
SECTIONS	W_1-W_5	D_{o1}	W_1-W_5	D_{o1}	W_1-W_5	D_{o1}	W_1-W_5	D_{o1}	W_1-W_5	D_{o1}	W_1-W_5	D_{o1}
	0.5	8.0	0.6	8.5	0.7	9.0	0.8	9.5	1.0	10.0	1.2	11.0
EB A	35	394	22	288	15	169	9	101	2	23	1	11
B	70	222	55	174	35	111	29	92	20	63	12	38
C	50	264	25	132	10	53	6	32	2	11	0	0
D	75	132	60	106	50	88	45	79	32	56	26	46
E	10	5	5	12	3	7	3	7	0	0	0	0
F	30	32	22	23	18	19	18	19	0	0	0	0
G	7	25	2	7	1	4	0	0	0	0	0	0
H	35	185	15	79	10	53	5	26	3	16	2	11
I	5	14	2	6	1	3	0	0	0	0	0	0
J	70	99	45	63	35	49	20	28	5	7	0	0
K	7	52	2	15	1	7	1	7	1	7	1	7
L	30	42	20	28	12	17	8	11	4	6	0	0
M	5	14	2	6	1	3	0	0	0	0	0	0
N	35	123	15	53	8	28	2	7	0	0	0	0
O	7	7	2	2	1	1	0	0	0	0	0	0

APPENDIX B

PROGRAM MODE

```
      PROGRAM MODE (INPUT,OUTPUT,TAPE5=INPUT,TAPE6=OUTPUT,TAPE1)
CC
C     THIS PROGRAM IS FOR USE WITH DYNAFLECT DEFLECTION MEASUREMENTS
C
C     THE PROGRAM PLOTS THE FREQUENCY AND CUMULATIVE DISTRIBUTIONS
C     OF A NUMBER OF DESIGN PARAMETERS CALCULATED FROM DYNAFLECT
C     DEFLECTION MEASUREMENTS.
C
C     THE RANGE OF THE DEFLECTION MEASUREMENTS IS DIVIDED INTO
C     INTERVALS.  THE LOWER AND UPPER LIMITS OF THE RANGE ARE
C     INPUT BY THE USER. (FDMIN,FDMAX,FSMIN,FSMAX)
C     FDMIN AND FDMAX REFER TO THE LIMITS OF THE RANGE OF SENSOR 1
C     AND SENSOR 5 DEFLECTIONS.
C     FSMIN AND FSMAX REFER TO THE LIMITS OF THE RANGE OF THE
C     BASIN SLOPES (SENSOR 1 - SENSOR 5)
C     A NUMBER OF STATISTICS RELATING TO THE DEFLECTIONS WITHIN A
C     SECTION, ARE CALCUATED.
C
C     MODE
C     AVERAGE
C     STANDARD DEVIATION
C
C     THESE STATISTICS ARE CALCULATED FOR SENSOR 1, SENSOR 5, AND THE
C     BASIN SLOPES (SENSOR 1 - SENSOR 5)
C
C     -----     ----     ----    ----    ----    ----    ----    -.--
C
C     IN ORDER TO USE THE PROGRAM IT SHOULD BE RUN TWICE ON THE SAME
C     DATA;  ONCE TO OBTAIN THE FREQUENCY DISTRIBUTION OF THE VARIOUS
C     DEFLECTION PARAMETERS, AND THEN AGAIN TO OBTAIN THE SUBGRADE
C     MODULUS, TENSILE STRESS, AND FATIGUE LIFE DISTRIBUTIONS.
C
C     ------------------------------------------------------------.-----
C
C     INPUTS
C
C     ------------------------------------------------------------.-.-----
C
C     THE INPUT TO THE PROGRAM REQUIRES 4 CARDS
C
C     CARD 1     I2,19A4
C          COLS  1 - 2   ISWELS= A SWITCH TO INDICATE WHETHER ELSYM5
C                                RUNS ARE REQUIRED TO CHECK THE
C                                REGRESSION STRESSES.
C
C         COLS   3 - 76  NTITLE= A SUITABLE TITLE.
C
C
C     CARD 2   I5,4F5.2,2I5
C          COLS  1 - 5   N    = THE NUMBER OF SECTIONS INTO WHICH
C                               THE ROADWAY IS DIVIDED, BASED ON
C                               THE DEFLECTION MEASUREMENTS IN THE
C                               SECTION
C
C                6 - 10  FDMIN= THE LOWER AND UPPER BOUNDARIES=
C               11 - 15  FDMAX= IN MILLI-INCHES, WITHIN WHICH MOST
C                               OF THE SENSOR 1 DEFLECTION MEASURE-
C                               MENTS ARE EXPECTED TO FALL.
C                               EXAMPLE  0.2  1.0
C                               FDMIN MUST BE GT 0.0
C
C                16 - 20  FSMIN= THE LOWER AND UPPER LIMITS , IN
C                21 - 25  FSMAX= MILLI-INCHES, WITHIN WHICH THE
C                               SLOPES OF THE DEFLECTION BASINS
C                               ARE EXPECTED TO FALL.
C                               EXAMPLE  0.1   1.0
C                               FSMIN MUST BE GT 0.0
C                26 - 30  NOPLT= THE NUMBER OF DEFLECTION FREQUENCY
C                               DISTRIBUTION DIAGRAMS TO BE PLOTTED.
C                               IF NOPLT = 0 SENSOR 5 PLOTTED
C                               IF NOPLT = 1 BASIN SLOPE PLOTTED
C                               IF NOPLT = 2 SLOPE AND SENS 5
C                               IF NOPLT = 3 SENS 1, SENS 5 AND
C                               BASIN SLOPES ARE PLOTTED
C
C
C               THE FOLLOWING DATA ON THIS CARD ONLY NEEDS TO BE INPUT
C               IF THE FATIGUE LIFE DISTRIBUTION OF THE SECTIONS OF
C               ROAD ARE TO BE PLOTTED
C
C                31 - 35  NFPLT= THE TYPES OF FREQUENCY DISTRIBUTION
C                               CURVES TO BE PLOTTED FROM THE
C                               FATIGUE ANALYSIS.
C                               IF NFPLT = 0 FATIGUE LIFE DIST.
C                               IS PLOTTED
C                               IF NFPLT = 1 TENSILE STRESS AND
C                               FATIGUE LIFE DISTRIBUTIONS ARE
C                               PLOTTED.
C                               IF NFPLT = 2 SUBGRADE MODULUS UNDER AN
C                               18 KIP AXLE LOAD,
C                               TENSILE STRESS AND FATIGUE LIFE,
C                               DISTRIBUTIONS ARE PLOTTED.
C
C
C     CARD 3,.NSECT+3  I5,6F10.0,2F5.3
C          COLS  1 -  5 NSEC(N)=THE NUMBER OF DEFLECTION
C                               BASINS MEASURED IN EACH SECTION
C                               OF THE ROADWAY.
C
C               COLS  6 - 15 D1(N)  =THICKNESS OF LAYER 1 (INCHES)
C                               VALID THICKNESSES ARE 7,8,9,10 AND 12
C                               DEFAULT = 7 INCHES
C
C               THE FOLLOWING DATA ON THIS CARD ONLY NEEDS TO BE INPUT
C               IF THE FATIGUE LIFE DISTRIBUTION OF THE SECTIONS OF
C               ROAD ARE TO BE PLOTTED
C
C               COLS 16 - 25 E1(N)  =MODULUS OF LAYER 1    (PSI)
C
C               COLS 26 - 35 D2(N)  =THICKNESS OF LAYER 2 (INCHES)
C
C               COLS 36 - 45 E2(N)  =MODULUS OF LAYER 2    (PSI)
C
C               COLS 46 - 55 D3(N)  =THICKNESS OF LAYER 3 (INCHES)
C                               THIS IS OPTIONAL.  IF LEFT BLANK
C                               THE PROGRAM ASSUMES THE SUBGRADE
C                               IS INFINITELY THICK.
C
C               COLS 56 - 65 F1(N)  =MODULUS OF RUPTURE OF CONCRETE
C                               SURFACE LAYER.
C
C               COLS 66 - 70 STATK(N) STATIC RATIO OF VERTICAL TO
```

```
C                              HORIZONTAL EFFECTIVE STRESS.
C                              OPTIONAL, IF LEFT BLANK THE
C                              PROGRAM WILL ASSUME THAT NO
C                              OVERBURDEN STRESSES ARE TO BE
C                              USED IN THE CALCULATION OF
C                              SUBGRADE MODULUS UNDER AN 18KIP
C                              AXLE LOAD.
C
C          COLS 71 - 75 SSG(N) -THE SLOPE OF THE SUBGRADE MODULUS
C                              DEVIATOR STRESS LINE WHEN LAB TEST
C                              DATA IS PLOTTED ON A LOG-LOG SCALE.
C                              OPTIONAL, IF LEFT BLANK PROGRAM
C                              ASSUMES ZERO STRESS SENSITIVITY.
C
C          COLS 76 - 80 STRSF(N)- AN INTERIOR TO EDGE STRESS FACTOR
C                                 FOR INCREASING THE STRESSES AS
C                                 CALCULATED BY LAYERED THEORY TO
C                                 ACCOUNT FOR EDGE LOADING CONDITIONS
C
C     THESE VALUES NEED ONLY BE INPUT ONCE IF THEY ARE THE SAME FOR
C     ALL SECTIONS. THE PROGRAM WILL ASSIGN PRECEDING VALUES FOR ALL
C     SUBSEQUENT SECTIONS.
C
C
C     CARD NSECT+4  16A4
C          COLS  1 - 64   IFORM - A SUITABLE FORMAT FOR READING
C                                 SENSOR 1 TO SENSOR 5 DYNAFLECT
C                                 DEFLECTIONS. DEFAULT IS
C                                (30X,5(F2.1,F3.2))
C
C     DATA CARDS
C
C     ------------------------------------------------------------
C
C     LIST OF VARIABLES.
C
C     ------------------------------------------------------------
C
C     DEFL(K,J)    - DEFLECTION AT SENSOR K UNDER THE DYNAFLECT
C                    LOAD
C
C     SLOPE(J)     - DIFFERENCE BETWEEN DEFLECTIONS AT SENSORS 1 AND 5
C
C     FD(I)        - UPPER LIMITS OF FREQUENCY INTERVAL (I) FOR MAX-
C                    IMUM DEFLECTIONS.
C
C     FS(L)        - UPPER LIMIT OF FREQUENCY INTERVAL (I) FOR
C                    DEFLECTION BASIN SLOPES
C
C
C     NSEC(N)      - NUMBER OF DEFLECTION POINTS IN SECTION N
C
C     NDGT         - NUMBER OF DEFLECTIONS WHICH FALL OUTSIDE THE
C                    MAXIMUM DEFLECTION INTERVAL.
C
C     NSGT         - NUMBER OF BASIN SLOPES WHICH FALL OUTSIDE THE
C                    MAXIMUM SLOPE INTERVAL.
C
C     NF           - THE NUMBER OF DEFLECTIONS WITHIN THE INTERVAL I
C
C     NS(I)        - THE NUMBER OF BASIN SLOPES WITHIN THE INTERVAL I
C
C     SLOPE(I)     - THE SLOPE OF THE DEFLECTION BASIN I
C                    EQUAL TO SENSOR1 - SENSOR5
C
C     FOLD(I)      - THE OLD LIMITS OF THE DEFLECTION INTERVALS
C                    SET BEFORE THE INTERVALS ARE SHIFTED.
C
C     SUM(I)       - THE SUM OF EACH SENSORS DEFLECTION FOR THOSE
C                    DEFLECTIONS WHICH FALL WITHIN THE MODAL INTERVAL.
C
C     AVEDEF(I)    - THE AVERAGE DEFLECTON
C     AVEDEF(I)    - THE AVERAGE DEFLECTION FOR THOSE DEFLECTIONS
C                    WHICH FALL WITHIN THE MODAL INTERVAL.
C
C     N            - A COUNTER WHICH COUNTS THE NUMBER OF SECTIONS.
C
C     FDMAX        - THE UPPER LIMIT OF THE DEFLECTIONS WITHIN
C                    WHICH THE MODE IS EXPECTED TO FALL.
C
C     FSMAX        - THE UPPER LIMIT OF THE BASIN SLOPES WITHIN
C                    WHITH THE MODE IS EXPECTED TO FALL
C
C     IFORM        - A SUITABLE FORMAT STATEMENT FOR READING THE INPUT
C                    DATA
C
C     NDINT        - THE NUMBER OF INTERVALS INTO WHICH THE RANGE OF
C                    DEFLECTIONS IS
C                    DEFLECTIONS IS DIVIDED.
C
C     NSINT        - THE NUMBER OF INTERVALS INTO WHICH THE RANGE OF
C                    DEFLECTION BASIN SLOPES IS DIVIDED.
C
C     IMODE        - THE MODE INTERVAL NUMBER
C
C     ISLOPE       - THE BASIN SLOPE MODE INTERVAL NUMBER.
C
C     UMODE        - THE UPPER LIMIT OF THE DEFLECTION MODAL INTERVAL.
C
C     USLOPE       - THE UPPER LIMIT OF THE BASIN SLOPE MODAL INTERVAL.
C
C     BMODE        - THE BOTTEM LIMIT OF THE DEFLECTION MODAL INTERVAL.
C
C     BSLOPE       - THE BOTTEM LIMIT OF THE BASIN SLOPE MODAL INTERVAL.
C
C
      COMMON /DTS/ FD(30),FS(30),FD5(60),NF(30),NS(30),NF5(60),NSEC(20),
     1IFORM(16),ELSTRS,ELSFAT
      COMMON /READ/ FDMAX,FSMAX,FDMIN,FSMIN,N,NPLT,NDPLT,JSW,KSW,NSECT
     1,ISWELS
      COMMON /FATIG/ D1(20),D2(20),D3(20),E1(20),E2(20),F1(20),STATK(20)
     1,SSG(20),STRSF(20)
C
      DIMENSION NTITLE(19), IFOR(16)
      INTEGER BLNK
      DATA IFOR/2H(3,2HOX,2H5(,2HF2,2H.1,2H,F,2H3.,2H2),2H ),7*1H /
      DATA BLNK/4H    /
C
C
      KSW=0
      READ (5,10) ISWELS,NTITLE
   10 FORMAT (I2,19A4)
      WRITE (6,20) NTITLE
   20 FORMAT (1H1///5X, 12HPROGRAM MODE///20A4)
```

```
C
      READ (5,30) NSECT,FDMIN,FDMAX,FSMIN,FSMAX,NDPLT,NFPLT
   30 FORMAT (I5,4F5.2,2I5)
      IF (NDPLT.GT.3) GO TO 130
      IF (NFPLT.GT.2) GO TO 130
C
      READ (5,40) ((NSEC(I),D1(I),E1(I),D2(I),E2(I),D3(I),F1(I)),STATK(I
     1),SSG(I),STRSF(I),I=1,NSECT)
   40 FORMAT (I5,6F10.0,3F5.3)
      IF (E1(1).LE.0.0) GO TO 60
      KSW=1
      IF (NSECT.EQ.1) GO TO 60
      DO 50 I=2,NSECT
         IF (E1(I).LE.0.0) E1(I)=E1(I-1)
         IF (E2(I).LE.0.0) E2(I)=E2(I-1)
         IF (D1(I).LE.0.0) D1(I)=D1(I-1)
         IF (D2(I).LE.0.0) D2(I)=D2(I-1)
         IF (D3(I).LE.0.0) D3(I)=D3(I-1)
         IF (F1(I).LE.0.0) F1(I)=F1(I-1)
         IF (STATK(I).LE.0.0) STATK(I)=STATK(I-1)
         IF (SSG(I).LE.0.0) SSG(I)=SSG(I-1)
         IF (STRSF(I).LE.0.0) STRSF(I)=STRSF(I-1)
   50 CONTINUE
   60 DO 70 I=1,NSECT
         IF (NSEC(I).GT.750) GO TO 150
   70 CONTINUE
C
      READ (5,80) IFORM
   80 FORMAT (16A4)
      IF (IFORM(1).NE.BLNK) GO TO 100
      DO 90 I=1,16
         IFORM(I)=IFOR(I)
   90 CONTINUE
C
  100 N=1
  110 JSW=0
      CALL DIST
      CALL PRINT
      CALL SGMOD
      CALL PLOT
      N=N+1
      IF (N.EQ.NSECT+1) GO TO 120
      GO TO 110
  120 CALL PRINT
      CALL EXIT
  130 WRITE (6,140)
  140 FORMAT (5X, 68HNFPLT OR NDPLT IS GREATER THAN 2 OR 3
     1      RESPECTIVELY)
  150 WRITE (6,160)
  160 FORMAT (5X, 27HNSEC(I) IS GREATER THAN 750)
C
      END
      SUBROUTINE DIST
      COMMON /AVE/ AVESCI,AVEBCI,AVESL,AVESP,AVEW1,AVEW5,STDSCI,STDBCI,S
     1TDSL,STDSP,STDW1,STDW5,CVW1,CVW5,CVSL,CVSP,CVSCI,CVBCI,AMODE1,AMOD
     2E5,AMDESL
      COMMON /READ/ FDMAX,FSMAX,FDMIN,FSMIN,N,NFPLT,NDPLT,JSW,KSW,NSECT
     1,ISWELS
      COMMON /MDOC/ BMODE,UMODE,BMODES,UMODES,NDGT5,NDGT,NDINT,NSINT,K,B
     1SLOPE,USLOPE,NSGT,NDINT5,AMSBG(20)
      COMMON /DTB/ FD(30),FS(30),FD5(60),NF(30),NS(30),NF5(60),NSEC(20),
     1IFORM(16),ELSTRS,FLSFAT
      DIMENSION DAT(5), DATM(5), DEFL(5,750), SLOPE(750), FOLD(30), NFOL
     1D(30), FOLD5(60), NFOLD5(60)
C
C     SET THE BOUNDARIES OF THE VARIOUS INTERVALS FOR FREQUENCY
C     CALCULATION.
C
      STD(A,B,C)=SQRT((A-B*B/C)/(C-1.0))
      SUMW1=0.0
      SUMW5=0.0
      SUMSP=0.0
      SUMSL=0.0
      SUMBCI=0.0
      SUMSCI=0.0
      SMSQSC=0.0
      SMSQBC=0.0
      SMSQSP=0.0
      SMSQSL=0.0
      SUMSQ1=0.0
      SUMSQ5=0.0
      TOTDEF=0.0
      NDINT=(FDMAX-FDMIN)/0.1
      NDINT=NDINT+1
      NDINT5=(FDMAX-FDMIN)/0.05
      NDINT5=NDINT5+1
      NSINT=(FSMAX-FSMIN)/0.05
      NSINT=NSINT+1
      FD(1)=FDMIN
      FD5(1)=FDMIN
      DO 10 I=1,NDINT
         FD(I+1)=FD(I)+0.1
   10 CONTINUE
      DO 20 I=1,NDINT5
         FD5(I+1)=FD5(I)+0.05
   20 CONTINUE
      FS(1)=FSMIN
      DO 30 I=1,NSINT
         FS(I+1)=FS(I)+0.05
   30 CONTINUE
      NCNT=NSEC(N)
      DO 70 J=1,NCNT
         READ (5,IFORM) ((DAT(IA),DATM(IB)),IB=1,5)
C
C
C     CHECK FOR ERRORS IN INPUT DATA , IF DATM IS LE. 0.0 THE PROGRAM
C     AUTOMATICALLY ASSUMES THAT DATM = 1.0
C
C
C
         DO 60 K=1,5
            DO 40 II=1,5
   40       IF (DATM(II).LE.0.0) DATM(II)=1.0
            DO 50 II=1,5
            IF (DAT(II).LE.0.0) GO TO 460
   50 CONTINUE
            DEFL(K,J)=DAT(K)*DATM(K)
   60    CONTINUE
         SLOPE(J)=DEFL(1,J)-DEFL(5,J)
   70 CONTINUE
      ISW=0
      DO 80 IA=1,30
         NS(IA)=0
   80 CONTINUE
      NSGT=0
```

```
   90 DO 100 IA=1,60
         NF5(IA)=0
      DO 100 IC=1,30
         NF(IC)=0
  100 CONTINUE
      NDGT=0
      NDGT5=0
C
C     DETERMINE THE NUMBER OF DEFLECTION MEASURMENTS AND THE
C     NUMBER OF DEFLECTION BASIN SLOPES WHICH FALL WITHIN EACH
C     INTERVAL.
C     ALSO CALCULATE AVERAGES AND STANDARD DEVIATIONS
C     FOR THE FOLLOWING: SCI, BCI, SP, SLOPE, DEFL(1) AND DEFL(5)
C
      DO 220 J=1,NCNT
         IF (ISW.EQ.1) GO TO 120
         SUMW1=SUMW1+DEFL(1,J)
         SUMW5=SUMW5+DEFL(5,J)
         SUMSQ1=SUMSQ1+DEFL(1,J)*DEFL(1,J)
         SUMSQ5=SUMSQ5+DEFL(5,J)*DEFL(5,J)
         SCI=DEFL(1,J)-DEFL(2,J)
         BCI=DEFL(4,J)-DEFL(5,J)
         SUMSL=SUMSL+SLOPE(J)
         SMSQSL=SMSQSL+SLOPE(J)*SLOPE(J)
         DO 110 K=1,5
            TOTDEF=TOTDEF+DEFL(K,J)
  110    CONTINUE
         SP=TOTDEF/(5.0*DEFL(1,J))
         TOTDEF=0.0
         SUMSCI=SUMSCI+SCI
         SUMBCI=SUMBCI+BCI
         SUMSP=SUMSP+SP
         SMSQSC=SMSQSC+SCI*SCI
         SMSQBC=SMSQBC+BCI*BCI
         SMSQSP=SMSQSP+SP*SP
  120    I=1
         L=1
         K=1
C
C     DETERMINE THE NUMBER OF W1 DEFLECTIONS WITHIN EACH INTERVAL.
C
  130    IF (DEFL(1,J).GT.FD(I)) GO TO 140
         NF(I)=NF(I)+1
         GO TO 160
  140    I=I+1
         IF (I.GT.(NDINT+1)) GO TO 150
         GO TO 130
  150    NDGT=NDGT+1
C
C     DETERMINE NUMBER OF W5 DEFLECTIONS WITHIN EACH INTERVAL.
C
  160    IF (DEFL(5,J).GT.FD5(K)) GO TO 170
         NF5(K)=NF5(K)+1
         GO TO 190
  170    K=K+1
         IF (K.GT.(NDINT5+1)) GO TO 180
         GO TO 160
  180    NDGT5=NDGT5+1
C
C     DETERMINE THE NUMBER OF DEFL. BASIN SLOPES WITHIN EACH INTERVAL.
C
  190    IF (ISW.EQ.1) GO TO 220
         IF (SLOPE(J).GT.FS(L)) GO TO 200
         NS(L)=NS(L)+1
         GO TO 220
  200    L=L+1
         IF (L.GT.(NSINT+1)) GO TO 210
         GO TO 190
  210    NSGT=NSGT+1
  220 CONTINUE
C
C
      IF (ISW.EQ.1) GO TO 230
C
C
C     CALC AVERAGES AND STD DEVIATIONS
C
C
      ASEC=NSEC(N)
      AVESCI=SUMSCI/ASEC
      AVEBCI=SUMBCI/ASEC
      AVESL=SUMSL/ASEC
      AVESP=SUMSP/ASEC
      AVEW1=SUMW1/ASEC
      AVEW5=SUMW5/ASEC
C
C
      STDSCI=STD(SMSQSC,SUMSCI,ASEC)
      STDBCI=STD(SMSQBC,SUMBCI,ASEC)
      STDSP=STD(SMSQSP,SUMSP,ASEC)
      STDSL=STD(SMSQSL,SUMSL,ASEC)
      STDW1=STD(SUMSQ1,SUMW1,ASEC)
      STDW5=STD(SUMSQ5,SUMW5,ASEC)
C
C
      CVW1=STDW1/AVEW1
      CVW5=STDW5/AVEW5
      CVSL=STDSL/AVESL
      CVSP=STDSP/AVESP
      CVBCI=STDBCI/AVESCI
      CVSCI=STDSCI/AVESCI
C
C     SET THE VALUES OF THE MODAL INTERVAL FOR THE DEFLECTIONS.
C
  230 IMODE=1
      IMODE5=1
      ISLOPE=1
      DO 240 I=1,NOINT
         IF (NF(IMODE).GT.NF(I+1)) GO TO 240
         IMODE=I+1
  240 CONTINUE
      DO 250 I=1,NOINT5
         IF (NF5(IMODE5).GT.NF5(I+1)) GO TO 250
         IMODE5=I+1
  250 CONTINUE
      IF (ISW.EQ.1) GO TO 370
      DO 260 I=1,NOINT
         IF (NS(ISLOPE).GT.NS(I+1)) GO TO 260
         ISLOPE=I+1
  260 CONTINUE
      ISW=1
      DO 270 I=1,NOINT
         NFOLD(I)=NF(I)
  270 CONTINUE
```

```
      IF (IMODE.EQ.1) GO TO 380
      BMODE=FD(IMODE-1)
      GO TO 410
  380 BMODE=0.0
      GO TO 410
  390 UMODE=UMODE1
      BMODE=BMODE1
      NDGT=NGT1
      NDINT=NDINT+1
      MDINT=NDINT+1
      DO 400 I=1,MDINT
         NF(I)=NFOLD(I)
         FD(I)=FOLD(I)
  400 CONTINUE
  410 IF (NFF5.GT.NF5(IMODE5)) GO TO 430
      UMODE5=FD5(IMODE5)
      IF (IMODE5.EQ.1) GO TO 420
      BMODE5=FD5(IMODE5-1)
      GO TO 450
  420 BMODE5=0.0
      GO TO 450
  430 UMODE5=UMODE5
      BMODE5=BMDEE5
      NDGT5=NGTT5
      NDINT5=NDINT5+1
      MDINT5=NDINT5+1
      DO 440 I=1,MDINT5
         NF5(I)=NFOLD5(I)
         FD5(I)=FOLD5(I)
  440 CONTINUE
  450 AMODE1=(UMODE1+BMODE1)/2.0
      AMODE5=(UMODE5+BMODE5)/2.0
      AMDESL=(USLOPE+BSLOPE)/2.0
      GO TO 480
  460 WRITE (6,470) J
  470 FORMAT (1X, 19HERROR IN DATA LINE ,I3, 12HAT ,LE, 8.0)
      STOP
  480 RETURN
C
      END
      SUBROUTINE SGMOD
CC
C     THIS SUBROUTINE CALCULATES:
C
C     1, SUBGRADE MODULUS FROM SENSOR 5 DEFLECTIONS
C     2, MODIFIED SUBGRADE MODULUS FOR A SUBGRADE OF FINITE THICKNESS
C     3, SUBGRADE MODULUS UNDER AN 18 KIP AXLE LOAD, (STRESS SENSITIVITY
C     4, TENSILE STRESS IN THE CONCRETE LAYER UNDER AN 18KIP AXLE.
C     5, FATIGUE LIFE OF THE PAVEMENT.
C
C
C     REGRESSION EQUATIONS, OBTAINED FROM LAYERED THEORY ANALYSIS,
C     ARE USED FOR ALL THE ABOVE CALCULATIONS.
C     THE ABOVE PARAMETERS ARE CALCULATED FOR ALL THE INTERVALS
C     USED IN THE PLOT OF W5 DEFLECTIONS.
C
      COMMON /DIS/ FD(30),FS(30),FD5(60),NF(30),NS(30),NF5(60),NSEF(20),
     1IFORM(16),ELSTRS,ELSFAT
      COMMON /MODC/ BMODE,UMODE,BMODE5,UMODE5,NDGT5,NDGT,NDINT,NSINT,K,R
     1SLOPE,USLOPE,NSGT,NDINT5,AMSBG(20)
      COMMON /READ/ FDMAX,FSMAX,FDMIN,FSMIN,N,NPLT,NDPLT,JJ=,KSW,NSECT
     1,ISWELS
      DO 280 I=1,MDINT5
         NFOLD5(I)=NF5(I)
  280 CONTINUE
      NF1=NF(IMODE)
      NFF5=NF5(IMODE5)
      NS1=NS(ISLOPE)
      NGT1=NDGT
      NGTT5=NDGT5
      UMODE1=FD(IMODE)
      UMDEE5=FD5(IMDDE5)
      IF (IMODE5.EQ.1) GO TO 290
      BMDEE5=FD5(IMODE5-1)
      GO TO 300
  290 BMDEE5=0.0
  300 IF (IMODE.EQ.1) GO TO 310
      BMODE1=FD(IMODE-1)
      GO TO 320
  310 BMODE1=0.0
  320 CONTINUE
C
C     SET THE VALUES OF THE MODAL INTERVAL FOR THE
C     SLOPES OF THE VARIOUS DEFLECTION BASINS.
C
      USLOPE=FS(ISLOPE)
      IF (ISLOPE.EQ.1) GO TO 330
      BSLOPE=FS(ISLOPE-1)
      GO TO 340
  330 BSLOPE=0.0
  340 CONTINUE
C
C
C     SET INTERMEDIATE INTERVAL LIMITS FOR DEFLECTION FREQUENCY
C     DISTRIBUTION CALCULATIONS.
C
C
      DO 350 I=1,NDINT
         FOLD(I)=FD(I)
         FD(I)=(FD(I)+FD(I+1))/2.0
  350 CONTINUE
      FOLD(NDINT+1)=FD(NDINT+1)
      NDINT=NDINT-1
      MDINT=NDINT+1
      DO 360 I=1,NDINT5
         FOLD5(I)=FD5(I)
         FD5(I)=(FD5(I)+FD5(I+1))/2.0
  360 CONTINUE
      FOLD5(NDINT5+1)=FD5(NDINT5+1)
      NDINT5=NDINT5-1
      MDINT5=NDINT5+1
C
C     RETURN TO THE CALCULATION OF THE MODAL DEFLECTION INTERVAL
C     USING INTERMEDIATE INTERVALS.
C
      GO TO 90
C
C     CHECK TO SEE WHICH INTERVALS HAVE THE MOST DEFLECTIONS
C     WITHIN THEM, THE FIRST SET OR THE SECOND SET &
C     SET THE MODAL INTERVAL TO BE THE INTERVAL WITH THE MOST
C     DEFLECTIONS WITHIN IT.
C
  370 IF (NF1.GT.NF(IMODE)) GO TO 390
      UMODE=FD(IMODE)
```

```
      COMMON /FATIG/ D1(20),D2(20),D3(20),E1(20),E2(20),F1(20),STATK(20)
     1,SSG(20),STRSF(20)
C
      DIMENSION THICK(5), AC(5), BC(5)
      DATA THICK/ 7.0, 8.0, 9.0, 10.0, 12.0/
      DATA AC/0.3670,0.2072,0.0967,-0.0072,-0.1944/
      DATA BC/-1.110,-1.156,-1.184,-1.208,-1.2507/
      NDINT5=NDINT5+1
C
C
C     CHECK WHICH REGRESSION EQUATION SHOULD BE USED FOR THE CALC.
C     OF SUBGRADE MODULUS FROM SENSOR 5 DEFLECTIONS.
C
      IF (JSW.GE.1) GO TO 90
      DO 10 IX=1,5
         IF (D1(N).LE.THICK(IX)) GO TO 20
         IF (IX.EQ.5) GO TO 100
   10 CONTINUE
C
C     IF ONLY THE SUBGRADE MODULUS UNDER THE DYNAFLECT LOAD IS REQUIRED
C
   20 IF (KSW.EQ.1) GO TO 30
      AMSSG(N)=10.**(AC(IX)+BC(IX)*ALOG10(((UMODE5*BMODE5)/2.)*.001))
      GO TO 130
C
C     CALCULATE THE SUBGRADE MODULUS UNDER THE DYNAFLECT LOAD
C
   30 DO 80 I=1,NDINT5
         FD5(I)=10.**(AC(IX)+BC(IX)*ALOG10(FD5(I)*.001))
C
C
         IF (D3(N).LE.0.0) GO TO 40
C
C     CALCULATE A REVISED SUBGRADE MODULUS BASED ON AN ESTIMATE OF
C     THE SUBGRADE THICKNESS.
C
      FD5(I)=FD5(I)*0.0011*10.**(-0.00166*D3(N)*1.338*ALOG10(D3(N)))
C
   40    IF (SSG(N).GT.-.01.AND.SSG(N).LT..01) GO TO 80
C
C     CALCULATE THE SUBGRADE MODULUS UNDER THE 18KIP AXLE LOAD
C     FOR THE INPUT STRESS SENSITIVITY OF THE SUBGRADE.
C     TWO OPTIONS EXIST:
C     1.  IF NO STATIC DEAD LOAD DEVIATOR STRESS IS INPUT THE
C      MODULUS UNDER THE 18KIP AXLE LOAD IS CALCULATED DIRECTLY.
C
C     2.  IF A STATIC DEAD LOAD DEVIATOR STRESS IS INPUT, AN
C      ITERATIVE PROCEDURE IS USED TO CALCULATE THE SUBGRADE
C      MODULUS UNDER THE AXLE LOAD.
C
        FREQ=-1.582-1.766E-2*D2(N)-1.928E-7*F2(N)-1.2972*ALOG10(D1(N))
       SDEVD=10.**(-2.71A-2.26E-2*D2(N)-2.387E-7*E2(N)-1.61*ALOG10(D1(N
     1   ))+.8362*ALOG10(FD5(I)))
C
        CONST=.6876
        IF (STATK(N).LE.0.0) GO TO 60
        SDEVS=STATK(N)*(.007*(D1(N)+D2(N)))
C
        SDEVD=SDEVD+SDEVS
C
        EOLD=1000.
   50  ENEW=10.**(ALOG10(FD5(I))-SSG(N)*(ALOG10(SDEVD)-ALOG10(SDEVS+10.*
     1   *(FREQ*CONST*ALOG10(EOLD))))
        IF (ABS(EOLD-ENEW).LT.100.) GO TO 70
        EOLD=(EOLD+ENEW)/2.0
        GO TO 50
   60   ENEW=10.**((ALOG10(FD5(I))-SSG(N)*ALOG10(SDEVD)+SSG(N)*FREQ)/(1.
     1   0-CONST*SSG(N)))
   70    FD5(I)=ENEW
C
   80 CONTINUE
C
C     IF THE SUBGRADE MODULUS FREQUENCY DIAGRAM IS TO BE PLOTTED
C     GO TO PLOT
C
C
C
      IF (NFPLT.EQ.2) CALL PLOT
   90 IF (JSW.EQ.2) GO TO 110
C
C     CALCULATE THE TENSILE STRESS IN THE SURFACE LAYER
C
C     IF ISHELS EQ 1 CALCULATE STRESSES FROM FLSYMS
C     ONLY THE STRESSES AT THE 90TH PERCENTILE
C     OF THE SENSOR 5 DEFLECTIONS ARE CALCULATED.
C
      IF(ISHELS .NE. 1)GO TO 95
      SUMM=0.0
      IC=0
      DO 91 I=1,NDINTS
      AA=NFS(I)
      BB=NSEC(N)
      SUMM=SUMM+AA/BB
      IF(SUMM .LT. 0.4 .OR. SUMM .GE. 0.99) GO TO 91
      IC=IC+1
      IF(IC .NE. 1) GO TO 92
      BSUM=SUMM
   92 IF(SUMM .GT. ASUM .AND. SUMM .LT. 0.9) BSUM=SUMM
      IF(SUMM .GE. 0.9) GO TO 93
      GO TO 91
   93 USUM=SUMM
      E390=FD5(I-1)+(0.90-BSUM)*((FD5(I)-FD5(I-1))/(USUM-BSUM))
C8    WRITE(1,*) BSUM,USUM,FD5(I-1),FD5(I),E390
      GO TO 94
   91 CONTINUE
   94 CALL STRESS(E390)
      IF(STRSF(N) .LE. 0.0) GO TO 96
      ELSTRS=ELSTRS*STRSF(N)
   96 ELSFAT=66000.*(F1(N)/ELSTRS)**3.0
C
C
   95 DO 100 I=1,NDINTS
        FD5(I)=10.**(2.88+1.972E-4*F1(N)-1.21E-6*E2(N)-1.72E-5*FD5(I)+8.
     1   1135E-2*D1(N)-5.896AF-4*E2(N)*D2(N)+6.12132E-8*E2(N)*D1(N)+7.13
     2   55E-10*E1(N)*E2(N)+3.8181E-10*FD5(I)*FD5(I)+3.312E-13*E2(N)*E2(
     3   N)+5.034E-33E-12*E2(N)*FD5(I))
C
C     IF A STRESS FACTOR IS INPUT INCREASE THE TENSILE STRESS.
C
         IF (STRSF(N).LE.0.0) GO TO 100
         FD5(I)=STRSF(N)*FD5(I)
  100 CONTINUE
C
C     IF THE STRESS DISTRIBUTION DIAGRAM IS TO BE PLOTTED CALL PLOT
```

```
C
      IF (NPPLT.GE.1) CALL PLOT
  110 CONTINUE
C
C     CALCULATE THE FATIGUE LIFE DISTRIBUTION OF THE SECTION
C
      DO 120 I=1,MDINT5
         FD5(I)=46000.*(F1(N)/FD5(I))**3.8
  120 CONTINUE
      JSW=3
      GO TO 130
  140 WRITE (6,150)
  150 FORMAT (1X, 37HTHE SURFACE THICKNESS IS OUT OF RANGE)
  130 RETURN
C
      END
      SUBROUTINE PRINT
C
C
      COMMON /DIS/ FD(30),FS(30),FD5(60),NF(30),NS(30),NF5(60),NSEC(20),
     1IFORM(16),ELSTRS,ELSFAT
      COMMON /READ/ FDMAX,FSMAX,FDMIN,FSMIN,N,NFPLT,NDPLT,JSW,KSW,NSECT
     1,ISWELS
      COMMON /AVE/ AVESCI,AVERCI,AVESL,AVESP,AVEW1,AVEW5,STDSCI,STDBCI,S
     1TDSL,STDSP,STDW1,STDW5,CVW1,CVW5,CVSL,CVSP,CVSCI,CVBCI,AMODE1,AMOD
     2E5,AMDESL
      COMMON /MODC/ BMODE,UMODE,BMODE5,UMODE5,NDGT5,NDGT,NDINT,NBINT,K,B
     1SLOPE,USLOPE,NBGT,NDINT5,AMSBG(20)
      COMMON /FATIG/ D1(20),D2(20),D3(20),E1(20),E2(20),F1(20),STATK(20)
     1,SBG(20),STRSF(20)
C
C     PRINT INPUT DATA
C
      IF (KSW.NE.1) GO TO 20
      IF (N.GT.NSECT) GO TO 80
      WRITE (6,10) N,D1(N),E1(N),D2(N),E2(N),D3(N),F1(N),STATK(N),SBG(N)
     1,STRSF(N)
   10 FORMAT (1H1,5X// 12HINPUT VALUES/5X, 14HSECTION NUMBER,I5/5X, 33
     1HLAYER THICKNESS     LAYER MODULUS/5X,2F15.0/5X,2F15.0/5X,F15.0/
     25X, 30HCONCRETE MODULUS OF RUPTURE = ,F10.0/5X, 43HSTATIC OVERBUR
     3DEN DEVIATOR STRESS FACTOR = ,F5.2/5X, 38HSUBGRADE STRESS SENSITIV
     4ITY = ,F10.2/5X, 33HSTRESS FACTOR FOR EDGE LOADING = ,F7.2)
C
C     PRINT RESULTS
C
C
   20 WRITE (1) N,NSEC(N),AVEW1,AMODE1,STDW1,CVW1,AVEW5,AMODE5,STDW5,CVW
     15,AVESL,AMDESL,STDSL,CVSL,AVESP,STDSP,CVSP,AVESCI,STDSCI,CVSCI,AVE
     2BCI,STDBCI,CVBCI
C
C
      IF (N.NE.NSECT+1) GO TO 80
      WRITE (6,30)
   30 FORMAT (1H1//5X, 40HTABLE OF DEFLECTION PARAMETER STATISTICS/5X,
     127HSLOPE = SENSOR 1 - SENSOR 5/5X, 27HSCI   = SENSOR 1 - SENSOR 2
     2/5X, 27HBCI   = SENSOR 4 - SENSOR 5/5X,   53HSPREADABILITY = (SENS
     3OR 1+2+3+4+5)/(5 TIMES SENSOR 1)/5X,  50HAVE = AVERAGE    MO = MOD
     4E    STD = STANDARD DEVIATION, 33H    CV = COEFFICIENT OF VARIATIO
     5N/5X, 40HNSEC  = NUMBER OF DEFLECTIONS IN SECTION//1X,   57HT  SEC
     6TION  I        SENSOR 1     I        SENSOR 5      I, 56H        SLO
     7PE          I  SPREADABILITY I        SCI      I, 17H        BCI
     8 I/1X,  57HI  N I NSEC I  AVE   MO  STD   CV I  AVE   MO  STD   CV
     9 I, 61H  AVE   MO  STD   CV I  AVE  STD   CV I  AVE  STD   CV I  A
     *VE, 12H  STD   CV I)
      REWIND 1
      DO 50 I=1,NSECT
         READ (1) N,NSEC(N),AVEW1,AMODE1,STDW1,CVW1,AVEW5,AMODE5,STDW5,C
     1   VW5,AVESL,AMDESL,STDSL,CVSL,AVESP,STDSP,CVSP,AVESCI,STDSCI,CVSC
     2   I,AVEBCI,STDBCI,CVBCI
         WRITE (6,40) N,NSEC(N),AVEW1,AMODE1,STDW1,CVW1,AVEW5,AMODE5,STD
     1   W5,CVW5,AVESL,AMDESL,STDSL,CVSL,AVESP,STDSP,CVSP,AVESCI,STDSCI,
     2   CVSCI,AVEBCI,STDBCI,CVBCI
   40 FORMAT (1X,1HI,I3,1X,1HI,I4,2X,1HI,4F5.2,1X,1HI,4F5.2,1X,1HI,4F5.2
     1,1X,1HI,3(3F5.2,1X,1HI)/1X,1HI,4X,1HI,6X,1HI,3(21X,1HI),3(16X,1HI)
     2)
   50 CONTINUE
      WRITE (6,60)
   60 FORMAT (///3X, 41HSUBGRADE MODULUS UNDER THE DYNAFLECT LOAD//3X,
     135HSECTION      MODAL SUBGRADE MODULUS)
      WRITE (6,70) (I,AMSBG(I),I=1,NSECT)
   70 FORMAT (3X,I5,10X,F10.0)
   80 RETURN
C
      END
      SUBROUTINE PLOT
      COMMON /DIS/ FD(30),FS(30),FD5(60),NF(30),NS(30),NF5(60),NSEC(20),
     1IFORM(16),ELSTRS,ELSFAT
      COMMON /READ/ FDMAX,FSMAX,FDMIN,FSMIN,N,NFPLT,NDPLT,JSW,KSW,NSECT
     1,ISWELS
      COMMON /MODC/ BMODE,UMODE,BMODE5,UMODE5,NDGT5,NDGT,NDINT,NBINT,K,B
     1SLOPE,USLOPE,NBGT,NDINT5,AMSBG(20)
C
      REAL ITIT
      INTEGER STP
      DIMENSION LINE(101), S(6), F(60), NUM(60), ITIT(18)
      DATA LINE/101*1H /
      DATA ITIT/4HSUBG,4HRADE,4H MOD,4HULUS,2*1H ,4HTENS,4HILE ,4H STR,4
     1HESS ,2*1H ,4HFATI,4HGUE ,4HLIFE,3*1H /
      DATA STP/3H***/
C
C     PLOT THE FREQUENCY DIAGRAMS FOR THE DEFLECTIONS
C     AND BASIN SLOPES.
C
C
      POINT(A,B)=(B/A*100.0)+1.5
      DATA ISTAR/1H*/
      DATA IPLUS/1H+/
      DATA IPER /1H./
      SCLEN=1.0
      MDINT=NDINT+1
      MDINT5=NDINT5+1
      MSINT=NSINT+1
      NSW=0
      IC=1
   10 LINE(IC)=IPER
      IF (IC.EQ.101) GO TO 20
      IC=IC+20
      GO TO 10
   20 DO 30 I=1,6
         C=I-1
         S(I)=0.2*C*SCLEN
   30 CONTINUE
      IF (KSW.EQ.1) GO TO 50
      IF (NDPLT.EQ.1.OR.NDPLT.EQ.2) GO TO 200
```

```
      IF (NDPLT.EQ.0) GO TO 230
      WRITE (6,40) N
   40 FORMAT (1H1//5X, 14HSECTION NUMBER,I5/5X, 37HFREQUENCY AND CUMULAT
     1IVE DISTRIBUTION/5X, 27HOF #I DYNAFLECT DEFLECTIONS/5X,  24HFREQU
     2ENCY DISTRIBUTION  ,1H*/5X, 24HCUMULATIVE DISTRIBUTION ,1H*)
      GO TO 70
   50 IF (NFPLT.EQ.2.AND.JSW.EQ.1) JSW=2
      IF (NFPLT.EQ.1.AND.JSW.EQ.0) JSW=2
      IF (NFPLT.EQ.2.AND.JSW.EQ.0) JSW=1
      ASW=JSW-1
      IST=6.0*ASW+1.0
      IEND=IST+5
      WRITE (6,60) N,(TITT(ICNT),ICNT=IST,IEND)
   60 FORMAT (1H1/5X, 18HSECTION NUMBER,I5/5X, 37HFREQUENCY AND CUMULATI
     1VE DISTRIBUTION/5X,  3HOF ,6A4)
C
   70 WRITE (6,80) S
   80 FORMAT (//15X,6(F6.4,14X)/15X,1HI,5(19(1H-),1HI))
      IF (KSW.EQ.1) GO TO 120
      IF (NSW.GE.1) GO TO 100
C
C     SET VALUES FOR PLOTTING #1 DEFLECTION FREQUENCY DIAGRAM.
C
      NEND=NDINT+1
      NUM(NDINT+2)=NDGT
      DO 90 I=1,NDINT
         NUM(I)=NF(I)
         F(I)=FD(I)
   90 CONTINUE
      GO TO 140
C
C     SET VALUES FOR PLOTTING THE BASIN SLOPE FREQUENCY DIAGRAM.
C
  100 IF (NSW.GT.1) GO TO 120
      NEND=NSINT+1
      NUM(NSINT+2)=NSGT
      DO 110 I=1,NSINT
         NUM(I)=NS(I)
         F(I)=FS(I)
  110 CONTINUE
      GO TO 140
C
C     SET VALUES FOR PLOTTING #5 DEFLECTION FREQUENCY DIAGRAM.
C
  120 NEND=NDINT5+1
      NSW=2
      NUM(NDINT5+2)=NDGT5
      DO 130 I=1,NDINT5
         NUM(I)=NF5(I)
         F(I)=FD5(I)
  130 CONTINUE
  140 SUMM=0.0
      NEND=NEND+1
      DO 170 I=1,NEND
         AA=NUM(I)
         BB=NSEC(N)
         FREQ=AA/BB
         SUMM=SUMM+FREQ
         ICOI=POINT(SCLEN,SUMM)
         LINOLI=LINE(ICOI)
         LINE(ICOI)=IPLUS
         ICFR=POINT(SCLEN,FREQ)
         LINOLD=LINE(ICFR)
         LINE(ICFR)=ISTAR
         ICNT=1
         WRITE (6,150) LINE
  150 FORMAT (15X,1P1A1)
         LINE(ICFR)=LINOLD
         LINE(ICOI)=LINOL1
C
         IF (I.EQ.NEND+1) GO TO 180
         WRITE (6,160) F(I)
  160 FORMAT (6X,G9.3,1HI)
  170 CONTINUE
  180 WRITE (6,190)
  190 FORMAT (15X,1HI,5(9(2H= ),2H=I))
      IF(ISWELS .NE. 1) GO TO 195
      IF(JSW .NE. 3) GO TO 195
      WRITE(6,193) ELSTRS,ELSFAT
  193 FORMAT(//5X, 23HSTRESS FROM ELSYM5 FOR ,
     1        /5X, 32H90TH PERCENTILE SUBGRADE MODULUS,3H = ,G9.3,
     2        /5X, 30HFATIGUE LIFE USING THIS STRESS,5H   = ,G9.3)
  195 IF (NSW.GE.1.AND.NDPLT.EQ.1) GO TO 250
      IF (NSW.GE.1.AND.NDPLT.EQ.2) GO TO 220
      IF (NSW.GF.1) GO TO 220
  200 NSW=NSW+1
      WRITE (6,210) N
  210 FORMAT (1H1//5X, 14HSECTION NUMBER,I5/5X, 40HFREQUENCY AND CUMULAT
     1IVE DISTRIBUTION OF/5X,  39HDYNAFLECT DEFLECTION BASIN SLOPE #1=N
     25)
      GO TO 70
  220 IF (NSW.EQ.2) GO TO 250
  230 NSW=2
      WRITE (6,240) N
  240 FORMAT (1H1//5X, 14HSECTION NUMBER,I5/5X, 40HFREQUENCY AND CUMULAT
     1IVE DISTRIBUTION OF/5X, 38HDYNAFLECT SENSOR 5 DEFLECTIONS)
      GO TO 70
  250 RETURN
C
      END
      SUBROUTINE STRESS (E3)
      COMMON /READ/ FDMAX,FSMAX,FDMIN,FSMIN,N,NFPLT,NDPLT,JSW,KSW
     >,NSECT,ISWELS
      COMMON /DIS/ FD(30),FS(30),FD5(60),NF(30),NS(30),NF5(60),
     >NSEC(20),IFORM(16),ELSTRS,ELSFAT
      COMMON /FATIG/ D1(20),D2(20),D3(20),E1(20),E2(20),F1(20),
     >               STATK(20),SSG(20),STRSF(20)
      COMMON /ELCTL/ KSW1, KSW2, KSW3, KSW4, NBZ, NEL, NEX, NGOP
     .             , NJ, NLSW, NTEST, NTST, NX, NRL
      COMMON /ELSYS/ NEL, E(5), V(5), TH(5), CI, DI(5)
      COMMON /ELCOM/ FDR, PRES, GL, NLO, XL(10), YL(10), NXY, NZ
     .             , XP(10), YP(10), Z(10), LAYZ(10), SNRM(3,2,1)
     .             , SSMR(3,2,1),   PS(3,2,1),  PSS(3,2,1)
     .             , DISP(3,2,1), ENRM(3,2,1), ESMR(3,2,1)
     .             ,   PE(3,2,1),  PSF(3,2,1)
      NBZ = 46
      NGOP = 0
      NLO = 2
      XL(1) = 0.0
      XL(2) = 13.11
      YL(1) = 0.0
      YL(2) = 0.0
      NXY = 1
      XP(1) = 0.0
```

```
      YP(1) = 0.0
      NZ = 1
      FOR = 4500.
      PRES = 75.
      NEL=3
      E(1) = E1(N)
      E(2) = E2(N)
      E(3)=E3
      TH(1) = D1(N)
      TH(2) = D2(N)
      TH(3) = 0.0
      V(1) = 0.15
      V(2) = 0.20
      V(3) = 0.45
      Z(1) = TH(1)
CA    WRITE(1,*) NEL,E,TH,V,Z
      CALL ELSYM5
      ELSTRS = PS(1,1,1)
      RETURN
      END
      SUBROUTINE ELSYM5
CC
C     ELSYM5 = FIVE LAYER ELASTIC PAVEMENT SYSTEM SYMULATION.
C
C         THIS SUBROUTINE WAS ADAPTED FROM THE ELSYM5 COMPUTER
C     PROGRAM, VERSION 3.1, WRITTEN BY GALE AHLBORN, ITTE, UNIVER-
C     SITY OF CALIFORNIA AT BERKELEY.  ELSYM5 IS BASED ON LAYER,
C     THE ORIGINAL ELASTIC LAYER PROGRAM, WHICH WAS DEVELOPED BY
C     CHEVRON.
C
C
C         COMMUNICATION BETWEEN THIS ROUTINE AND ITS CALLER IS
C     THROUGH THE /ELSYS/ AND /ELCOM/ COMMON BLOCKS.  THE ENTRY
C     AND EXIT CONDITIONS ARE DESCRIBED IN THE COMMENTS WHICH
C     ACCOMPANY THESE COMMON BLOCKS.
C
C
C     /ELCTL/ = ELSYM5 CONTROL SWITCHES.
C
C     KSW1  =  1 IF UNDERLYING BASE IS ELASTIC,
C              2 IF RIGID UNDERLYING BASE.
C     KSW2  =  1 FOR FULL FRICTION RIGID BASE INTERFACE,
C              2 FOR NO FRICTION RIGID BASE INTERFACE.
C     KSW3  =  1 IF CURRENT RADIAL POINT NOT BENEATH LOAD,
C              2 IF CURRENT POINT DIRECTLY UNDER LOAD.
C     KSW4  =  1 IF CURRENT DEPTH NOT AT SURFACE,
C              2 IF CURRENT DEPTH AT SURFACE.
C     NGQP  =  NUMBER OF GAUSSIAN QUADRATURE POINTS.
C     NI    =  NUMBER OF INTERFACES BETWEEN LAYERS.
C     NLSW  =  3 FOR ONE ELASTIC LAYER,
C              2 FOR TWO ELASTIC LAYERS,
C              1 FOR THREE OR MORE ELASTIC LAYERS.
C
      COMMON /ELCTL/ KSW1, KSW2, KSW3, KSW4, NBZ, NEI, NEX, NGQP
     .             , NI, NLSW, NTEST, NTSI, NX, WRL
CC
C     /ELCYLN/ = ELSYM5 CYLINDRICAL COORDINATE VARIABLES.
C
C     NRC   =  INDEX OF CURRENT RADIAL DISTANCE IN R.
C     NZC   =  INDEX OF CURRENT DEPTH IN Z.
C     LAY   =  LAYER IN WHICH POINT IS LOCATED.
C     NR    =  NUMBER OF RADIAL DISTANCES AT WHICH CALCULATIONS
C              MUST BE MADE.
C     R     =  ARRAY OF DISTANCES BETWEEN LOADS AND XY POINTS IN
C              ASCENDING ORDER WITH DUPLICATE VALUES REMOVED.
C     IXR   =  ARRAY OF POINTERS TO THE ELEMENT IN R WHICH GIVES THE
C              DISTANCE FROM EACH XY POINT TO EACH LOAD.
C     ANS   =  ARRAY OF CALCULATED RESPONSES AT EACH DEPTH AND
C              FOR EACH RADIAL DISTANCE.
C     RLP   =  RADIUS OF LOAD * PRESSURE.
C     WR    =  CURRENT RADIAL DISTANCE.
C     WZ    =  CURRENT DEPTH.
C
C     DIMENSIONS ON ANS CHANGED FROM (6,100,10) TO SAVE SPACE.
C     IN REPAIR, ONLY ONE DEPTH POINT, 2 X-Y POINTS, AND 4 LOADS ARE
C     USED.
      COMMON /ELCYLN/ NRC, NZC, LAY, NR, R(100), IXR(100), ANS(6,6,1)
     .              , RSE, TSE, VSE, SSE, RDP, VRP, RLP, WR, WZ
CC
C
C     BLANK COMMON = USED AS WORKING STORAGE BY INPUT AND BY ELSYM5.
C
      COMMON  ST1, ST2, ST3, ST4, TST1, TST2, TST3, TST4
     .              , CDAB(5,736), AJ1(184), RJ0(184), RJ1(184), Ex(32)
CC
C     /ELPART/ = PARTITION USED FOR NUMERICAL INTEGRATION.
C
      COMMON /ELPART/ GP(184)
CC
C
C     /ELSYS/ = ELASTIC LAYERED SYSTEM DESCRIPTION.
C
C
C     THE FOLLOWING INFORMATION MUST BE PROVIDED BEFORE ELSYM5 IS
C     CALLED, THESE LOCATIONS ARE NOT DISTURBED.
C
C     NEL   =  NUMBER OF ELASTIC LAYERS.
C     E     =  ARRAY OF MODULI FOR THE LAYERS.
C     V     =  ARRAY OF POISSON'S RATIOS FOR THE LAYERS.
C     TH    =  ARRAY OF THICKNESS FOR THE LAYERS.
C              TH(NEL) = 0.0  IF ELASTIC HALFSPACE,
C                      = DISTANCE TO RIGID BASE INTERFACE OTHERWISE.
C     CI    =  2HFF IF FULL FRICTION RIGID BASE INTERFACE,
C           =  2HNF IF NO FRICTION RIGID BASE INTERFACE.
C              (IGNORED IF TH(NEL) = 0.0)
C
C
C     ON EXIT FROM ELSYM5 THE FOLLOWING INFORMATION IS AVAILABLE.
C
C     DI    =  DEPTHS OF THE INTERFACES BETWEEN LAYERS.
C
      COMMON /ELSYS/ NEL, E(5), V(5), TH(5), CI, DI(5)
CC
C
C     /ELCOM/ = ELSYM5 COMMUNICATIONS BLOCK.
C
C
C     THE FOLLOWING INFORMATION MUST BE PROVIDED BEFORE ELSYM5 IS
C     CALLED, THESE LOCATIONS ARE NOT DISTURBED.
C
C     FOR   =  LOAD FORCE (POUNDS).
C     PRES  =  LOAD PRESSURE (PSI).
C     NLO   =  NUMBER OF LOADS.
C     XL    =  ARRAY OF X COORDINATES (IN).
```

```
C     YL    =  ARRAY OF Y COORDINATES (IN).
C     NXY   =  NUMBER OF XY POINTS FOR RESULTS.
C     NZ    =  NUMBER OF DEPTHS FOR RESULTS.
C     XP    =  ARRAY OF X COORDINATES FOR RESULTS (IN).
C     YP    =  ARRAY OF Y COORDINATES FOR RESULTS (IN).
C     Z     =  ARRAY OF DEPTHS FOR RESULTS (IN).
C
C
C     ON EXIT FROM ELSYMS THE FOLLOWING INFORMATION IS AVAILABLE.
C
C     RL    =  RADIUS OF ASSUMED CIRCULAR LOADS (IN).
C     LAYZ  =  ARRAY OF LAYERS IN WHICH Z VALUES FALL.
C
C     THE FOLLOWING ARRAYS ARE USED TO RETURN THE RESULTS OF THE
C     ELASTIC LAYER SOLUTION.  THEY ARE TRIPLY-DIMENSIONED, THE
C     INDICES ARE:
C             1ST INDEX = DIRECTION OF RESPONSE. (FOR PRINCIPAL
C                         STRESSES AND STRAINS: 1, 2, 3; OTHER
C                         RESPONSES ARE CODED: 1=X, 2=Y, 3=Z)
C             2ND INDEX = INDEX OF XY POSITION IN XP AND YP.
C             3RD INDEX = INDEX OF DEPTH IN Z.
C
C     SNRM  =  NORMAL STRESSES.
C     SSHR  =  SHEAR STRESSES.
C     PS    =  PRINCIPAL STRESSES.
C     PSS   =  PRINCIPAL SHEAR STRESSES.
C     DISP  =  DISPLACEMENTS.
C     ENRM  =  NORMAL STRAINS.
C     ESHR  =  SHEAR STRAINS.
C     PE    =  PRINCIPAL STRAINS.
C     PSE   =  PRINCIPAL SHEAR STRAINS.
C
C
      COMMON /ELCOM/ FOR, PRES, RL, NLD, XL(10), YL(10), NXY, NZ
     *              , XP(10), YP(10), Z(10), LAYZ(10), SNRM(3,2,1)
     *              , SSHR(3,2,1),   PS(3,2,1),  PSS(3,2,1)
     *              , DISP(3,2,1), ENRM(3,2,1), ESHR(3,2,1)
     *              ,   PE(3,2,1),  PSE(3,2,1)
C     DIMENSIONS CHANGED FROM (3,10,10) FOR LIMITED REQUIREMENTS OF
C     RPOD PROGRAM.  ONLY 2 X-Y, 1 Z VALUE USED.
C
      DATA IFIRST / 0 /
C
C     PERFORM SYSTEM INITIALIZATIONS.
C
      IF (IFIRST.EQ.0) CALL ELPRS
      IFIRST=1
      CALL ELINIT
C
C     CALCULATE COEFFICIENTS OF THE SYSTEM ONCE FOR EACH DISTINCT
C     RADIAL DISTANCE FROM A LOAD TO AN XY POINT (USING CYLINDRICAL
C     COORDINATES).
C
      IF (NLSW .LT. 3) GO TO 20
   10 CALL ELSNGL
      GO TO 50
   20 CALL ELPCP
   30 K4=1
      K1=1
      DO 40 K2=1,NBZ
      DO 40 K3=1,NGQP
         FM=GP(K1)/WRL
         CALL ELDEVL (FM)
         CALL ELMULT (FM)
         CALL ELBKS (FM,K8)
         K1=K1+1
         K4=K4+8
   40 CONTINUE
   50 K1=1
      RLDWRL=RL/WRL
      DO 60 K2=1,NBZ
      DO 60 K3=1,NGQP
         X=GP(K1)*RLDWRL
         AJ1(K1)=BESSEL(X,1)
         K1=K1+1
   60 CONTINUE
      IF (KS=3 .EQ. 1) GO TO 80
   70 NTEST=2
      GO TO 120
   80 K1=1
      WRDWRL=WR/WRL
      DO 90 K2=1,NBZ
      DO 90 K3=1,NGQP
         X=GP(K1)*WRDWRL
         RJ0(K1)=BESSEL(X,0)
         RJ1(K1)=BESSEL(X,1)
         K1=K1+1
   90 CONTINUE
      IF (WR=RL) 100,100,110
  100 NTEST=RL/WR+0.0001
      GO TO 120
  110 NTEST=WR/RL+0.0001
  120 NTEST=NTEST+1
      IF (NTEST-10) 140,140,130
  130 NTEST=10
  140 NTST=NTEST+1
C
C     CALCULATE RESPONSES AT EACH DEPTH FOR CURRENT RADIAL DISTANCE.
C
      DO 200 K1=1,NZ
         KS=4
         NZC=K1
         WZ=Z(NZC)
         IF (WZ.EQ.0.0) KS=4
C                                  DETERMINE LAYER IN WHICH CURRENT
C                                  DEPTH POINT RESIDES.
      IF (NLSW .LT. 3) GO TO 160
  150    LAY=1
         GO TO 190
  160    DO 180 K2=1,NEI
            IF (WZ-(DI(K2)+0.001)) 170,170,180
  170       LAY=K2
            GO TO 190
  180    CONTINUE
         LAY=NEL
  190    LAYZ(NZC)=LAY
         CALL ELCALC
         CALL ELBRP
  200 CONTINUE
      K=K+1
      NRC=NRC+1
      IF (NRC.GT.NR) GO TO 210
      WR=R(NRC)
      IF (WR.LE.RL) GO TO 40
```

```
      WRL=WR
      IF (NLSW - 2) 30,30,10
C
C     RETURN ANSWERS TO CALLER.
C
  210 CALL ELOUT
      RETURN
C
      END
      SUBROUTINE ELPRS
CC
C     ELPRS = PRESET ELASTIC LAYER PROCEDURE.
C
C         THIS SUBROUTINE IS ONLY CALLED THE FIRST TIME ELSYMS
C     IS EXECUTED.  IT INITIALIZES STORAGE LOCATIONS WHICH ARE
C     NOT CHANGED WHILE SOLUTIONS ARE BEING PERFORMED.
C
C         THE NUMERICAL INTEGRATION TECHNIQUE USED FOR THE
C     ELASTIC LAYER SOLUTIONS IS A 4 POINT GAUSSIAN QUADRATURE
C     WITH NBZ = 46.  CONSTANTS REQUIRED FOR THIS METHOD ARE
C     DEVELOPED HERE.
C
      COMMON /ELCTL/ KSW1, KSW2, KSW3, KSW4, NBZ, NEI, NEX, NGQP
     .             , NI, NLSW, NTEST, NTSI, NX, WRL
C
C     BLANK COMMON = USED AS WORKING STORAGE BY INPUT AND BY ELSYMS.
C
      COMMON  ST1, ST2, ST3, ST4, TST1, TST2, TST3, TST4
     .             , CDAB(5,736), AJ1(184), BJ0(184), BJ1(184), Ex(32)
      COMMON /ELPART/ GP(184)
C
C *** EXCLUSIVE ROUTINE ARRAYS
      DIMENSION BZ(46),GU(4)
C
      DATA BZ/ 1.0,
     1 2.40482556 , 3.83170597 , 5.52007811 , 7.01558667 , 8.65372791 ,
     2 10.1734681 , 11.7915344 , 13.3236919 , 14.9309177 , 16.4706301 ,
     3 18.0710640 , 19.6158585 , 21.2116366 , 22.7600844 , 24.3524715 ,
     4 25.9036721 , 27.4934791 , 29.0468285 , 30.6346065 , 32.1896799 ,
     5 33.7758202 , 35.3323076 , 36.9170984 , 38.4747662 , 40.0584258 ,
     6 41.6170942 , 43.1997917 , 44.7593190 , 46.3411884 , 47.9818409 ,
     7 49.4826099 , 51.0435352 , 52.6200518 , 54.1855536 , 55.7655108 ,
     8 57.3275254 , 58.9069839 , 60.4694578 , 62.0484692 , 63.6113467 ,
     9 65.1899648 , 66.7532267 , 68.3314693 , 69.8950718 , 71.4729816 /
C
      DATA GU /
     1 .430568156 ,-.169990522 , .169990522 , .430568156 /
C
C     THIS DATA STATEMENT MOVED TO BLOCK DATA (FOR IBM)
C     DATA NBZ, NGQP / 46, 4 /
C
      K3=0
      FMB=0.0
      DO 20 K1=1,NBZ
         FM=BZ(K1)
         SBA=(FM+FMB)/2.0
         DBA=FM-FMB
         DO 10 K2=1,NGQP
            K3=K3+1
            GP(K3)=SBA+DBA*GU(K2)
   10    CONTINUE
         FMB=FM
   20 CONTINUE
      RETURN
C
      END
      SUBROUTINE ELINIT
CC
C     ELINIT = ELSYMS INITIALIZATION ROUTINE.
C
C         THIS SUBROUTINE SETS SYSTEM CONTROL VARIABLES AND FLAGS
C     AS REQUIRED TO PERFORM THE CALCULATIONS SPECIFIED BY THE
C     CALLER IN COMMON BLOCKS /ELSYS/ AND /ELCOM/.
C
C     ENTRY:   INPUT VALUES SET IN /ELSYS/ AND /ELCOM/.
C
C     EXIT:    DI   =  ARRAY OF DEPTHS TO INTERFACES.
C              EX   =  EXPONENT TEST ARRAY.
C              IXR  =  ARRAY OF POINTERS TO THE ELEMENT IN R WHICH
C                      GIVES THE DISTANCE FROM EACH XY POINT TO
C                      EACH LOAD.
C              KSW1 =  1 IF UNDERLYING BASE IS ELASTIC,
C                   =  2 IF RIGID UNDERLYING BASE.
C              KSW2 =  1 FOR FULL FRICTION RIGID BASE INTERFACE.
C                   =  2 FOR NO FRICTION RIGID BASE INTERFACE.
C              KSW3 =  1 IF FIRST RADIAL POINT NOT BENEATH LOAD.
C                   =  2 IF FIRST POINT DIRECTLY UNDER LOAD.
C              NEI  =  NEL - 1
C              NI   =  NUMBER OF INTERFACES.
C              NLSW =  3 FOR ONE ELASTIC LAYER,
C                   =  2 FOR TWO ELASTIC LAYERS,
C                   =  1 FOR THREE OR MORE ELASTIC LAYERS.
C              NR   =  NUMBER OF RADIAL DISTANCES AT WHICH CALCULATIONS
C                      MUST BE MADE.
C              NX   =  1 IF RIGID BASE,
C                   =  2 IF ELASTIC BASE.
C              R    =  ARRAY OF DISTANCES BETWEEN LOADS AND XY POINTS
C                      IN ASCENDING ORDER WITH DUPLICATE VALUES REMOVED.
C              RL   =  RADIUS OF LOADED AREA.
C              RLP  =  RADIUS OF LOAD * PRESSURE.
C              WR   =  FIRST RADIAL DISTANCE AT WHICH CALCULATIONS
C                      WILL BE PERFORMED.
C
C
C
C     /CONST/ = PROGRAM CONSTANTS.
C
      COMMON /CONST/ ICO, IPR, RLMIN, RLMAX, EMBKUP, DSNLD, DSNPR, DBLDS
     .             , XK1, XK2, FLOC1, FLOC2, ZSRGM, ECRACK, THRRL
     .             , FVOID
      COMMON /ELCTL/ KSW1, KSW2, KSW3, KSW4, NBZ, NEI, NEX, NGQP
     .             , NI, NLSW, NTEST, NTSI, NX, WRL
C     DIMENSIONS ON ANS CHANGED FROM (6,100,10) TO SAVE SPACE.
C     IN REPAIR, ONLY ONE DEPTH POINT, 2 X-Y POINTS, AND 4 LOADS ARE
C     USED.
      COMMON /ELCYLN/ NRC, NZC, LAY, NR, R(100), IXR(100), ANS(6,8,1)
     .             , RSE, TSF, VSE, SSE, RDP, VDP, RLP, WR, WZ
C
C     BLANK COMMON = USED AS WORKING STORAGE BY INPUT AND BY ELSYMS.
C
      COMMON  ST1, ST2, ST3, ST4, TST1, TST2, TST3, TST4
     .             , CDAB(5,736), AJ1(184), BJ0(184), BJ1(184), Ex(32)
C
C     /ELSYS/ = ELASTIC LAYERED SYSTEM DESCRIPTION.
```

```
C
C
C     THE FOLLOWING INFORMATION MUST BE PROVIDED BEFORE ELSYM5 IS
C     CALLED, THESE LOCATIONS ARE NOT DISTURBED.
C
C     NEL   =  NUMBER OF ELASTIC LAYERS.
C     E     =  ARRAY OF MODULI FOR THE LAYERS.
C     V     =  ARRAY OF POISSON'S RATIOS FOR THE LAYERS.
C     TH    =  ARRAY OF THICKNESS FOR THE LAYERS.
C              TH(NEL) = 0.0  IF ELASTIC HALFSPACE,
C                      = DISTANCE TO RIGID BASE INTERFACE OTHERWISE.
C     CI    =  2HFF IF FULL FRICTION RIGID BASE INTERFACE,
C           =  2HNF IF NO FRICTION RIGID BASE INTERFACE.
C              (IGNORED IF TH(NEL) = 0.0)
C
C
C     ON EXIT FROM ELSYM5 THE FOLLOWING INFORMATION IS AVAILABLE.
C
C     DI    =  DEPTHS OF THE INTERFACES BETWEEN LAYERS.
C
      COMMON /ELSYS/ NEL, E(5), V(5), TH(5), CI, DI(5)
C
C     /ELCOM/ = ELSYM5 COMMUNICATIONS BLOCK.
C
C
C     THE FOLLOWING INFORMATION MUST BE PROVIDED BEFORE ELSYM5 IS
C     CALLED, THESE LOCATIONS ARE NOT DISTURBED.
C
C     FOR   =  LOAD FORCE (POUNDS).
C     PRES  =  LOAD PRESSURE (PSI).
C     NLO   =  NUMBER OF LOADS.
C     XL    =  ARRAY OF X COORDINATES (IN).
C     YL    =  ARRAY OF Y COORDINATES (IN).
C     NXY   =  NUMBER OF XY POINTS FOR RESULTS.
C     NZ    =  NUMBER OF DEPTHS FOR RESULTS.
C     XP    =  ARRAY OF X COORDINATES FOR RESULTS (IN).
C     YP    =  ARRAY OF Y COORDINATES FOR RESULTS (IN).
C     Z     =  ARRAY OF DEPTHS FOR RESULTS (IN).
C
C
C     ON EXIT FROM ELSYM5 THE FOLLOWING INFORMATION IS AVAILABLE.
C
C     RL    =  RADIUS OF ASSUMED CIRCULAR LOADS (IN).
C     LAYZ  =  ARRAY OF LAYERS IN WHICH Z VALUES FALL.
C
C     THE FOLLOWING ARRAYS ARE USED TO RETURN THE RESULTS OF THE
C     ELASTIC LAYER SOLUTION.  THEY ARE TRIPLY-DIMENSIONED, THE
C     INDICES ARE:
C              1ST INDEX = DIRECTION OF RESPONSE.  (FOR PRINCIPAL
C                          STRESSES AND STRAINS: 1, 2, 3; OTHER
C                          RESPONSES ARE CODED: 1=X, 2=Y, 3=Z)
C              2ND INDEX = INDEX OF XY POSITION IN XP AND YP.
C              3RD INDEX = INDEX OF DEPTH IN Z.
C
C     SNRM  =  NORMAL STRESSES.
C     SSHR  =  SHEAR STRESSES.
C     PS    =  PRINCIPAL STRESSES.
C     PSS   =  PRINCIPAL SHEAR STRESSES.
C     DISP  =  DISPLACEMENTS.
C     ENRM  =  NORMAL STRAINS.
C     ESHR  =  SHEAR STRAINS.
C     PE    =  PRINCIPAL STRAINS.
C     PSE   =  PRINCIPAL SHEAR STRAINS.
C
C
      COMMON /ELCOM/ FOR, PRES, RL, NLO, XL(10), YL(10), NXY, NZ
     ,             , XP(10), YP(10), Z(10), LAYZ(10), SNRM(3,2,1)
     ,             , SSHR(3,2,1),   PS(3,2,1),  PSS(3,2,1)
     ,             , DISP(3,2,1), ENRM(3,2,1), ESHR(3,2,1)
     ,             ,   PE(3,2,1),  PSE(3,2,1)
C     DIMENSIONS CHANGED FROM (3,10,10) FOR LIMITED REQUIREMENTS OF
C     RPOD PROGRAM.  ONLY 2 X-Y, 1 Z VALUE USED.
C
C *** EXCLUSIVE ROUTINE ARRAYS
      DIMENSION XR(100)
C
C
C *** ERROR MESSAGES ARRAY
      DIMENSION ERMSG(12,8)
C *** ERROR MESSAGES
      DATA ERMSG /
     1 4HNUMB,4HER O,4HF EL,4HASTI,4HC LA,4HYERS,4H OUT,4HSIDE,
     2 4H LIM,4HIT O,4HF 1 ,4H= 5 ,
     3 4HNUMB,4HER O,4HF XY,4H VAL,4HUES ,4HOUTS,4HIDE ,4HLIMI,
     4 4HT OF,4H 1 =,4H 10 ,4H    ,
     5 4HNUMB,4HER O,4HF Z ,4HVALU,4HES O,4HUTSI,4HDE L,4HIMIT,
     6 4H OF ,4H1 = ,4H10  ,4H    ,
     7 4HLOAD,4H IMP,4HROPE,4HRLY ,4HOESC,4HRISE,4HD   ,4H    ,
     8 4H    ,4H    ,4H    ,4H    ,
     9 4HELAS,4HTIC ,4HLAYE,4HR DA,4HTA I,4HMPRO,4HPER ,4H    ,
     * 4H    ,4H    ,4H    ,4H    ,
     * 4HZ VA,4HLUE ,4HIMPR,4HOPER,4H    ,4H    ,4H    ,4H    ,
     * 4H    ,4H    ,4H    ,4H    ,
     * 4HNUMB,4HER O,4HF LO,4HADS ,4HOUTS,4HIDE ,4HLIMI,4HT OF,
     * 4H 1 =,4H 10 ,4H    ,4H    ,
     * 4HRIGI,4HD BA,4HSE I,4HNTER,4HFACE,4H IMP,4HROPE,4HRLY ,
     * 4HDEFI,4HNED ,4H    ,4H    /
C
C
C *** ALPHA CONDITION OF INTERFACE
      DATA AFF,ANF/2HFF,2HNF/
      IND1=0
      TST1=60.0
      TST2=0.0001
C
C     TEST NUMBER OF ELASTIC LAYERS (NEL)
C     SET NUMBER OF LAYERS SWITCH (NLSW)
C
      IF (NEL-1) 500,10,20
C *** NLSW=3 FOR 1 ELASTIC LAYER
   10 NLSW=3
      GO TO 50
   20 IF (NEL-3) 30,40,40
C *** NLSW=2 FOR 2 ELASTIC LAYERS
   30 NLSW=2
      GO TO 50
C *** NLSW=1 FOR 3 OR MORE ELASTIC LAYERS
   40 NLSW=1
      IF (NEL-5) 50,50,500
C
C     TEST NUMBER OF LOADS (NLO), NUMBER OF XY VALUES (NXY), AND
C     NUMBER OF Z VALUES (NZ).
C
   50 CONTINUE
```

```
      IF (NLD.LE.0.OR.NLD.GT.10) GO TO 560
      IF (NXY.LE.0.OR.NXY.GT.10) GO TO 510
      IF (NZ.LE.0.OR.NZ.GT.10) GO TO 520
C
C     TEST /ELSYS/ VALUES.
C
      DO 110 K1=1,NEL
         IF (E(K1).LE.0.0) GO TO 540
         IF (V(K1).LE.0.0.OR.V(K1).GT.0.99) GO TO 540
         IF (K1.EQ.NEL) GO TO 60
         IF (TH(K1)) 540,540,110
C *** TEST BASE CONDITION
   60    IF (TH(K1)) 540,70,80
C *** SET BASE CONDITION TO ELASTIC
   70    NI=NEL-1
         NX=2
         KSW1=1
         GO TO 100
C *** SET BASE CONDITION TO RIGID
   80    NI=NEL
         NX=1
         KSW1=2
C *** CHECK BASE INTERFACE CONDITION
         IF (CI.NE.AFF) GO TO 90
         KSW2=1
         GO TO 100
   90    IF (CI.NE.ANF) GO TO 570
         KSW2=2
  100    NEI=NEL-1
  110 CONTINUE
C
C     COMPUTE LOAD RADIUS, CHECK VALUES OF FOR AND PRES.
C
      IF (FOR.LE.0.0) GO TO 530
      IF (PRES.LE.0.0) GO TO 530
      RL=SQRT(.31831099*FOR/PRES)
C
C     CHECK FOR NEGATIVE Z VALUES, SORT IN ASCENDING ORDER.
C
      DO 120 K1=1,NZ
         IF (Z(K1)) 550,120,120
  120 CONTINUE
      IF (NZ-1) 160,160,130
  130 K1=NZ-1
      DO 150 K2=1,K1
         K3=K2+1
      DO 150 K4=K3,NZ
         IF (Z(K2)-Z(K4)) 150,550,140
  140    TEMP=Z(K2)
         Z(K2)=Z(K4)
         Z(K4)=TEMP
  150 CONTINUE
C
C     DEVELOP DEPTH TO INTERFACE ARRAY (DI), AND EXPONENT TEST
C     ARRAY (EX).
C
  160 IF (NLSW .LT. 3) GO TO 180
  170 DI(1)=TH(1)
      EX(1)=0.0
      EX(2)=2.0*TH(1)
      GO TO 230
  180 DI(1)=TH(1)
      IF (NI.LT.2) GO TO 200
      DO 190 K1=2,NI
         DI(K1)=DI(K1-1)+TH(K1)
  190 CONTINUE
  200 NEX=2**NI
      K1=1
      K2=1
      EX(1)=0.0
      DO 220 K3=1,NEL
         K4=NEL+1-K3
         TEMP=2.0*TH(K4)
         DO 210 K5=1,K2
            K1=K1+1
            EX(K1)=TEMP+EX(K5)
  210    CONTINUE
         K2=K2+2
  220 CONTINUE
C
C     IF RIGID BASE, CHECK Z VALUES NOT TOO BIG AND V(NEL) NOT .75
C
  230 CONTINUE
      IF (KSW1.EQ.1) GO TO 250
      DINI=DI(NI)
      NZL=NZ
      DO 240 K1=1,NZL
         K2=NZ-K1+1
         IF (DINI+.0001.GE.Z(K2)) GO TO 240
         NZ=NZ-1
  240 CONTINUE
      IF (ABS(V(NEL)-.75).LT..002) GO TO 540
C
C     DEVELOP R ARRAY BY LOAD WITHIN XY POINT
C
  250 NR=NXY*NLD
      NXR=NR
      K1=1
      DO 260 K2=1,NXY
         XPI=XP(K2)
         YPI=YP(K2)
      DO 260 K3=1,NLD
         R(K1)=SQRT((YPI-YL(K3))**2+(XPI-XL(K3))**2)
         XR(K1)=R(K1)
         K1=K1+1
  260 CONTINUE
C *** SORT R ARRAY IN ORDER OF INCREASING VALUE
      IF (NR.LE.1) GO TO 340
      K2=NR-1
      DO 270 K1=1,K2
         K3=K1+1
      DO 270 K4=K3,NR
         IF (R(K1).LE.R(K4)) GO TO 270
         TEMP=R(K1)
         R(K1)=R(K4)
         R(K4)=TEMP
  270 CONTINUE
C
C     ELIMINATE NEAR DUPLICATE R VALUES.
C
      M = 1
  290 IF (M .EQ. NR) GO TO 330
      M1 = M+1
  300 IF (ABS(R(M)-R(M1)) .GE. .02) GO TO 320
```

```
      NR = NR-1
      DO 310 K1=M1,NR
         R(K1) = R(K1+1)
  310 CONTINUE
      IF (M .EQ. NR) GO TO 330
      GO TO 300
  320 M = M1
      GO TO 290
  330 CONTINUE
C
C     DEVELOP IXR ARRAY AS A POINTER
C
  340 DO 370 K1=1,NXR
         XRI=XR(K1)
         DO 360 K2=1,NR
            IF (ABS(XRI-R(K2))-.02) 350,350,360
  350       IXR(K1)=K2
            GO TO 370
  360    CONTINUE
         WRITE (IPR,590)
         STOP
  370 CONTINUE
      IF (ABS(RL-R(1))-.0001) 390,390,380
  380 IF (RL-R(1)) 400,390,390
  390 WRL=RL
      GO TO 410
  400 WRL=R(1)
  410 WR=R(1)
      IF (WR-.0001) 420,420,430
  420 WR=.0
      KSW3=2
      GO TO 440
  430 KSW3=1
  440 NRC=1
C
C     WITH SORTED Z VALUES - ONLY HAVE TO TEST ONE VALUE
C     DETERMINE BACK SUBSTITION LIMIT
C
      ZT=Z(NZ)
      DO 450 K1=1,NEI
         NBLL=K1
         IF (ZT-DI(K1)) 460,460,450
  450 CONTINUE
      NBLL=NEL
C
C     SET RELATIVE (PSI), OR ABSOLUTE OUTPUT
C
  460 IF (IND1) 470,480,470
  470 RLP=RL
      GO TO 490
  480 RLP=RL*PRES
  490 CONTINUE
      RETURN
C
C     INPUT DATA ERROR TRAP
C     SET ERROR INDICATOR
C
  500 NER=1
      GO TO 580
  510 NER=2
      GO TO 580
  520 NER=3
      GO TO 580
  530 NER=4
      GO TO 580
  540 NER=5
      GO TO 580
  550 NER=6
      GO TO 580
  560 NER=7
      GO TO 580
  570 NER=8
  580 CONTINUE
      WRITE (IPR,600)
      WRITE (IPR,610) (ERMSG(K1,NER),K1=1,12)
      STOP
C
  590 FORMAT (13H ERROR IN IXR)
  600 FORMAT (1H0,4X,38HFATAL ERROR IN ELSYMS INPUT PARAMETER(S))
  610 FORMAT (1H0,4X,12A4)
C
      END
      SUBROUTINE ELSNGL
CC
C     ELSNGL - SINGLE LAYER ELASTIC SYSTEM.
C
      COMMON /ELCTL/ KSW1, KSW2, KSW3, KSW4, NBZ, NEI, NEX, NGQP
     *             , NI, NLSM, NTEST, NTSI, NX, WRL
C
C     BLANK COMMON - USED AS WORKING STORAGE BY INPUT AND BY ELSYMS.
C
      COMMON  ST1, ST2, ST3, ST4, TST1, TST2, TST3, TST4
     *             , CDAB(5,736), AJ1(184), AJP(184), RJ1(184), EX(32)
      COMMON /ELPART/ GP(184)
C
C     /ELSYS/ - ELASTIC LAYERED SYSTEM DESCRIPTION.
C
C
C     THE FOLLOWING INFORMATION MUST BE PROVIDED BEFORE ELSYMS IS
C     CALLED, THESE LOCATIONS ARE NOT DISTURBED.
C
C     NEL   =  NUMBER OF ELASTIC LAYERS.
C     E     =  ARRAY OF MODULI FOR THE LAYERS.
C     V     =  ARRAY OF POISSON'S RATIOS FOR THE LAYERS.
C     TH    =  ARRAY OF THICKNESS FOR THE LAYERS.
C                TH(NEL) = 0.0  IF ELASTIC HALFSPACE,
C                        = DISTANCE TO RIGID BASE INTERFACE OTHERWISE.
C     CI    =  2HFF IF FULL FRICTION RIGID BASE INTERFACE,
C           =  2HNF IF NO FRICTION RIGID BASE INTERFACE,
C              (IGNORED IF TH(NEL) = 0.0)
C
C
C     ON EXIT FROM ELSYMS THE FOLLOWING INFORMATION IS AVAILABLE.
C
C     DI    =  DEPTHS OF THE INTERFACES BETWEEN LAYERS.
C
      COMMON /ELSYS/ NEL, E(5), V(5), TH(5), CI, DI(5)
C
C *** EXCLUSIVE ROUTINE ARRAYS
      DIMENSION SA(2,2)
C
      ST1=2.0*V(1)
      ST2=ST1-1.0
      IF (KSW1 .EQ. 1) GO TO 20
```

```
C *** SINGLE ELASTIC LAYER WITH RIGID BASE
   10 PC1=1.0/(3.0+4.0*V(1))
      PC2=1.0-4.0*V(1)
      PC3=2.0*PC1
      PC4=2.0*DI(1)
      PC5=PC4*DI(1)
      PC6=4.0*ST2
C *** END RIGID BASE ROUTINE
   20 K6=-3
      K5=0
      DO 110 K2=1,NBZ
      DO 110 K1=1,NGQP
         K6=K6+4
         K5=K5+1
         FM=GP(K5)/WRL
         RFM=1.0/FM
         RFM2=RFM*RFM
      IF (KSW1 .EQ. 1) GO TO 100
C *** SINGLE ELASTIC LAYER WITH RIGID BASE
   30    VAL=FM*EX(2)
C *** SINGLE ELASTIC LAYER WITH RIGID BASE REVERTS TO
C *** SINGLE ELASTIC LAYER WITH NO BASE WHEN VAL EXCEEDS TEST
         IF (VAL-ST1) 40,40,100
   40    VAL=EXP(-VAL)
      IF (KSW2 .EQ. 2) GO TO 60
C *** RIGID BASE WITH FULL FRICTION
   50    CM1=(PC2-FM*PC4)*PC1*VAL
         CM2=(PC6-FM*FM*PC5)*PC1*RFM*VAL
         CM3=PC3*FM*VAL
         CM4=(PC2+FM*PC4)*PC1*VAL
         SA(1,1)=FM*FM*CM1+ST1*CM3
         SA(1,2)=-ST1+FM*CM2+ST1*CM4
         SA(2,1)=-FM+FM*CM1+ST2*CM3
         SA(2,2)=ST2+FM*CM2+ST2*CM4
         GO TO 70
C *** RIGID BASE WITH NO FRICTION
   60    SA(1,1)=FM-FM*VAL
         SA(1,2)=-ST1+(ST1-2.0*FM*DI(1))*VAL
         SA(2,1)=-FM+FM*VAL
         SA(2,2)=ST2+(ST2-2.0*FM*DI(1))*VAL
   70    CDAB(1,K6)=-SA(1,2)*RFM2/(SA(2,1)*(-SA(1,2))+SA(2,2)*SA(1,1))
         CDAB(1,K6+1)=SA(1,1)*CDAB(1,K6)/(-SA(1,2))
      IF (KSW2 .EQ. 2) GO TO 90
C *** RIGID BASE WITH FULL FRICTION
   80    CDAB(1,K6+2)=CM1*CDAB(1,K6)+CM2*CDAB(1,K6+1)
         CDAB(1,K6+3)=CM3*CDAB(1,K6)+CM4*CDAB(1,K6+1)
         GO TO 110
C *** RIGID BASE WITH NO FRICTION
   90    CDAB(1,K6+2)=-(CDAB(1,K6)+2.0*DI(1)*CDAB(1,K6+1))*VAL
         CDAB(1,K6+3)=CDAB(1,K6+1)*VAL
         GO TO 110
C *** SINGLE ELASTIC LAYER - NO BASE
  100    CDAB(1,K6)=-ST1*RFM2*RFM
         CDAB(1,K6+1)=-RFM2
         CDAB(1,K6+2)=0.0
         CDAB(1,K6+3)=0.0
  110 CONTINUE
      RETURN
C
      END
      SUBROUTINE ELPCC
CC
C     ELPCC - PRESET COEFFICIENT CALCULATIONS FOR MULTI-LAYER SYSTEM.
C
      COMMON /ELCTL/ KSW1, KSW2, KSW3, KSW4, NBZ, NEI, NEX, NGQP
     *               , NI, NLSW, NTEST, NTSI, NX, WRL
      COMMON /ELCOEF/
     1 EI(16,2,2),S(2,2,2),SV(4,9),ISC(4),SA(2,2),PB(2,2),BA(2,2,2),
     2 TB1,TB2,TB3,TB4,TB5,
     3 NE,NEX02,NFIM1
C
C     /ELSYS/ - ELASTIC LAYERED SYSTEM DESCRIPTION.
C
C
C     THE FOLLOWING INFORMATION MUST BE PROVIDED BEFORE ELSYMS IS
C     CALLED. THESE LOCATIONS ARE NOT DISTURBED.
C
C     NEL   =  NUMBER OF ELASTIC LAYERS.
C     E     =  ARRAY OF MODULI FOR THE LAYERS.
C     V     =  ARRAY OF POISSON/S RATIOS FOR THE LAYERS.
C     TH    =  ARRAY OF THICKNESS FOR THE LAYERS.
C                TH(NEL) = 0.0  IF ELASTIC HALFSPACE,
C                        = DISTANCE TO RIGID BASE INTERFACE OTHERWISE.
C     CI    =  2HFF IF FULL FRICTION RIGID BASE INTERFACE,
C           =  2HNF IF NO FRICTION RIGID BASE INTERFACE.
C              (IGNORED IF TH(NEL) = 0.0)
C
C
C     ON EXIT FROM ELSYMS THE FOLLOWING INFORMATION IS AVAILABLE.
C
C     DI    =  DEPTHS OF THE INTERFACES BETWEEN LAYERS.
C
      COMMON /ELSYS/ NEL, E(5), V(5), TH(5), CI, DI(5)
C
C *** EXCLUSIVE ROUTINE ARRAYS
      DIMENSION RDET(4)
C
      DO 10 K1=1,NEI
         RDET(K1)=1.0/(4.0*(1.0-V(K1)))
   10 CONTINUE
      NEX02=NEX/2
      NFIM1=NEI-1
      NE=NEIM1+4+1
C *** DEVELOP ISC ARRAY
      ISC(NEI)=1
      IF (NLSW .EQ. 2) GO TO 40
   20 DO 30 K1=1,NEIM1
         K2=NEI-K1
         ISC(K2)=ISC(K2+1)+2
   30 CONTINUE
   40 K1=1
      DO 50 K2=1,NE,4
         T1=(1.0+V(K1+1))*E(K1)/(E(K1+1)*(1.0+V(K1)))
         T2=1.0+T1
C *** ELEMENTS TOTALLY INDEPENDENT OF M
         EI(K2,1,1)=(-4.0*V(K1)+T1+3.0)*RDET(K1)
         EI(K2+3,1,1)=EI(K2,1,1)
         EI(K2,2,2)=(-T1*(4.0*V(K1+1)-3.0)+1.0)*RDET(K1)
         EI(K2+3,2,2)=EI(K2,2,2)
         EI(K2,2,1)=0.0
         EI(K2+3,2,1)=0.0
C *** PORTIONS OF ELEMENTS INDEPENDENT OF M
         SV(K1,1)=(-2.0*DI(K1)*(2.0*V(K1)-1.0-T1*(2.0*V(K1+1)-1.0)))*RDE
     1   T(K1)
```

```
      SV(K1,2)=(-T2*(4.0*V(K1)-1.0))*RDET(K1)
      SV(K1,3)=(-4.0*DI(K1)*(T2*(V(K1)-V(K1+1))))*RDET(K1)
      SV(K1,8)=(-T2*(4.0*V(K1+1)-1.0))*RDET(K1)
C *** PORTION OF ELEMENTS DEPENDENT ON 1.0/M
      SV(K1,5)=(1.0+2.0*V(K1+1)*(4.0*V(K1)-3.0)-T1*(1.0+2.0*V(K1)*(4.
     !   0*V(K1+1)-3.0)))*RDET(K1)
      SV(K1,6)=(1.0-2.0*V(K1+1)*(4.0*V(K1)-1.0)-T1*(1.0-2.0*V(K1)*(4.
     1   0*V(K1+1)-1.0)))*RDET(K1)
C *** PORTIONS OF ELEMENTS DEPENDENT ON M
      T1=(-2.0*T2)*RDET(K1)
      SV(K1,7)=-DI(K1)*T1
      SV(K1,8)=-DI(K1)**2*T1
      SV(K1,9)=T1
      K1=K1+1
   50 CONTINUE
C *** SET UP SURFACE ARRAY ELEMENTS INDEPENDENT OF M
      S(1,1,2)=-2.0*V(1)
      S(1,2,2)=2.0*V(1)-1.0
      S(2,1,2)=2.0*V(1)
      S(2,2,2)=2.0*V(1)-1.0
      IF (KSW1 .EQ. 1) GO TO 70
C *** RIGID BASE WITH ROUGH INTERFACE
   60 T1=3.0-4.0*V(NEL)
C *** PORTIONS OF RIGID BASE ELEMENTS INDEPENDENT OF M
      TB1=(1.0-4.0*V(NEL))/T1
C *** PORTIONS OF RIGID BASE ELEMENTS DEPENDENT ON M
      TB3=2.0/T1
      TB4=TB3*DI(NI)
      TB5=TB4*DI(NI)
C *** PORTIONS OF RIGID BASE ELEMENTS DEPENDENT ON 1.0/M
      TB2=4.0*(2.0*V(NEL)-1.0)/T1
   70 RETURN
C
      END
      SUBROUTINE ELDEVL ( FM )
CC
C     ELDEVL = DEVELOP EI(K,I,J), S(K,I,J), AND RR(I,J) ARRAYS FOR FM.
C
      COMMON /ELCTL/ KSW1, KSW2, KSW3, KSW4, NBZ, NEI, NEX, NGQP
     *             , NI, NLSW, NTEST, NTSI, NX, WRL
      COMMON /ELCOEF/
     1 EI(16,2,2),S(2,2,2),SV(4,9),ISC(4),SA(2,2),RR(2,2),BA(2,2,2),
     2 TB1,TB2,TB3,TB4,TB5,
     3 NE,NEX02,NEIM1
C
C     /ELSYS/ = ELASTIC LAYERED SYSTEM DESCRIPTION.
C
C
C     THE FOLLOWING INFORMATION MUST BE PROVIDED BEFORE ELSYMS IS
C     CALLED, THESE LOCATIONS ARE NOT DISTURBED.
C
C     NEL   =  NUMBER OF ELASTIC LAYERS.
C     E     =  ARRAY OF MODULI FOR THE LAYERS.
C     V     =  ARRAY OF POISSON'S RATIOS FOR THE LAYERS.
C     TH    =  ARRAY OF THICKNESS FOR THE LAYERS.
C                TH(NEL) = 0.0  IF ELASTIC HALFSPACE,
C                        = DISTANCE TO RIGID BASE INTERFACE OTHERWISE.
C     CI    =  2HFF IF FULL FRICTION RIGID BASE INTERFACE.
C           =  2HNF IF NO FRICTION RIGID BASE INTERFACE.
C              (IGNORED IF TH(NEL) = 0.0)
C
C
C     ON EXIT FROM ELSYMS THE FOLLOWING INFORMATION IS AVAILABLE.
C
C     DI    =  DEPTHS OF THE INTERFACES BETWEEN LAYERS.
C
      COMMON /ELSYS/ NEL, E(5), V(5), TH(5), CI, DI(5)
C
      RFM=1.0/FM
      K1=1
C *** SET UP ELEMENTS DEPENDENT ON M AND 1.0/M
      DO 10 K2=1,NE,4
         EI(K2,1,2)=SV(K1,1)+RFM*SV(K1,5)
         EI(K2+1,1,1)=SV(K1,2)+FM*SV(K1,7)
         EI(K2+1,1,2)=SV(K1,3)+FM*SV(K1,8)+RFM*SV(K1,6)
         EI(K2+1,2,1)=FM*SV(K1,9)
         EI(K2+1,2,2)=SV(K1,4)-FM*SV(K1,7)
         EI(K2+2,1,1)=SV(K1,2)-FM*SV(K1,7)
         EI(K2+2,1,2)=SV(K1,3)-FM*SV(K1,8)-RFM*SV(K1,6)
         EI(K2+2,2,1)=-FM*SV(K1,9)
         EI(K2+2,2,2)=SV(K1,4)+FM*SV(K1,7)
         EI(K2+3,1,2)=SV(K1,1)-RFM*SV(K1,5)
         K1=K1+1
   10 CONTINUE
C *** SET UP SURFACE ARRAY ELEMENTS THAT ARE DEPENDENT ON M
      S(1,1,1)=FM
      S(1,2,1)=-FM
      S(2,1,1)=FM
      S(2,2,1)=FM
      IF (KSW1 .EQ. 1) GO TO 90
      IF (KSW2 .EQ. 2) GO TO 80
C *** RIGID BASE WITH FULL FRICTION
   30 RR(1,1)=TB1-FM*TB4
      RR(1,2)=RFM*TB2-FM*TB5
      RR(2,1)=FM*TB3
      RR(2,2)=TB1+FM*TB4
      GO TO 50
C *** RIGID BASE WITH NO FRICTION
   40 RR(1,1)=-1.0
      RR(1,2)=-2.0*DI(NI)
      RR(2,1)=0.0
      RR(2,2)=1.0
   50 K7=1
      K1=NE+1
      K3=K1+2
      DO 60 K2=K1,K3,2
         DO 70 K4=1,2
         DO 70 K5=1,2
            SUM=0.0
            DO 60 K6=1,2
               SUM=SUM+EI(K2,K4,K6)*RR(K6,K5)
   60       CONTINUE
            SA(K7,K4,K5)=SUM
   70    CONTINUE
         K7=K7+1
   80 CONTINUE
   90 RETURN
C
      END
      SUBROUTINE ELMULT ( FM )
CC
C     ELMULT = MULTIPLY S(K,I,J) AND EI(K,I,J) FOR ALL FM VALUES.
C
      COMMON /ELCTL/ KSW1, KSW2, KSW3, KSW4, NBZ, NEI, NEX, NGQP
```

```
     .              , NI, NLSW, NTEST, NTSI, NX, WRL
C
C      BLANK COMMON = USED AS WORKING STORAGE BY INPUT AND BY ELSYMS.
C
      COMMON  ST1, ST2, ST3, ST4, TST1, TST2, TST3, TST4
     .              , CDAR(5,736), AJ1(184), RJ0(184), RJ1(184), EX(32)
      COMMON /ELCOEF/
     1 EI(16,2,2),S(2,2,2,2),SV(4,9),ISC(4),SA(2,2),RR(2,2),BA(2,2,2),
     2 TB1,TB2,TB3,TB4,TB5,
     3 NE,NEXD2,NEIM1
C
C *** EXCLUSIVE ROUTINE ARRAYS
      DIMENSION TP(5,2,2),ITA(4),ITAB(4),SEI(2,2,2)
C
      RFM=1.0/FM
      IF (K8W1 .EQ. 1) GO TO 30
C *** START RIGID BASE ROUTINE
   10 K6=0
      K1=NE+1
      K3=K1+2
      DO 20 K2=K1,K3,2
         K6=K6+1
      DO 20 K4=1,2
      DO 20 K5=1,2
         SEI(K6,K5,K4)=EI(K2,K5,K4)
         EI(K2,K5,K4)=BA(K6,K5,K4)
   20 CONTINUE
C *** END RIGID BASE ROUTINE
   30 DO 40 K1=1,2
      DO 40 K2=1,2
         SA(K1,K2)=0.0
   40 CONTINUE
      ITAB(1)=3
      K5=1
      DO 200 K1=1,2
         DO 50 K2=1,2
         DO 50 K3=1,2
            TP(1,K2,K3)=S(K1,K2,K3)
   50    CONTINUE
         DO 190 K4=1,NEXD2
C *** CHECK EXPONENT VALUE
            VAL=FM*EX(K5)
            IF (VAL-T8T1) 60,60,180
   60       VAL=EXP(-VAL)
C *** DEVELOP INDEX TO ADD ARRAY
            DO 100 K2=1,NEI
               IT=K5=1
   70          ITT=IT/ISC(K2)
               IF (ITT-3) 90,90,80
   80          IT=IT-4*ISC(K2)
               GO TO 70
   90          ITA(K2)=ITT
  100       CONTINUE
C *** CHECK AGAINST BACK INDEX TO ADD ARRAY
            DO 110 K2=1,NEI
               K3=K2
               IF (ITA(K2)-ITAB(K2)) 120,110,120
  110       CONTINUE
C *** K3 IS NOW THE INDEX FOR THE TP AND THE ITA ARRAYS
C *** SET ITA BACK ARRAY
  120       DO 130 K2=1,NEI
               ITAB(K2)=ITA(K2)
  130       CONTINUE
            K2=(K3-1)*4+1
            DO 160 K10=K2,NE,4
               K6=K10+ITA(K3)
               DO 150 K7=1,2
               DO 150 K8=1,2
                  SUM=0.0
                  DO 140 K9=1,2
                     SUM=SUM+TP(K3,K7,K9)*EI(K6,K9,K8)
  140             CONTINUE
                  TP(K3+1,K7,K8)=SUM
  150          CONTINUE
               K3=K3+1
  160       CONTINUE
            DO 170 K7=1,2
            DO 170 K8=1,2
               SA(K7,K8)=SA(K7,K8)+TP(K3,K7,K8)*VAL
  170       CONTINUE
  180       K5=K5+NX
  190    CONTINUE
  200 CONTINUE
      IF (K8W1 .EQ. 1) GO TO 230
C *** START RIGID BASE ROUTINE
C *** REPLACE BOTTOM EI ELEMENTS
  210 K6=0
      K1=NE+1
      K3=K1+2
      DO 220 K2=K1,K3,2
         K6=K6+1
      DO 220 K4=1,2
      DO 220 K5=1,2
         EI(K2,K5,K4)=SEI(K6,K5,K4)
  220 CONTINUE
C *** END RIGID BASE ROUTINE
  230 RETURN
C
      END
      SUBROUTINE ELBKS ( FM,M )
CC
C      ELBKS = BACK SOLVE FOR A(I,J),B(I,J),C(I,J) AND D(I,J).
C
      COMMON /ELCTL/ K8W1, K8W2, K8W3, K8W4, N87, NEI, NEX, NGQP
     .              , NI, NLSW, NTEST, NTSI, NX, WRL
C
C      BLANK COMMON = USED AS WORKING STORAGE BY INPUT AND BY ELSYMS.
C
      COMMON  ST1, ST2, ST3, ST4, TST1, TST2, TST3, TST4
     .              , CDAR(5,736), AJ1(184), RJ0(184), RJ1(184), EX(32)
      COMMON /ELCOEF/
     1 EI(16,2,2),S(2,2,2,2),SV(4,9),ISC(4),SA(2,2),RR(2,2),BA(2,2,2),
     2 TB1,TB2,TB3,TB4,TB5,
     3 NE,NEXD2,NEIM1
C
C      /ELSYS/ = ELASTIC LAYERED SYSTEM DESCRIPTION.
C
C
C      THE FOLLOWING INFORMATION MUST BE PROVIDED BEFORE ELSYMS IS
C      CALLED, THESE LOCATIONS ARE NOT DISTURBED.
C
C      NEL  =  NUMBER OF ELASTIC LAYERS.
C      E    =  ARRAY OF MODULI FOR THE LAYERS.
C      V    =  ARRAY OF POISSON'S RATIOS FOR THE LAYERS.
```

```
C     TH    =  ARRAY OF THICKNESS FOR THE LAYERS.
C              TH(NEL) = 0.0  IF ELASTIC HALFSPACE,
C                      = DISTANCE TO RIGID BASE INTERFACE OTHERWISE.
C     CI    =  2HFF IF FULL FRICTION RIGID BASE INTERFACE,
C           =  2HNF IF NO FRICTION RIGID BASE INTERFACE.
C              (IGNORED IF TH(NEL) = 0.0)
C
C
C     ON EXIT FROM ELBYMS THE FOLLOWING INFORMATION IS AVAILABLE.
C
C     DI    =  DEPTHS OF THE INTERFACES BETWEEN LAYERS.
C
      COMMON /ELBYS/ NEL, E(5), V(5), TH(5), CI, DI(5)
C
C *** EXCLUSIVE ROUTINE ARRAYS
      DIMENSION VA(4)
C
      VA(1)=1.0
      VA(4)=1.0
      RFM=1.0/FM
      CDAB(NEL,M)=-BA(1,2)*RFM*RFM/(-BA(2,1)*BA(1,2)+BA(2,2)*BA(1,1))
      CDAB(NEL,M+1)=BA(1,1)*CDAB(NEL,M)/(-BA(1,2))
      IF (KBW1 .EQ. 1) GO TO 30
C *** START RIGID BASE ROUTINE
   10 VAL=FM*DI(NI)*2.0
      IF (VAL-TST1) 20,20,30
   20 VAL=EXP(-VAL)
      CDAB(NEL,M+2)=(RB(1,1)*CDAB(NEL,M)+RB(1,2)*CDAB(NEL,M+1))*VA(
      CDAB(NEL,M+3)=(RB(2,1)*CDAB(NEL,M)+RB(2,2)*CDAB(NEL,M+1))*VA(
      GO TO 40
C *** END RIGID BASE ROUTINE
   30 CDAB(NEL,M+2)=0.0
      CDAB(NEL,M+3)=0.0
   40 DO 140 K10=1,NEI
         K11=NEI-K10+1
         MP3=M+3
         DO 50 K1=M,MP3
            CDAB(K11,K1)=0.0
   50    CONTINUE
         K12=K11+1
         K13=(K11-1)*4+1
         VAL=2.0*FM*DI(K11)
         IF (VAL-TST1) 70,70,60
   60    K6=1
         K4=1
         GO TO 100
   70    VA(2)=EXP(-VAL)
         K4=2
         VA(3)=1.0/VA(2)
         IF (CDAB(K12,M+2)) 90,80,90
   80    K6=1
         GO TO 100
   90    K6=2
  100    K8=M-2
         K7=0
         DO 130 K5=1,K4
            K2=M-1
            K8=K8+2
            K9=K8+1
            DO 120 K3=1,K4
               K7=K7+1
               DO 110 K1=1,2
                  K2=K2+1
                  CDAB(K11,K2)=CDAB(K11,K2)+VA(K7)*(EI(K13,K1,1)*CDAB(K1
     1            2,K8)+EI(K13,K1,2)*CDAB(K12,K9))
  110          CONTINUE
               K13=K13+2
  120       CONTINUE
            K13=K13-3
  130    CONTINUE
  140 CONTINUE
      RETURN
C
      END
      FUNCTION BESSEL (X,N)
CC
C     BESSEL = EVALUATE N-TH ORDER BESSEL FUNCTION (N = 0, 1 OR 2).
C
C *** EXCLUSIVE ROUTINE ARRAYS
      DIMENSION A1(12),A2(5),A3(5),A4(12),A5(5),A6(5)
      DIMENSION A7(12),A8(5),A9(5)
C
      DATA A1      /-.000000003 , .000000076 ,
     1-.000001762 , .000032460 ,-.000460626 , .004819180 ,-.038A03769 ,
     2 .158867102 ,-.370004994 , .265178613 ,-.008723442 , .315455043 /
      DATA A2      /
     1-.000000001 , .000000018 ,-.000000741 , .000068385 ,-.031111799 /
      DATA A3      /
     1 .000000002 ,-.000000052 , .000003075 ,-.000536522 , 1.99802070 /
C
      DATA A4      /-.000000001 , .000000029 ,
     1-.000000762 , .000015887 ,-.000260444 , .003240270 ,-.029175525 ,
     2 .177709120 ,-.661043934 , 1.28799410 ,-1.19180120 , 1.29671754 /
      DATA A5      /
     1 .000000001 ,-.000000021 , .000000914 ,-.000096277 , .093555574 /
      DATA A6      /
     1-.000000002 , .000000062 ,-.000003987 , .000898990 , 2.001A0A1A /
C
      DATA A7      / 0.0        , .000000010 ,
     1-.000000300 , .000006870 ,-.000127390 , .001829980 ,-.019569010 ,
     2 .147707600 ,-.730485480 , 2.13203940 ,-3.10639360 , 3.32300070 /
      DATA A8      /
     1 0.0         , .000000008 ,-.000001730 , .000293150 ,-.469339A2 /
      DATA A9      /
     1 0.0         ,-.000000112 , .000008970 ,-.006371780 , 1.9A723A30 /
C
      NM1 = N + 1
      IF (X-8.) 10,10,50
   10 XZ=X*X*.0625-2.
      IF (NM1) 20, 30, 40
   20 BESS=CHEB(A1,12,XZ)
      GO TO 90
   30 BESS=X*CHEB(A4,12,XZ)/8.0
      GO TO 90
   40 BESS=X*X/60.0*CHEB(A7,12,XZ)
      GO TO 90
   50 XZ=256./(X*X)-2.0
      A=0.78539816
      A=2.3561945
      C=0.79788456
      D=3.9269908
      IF (NM1) 60, 70, 80
   60 BESS=(4.0/X)*CHEB(A2,5,XZ)*SIN(X-A)
      BESS=BESS+CHEB(A3,5,XZ)*COS(X-A)
```

```
      BESS=BESS*C/SQRT(X)
      GO TO 90
   70 BESS=-(8.0/X)*CHEB(A5,5,XZ)*SIN(X-B)
      BESS=BESS+CHEB(B6,5,XZ)*COS(X-B)
      BESS=BESS*C/SQRT(X)
      GO TO 90
   80 BESS=-(8.0/X)*CHEB(A8,5,XZ)*SIN(X-D)
      BESS=BESS+CHEB(A9,5,XZ)*COS(X-D)
      BESS=BESS*C/SQRT(X)
   90 BESSEL=BESS
      RETURN
C
      END
      FUNCTION CHEB (A,N,Z)
CC
C     CHEB = CHEBYACHEV EVALUATION FOR BESSEL.
C
      DIMENSION A(12),B(10)
      B(1)=0.
      B(2)=0.
      DO 10 I=1,N
         B(I+2)=Z*B(I+1)-B(I)+A(I)
   10 CONTINUE
      CHEB=.5*(B(N+2)-B(N))
      RETURN
C
      END
      SUBROUTINE ELCALC
CC
C     ELCALC = CALCULATE ELASTIC LAYER RESPONSES AT CURRENT POINT.
C
      COMMON /ELCTL/ KSW1, KSW2, KSW3, KSW4, NBZ, NEL, NEX, NGOP
     *              , NI, NLSW, NTEST, NTSI, NX, WRL
C     DIMENSIONS ON ANS CHANGED FROM (6,100,10) TO SAVE SPACE.
C     IN REPAIR, ONLY ONE DEPTH POINT, 2 X-Y POINTS, AND 4 LOADS ARE
C     USED.
      COMMON /ELCYLN/ NRC, NZC, LAY, NR, R(100), TXR(100), ANS(6,8,1)
     *              , RSE, TSE, VSE, SSE, RDP, VDP, RLP, WR, WZ
C
C     BLANK COMMON = USED AS WORKING STORAGE BY INPUT AND BY ELSYM5.
C
      COMMON  ST1, ST2, ST3, ST4, TST1, TST2, TST3, TST4
     *      , CDAR(5,736), AJ1(184), RJ0(184), RJ1(184), Ex(32)
      COMMON /ELPART/ GP(184)
C
C     /ELSYS/ = ELASTIC LAYERED SYSTEM DESCRIPTION.
C
C
C     THE FOLLOWING INFORMATION MUST BE PROVIDED BEFORE ELSYM5 IS
C     CALLED, THESE LOCATIONS ARE NOT DISTURBED.
C
C     NEL  =  NUMBER OF ELASTIC LAYERS.
C     E    =  ARRAY OF MODULI FOR THE LAYERS.
C     V    =  ARRAY OF POISSON/S RATIOS FOR THE LAYERS.
C     TH   =  ARRAY OF THICKNESS FOR THE LAYERS.
C             TH(NEL) = 0.0  IF ELASTIC HALFSPACE.
C                     = DISTANCE TO RIGID BASE INTERFACE OTHERWISE.
C     CI   =  2HFF IF FULL FRICTION RIGID BASE INTERFACE,
C             2HNF IF NO FRICTION RIGID BASE INTERFACE.
C             (IGNORED IF TH(NEL) = 0.0)
C
C
C     ON EXIT FROM ELSYM5 THE FOLLOWING INFORMATION IS AVAILABLE.
C
C     DI   =  DEPTHS OF THE INTERFACES BETWEEN LAYERS.
C
      COMMON /ELSYS/ NEL, E(5), V(5), TH(5), CI, DI(5)
C
C     /ELCOM/ = ELSYM5 COMMUNICATIONS BLOCK.
C
C
C     THE FOLLOWING INFORMATION MUST BE PROVIDED BEFORE ELSYM5 IS
C     CALLED, THESE LOCATIONS ARE NOT DISTURBED.
C
C     FOR  =  LOAD FORCE (POUNDS).
C     PRES =  LOAD PRESSURE (PSI).
C     NLD  =  NUMBER OF LOADS.
C     XL   =  ARRAY OF X COORDINATES (IN),
C     YL   =  ARRAY OF Y COORDINATES (IN).
C     NXY  =  NUMBER OF XY POINTS FOR RESULTS.
C     NZ   =  NUMBER OF DEPTHS FOR RESULTS.
C     XP   =  ARRAY OF X COORDINATES FOR RESULTS (IN),
C     YP   =  ARRAY OF Y COORDINATES FOR RESULTS (IN).
C     Z    =  ARRAY OF DEPTHS FOR RESULTS (IN).
C
C
C     ON EXIT FROM ELSYM5 THE FOLLOWING INFORMATION IS AVAILABLE.
C
C     RL   =  RADIUS OF ASSUMED CIRCULAR LOADS (IN).
C     LAYZ =  ARRAY OF LAYERS IN WHICH Z VALUES FALL.
C
C     THE FOLLOWING ARRAYS ARE USED TO RETURN THE RESULTS OF THE
C     ELASTIC LAYER SOLUTION.  THEY ARE TRIPLY-DIMENSIONED, THE
C     INDICES ARE:
C             1ST INDEX = DIRECTION OF RESPONSE. (FOR PRINCIPAL
C                         STRESSES AND STRAINS: 1, 2, 3; OTHER
C                         RESPONSES ARE CODED: 1=X, 2=Y, 3=Z)
C             2ND INDEX = INDEX OF XY POSITION IN XP AND YP.
C             3RD INDEX = INDEX OF DEPTH IN Z.
C
C     SNRM =  NORMAL STRESSES.
C     SSHR =  SHEAR STRESSES.
C     PS   =  PRINCIPAL STRESSES.
C     PSS  =  PRINCIPAL SHEAR STRESSES.
C     DISP =  DISPLACEMENTS.
C     ENRM =  NORMAL STRAINS.
C     ESHR =  SHEAR STRAINS.
C     PE   =  PRINCIPAL STRAINS.
C     PSE  =  PRINCIPAL SHEAR STRAINS.
C
C
      COMMON /ELCOM/ FOR, PRES, RL, NLD, XL(10), YL(10), NXY, NZ
     *             , XP(10), YP(10), Z(10), LAYZ(10), SNRM(3,2,1)
     *             , SSHR(3,2,1),   PS(3,2,1),  PSS(3,2,1)
     *             , DISP(3,2,1), ENRM(3,2,1), ESHR(3,2,1)
     *             ,   PE(3,2,1),  PSE(3,2,1)
C     DIMENSIONS CHANGED FROM (3,10,10) FOR LIMITED REQUIREMENTS OF
C     WPOD PROGRAM.  ONLY 2 X-Y, 1 Z VALUE USED.
C
C *** EXCLUSIVE ROUTINE ARRAYS
      DIMENSION GF(4),TEST(11)
C
      DATA GF /
     1 .173927423 , .326072577 , .326072577 , .173927423 /
```

```
      DATA DIV /    .861136312 /
C
      ITS=1
      VSE=0.0
      SSE=0.0
      RDP=0.0
      VDP=0.0
      RSE=0.0
      TSE=0.0
      ST1=2.0*V(LAY)
      ST2=1.0/ST1
      ST3=2.0*ST2
      ST4=1.0*ST1
      KSW5=1
      KSW6=1
      NAB=0
      NRZC=0
      K1=0
      K2=-3
      DO 270 K3=1,NBZ
         S1=0.0
         S2=0.0
         S3=0.0
         S4=0.0
         S5=0.0
         S6=0.0
         NBZC=NRZC+1
         DO 170 K4=1,NGDP
            K1=K1+1
            K2=K2+4
            FM=GP(K1)/WRL
      IF (KSW4 .EQ. 1) GO TO 20
   10       VAL=1.0
            GO TO 50
   20       VAL=FM*WZ
            IF (VAL-TST1) 40,40,30
   30       KSW6=2
            GO TO 170
   40       VAL=EXP(VAL)
   50       T2=FM*AJ1(K1)*GF(K4)
      IF (KSW3 .EQ. 1) GO TO 70
   60       T1=FM*T2
            GO TO 80
   70       T1=T2*RJ0(K1)
            T2=T2*RJ1(K1)
            T3=FM*T1
C *** C - D  SECTION
   80       D=CDAB(LAY,K2+1)
            CD=FM*(CDAB(LAY,K2)+D*WZ)/VAL
            DE=D/VAL
      IF (KSW3 .EQ. 1) GO TO 100
   90       S1=S1+T1*(ST2*DE+CD)
            S4=S4+T2*(-ST3*DE-CD)
C *** FORMULAS CHANGED FROM
C     S5=S5+T1*(ST4*DE+CD)
C     S6=S6+T1*DE
C *** TO
            S5=S5+T1*((ST1+0.5)*DE+0.5*CD)
            GO TO 110
  100       S1=S1+T3*(ST2*DE+CD)
            S2=S2+FM*T2*(-ST1*DE+CD)
            S3=S3+T2*(DE-CD)
            S4=S4-T1*(ST3*DE+CD)
            S5=S5+T3*(ST4*DE+CD)
            S6=S6+T3*DE
C *** A - B  SECTION
  110 IF (KSW5 .EQ. 2) GO TO 170
  120       B=CDAB(LAY,K2+3)
            IF (B) 140,130,140
  130       KSW5=2
            NAB=NRZC
            GO TO 170
  140       AB=FM*(CDAB(LAY,K2+2)+B*WZ)*VAL
            BE=B*VAL
      IF (KSW3 .EQ. 1) GO TO 160
  150       S1=S1+T1*(ST2*BE-AB)
            S4=S4+T2*(ST3*BE-AB)
C *** FORMULAS CHANGED FROM
C     S5=S5+T1*(ST4*BE+AB)
C     S6=S6+T1*BE
C *** TO
            S5=S5+T1*((ST1+0.5)*BE+0.5*AB)
            GO TO 170
  160       S1=S1+T3*(ST2*BE-AB)
            S2=S2+FM*T2*(ST1*BE+AB)
            S3=S3+T2*(BE+AB)
            S4=S4+T1*(ST3*BE-AB)
            S5=S5+T3*(ST4*BE+AB)
            S6=S6+T3*BE
  170    CONTINUE
         SF=(GP(K1)-GP(K1-3))/(DIV*WRL)
         VSF=VSF+S1*SF
         VDP=VDP+S4*SF
      IF (KSW3 .EQ. 1) GO TO 190
  180    RSE=RSF+S5*SF
C *** FORMULAS CHANGED FROM
C     TSE=TSE+ST1-S6*SF
C *** TO
         TSE=RSF
         GO TO 200
  190    RSE=SSE+S2*SF
         RDP=RDP+S3*SF
         RSE=RSE+SF*(S5-S3/WR)
         TSE=TSE+SF*(ST1+S6+S3/WR)
  200    TESTH=ABS(2.0*S1+RL*SF)-TST2
         IF (ITS-NTSI) 210,220,220
  210    TEST(ITS)=TESTH
         ITS=ITS+1
         GO TO 260
  220    TEST(NTSI)=TESTH
         DO 250 K4=1,NTEST
            IF (TESTH-TEST(K4)) 230,240,240
  230       TESTH=TEST(K4)
  240       TEST(K4)=TEST(K4+1)
  250    CONTINUE
         IF (TESTH) 280,280,260
  260 IF (KSW6 .EQ. 2) GO TO 290
  270 CONTINUE
      IND=1
      GO TO 300
  280 IND=2
      GO TO 300
  290 IND=3
  300 RETURN
```

```
C
      END
      SUBROUTINE ELSRP
CC
C     ELSRP - STORE ELASTIC RESPONSE FOR SINGLE CYLINDRICAL POINT.
C
C     DIMENSIONS ON ANS CHANGED FROM (6,100,10) TO SAVE SPACE.
C     IN REPAIR, ONLY ONE DEPTH POINT, 2 X-Y POINTS, AND 4 LOADS ARE
C     USED.
      COMMON /ELCYLN/ NRC, NZC, LAY, NR, R(100), IXR(100), ANS(6,8,1)
     .              , RSE, TSE, VSE, SSE, RDP, VDP, RLP, WR, WZ
C
C     /ELSYS/ - ELASTIC LAYERED SYSTEM DESCRIPTION.
C
C
C     THE FOLLOWING INFORMATION MUST BE PROVIDED BEFORE ELSYM5 IS
C     CALLED, THESE LOCATIONS ARE NOT DISTURBED.
C
C     NEL   =  NUMBER OF ELASTIC LAYERS.
C     E     =  ARRAY OF MODULI FOR THE LAYERS.
C     V     =  ARRAY OF POISSON'S RATIOS FOR THE LAYERS.
C     TH    =  ARRAY OF THICKNESS FOR THE LAYERS.
C                TH(NEL) = 0.0  IF ELASTIC HALFSPACE,
C                        = DISTANCE TO RIGID BASE INTERFACE OTHERWISE.
C     CI    =  2HFF IF FULL FRICTION RIGID BASE INTERFACE,
C           =  2HNF IF NO FRICTION RIGID BASE INTERFACE.
C              (IGNORED IF TH(NEL) = 0.0)
C
C
C     ON EXIT FROM ELSYM5 THE FOLLOWING INFORMATION IS AVAILABLE.
C
C     DI    =  DEPTHS OF THE INTERFACES BETWEEN LAYERS.
C
      COMMON /ELSYS/ NEL, E(5), V(5), TH(5), CI, DI(5)
C
C *** EXCLUSIVE ROUTINE ARRAYS
      DIMENSION A(6)
C
      A(1)=RSE*RLP
      A(2)=TSE*RLP
      A(3)=VSE*RLP
      A(4)=SSE*RLP
      A(5)=(1.0+V(LAY))/E(LAY)*RDP*RLP
      A(6)=(1.0+V(LAY))/E(LAY)*VDP*RLP
      ANS(1,NRC,NZC)=A(1)
      ANS(2,NRC,NZC)=A(2)
      ANS(3,NRC,NZC)=A(3)
      ANS(4,NRC,NZC)=A(4)
      ANS(5,NRC,NZC)=A(5)
      ANS(6,NRC,NZC)=A(6)
      RETURN
C
      END
      SUBROUTINE ELOUT
CC
C     ELOUT - OUTPUT RESULTS OF ELASTIC LAYER SYMULATION IN /ELCOM/.
C
C         THIS SUBROUTINE CONVERTS THE RESULTS, WHICH WERE CALCULATED
C     USING CYLINDRICAL COORDINATES AND A SINGLE LOAD, TO CARTESIAN
C     COORDINATES WITH SUPERPOSITION OF LOADS.  IT ALSO CALCULATES
C     THE PRINCIPAL STRESSES AND STRAINS.
C
C     DIMENSIONS ON ANS CHANGED FROM (6,100,10) TO SAVE SPACE.
C     IN REPAIR, ONLY ONE DEPTH POINT, 2 X-Y POINTS, AND 4 LOADS ARE
C     USED.
      COMMON /ELCYLN/ NRC, NZC, LAY, NR, R(100), IXR(100), ANS(6,8,1)
     .              , RSE, TSE, VSE, SSE, RDP, VDP, RLP, WR, WZ
C
C     /ELSYS/ - ELASTIC LAYERED SYSTEM DESCRIPTION.
C
C
C     THE FOLLOWING INFORMATION MUST BE PROVIDED BEFORE ELSYM5 IS
C     CALLED, THESE LOCATIONS ARE NOT DISTURBED.
C
C     NEL   =  NUMBER OF ELASTIC LAYERS.
C     E     =  ARRAY OF MODULI FOR THE LAYERS.
C     V     =  ARRAY OF POISSON'S RATIOS FOR THE LAYERS.
C     TH    =  ARRAY OF THICKNESS FOR THE LAYERS.
C                TH(NEL) = 0.0  IF ELASTIC HALFSPACE,
C                        = DISTANCE TO RIGID BASE INTERFACE OTHERWISE.
C     CI    =  2HFF IF FULL FRICTION RIGID BASE INTERFACE,
C           =  2HNF IF NO FRICTION RIGID BASE INTERFACE.
C              (IGNORED IF TH(NEL) = 0.0)
C
C
C     ON EXIT FROM ELSYM5 THE FOLLOWING INFORMATION IS AVAILABLE.
C
C     DI    =  DEPTHS OF THE INTERFACES BETWEEN LAYERS.
C
      COMMON /ELSYS/ NEL, E(5), V(5), TH(5), CI, DI(5)
C
C     /ELCOM/ - ELSYM5 COMMUNICATIONS BLOCK.
C
C
C     THE FOLLOWING INFORMATION MUST BE PROVIDED BEFORE ELSYM5 IS
C     CALLED, THESE LOCATIONS ARE NOT DISTURBED.
C
C     FOR   =  LOAD FORCE (POUNDS).
C     PRES  =  LOAD PRESSURE (PSI).
C     NLO   =  NUMBER OF LOADS.
C     XL    =  ARRAY OF X COORDINATES (IN).
C     YL    =  ARRAY OF Y COORDINATES (IN).
C     NXY   =  NUMBER OF XY POINTS FOR RESULTS.
C     NZ    =  NUMBER OF DEPTHS FOR RESULTS.
C     XP    =  ARRAY OF X COORDINATES FOR RESULTS (IN).
C     YP    =  ARRAY OF Y COORDINATES FOR RESULTS (IN).
C     Z     =  ARRAY OF DEPTHS FOR RESULTS (IN).
C
C
C     ON EXIT FROM ELSYM5 THE FOLLOWING INFORMATION IS AVAILABLE.
C
C     RL    =  RADIUS OF ASSUMED CIRCULAR LOADS (IN).
C     LAYZ  =  ARRAY OF LAYERS IN WHICH Z VALUES FALL.
C
C     THE FOLLOWING ARRAYS ARE USED TO RETURN THE RESULTS OF THE
C     ELASTIC LAYER SOLUTION.  THEY ARE TRIPLY-DIMENSIONED, THE
C     INDICES ARE:
C             1ST INDEX = DIRECTION OF RESPONSE.  (FOR PRINCIPAL
C                         STRESSES AND STRAINS: 1, 2, 3; OTHER
C                         RESPONSES ARE CODED: 1=X, 2=Y, 3=Z)
C             2ND INDEX = INDEX OF XY POSITION IN XP AND YP.
C             3RD INDEX = INDEX OF DEPTH IN Z.
C
C     SNRM  =  NORMAL STRESSES.
```

```
C     SSHR =  SHEAR STRESSES.
C     PS   =  PRINCIPAL STRESSES.
C     PSS  =  PRINCIPAL SHEAR STRESSES.
C     DISP =  DISPLACEMENTS.
C     ENRM =  NORMAL STRAINS.
C     ESHR =  SHEAR STRAINS.
C     PE   =  PRINCIPAL STRAINS.
C     PSE  =  PRINCIPAL SHEAR STRAINS.
C
C
      COMMON /ELCOM/ FOR, PRES, RL, NLD, XL(10), YL(10), NXY, NZ
     *             , XP(10), YP(10), Z(10), LAYZ(10), SNRM(3,2,1)
     *             , SSHR(3,2,1),   PS(3,2,1),  PSS(3,2,1)
     *             , DISP(3,2,1), ENRM(3,2,1), ESHR(3,2,1)
     *             ,   PE(3,2,1),  PSE(3,2,1)
C     DIMENSIONS CHANGED FROM (3,10,10) FOR LIMITED REQUIREMENTS OF
C     RPOD PROGRAM.  ONLY 2 X-Y, 1 Z VALUE USED.
C
C *** EXCLUSIVE ROUTINE ARRAYS
      DIMENSION A(6),SET(3,3),DC(3,3),T(3)
C
C     LOOP THROUGH ENTIRE ROUTINE ONCE FOR EACH DEPTH.
C
      DO 120 NZR=1,NZ
      NZC = NZR
         LAY=LAYZ(NZC)
         ELAY=E(LAY)
         VLAY=V(LAY)
         SSC=2.0*(1.0+VLAY)/ELAY
         DO 10 K2=1,NXY
         DO 10 K1=1,3
            SNRM(K1,K2,NZC)=0.0
            SSHR(K1,K2,NZC)=0.0
            PS(K1,K2,NZC)=0.0
            PSS(K1,K2,NZC)=0.0
            DISP(K1,K2,NZC)=0.0
            ENRM(K1,K2,NZC)=0.0
            ESHR(K1,K2,NZC)=0.0
            PE(K1,K2,NZC)=0.0
            PSE(K1,K2,NZC)=0.0
   10    CONTINUE
         K9=1
C
C     CALCULATE RESPONSES AT EACH XY POINT FOR CURRENT DEPTH.
C
         DO 110 NXYC=1,NXY
            XPI=XP(NXYC)
            YPI=YP(NXYC)
            DO 60 NLOC=1,NLD
               IR=IXR(K9)
               DO 20 K1=1,6
                  A(K1)=ANS(K1,IR,NZC)
   20          CONTINUE
               RI=R(IR)
               IF (RI-.001) 40,40,30
   30          SINT=(YPI-YL(NLOC))/RI
               SINT2=SINT**2
               COST=(XPI-XL(NLOC))/RI
               COST2=COST**2
               SNRM(1,NXYC,NZC)=SNRM(1,NXYC,NZC)+COST2*A(1)+SINT2*A(2)
               SNRM(2,NXYC,NZC)=SNRM(2,NXYC,NZC)+COST2*A(2)+SINT2*A(1)
               SNRM(3,NXYC,NZC)=SNRM(3,NXYC,NZC)+A(3)
               SSHR(1,NXYC,NZC)=SSHR(1,NXYC,NZC)+COST*SINT*(A(1)-A(2))
               SSHR(2,NXYC,NZC)=SSHR(2,NXYC,NZC)+COST*A(4)
               SSHR(3,NXYC,NZC)=SSHR(3,NXYC,NZC)+SINT*A(4)
               DISP(1,NXYC,NZC)=DISP(1,NXYC,NZC)+COST*A(5)
               DISP(2,NXYC,NZC)=DISP(2,NXYC,NZC)+SINT*A(5)
               DISP(3,NXYC,NZC)=DISP(3,NXYC,NZC)+A(6)
               GO TO 50
C
   40          SNRM(1,NXYC,NZC)=SNRM(1,NXYC,NZC)+A(1)
               SNRM(2,NXYC,NZC)=SNRM(2,NXYC,NZC)+A(2)
               SNRM(3,NXYC,NZC)=SNRM(3,NXYC,NZC)+A(3)
               SSHR(2,NXYC,NZC)=SSHR(2,NXYC,NZC)+A(4)
               DISP(1,NXYC,NZC)=DISP(1,NXYC,NZC)+A(5)
               DISP(3,NXYC,NZC)=DISP(3,NXYC,NZC)+A(6)
   50          K9=K9+1
   60       CONTINUE
            DO 70 K1=1,3
               SET(K1,K1)=SNRM(K1,NXYC,NZC)
   70       CONTINUE
            SET(1,2)=SSHR(1,NXYC,NZC)
            SET(1,3)=SSHR(2,NXYC,NZC)
            SET(2,3)=SSHR(3,NXYC,NZC)
            SET(2,1)=SET(1,2)
            SET(3,1)=SET(1,3)
            SET(3,2)=SET(2,3)
            CALL ELSMTX (SET,DC,3,0)
            DO 80 K1=1,3
               T(K1)=SET(K1,K1)
   80       CONTINUE
            DO 100 K1=1,2
               K2=K1+1
            DO 100 K3=K2,3
               IF (T(K1)-T(K3)) 90,100,100
   90          TEMP=T(K1)
               T(K1)=T(K3)
               T(K3)=TEMP
  100       CONTINUE
            PS(1,NXYC,NZC)=T(1)
            PS(2,NXYC,NZC)=T(2)
            PS(3,NXYC,NZC)=T(3)
            PSS(1,NXYC,NZC)=0.5*(T(1)-T(3))
            PSS(2,NXYC,NZC)=0.5*(T(1)-T(2))
            PSS(3,NXYC,NZC)=0.5*(T(2)-T(3))
            ENRM(1,NXYC,NZC)=(SNRM(1,NXYC,NZC)-VLAY*(SNRM(2,NXYC,NZC)+SN
     1      RM(3,NXYC,NZC)))/ELAY
            ENRM(2,NXYC,NZC)=(SNRM(2,NXYC,NZC)-VLAY*(SNRM(1,NXYC,NZC)+SN
     1      RM(3,NXYC,NZC)))/ELAY
            ENRM(3,NXYC,NZC)=(SNRM(3,NXYC,NZC)-VLAY*(SNRM(1,NXYC,NZC)+SN
     1      RM(2,NXYC,NZC)))/ELAY
            ESHR(1,NXYC,NZC)=SSC*SSHR(1,NXYC,NZC)
            ESHR(2,NXYC,NZC)=SSC*SSHR(2,NXYC,NZC)
            ESHR(3,NXYC,NZC)=SSC*SSHR(3,NXYC,NZC)
            PE(1,NXYC,NZC)=(T(1)-VLAY*(T(2)+T(3)))/ELAY
            PE(2,NXYC,NZC)=(T(2)-VLAY*(T(1)+T(3)))/ELAY
            PE(3,NXYC,NZC)=(T(3)-VLAY*(T(1)+T(2)))/ELAY
            PSE(1,NXYC,NZC)=SSC*PSS(1,NXYC,NZC)
            PSE(2,NXYC,NZC)=SSC*PSS(2,NXYC,NZC)
            PSE(3,NXYC,NZC)=SSC*PSS(3,NXYC,NZC)
  110    CONTINUE
  120 CONTINUE
      RETURN
C
```

```
      END
      SUBROUTINE FLSMTX (H,U,N,IVEC)
CC
C     ELSMTX = SYMMETRIC MATRIX ROUTINE FOR ELOUT.
C
      DIMENSION H(3,3),U(3,3),W(3),IQ(3)
C
      AN=N
      NMI1=N-1
      IF (IVEC-1) 60,10,60
   10 DO 50 I=1,N
         DO 40 J=1,N
            IF (I-J) 30,20,30
   20       U(I,J)=1.0
            GO TO 40
   30       U(I,J)=0.0
   40    CONTINUE
   50 CONTINUE
   60 DO 90 I=1,NMI1
         W(I)=0.0
         IPL1=I+1
         DO 80 J=IPL1,N
            IF (W(I)-ABS(H(I,J))) 70,70,80
   70       W(I)=ABS(H(I,J))
            IQ(I)=J
   80    CONTINUE
   90 CONTINUE
C
C     XMAX SET EQUAL TO ZERO TO AVOID AN IRRELEVANT COMPILER
C     DIAGNOSTIC.
C
      XMAX = 0.0
      DO 120 I=1,NMI1
C
         IF (I-1) 110,110,100
  100    IF (XMAX-W(I)) 110,120,120
C
  110    XMAX=W(I)
         IPIV=I
         JPIV=IQ(I)
  120 CONTINUE
      IF (XMAX-1.E-12/AN) 190,190,130
  130 Z=H(IPIV,IPIV)-H(JPIV,JPIV)
C
C     Y=2.00*H(IPIV,JPIV) ***
C     TA=Y/(DABS(Z)+DSQRT(Z*Z+Y*Y)) ***
C     IF(Z.LT.0.0 TA) TA=-TA ***
C     CO=1.D0/DSQRT(1.D0+TA*TA) ***
      Y=2.0*H(IPIV,JPIV)
      TA=Y/(ABS(Z)+SQRT(Z*Z+Y*Y))
      IF (Z) 140,150,150
  140 TA=-TA
  150 CO=1.0/SQRT(1.0+TA*TA)
C
      SI=TA*CO
      HII=H(IPIV,IPIV)
      HJJ=H(JPIV,JPIV)
      HIJ=H(IPIV,JPIV)
      DO 160 K=1,N
         HTE=H(K,IPIV)
         H(K,IPIV)=H(K,IPIV)*CO+H(K,JPIV)*SI
         H(K,JPIV)=H(K,JPIV)*CO-HTE*SI
         H(IPIV,K)=H(K,IPIV)
  160 H(JPIV,K)=H(K,JPIV)
      H(IPIV,JPIV)=0
      H(JPIV,IPIV)=0
      AA=HIJ*TA
      H(IPIV,IPIV)=HII+AA
      H(JPIV,JPIV)=HJJ-AA
      IF (IVEC) 60,60,170
  170 DO 180 K=1,N
         UTE=U(K,IPIV)
         U(K,IPIV)=U(K,IPIV)*CO+U(K,JPIV)*SI
  180 U(K,JPIV)=U(K,JPIV)*CO-UTE*SI
      GO TO 60
  190 RETURN
C
      END
```

```
07 APR 80 UNIVERSITY OF TEXAS 170/7504 UT20=208

CEDP862=395


        CHARGES THROUGH 6 APR 80 ; TIME $ 1577.36 SUPPLIES $ 187.46

20.51.49 JOB INITIALIZED.
20.52.09 EDITPF 9756 HUEBMID
20.54.32 EDITPF 9756 HUMBJNT
20.55.08 EDITPF 9756 HUEBJNT
20.55.55 READPF 6899 FATLIF
20.55.58  COPIED FILE FATLIF.
20.56.15 RFL 600HR
20.56.16 MNF I=FATLIF
20.56.16  .. 00001. INFORMATIVE DIAGNOSTICS IN   MODE
20.56.17  .. 00002. INFORMATIVE DIAGNOSTICS IN   $GMOD
20.56.17  .. 00001. INFORMATIVE DIAGNOSTICS IN   PRINT
20.56.17  .. 00001. INFORMATIVE DIAGNOSTICS IN   PLOT
20.56.17  .. 00003. INFORMATIVE DIAGNOSTICS IN   ELSYMS
20.56.18  .. 00003. INFORMATIVE DIAGNOSTICS IN   ELINIT
20.56.18  .. 00004. INFORMATIVE DIAGNOSTICS IN   ELSNGL
20.56.18  .. 00002. INFORMATIVE DIAGNOSTICS IN   ELPCC
20.56.18  .. 00002. INFORMATIVE DIAGNOSTICS IN   ELDEVL
20.56.18  .. 00002. INFORMATIVE DIAGNOSTICS IN   ELMULT
20.56.18  .. 00022. INFORMATIVE DIAGNOSTICS IN   ELBKS
20.56.19  .. 00007. INFORMATIVE DIAGNOSTICS IN   BESSEL
20.56.19  .. 00006. INFORMATIVE DIAGNOSTICS IN   ELCALC
20.56.19  .. 00001. INFORMATIVE DIAGNOSTICS IN   ELSMTX
20.56.28  .. CTIME =   5.881 TM SECS,  FL USED =  0544000
20.56.47 EDIT OUTPUT
20.57.39 PRINT FATLIF/57 HD=$MODE PR

#######  CEDP862.
#######  CEDP862.
#######  CEDP862.
```

Output from Program MODE for 15' jointed concrete pavement along IH-30 in Hunt County, Texas. West bound lane - all deflections at joints.

TABLE OF DEFLECTION PARAMETER STATISTICS
SLOPE = SENSOR 1 - SENSOR 5
SCI = SENSOR 1 - SENSOR 2
BCI = SENSOR 4 - SENSOR 5
SPREADABILITY = (SENSOR 1+2+3+4+5)/(5 TIMES SENSOR 1)
AVE = AVERAGE MD = MODE STD = STANDARD DEVIATION CV = COEFFICIENT OF VARIATION
NSEC = NUMBER OF DEFLECTIONS IN SECTION

SECTION		SENSOR 1				SENSOR 5				SLOPE				SPREADABILITY			SCI			BCI		
N	NSEC	AVE	MD	STD	CV	AVE	MD	STD	CV	AVE	MD	STD	CV	AVE	STD	CV	AVE	STD	CV	AVE	STD	CV
1	23	1.22	.75	.50	.41	.59	.60	.14	.23	.63	.25	.52	.83	.74	.06	.09	.18	.10	.54	.11	.16	1.49
2	16	.81	.65	.21	.26	.54	.43	.10	.34	.27	.25	.07	.27	.83	.04	.04	.06	.03	.49	.04	.03	.69
3	15	1.12	.95	.28	.25	.62	.70	.14	.22	.50	.45	.16	.32	.77	.04	.05	.15	.07	.46	.10	.09	.91
4	38	.77	.65	.23	.29	.49	.43	.12	.25	.28	.25	.13	.47	.82	.04	.05	.07	.05	.74	.06	.04	.65
5	72	1.02	.85	.34	.33	.54	.60	.14	.27	.48	.35	.24	.50	.77	.06	.08	.13	.10	.77	.10	.06	.55
6	84	.84	.85	.24	.27	.54	.60	.13	.24	.34	.25	.18	.51	.82	.05	.06	.08	.05	.68	.11	.12	1.12
7	10	1.07	.65	.46	.43	.55	.38	.23	.42	.52	.45	.26	.50	.75	.05	.07	.19	.11	.57	.11	.05	.47
8	97	.88	.85	.22	.25	.56	.45	.13	.23	.33	.25	.15	.46	.83	.05	.07	.09	.06	.74	.09	.06	.65
9	85	1.01	.95	.32	.32	.59	.60	.13	.22	.42	.25	.23	.54	.79	.05	.07	.12	.09	.75	.09	.06	.68
10	83	1.51	.75	.75	.50	.77	.58	.24	.31	.74	.35	.55	.74	.76	.07	.09	.24	.17	.71	.16	.16	1.02
11	119	1.22	.85	.40	.33	.65	.60	.15	.23	.56	.45	.28	.50	.78	.13	.16	.18	.11	.58	.14	.08	.55

SUBGRADE MODULUS UNDER THE DYNAFLECT LOAD

SECTION	MODAL SUBGRADE MODULUS
1	6653.
2	12867.
3	7395.
4	12867.
5	8775.
6	8775.
7	14785.
8	12876.
9	8775.
10	9200.
11	8775.

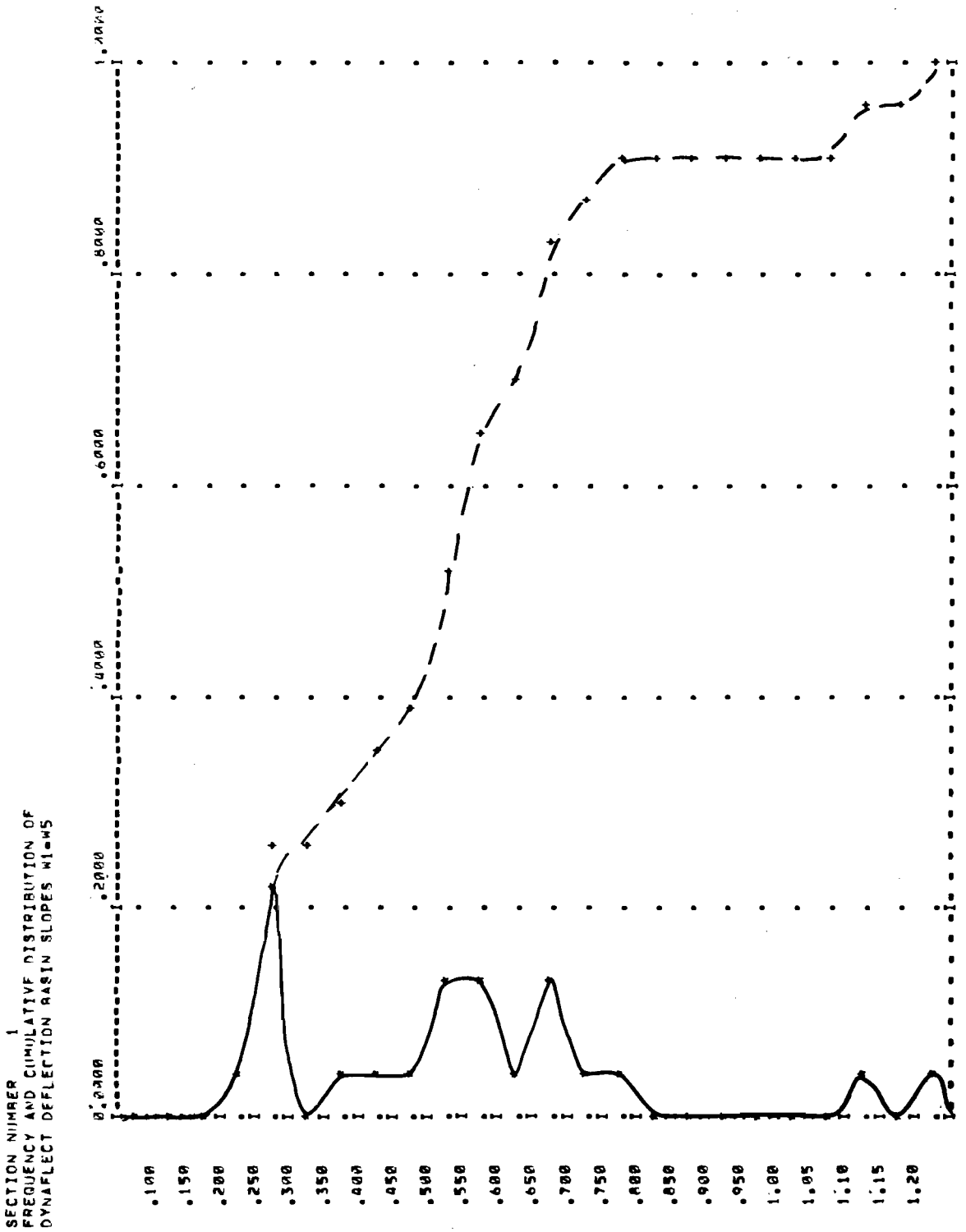
SECTION NUMBER 1
FREQUENCY AND CUMULATIVE DISTRIBUTION OF
DYNAFLECT DEFLECTION BASIN SLOPES W1-W5
.2000
.4000
.6000
.8000
1.0000
.100
.150
.200
.250
.300
.350
.400
.450
.500
.550
.600
.650
.700
.750
.800
.850
.900
.950
1.00
1.05
1.10
1.15
1.20

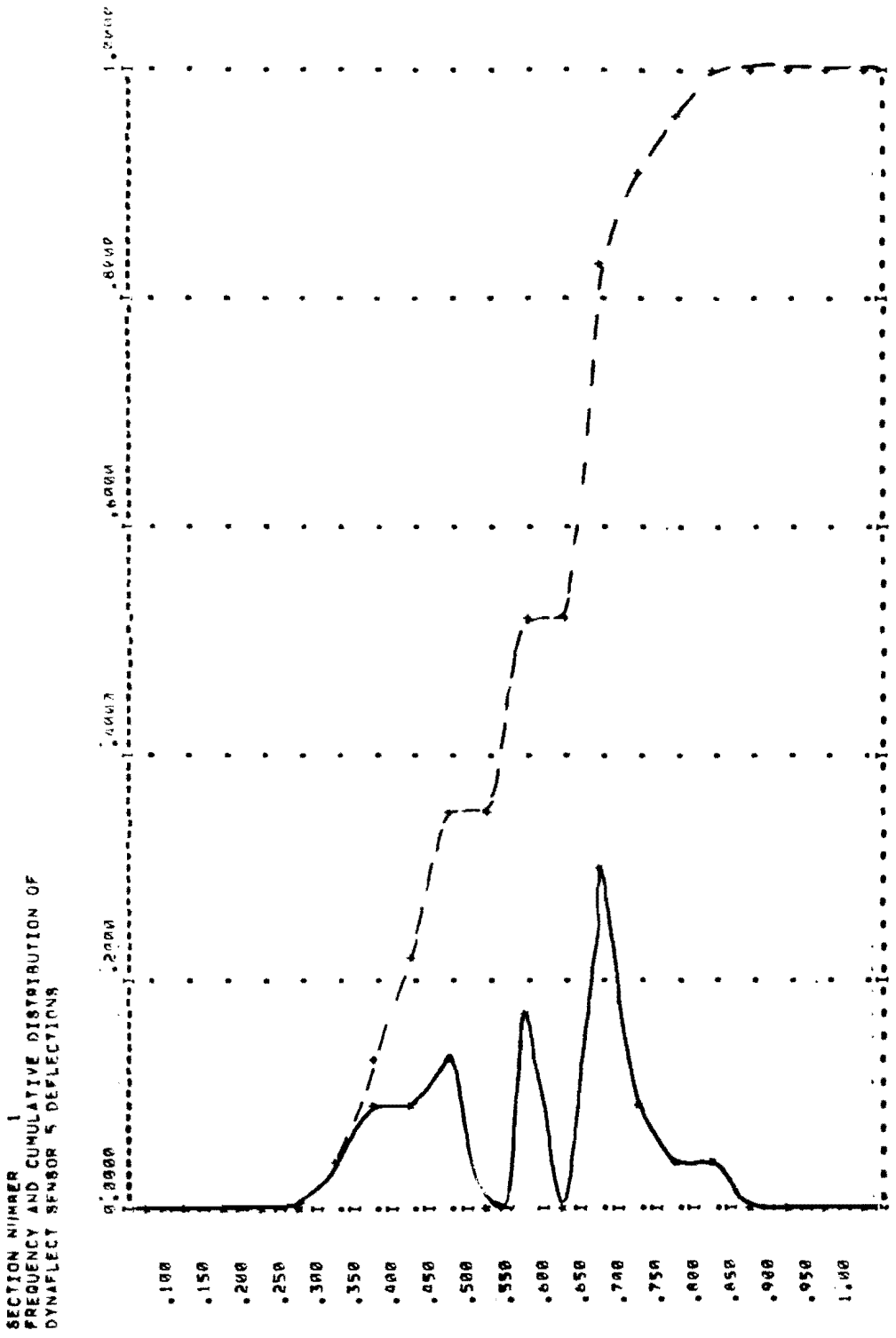
SECTION NUMBER 1
FREQUENCY AND CUMULATIVE DISTRIBUTION OF
DYNAFLECT SENSOR 5 DEFLECTIONS
.100
.150
.200
.250
.300
.350
.400
.450
.500
.550
.600
.650
.700
.750
.800
.850
.900
.950
1.000

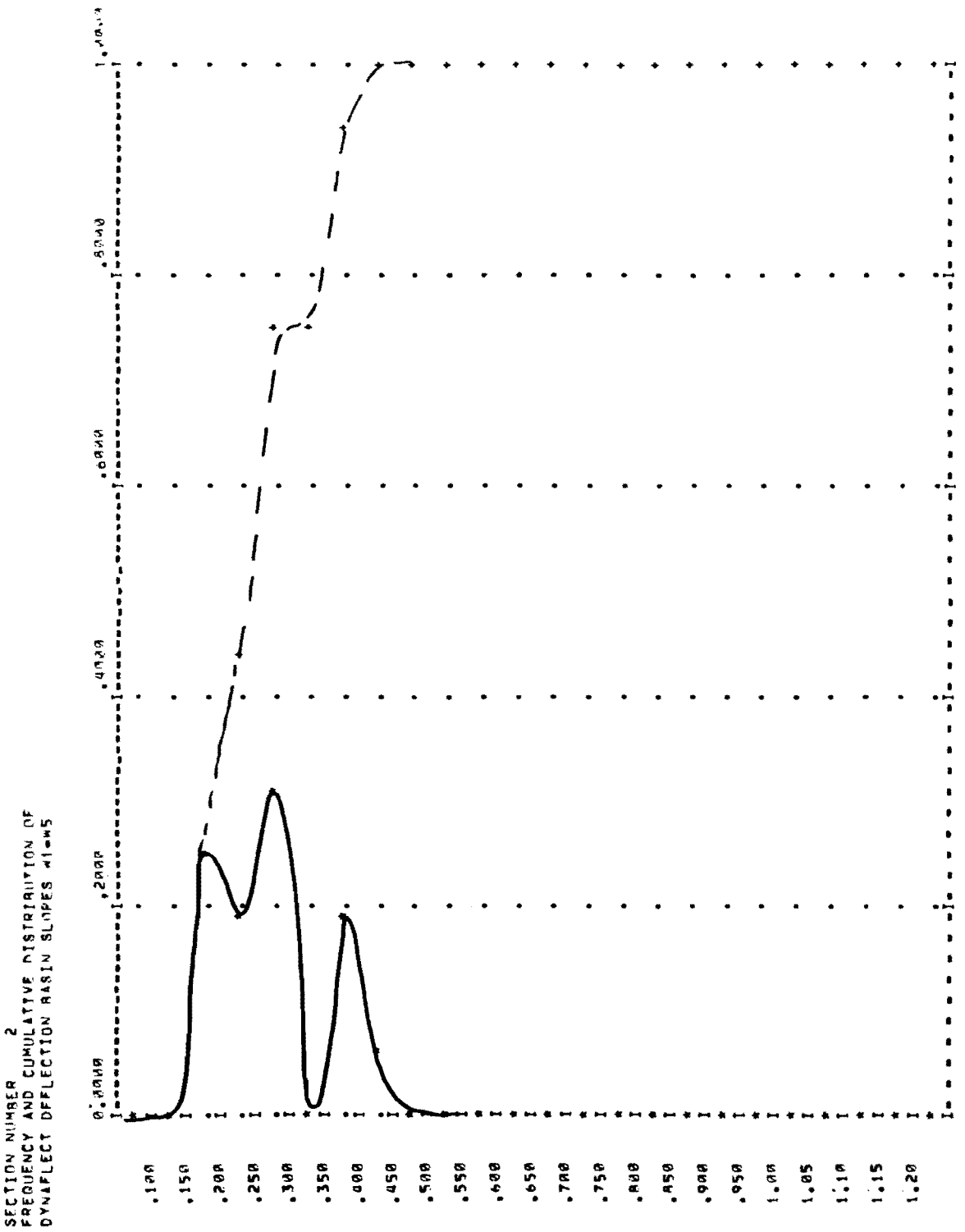
SECTION NUMBER 2
FREQUENCY AND CUMULATIVE DISTRIBUTION OF
DYNAFLECT DEFLECTION BASIN SLOPES #1-#5
0.0000
.2000
.4000
.6000
.8000
1.0000
.100
.150
.200
.250
.300
.350
.400
.450
.500
.550
.600
.650
.700
.750
.800
.850
.900
.950
1.000
1.050
1.100
1.150
1.200

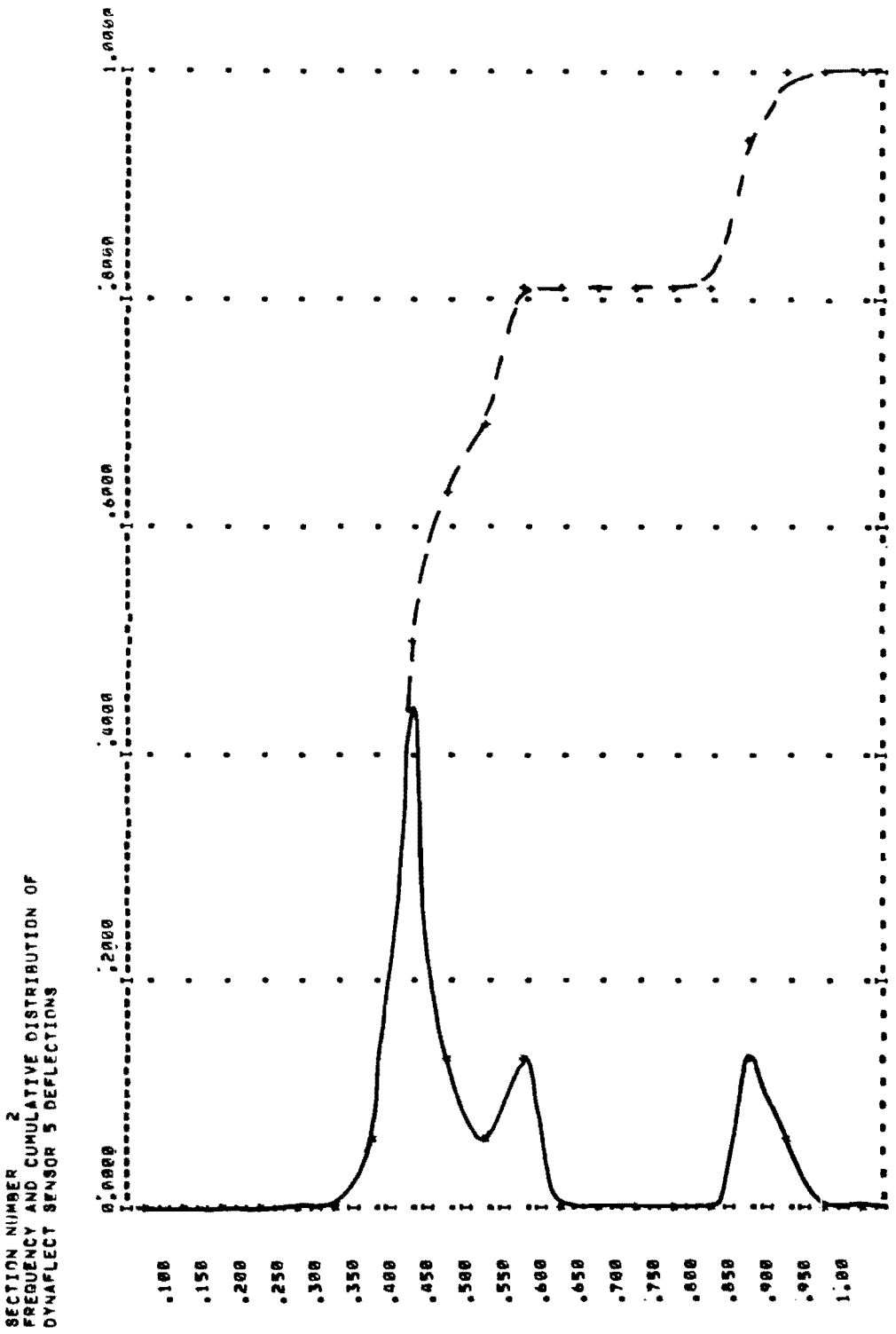
SECTION NUMBER 2
FREQUENCY AND CUMULATIVE DISTRIBUTION OF
DYNAFLECT SENSOR 5 DEFLECTIONS
0.0000
.2000
.4000
.6000
.8000
1.0000
.100
.150
.200
.250
.300
.350
.400
.450
.500
.550
.600
.650
.700
.750
.800
.850
.900
.950
1.00

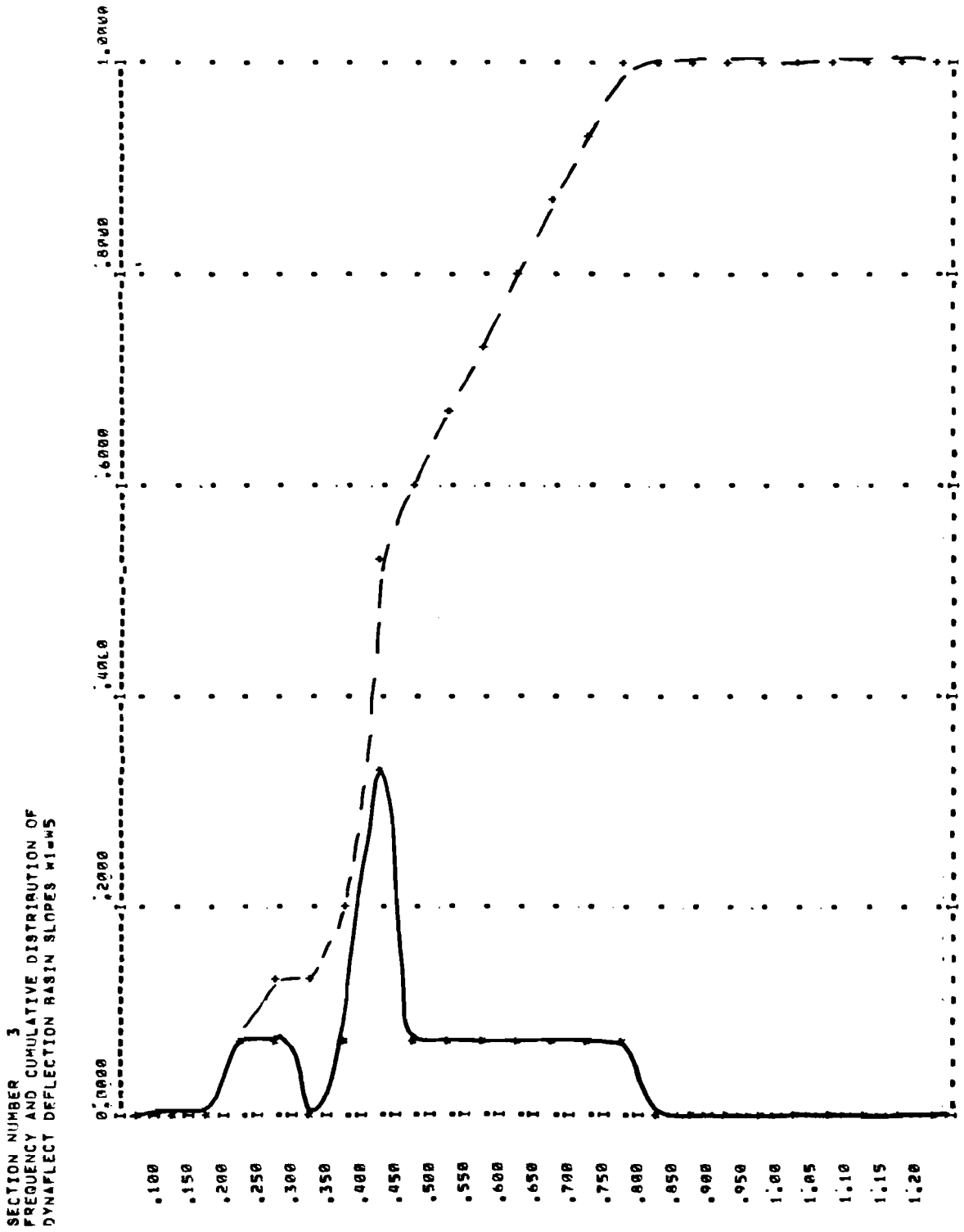
SECTION NUMBER 3
FREQUENCY AND CUMULATIVE DISTRIBUTION OF
DYNAFLECT DEFLECTION BASIN SLOPES W1-W5
0.0000
.2000
.4000
.6000
.8000
1.0000
.100
.150
.200
.250
.300
.350
.400
.450
.500
.550
.600
.650
.700
.750
.800
.850
.900
.950
1.00
1.05
1.10
1.15
1.20

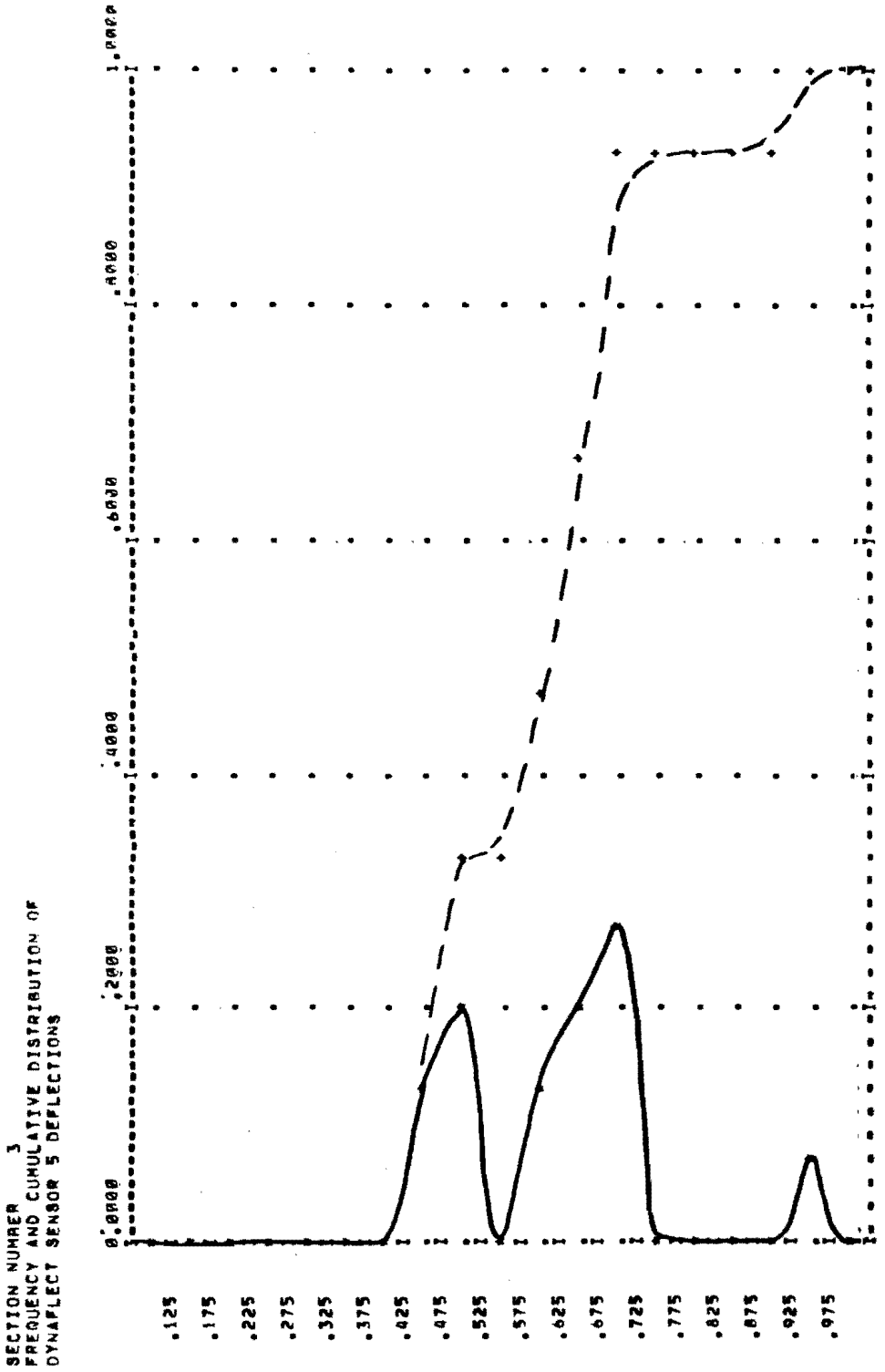
SECTION NUMBER 3
FREQUENCY AND CUMULATIVE DISTRIBUTION OF
DYNAFLECT SENSOR 5 DEFLECTIONS
0.0000
.2000
.4000
.6000
.8000
1.0000
.125
.175
.225
.275
.325
.375
.425
.475
.525
.575
.625
.675
.725
.775
.825
.875
.925
.975

SECTION NUMBER 4
FREQUENCY AND CUMULATIVE DISTRIBUTION OF
DYNAFLECT DEFLECTION BASIN SLOPES W1-W5

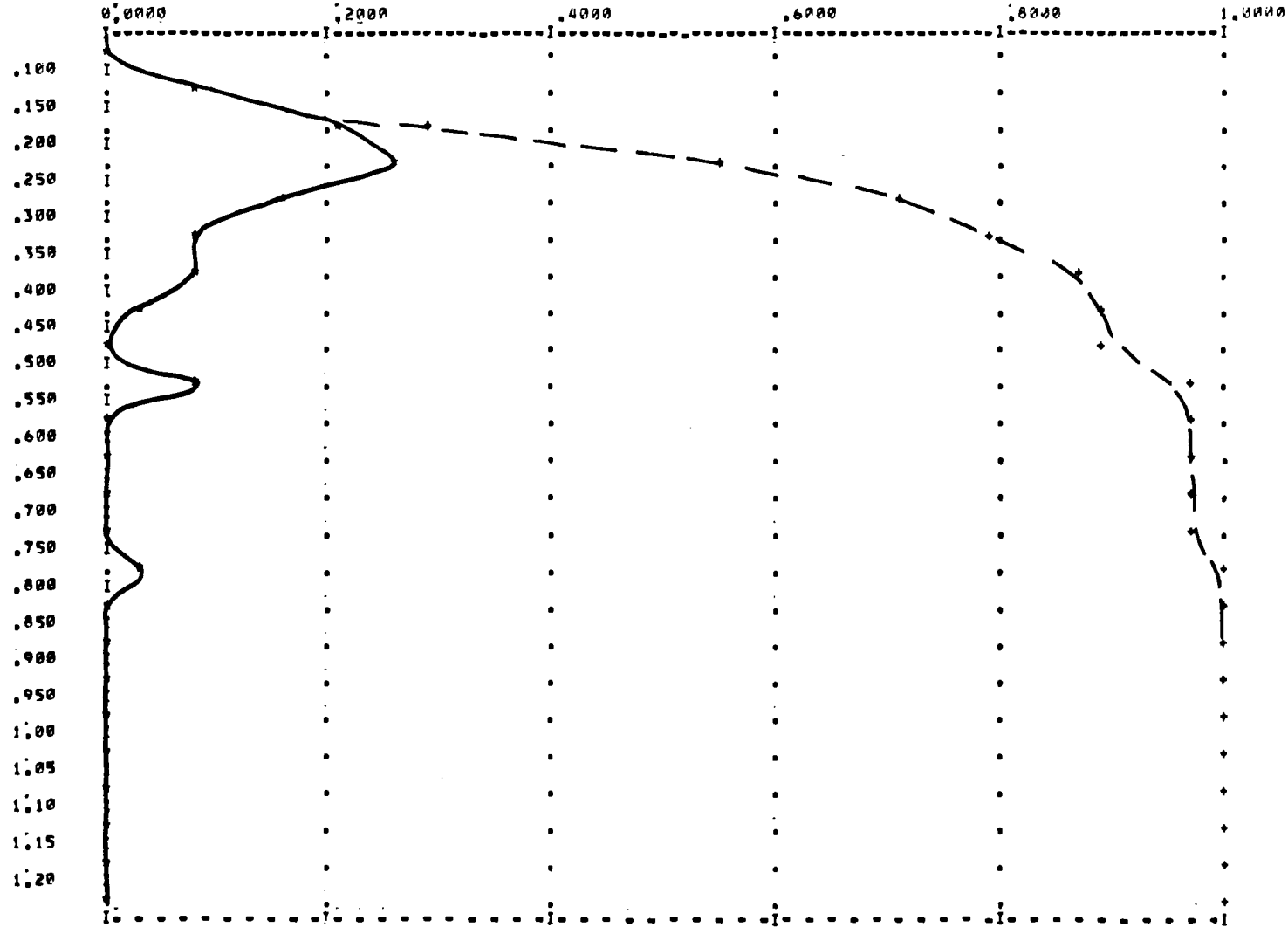

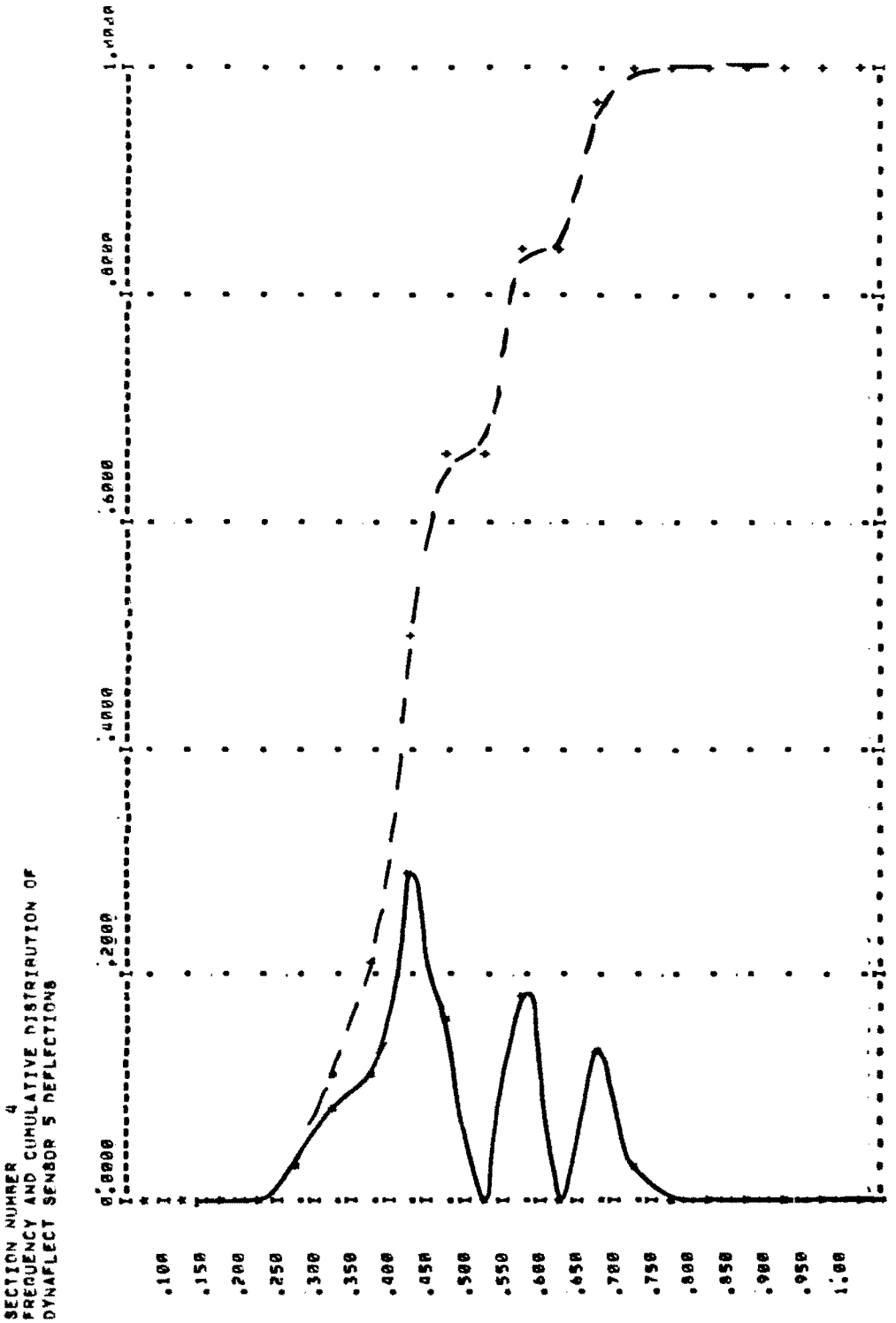
SECTION NUMBER 4
FREQUENCY AND CUMULATIVE DISTRIBUTION OF
DYNAFLECT SENSOR 5 DEFLECTIONS
0.0000
.2000
.4000
.6000
.8000
1.0000
.100
.150
.200
.250
.300
.350
.400
.450
.500
.550
.600
.650
.700
.750
.800
.850
.900
.950
1.00

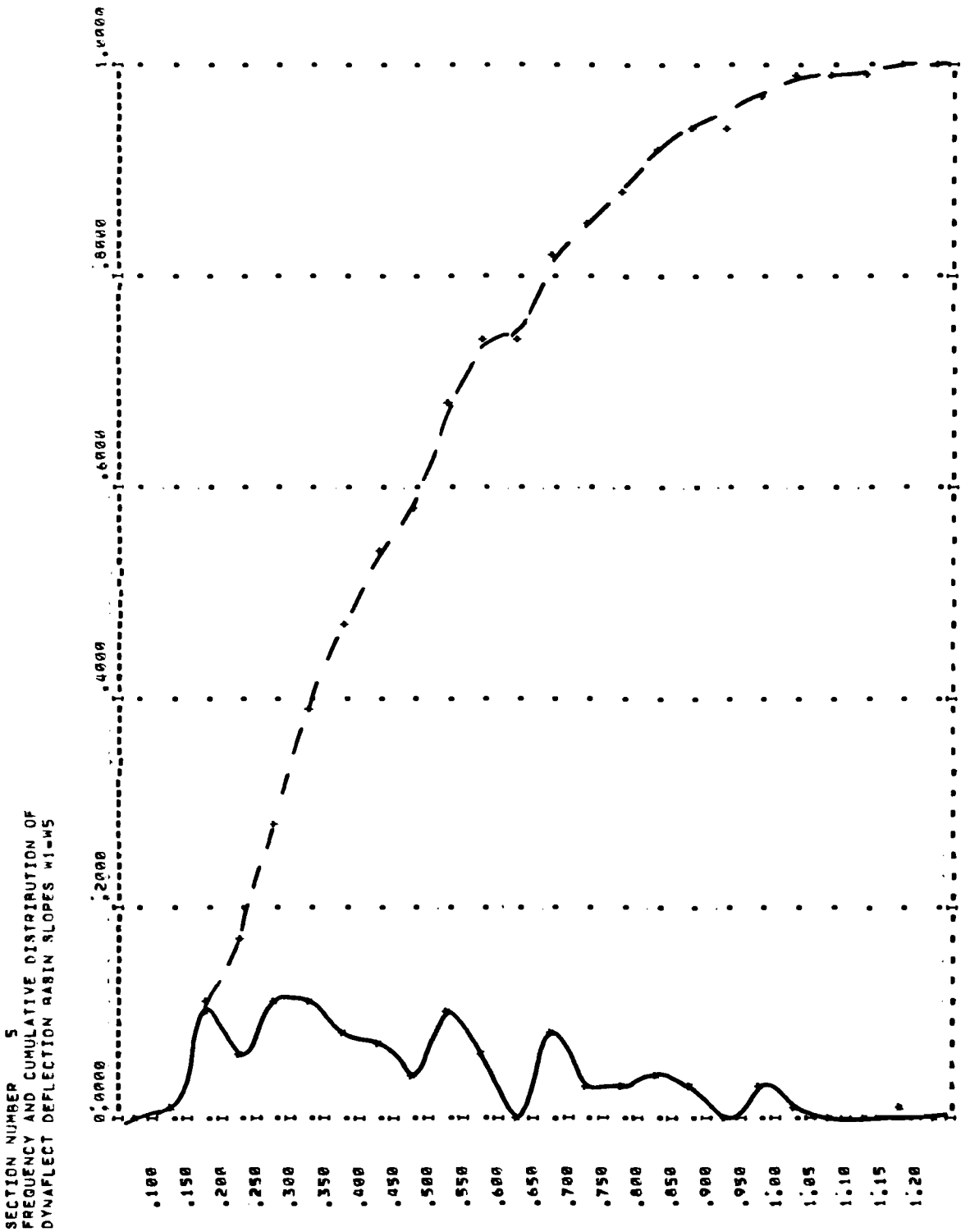
SECTION NUMBER 5
FREQUENCY AND CUMULATIVE DISTRIBUTION OF
DYNAFLECT DEFLECTION BASIN SLOPES W1-W5
0.0000
.2000
.4000
.6000
.8000
1.0000
.100
.150
.200
.250
.300
.350
.400
.450
.500
.550
.600
.650
.700
.750
.800
.850
.900
.950
1.00
1.05
1.10
1.15
1.20

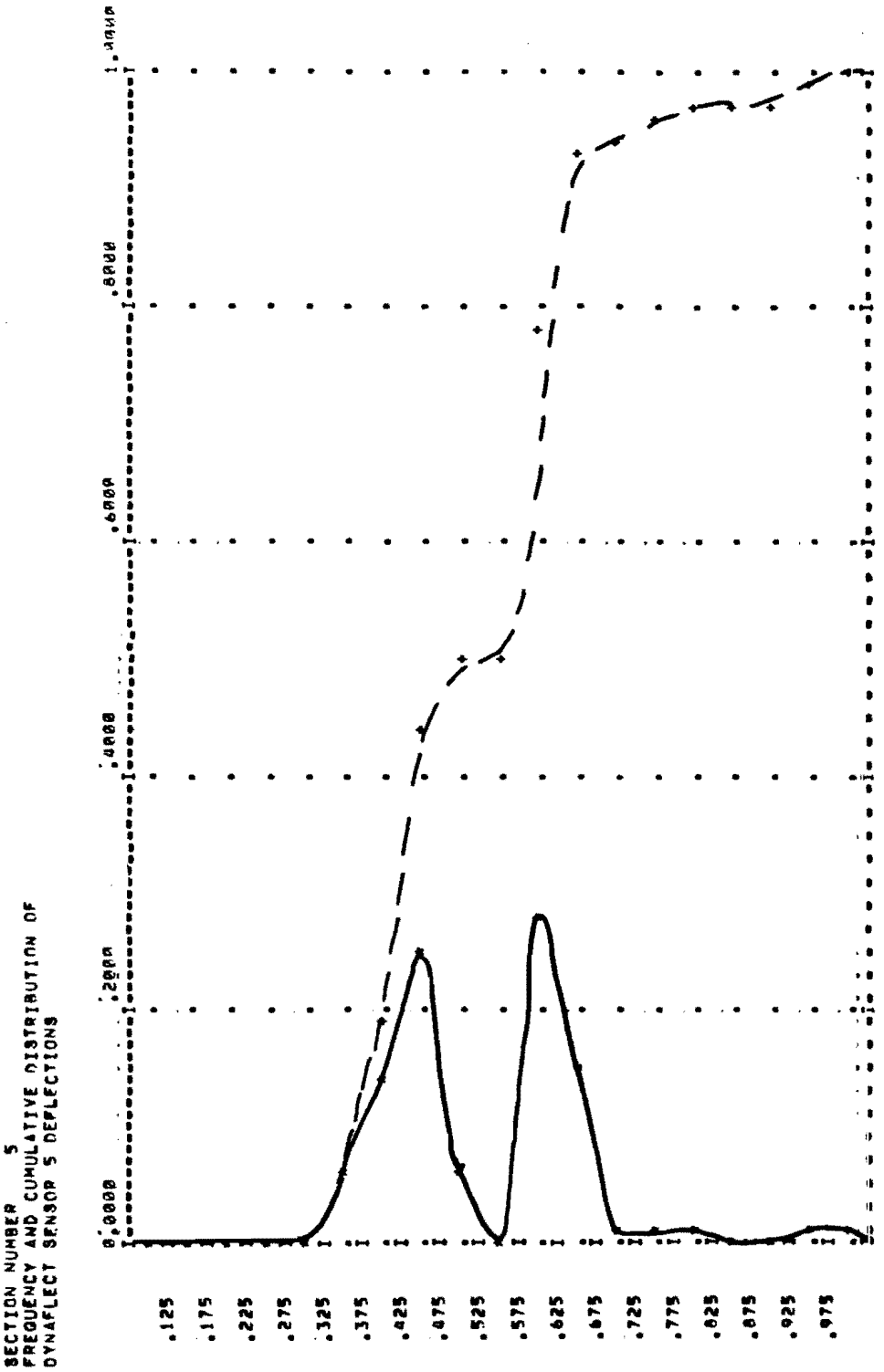
SECTION NUMBER 5
FREQUENCY AND CUMULATIVE DISTRIBUTION OF
DYNAFLECT SENSOR 5 DEFLECTIONS
0.0000
.2000
.4000
.6000
.8000
1.0000
.125
.175
.225
.275
.325
.375
.425
.475
.525
.575
.625
.675
.725
.775
.825
.875
.925
.975

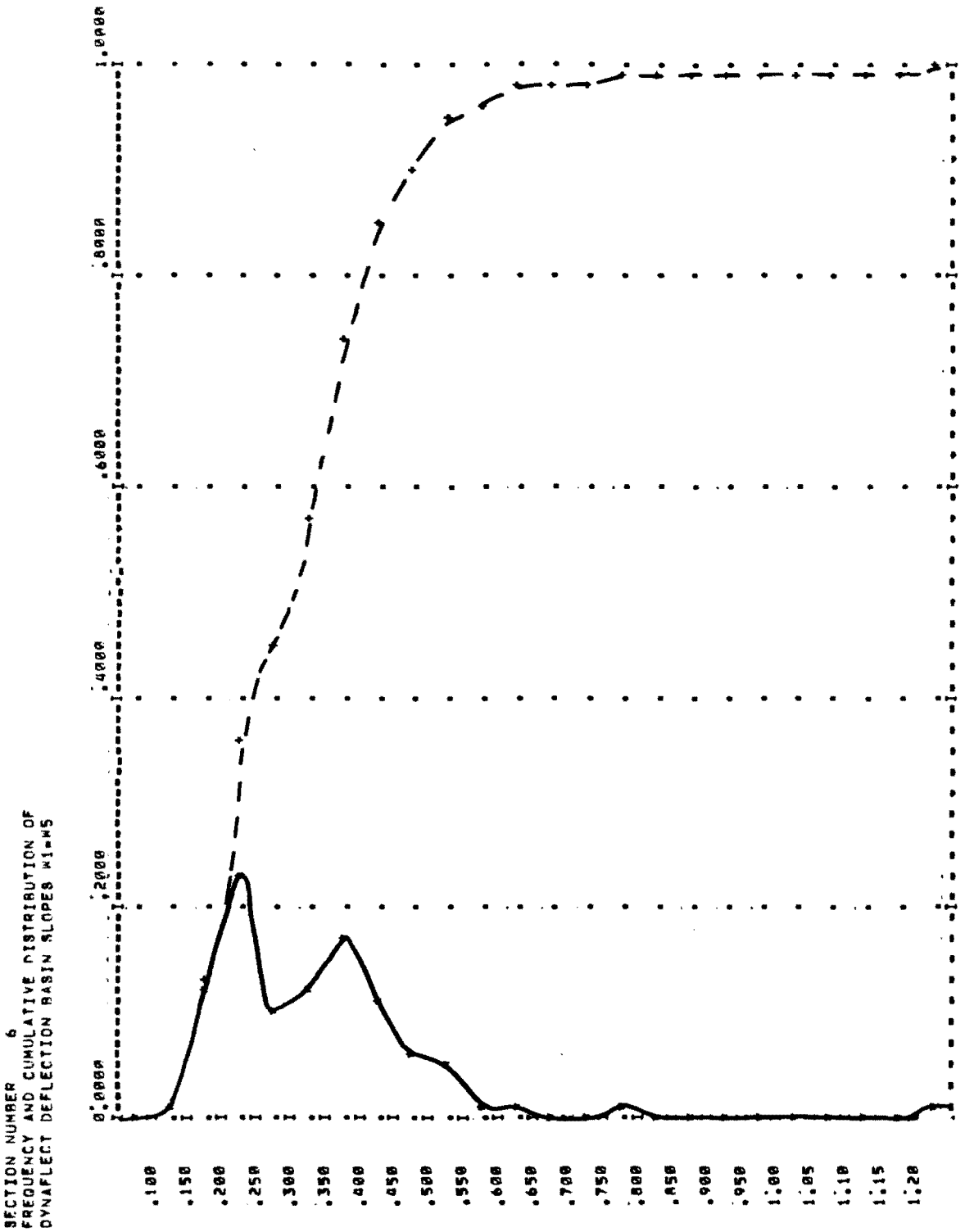
SECTION NUMBER 6
FREQUENCY AND CUMULATIVE DISTRIBUTION OF
DYNAFLECT DEFLECTION BASIN SLOPES W1-W5
0.0000
.2000
.4000
.6000
.8000
1.0000
.100
.150
.200
.250
.300
.350
.400
.450
.500
.550
.600
.650
.700
.750
.800
.850
.900
.950
1.00
1.05
1.10
1.15
1.20

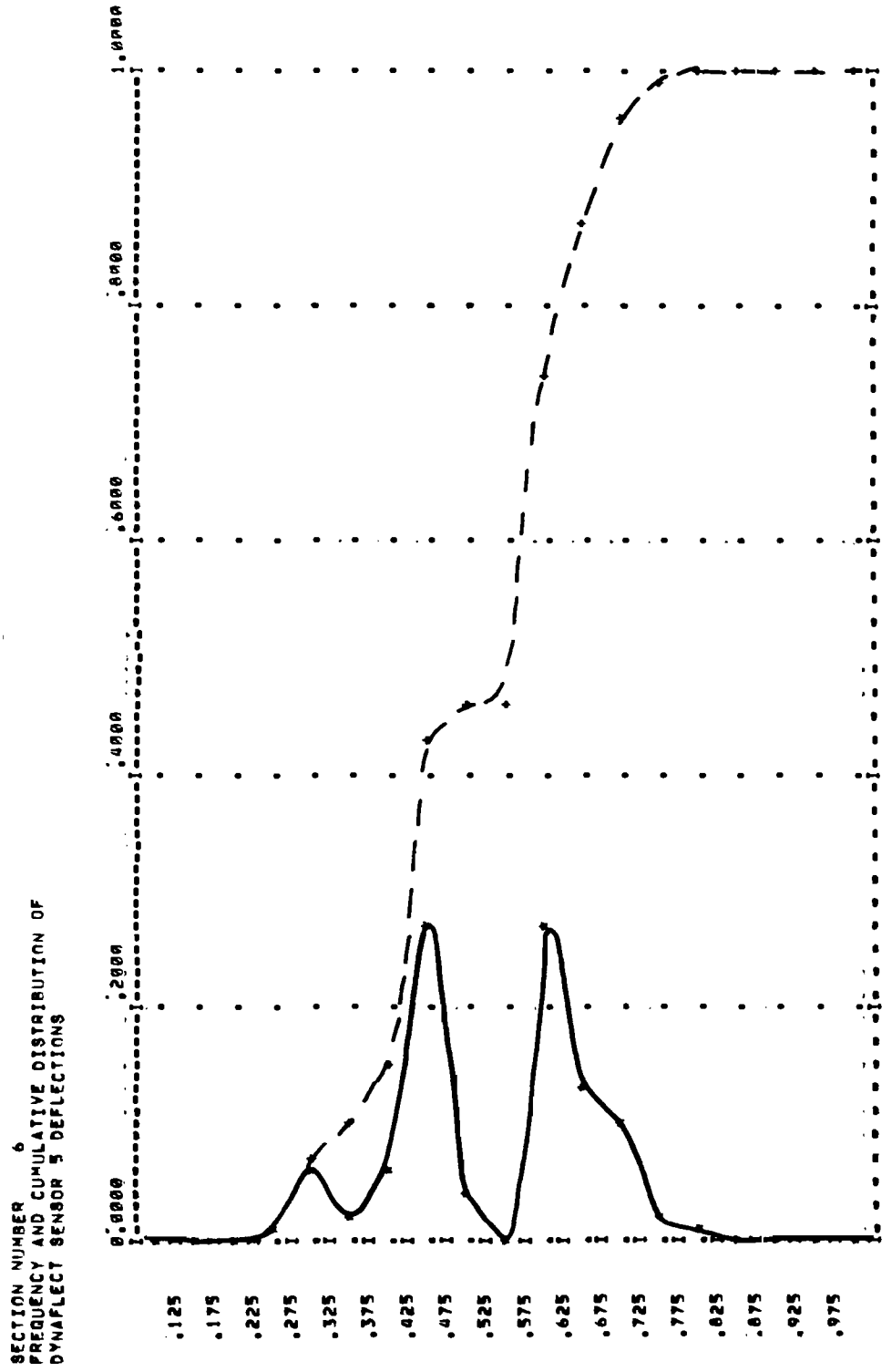
SECTION NUMBER 6
FREQUENCY AND CUMULATIVE DISTRIBUTION OF
DYNAFLECT SENSOR 5 DEFLECTIONS
0.0000
.2000
.4000
.6000
.8000
1.0000
.125
.175
.225
.275
.325
.375
.425
.475
.525
.575
.625
.675
.725
.775
.825
.875
.925
.975

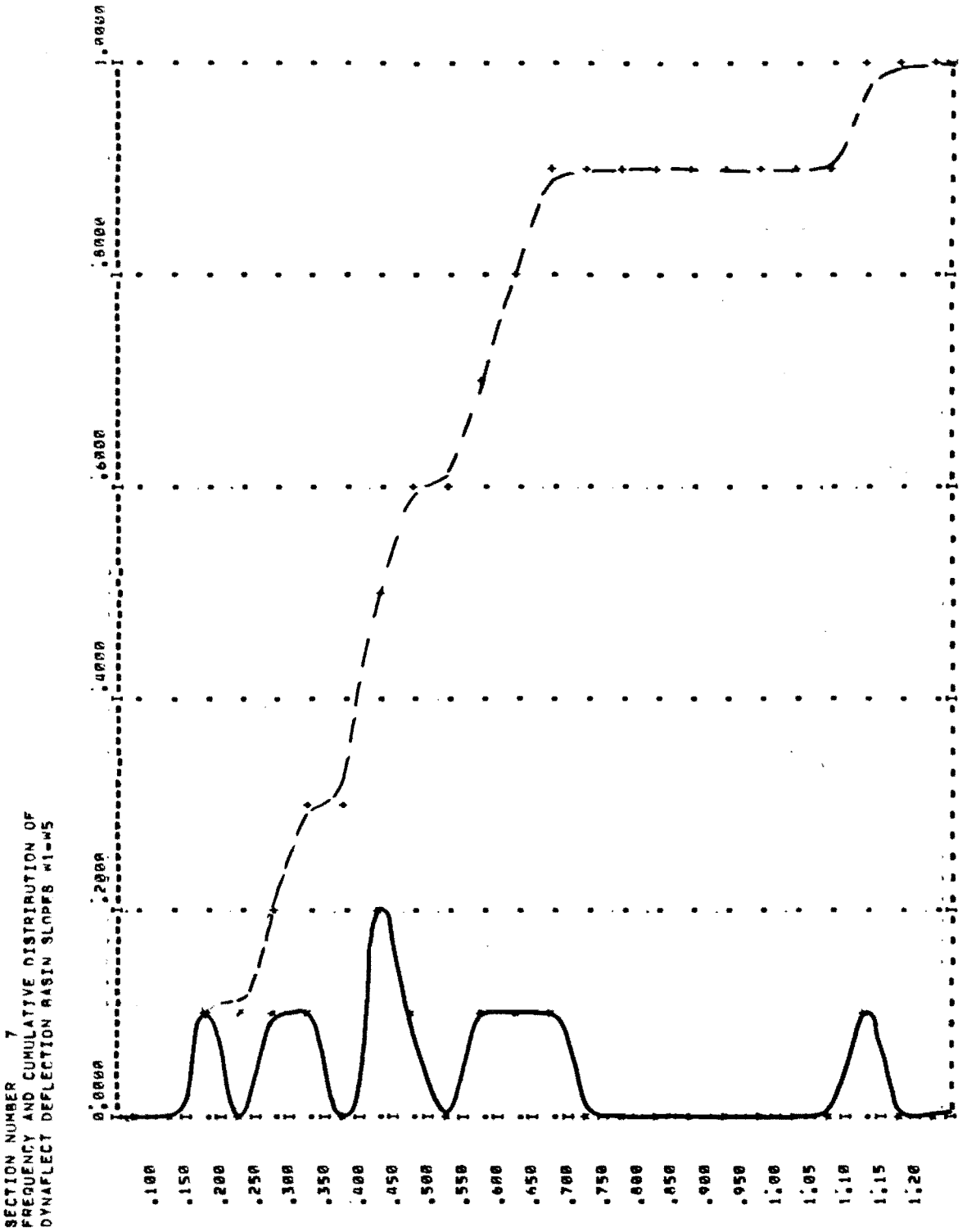
SECTION NUMBER 7
FREQUENCY AND CUMULATIVE DISTRIBUTION OF
DYNAFLECT DEFLECTION BASIN SLOPES #1-#5
0.0000
.2000
.4000
.6000
.8000
1.0000
.100
.150
.200
.250
.300
.350
.400
.450
.500
.550
.600
.650
.700
.750
.800
.850
.900
.950
1.00
1.05
1.10
1.15
1.20

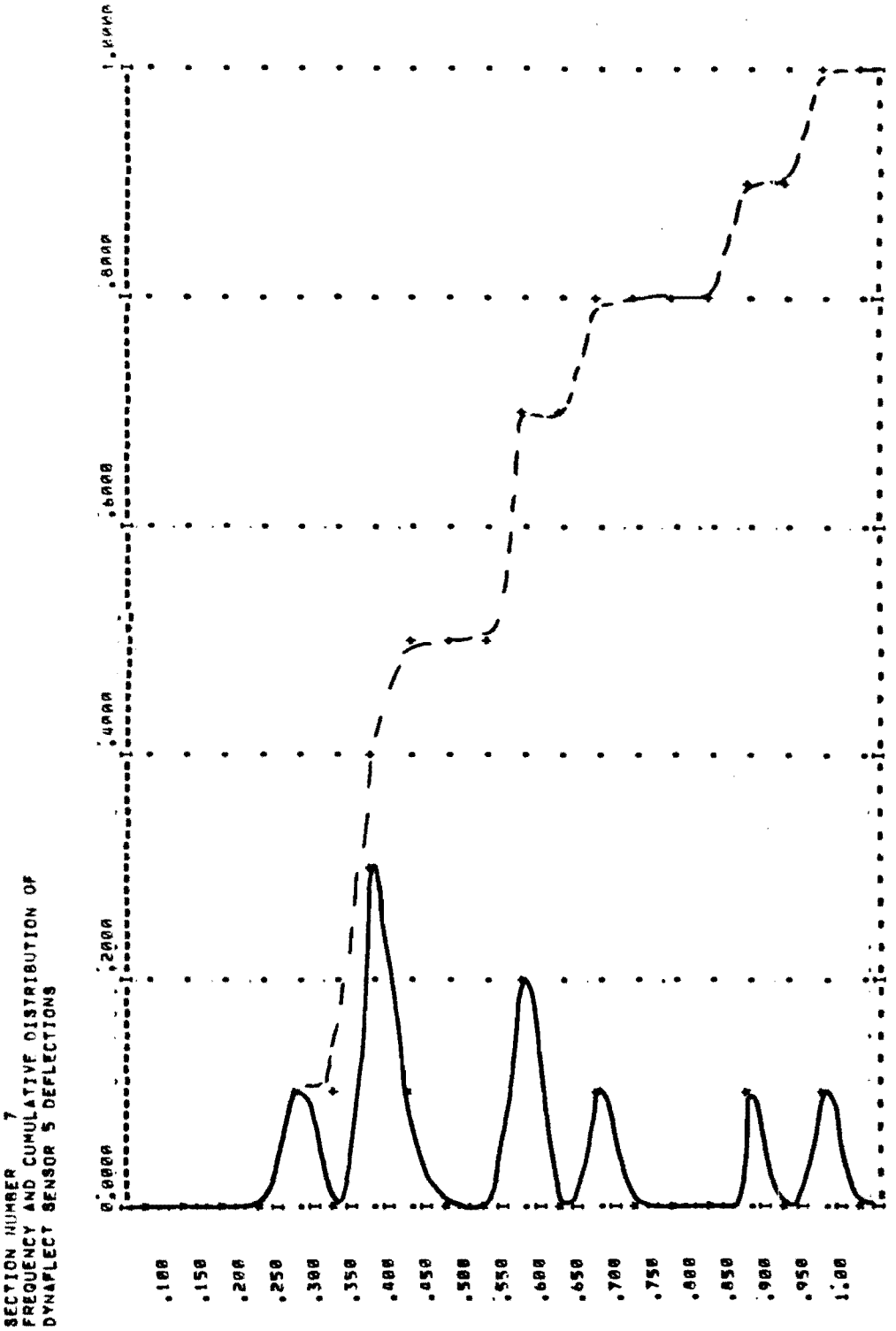
SECTION NUMBER 7
FREQUENCY AND CUMULATIVE DISTRIBUTION OF
DYNAFLECT SENSOR 5 DEFLECTIONS
0.0000
.2000
.4000
.6000
.8000
1.0000
.100
.150
.200
.250
.300
.350
.400
.450
.500
.550
.600
.650
.700
.750
.800
.850
.900
.950
1.00

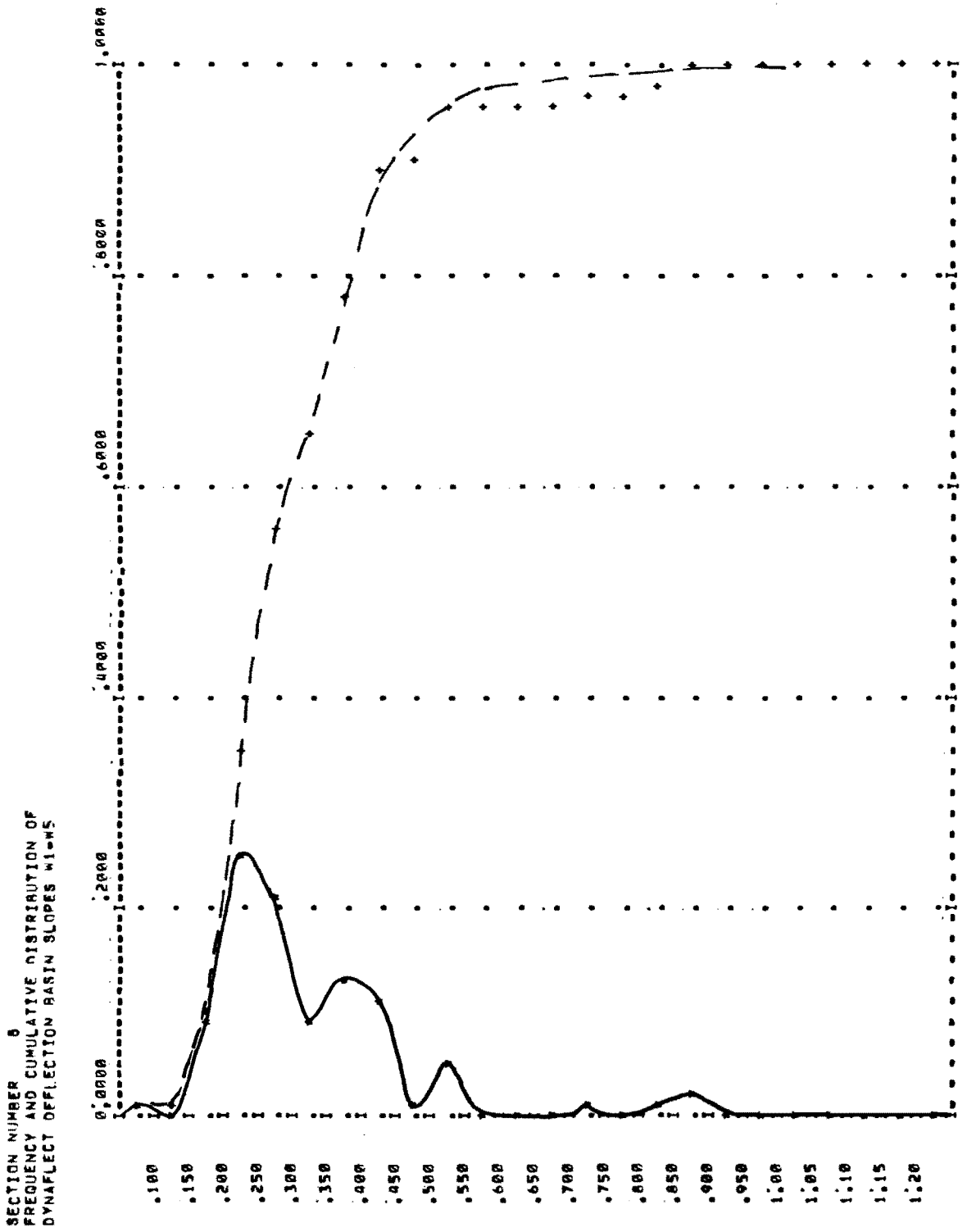
SECTION NUMBER 8
FREQUENCY AND CUMULATIVE DISTRIBUTION OF
DYNAFLECT DEFLECTION BASIN SLOPES W1-W5
0.0000
.2000
.4000
.6000
.8000
1.0000
.100
.150
.200
.250
.300
.350
.400
.450
.500
.550
.600
.650
.700
.750
.800
.850
.900
.950
1.00
1.05
1.10
1.15
1.20

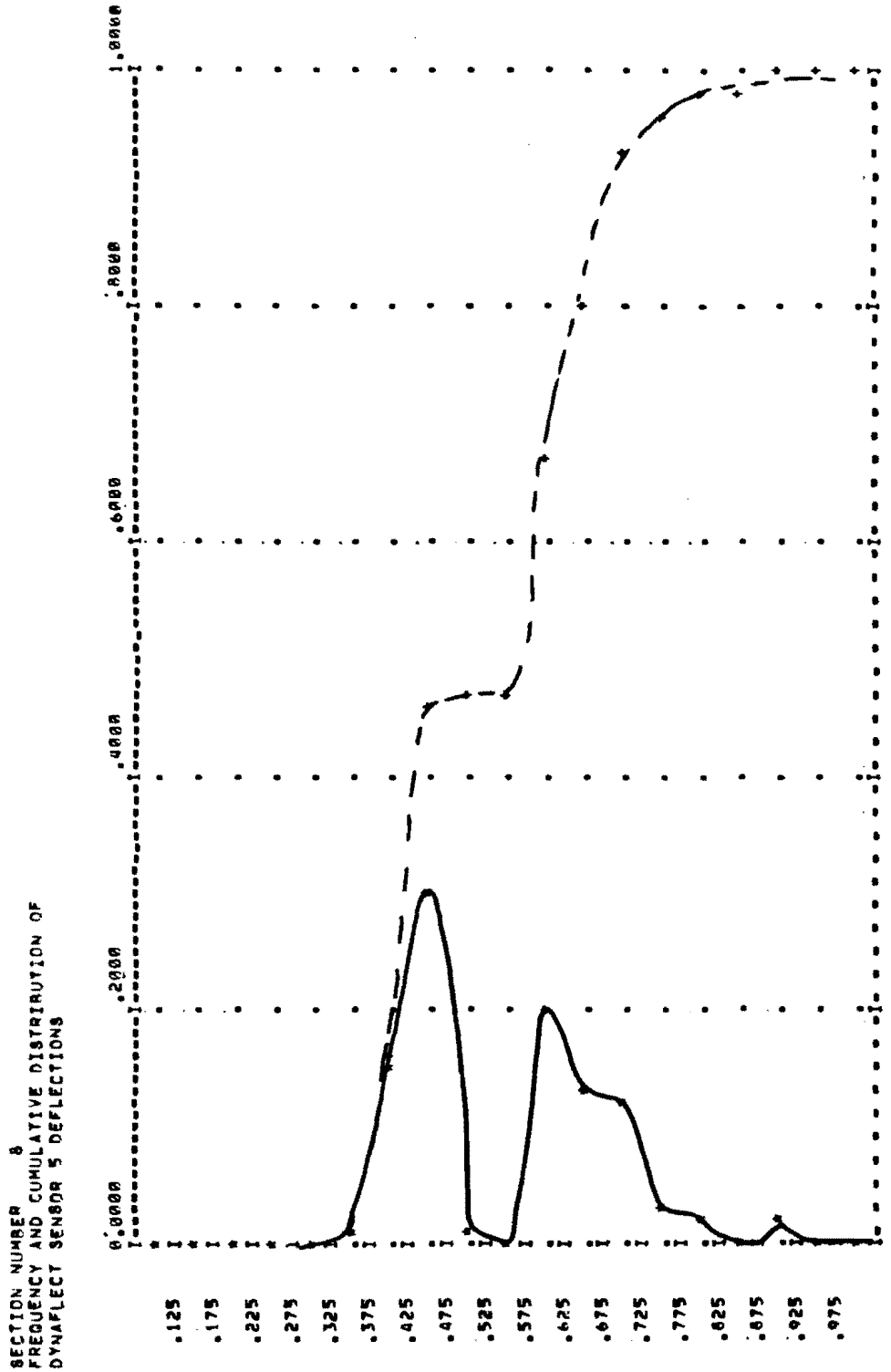
SECTION NUMBER 8
FREQUENCY AND CUMULATIVE DISTRIBUTION OF
DYNAFLECT SENSOR 5 DEFLECTIONS
0.0000
.2000
.4000
.6000
.8000
1.0000
.125
.175
.225
.275
.325
.375
.425
.475
.525
.575
.625
.675
.725
.775
.825
.875
.925
.975

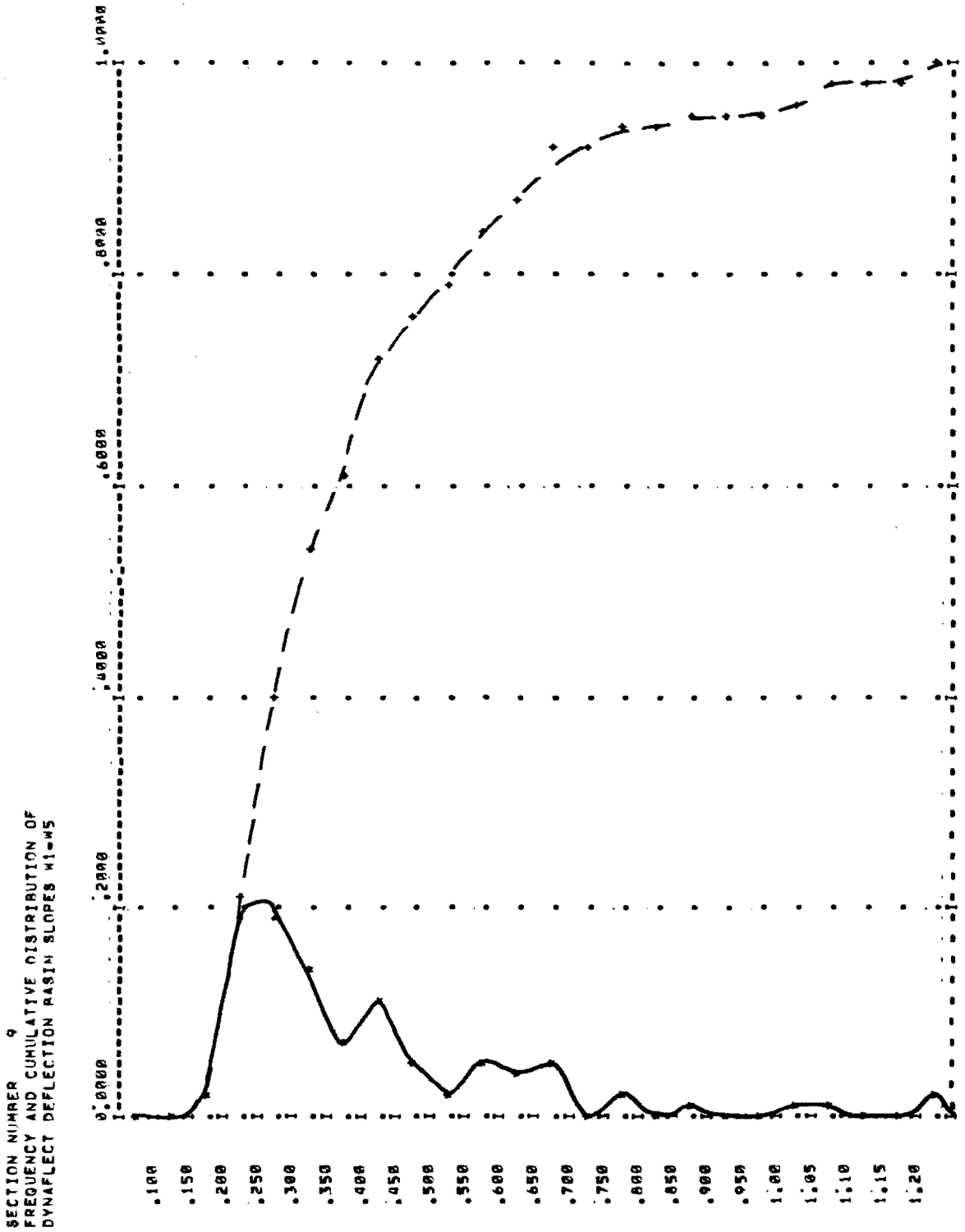
SECTION NUMBER 9
FREQUENCY AND CUMULATIVE DISTRIBUTION OF
DYNAFLECT DEFLECTION BASIN SLOPES W1-W5
0.0000
.2000
.4000
.6000
.8000
1.0000
.100
.150
.200
.250
.300
.350
.400
.450
.500
.550
.600
.650
.700
.750
.800
.850
.900
.950
1.00
1.05
1.10
1.15
1.20

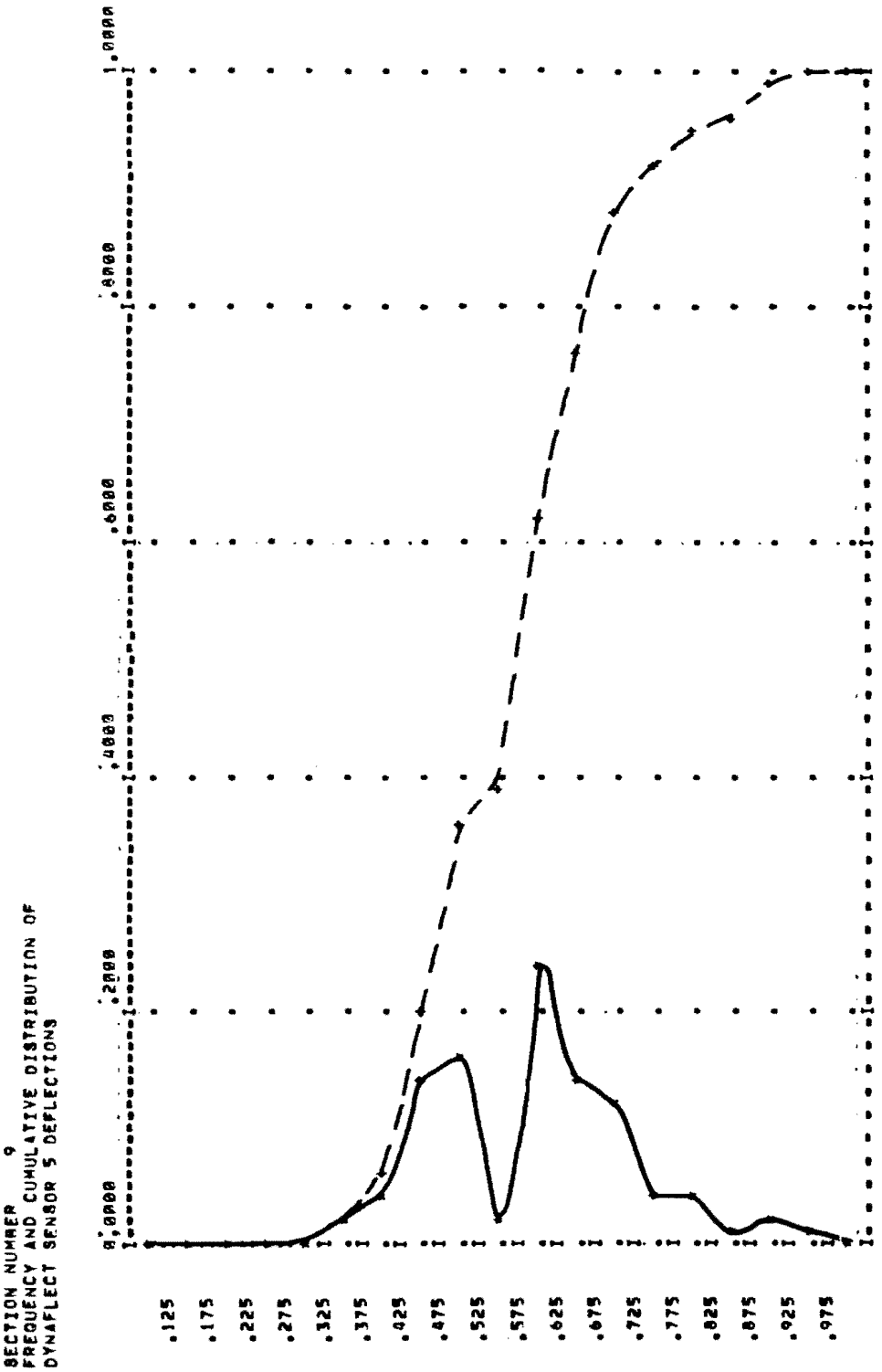
SECTION NUMBER 9
FREQUENCY AND CUMULATIVE DISTRIBUTION OF
DYNAFLECT SENSOR 5 DEFLECTIONS
0.0000
.2000
.4000
.6000
.8000
1.0000
.125
.175
.225
.275
.325
.375
.425
.475
.525
.575
.625
.675
.725
.775
.825
.875
.925
.975

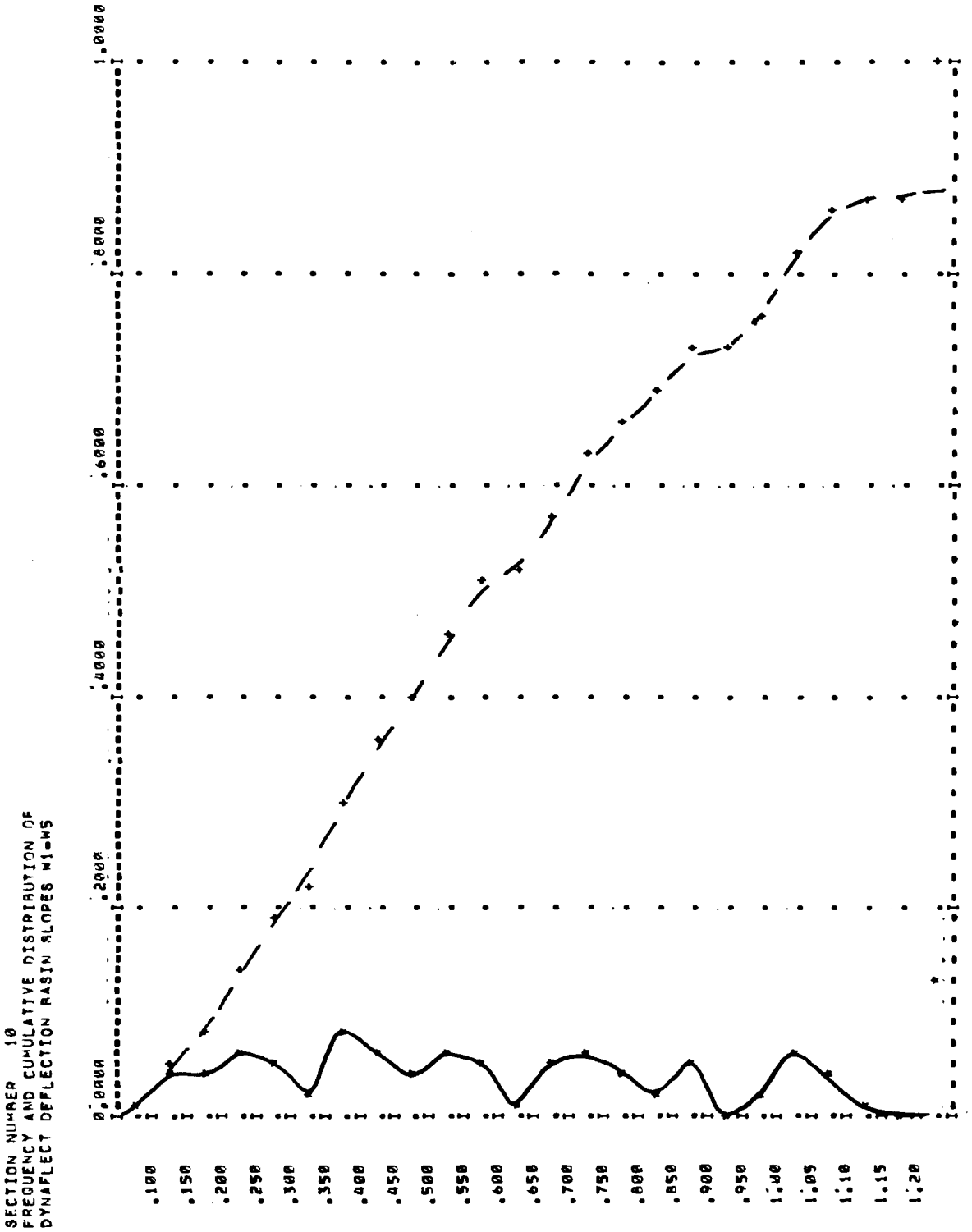
SECTION NUMBER 10
FREQUENCY AND CUMULATIVE DISTRIBUTION OF
DYNAFLECT DEFLECTION BASIN SLOPES W1-W5
0.0000
.2000
.4000
.6000
.8000
1.0000
.100
.150
.200
.250
.300
.350
.400
.450
.500
.550
.600
.650
.700
.750
.800
.850
.900
.950
1.00
1.05
1.10
1.15
1.20

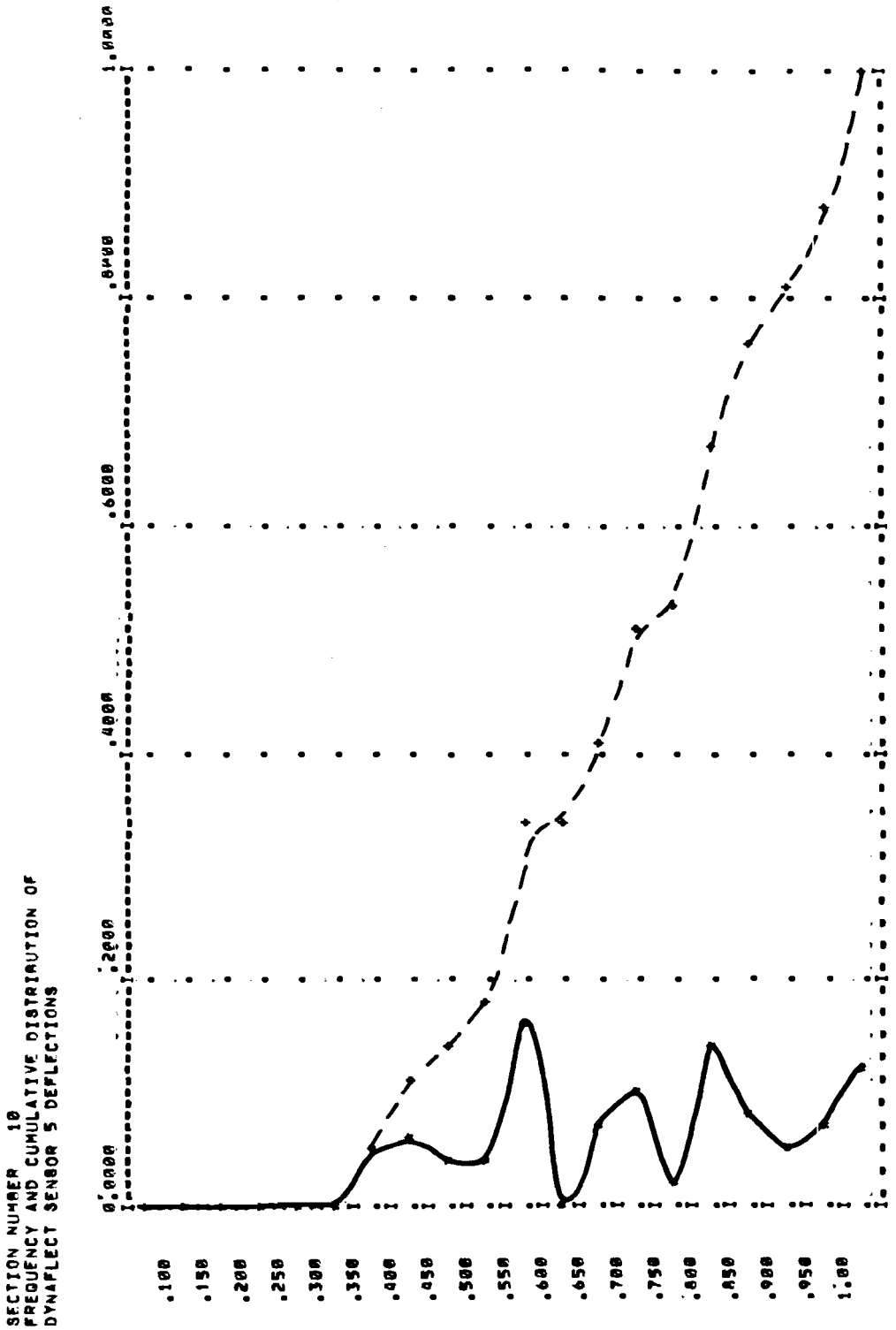
SECTION NUMBER 10
FREQUENCY AND CUMULATIVE DISTRIBUTION OF
DYNAFLECT SENSOR 5 DEFLECTIONS
0.0000
.2000
.4000
.6000
.8000
1.0000
.100
.150
.200
.250
.300
.350
.400
.450
.500
.550
.600
.650
.700
.750
.800
.850
.900
.950
1.00

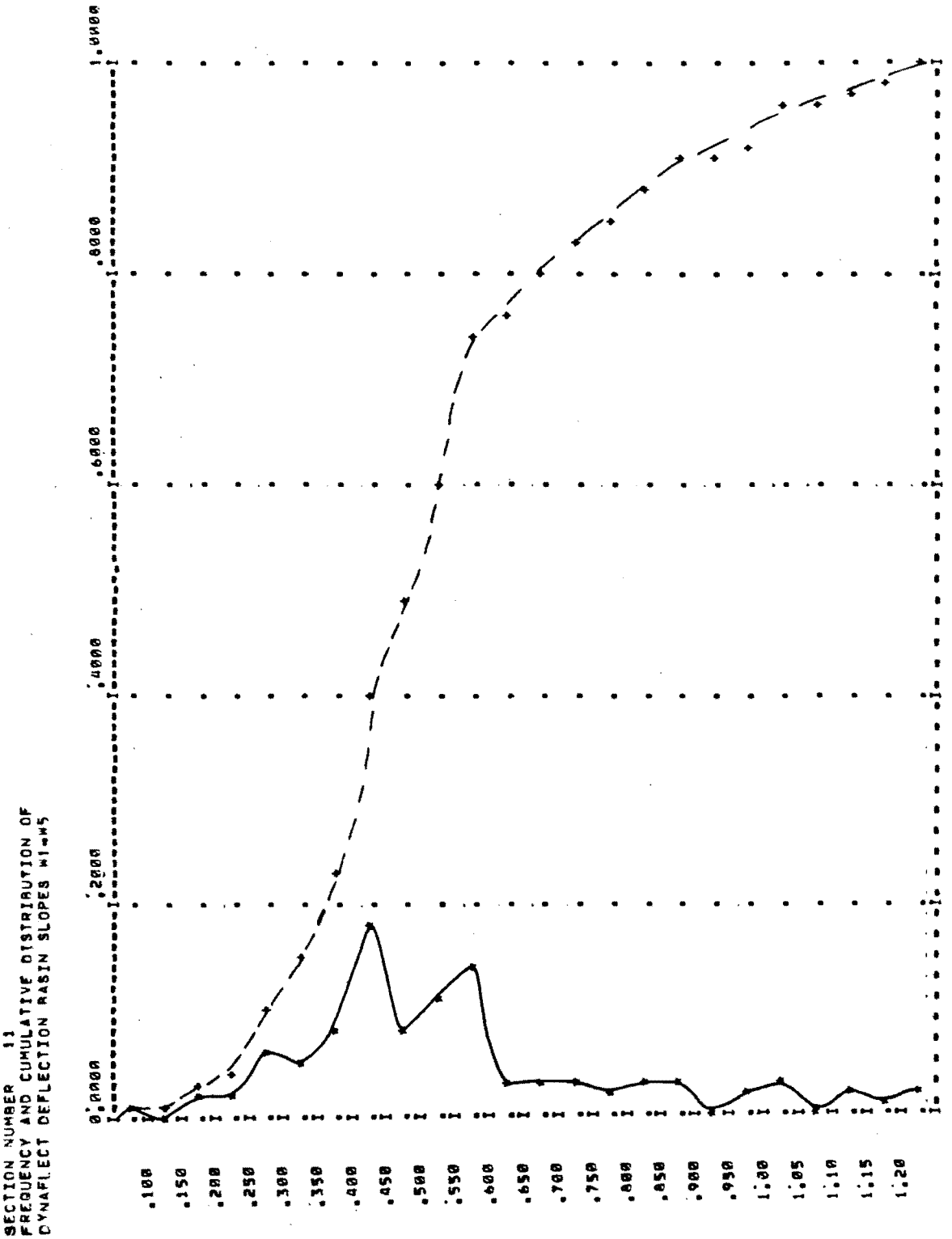
SECTION NUMBER 11
FREQUENCY AND CUMULATIVE DISTRIBUTION OF
DYNAFLECT DEFLECTION BASIN SLOPES W1-W5
0.0000
.2000
.4000
.6000
.8000
1.0000
.100
.150
.200
.250
.300
.350
.400
.450
.500
.550
.600
.650
.700
.750
.800
.850
.900
.950
1.00
1.05
1.10
1.15
1.20

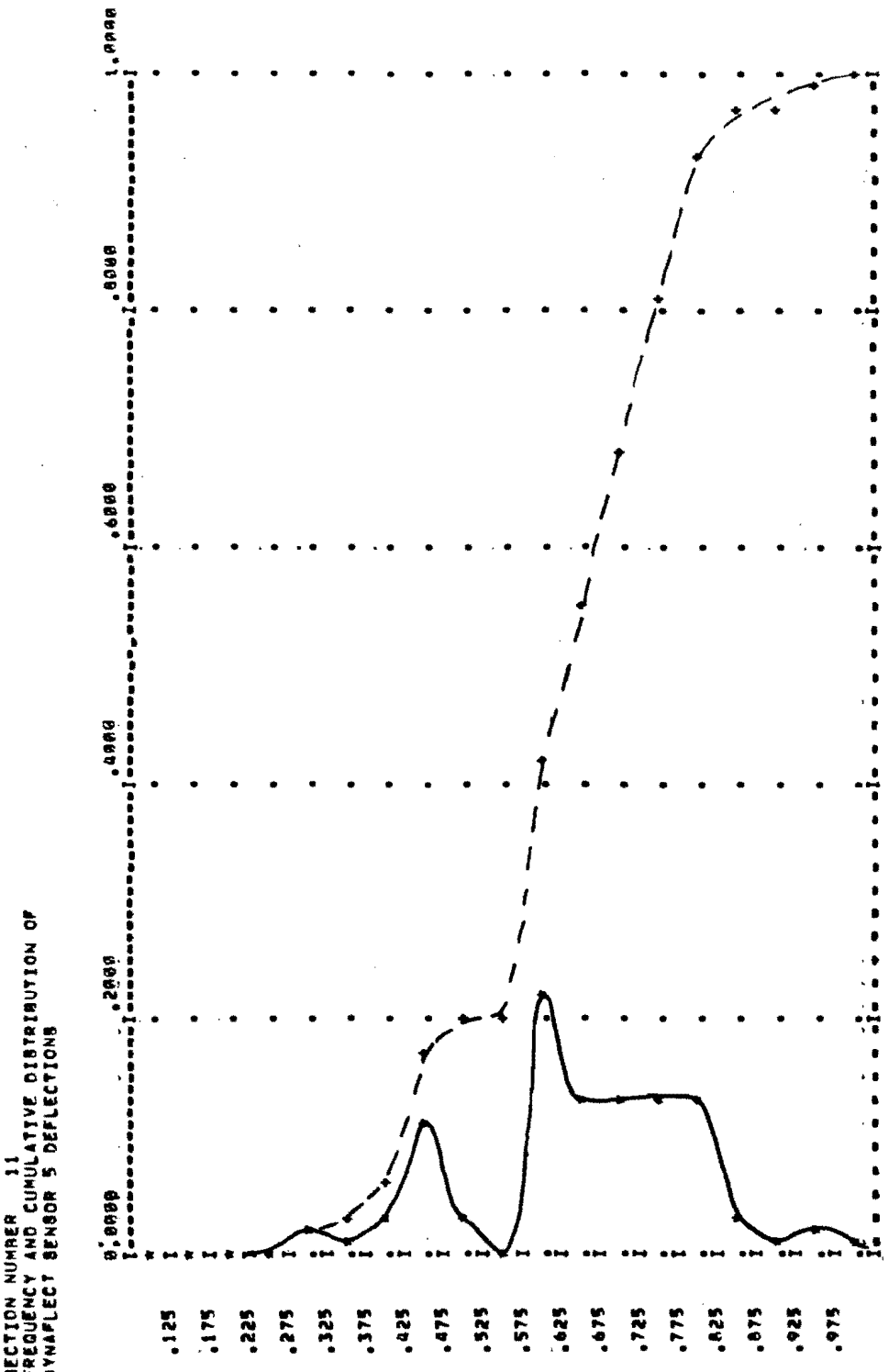
SECTION NUMBER 11
FREQUENCY AND CUMULATIVE DISTRIBUTION OF
DYNAFLECT SENSOR 5 DEFLECTIONS
0.0000
.2000
.4000
.6000
.8000
1.0000
.125
.175
.225
.275
.325
.375
.425
.475
.525
.575
.625
.675
.725
.775
.825
.875
.925
.975

APPENDIX C

CALCULATION OF SUBGRADE

MODULUS FROM DEFLECTION MEASUREMENTS

APPENDIX C. CALCULATION OF THE SUBGRADE MODULUS FROM DEFLECTION MEASUREMENTS

If the moduli of the upper pavement layers are known then the modulus of an infinitely thick subgrade can be calculated from deflection measurements, by using layered theory, as follows:

(1) Assume the value of E, say E_A which is below the expected value of E. Using layered theory compute the surface deflection, W_A with the load used for the deflection measurement and at the point of measurement.

(2) Now recompute the deflection for an assumed subgrade modulus E_B which is larger than the expected value of E.

(3) The surface deflections as computed by layered theory are practically linearly related to the subgrade modulus when plotted on a log-log scale as indicated in Fig C.1. (The closer E_A and E_B are to E, the more accurate is the result.)

(4) The equation of the line relating E to W is of the form

$$\log E = X + Y \log W$$

and

$$X = \frac{\log E_A - \log E_B}{\log W_A - \log W_B} = \text{slope of the line}$$

and

$$\log E_A = X + Y \log W_A$$

$$\therefore Y = \frac{X - \log E_A}{\log W_A} = \text{intercept}$$

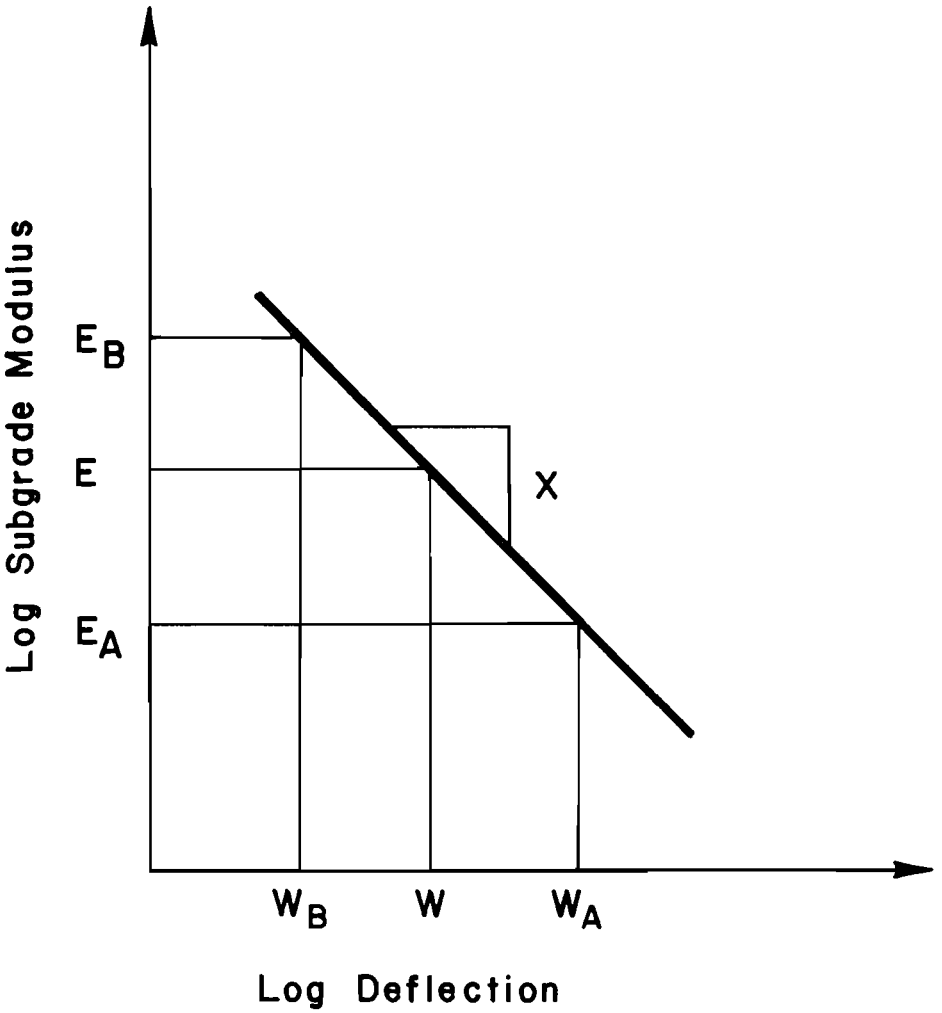

Fig C.1. Diagram illustrating the calculation of subgrade modulus from deflection.

APPENDIX D

CALCULATION OF EQUIVALENT STRESS

APPENDIX D. A METHOD FOR CALCULATING AN EQUIVALENT STRESS AT WHICH A NUMBER OF APPLICATIONS RESULTS IN THE SAME DAMAGE AS WHEN A SIMILAR NUMBER OF APPLICATIONS IS DISTRIBUTED AMONG A NUMBER OF STRESS LEVELS

These calculations assume that miners Hypothesis is valid; i.e., that the ratios of stress applications, relative to the allowable number of applications at that stress level, may be linearly summed over the life of the structure to calculate the damage to that structure, or

$$D = \sum_{i=1}^{P} \frac{n_i}{N_i}$$

where

D = fatigue damage to the structure,

N_i = allowable number of applications at stress level i,

n_i = number of stress applications at level i, and

P = number of stress levels used in the calculation.

For the two stress levels A and B and the equivalent stress level E, shown in Fig D.1:

$$D = \frac{n_e}{N_E} = \frac{n_A}{N_A} + \frac{n_B}{N_B}$$

Therefore

$$N_e = \frac{n_E N_A N_B}{N_A N_B + n_B N_A} \quad \text{and} \quad N = K_1 (f/\sigma)^{K_2}$$

where

f = flexural strength of the concrete,

σ = stress in the structure, and

K_1 and K_2 are constants for each particular fatigue equation.

Therefore

$$K_1 (f/\sigma_E)^{K_2} = \frac{(n_A + n_B) N_A N_B}{n_A N_B + n_B N_A}$$

and

$$\left(\frac{f}{\sigma_E}\right) = \left[\frac{(n_A + n_B) N_A N_B}{K_1 (n_A N_B + n_B N_A)}\right]^{1/K_2}$$

Therefore

$$\sigma_E = f K_1^{1/K_2} \left[\frac{n_A N_B + n_B N_A}{(n_A + n_B) N_A N_B}\right]^{1/K_2}$$

and similarly for any number of initial stress levels.

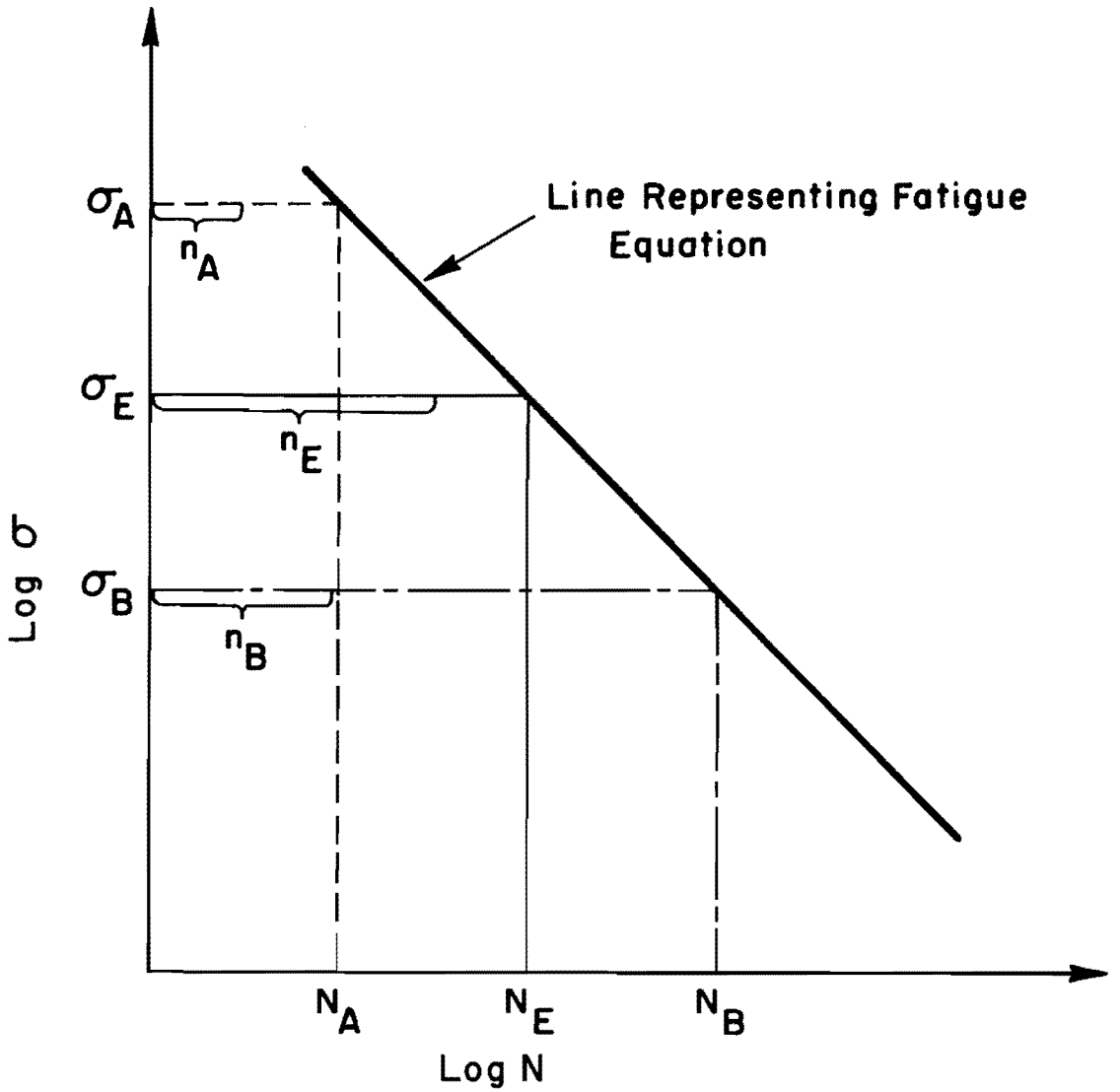

Fig D.2. Figure illustrating the calculation of an effective stress at which a number of applications will result in the same damage, as when a similar number of applications is distributed among a pair of stress levels.

APPENDIX E

COST ANALYSIS, MAINTENANCE OR OVERLAY

APPENDIX E. MAINTENANCE AND REHABILITATION COSTS AS A FUNCTION OF PAVEMENT DISTRESS

ECONOMIC ANALYSIS

Economic failure may be defined as that point at which the present value of maintenance costs and the corresponding user costs taken over a period of time exceed the cost of a rehabilitation strategy which would last for the same length of time. The variables which need to be estimated for an economic analysis, to estimate the failure point, are as follows:

(1) The future pavement distress and associated costs,

(2) The life of a rehabilitation strategy and construction and maintenance costs,

(3) The user costs, and

(4) The discount rate.

Each of these items will be described below.

(1) Results from condition surveys conducted on CRC pavements during 1974 and 1978 in Texas are shown in Figs E.1 to E.4. In each of these figures the number of defects per mile versus pavement age for approximately 25 pavement sections are shown. Defects include severe punch outs and patches. For each of the sections a polynomial curve was fitted through the data points.

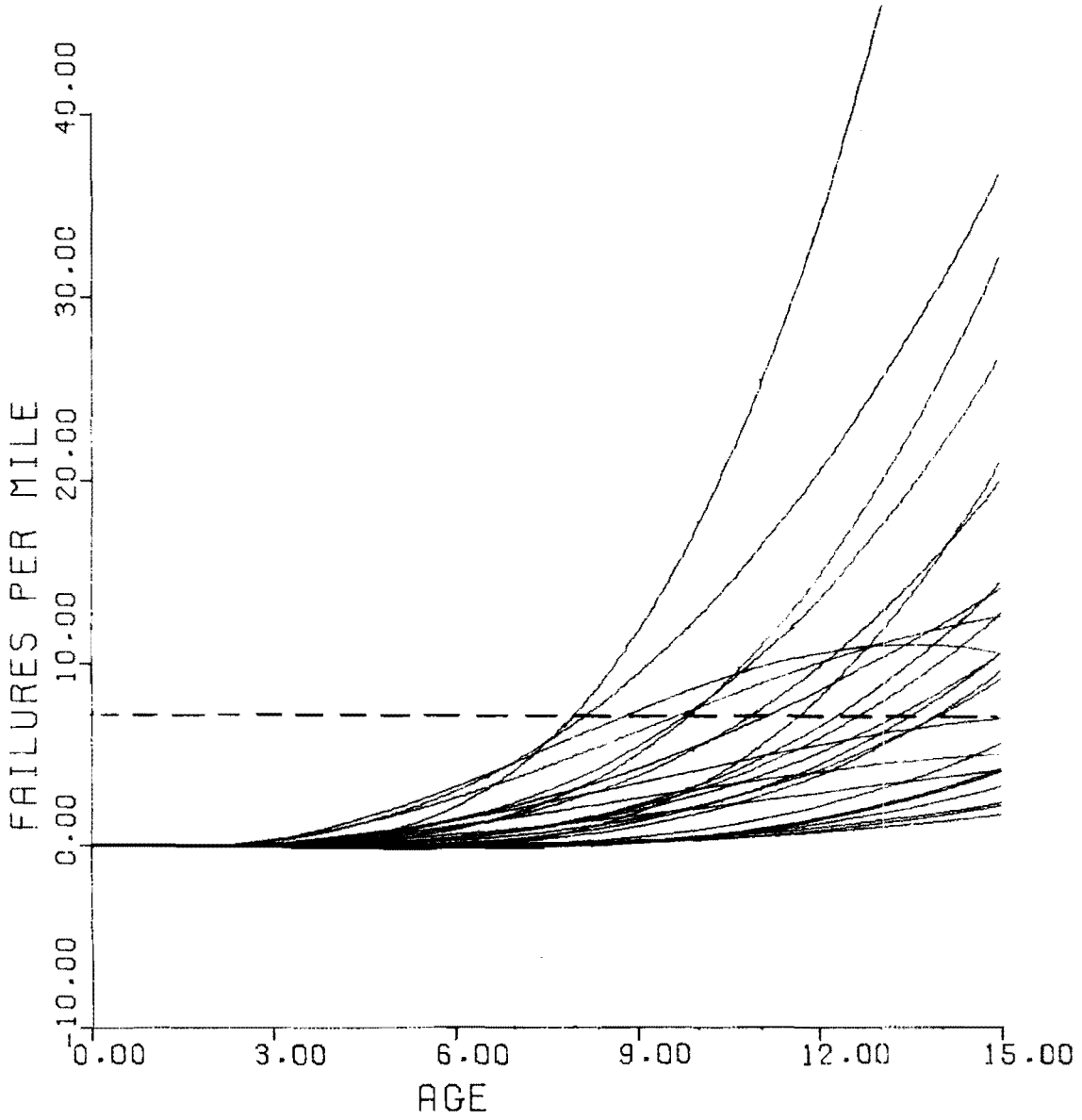

Fig E.1. Continuously reinforced concrete pavement defects (punch outs and patches) as a function of pavement age (1/4 of project).

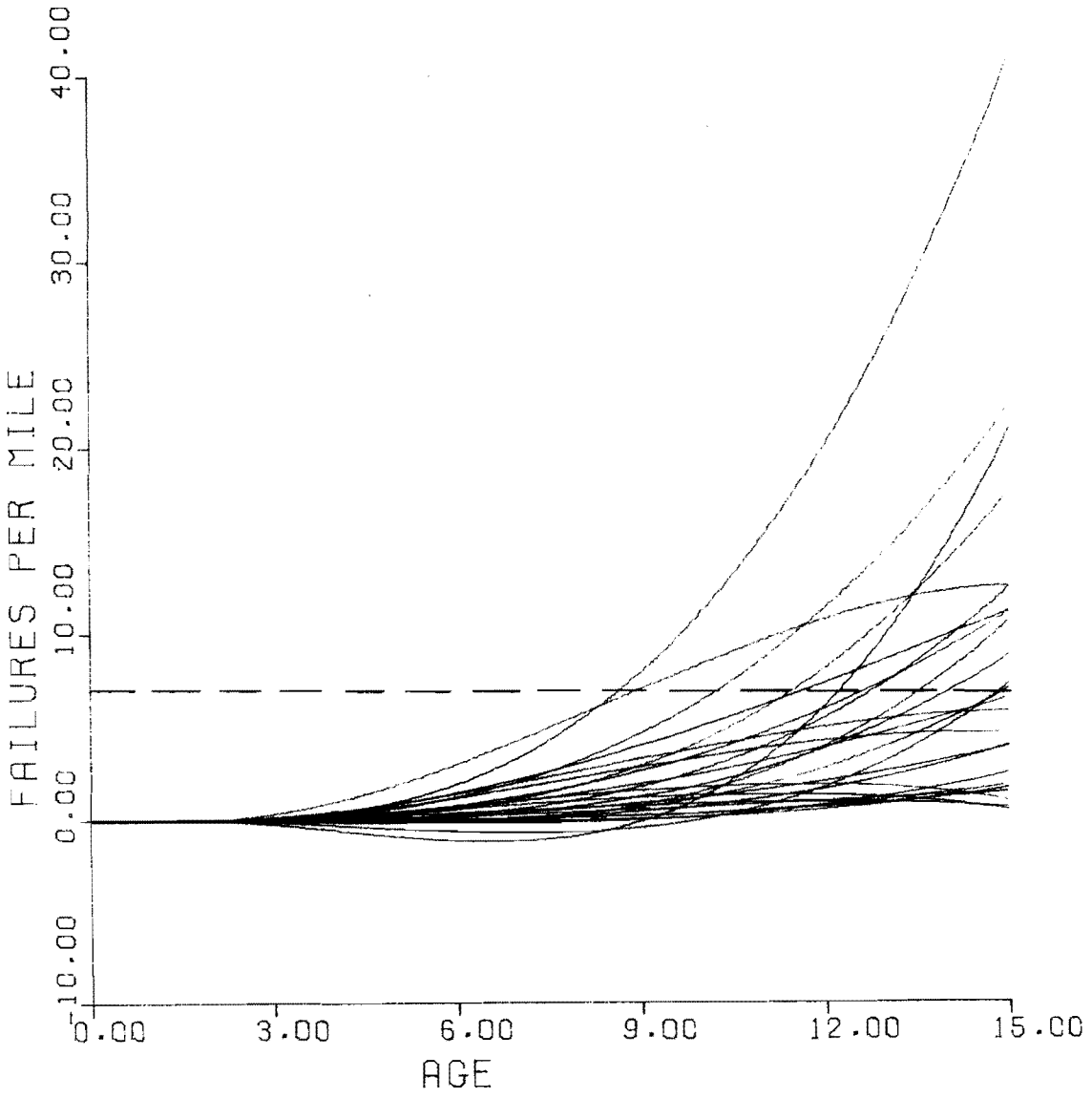

Fig E.2. Continuously reinforced concrete pavement defects (punch outs and patches) as a function of pavement age (1/4 of project).

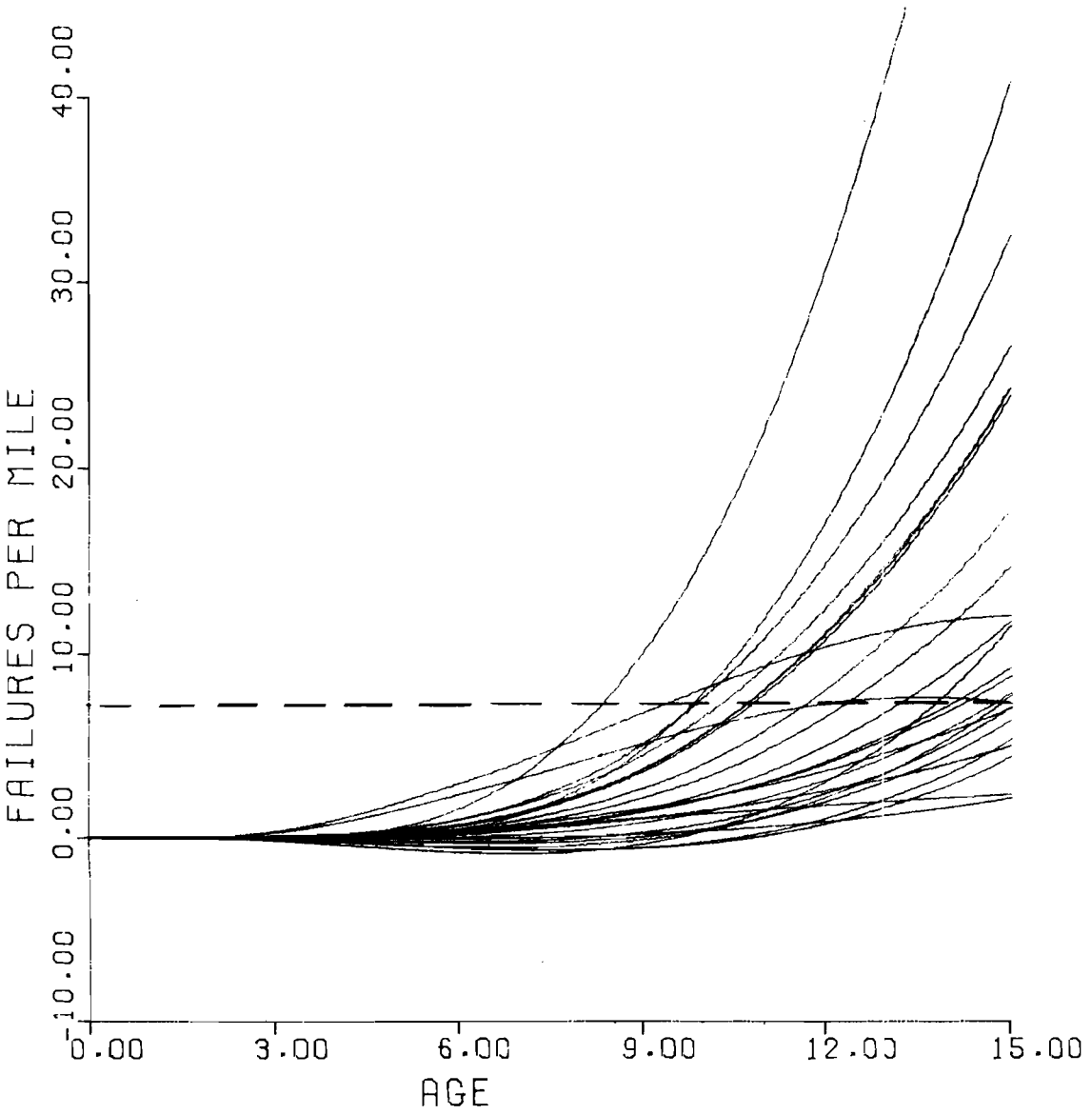

Fig E.3 Continuously reinforce concrete pavement defects (punch outs and patches) as a function of pavement age (1/4 of project).

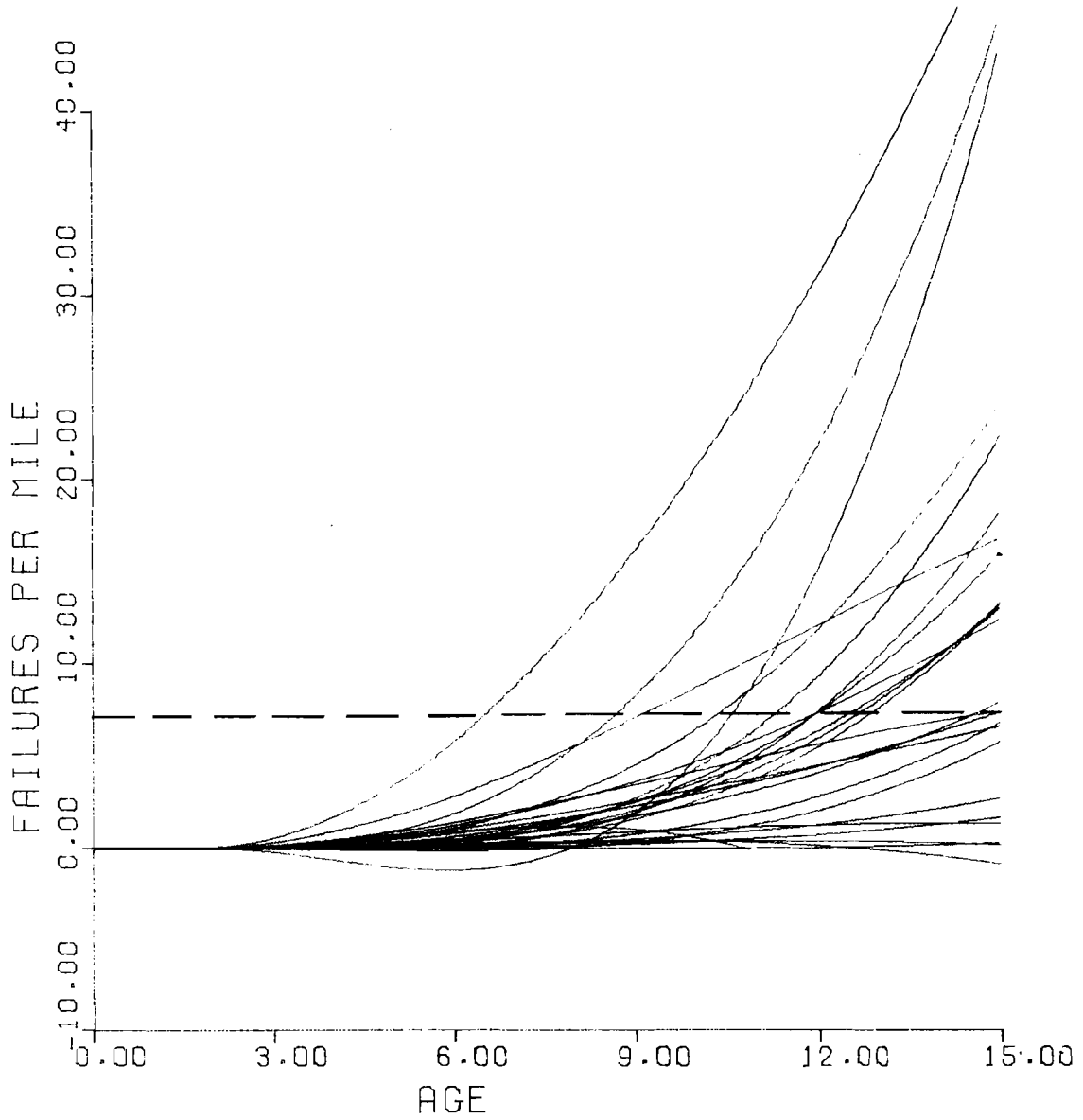

Fig E.4 Continuously reinforce concrete pavement defects (punch outs and patches) as a function of pavement age (1/4 of project).

As indicated in the figures, the rate of defect occurrence increases with time and, correspondingly, the maintenance cost increases with time. The rate of defect occurrence at which the future maintenance costs will exceed the cost of a rehabilitation strategy designed for the same period of time needs to be found.

(2) The life of a rehabilitation strategy depends on a variety of aspects, which cannot be fully discussed in this paragraph. Because of the numerous other variables associated with a cost analysis, a fixed overlay life will be assumed in this analysis. The assumption is therefore made that a 3-inch overlay will last for 5 years with nominal maintenance costs.

(3) User costs depend on both the roughness of the road and the user delay costs associated with construction and maintenace. In this analysis the roughness related user costs are ignored and only the user delay costs during construction and maintenance are considered.

(4) The discount rate used in an economic analysis depends on inflation and the interest rate on borrowed capital. Both of these factors may vary considerably with time and are difficult to predict with any reliability. In this analysis a number of discount rates will be used in order to account for the variability.

ECONOMIC ANALYSIS

The present value of a rehabilitation strategy will be compared to the present value of continued maintenance.

(1) Distress quantities are determined from typical curves in Figs E.1 to E.4.

(2) The average cost of a patch is assumed to be $1,000. This figure was obtained from the Texas SDHPT maintenance department.

(3) User delay costs due to patching are based on a 4-lane divided highway of which one lane is closed for one mile for three days to effect repairs. Three patches will be repaired within this mile of road during three days. The AADT along the road is assumed to be 20,000, which corresponds to a fairly heavily travelled Interstate Highway. The traffic speed is assumed to slow down from 55 mph to 35 mph for 2 miles due to the one mile of lane closure. The user time costs are assumed to be $0.40 per hour, which may be high enough to account for economic and political factors.

User delay cost for three patches/mi = $24.00

Therefore the user delay cost per patch = $800.00

Total patch cost = $1,000 + $800 = $1,800.00

(4) Rehabilitation costs are based on an asphalt concrete overlay costing $30.00 per ton and applied only over the main lanes. User delay costs per mile of rehabilitation are the same as those for three patches ($2,400.00). Density of asphalt concrete is assumed to be 150 lb/ft^3 .

(5) Compare the present value of rehabilitation costs to the present value of maintenance costs, starting at the stage where defects are occurring at a rate of 3 per year:

Year	1	2	3	4	5
Number of patches	3	5	8	12	18

(6) The present value of continued maintenance is compared to the present value of maintenance costs for the above assumptions in Fig E.5.

CONCLUSIONS

From Fig E.5 it is apparent that, for the assumptions listed above, the cost of continued maintenance may exceed that of rehabilitation when the rate of distress occurrence exceeds three defects per year. This defect-rate may occur at different pavement lives for different pavements, depending on the pavement structure, traffic, environment, etc. However, Figs E.1 to E.4 indicate that once this defect rate has occurred, further increases in defect occurrences may follow similar trends. It may therefore be prudent to use this rate of defect occurrence as a terminal condition for the pavement.

Furthermore, from Figs E.1 to E.4 it becomes apparent that, on the average, the critical rate of defect occurrence occurs when the number of defects per mile in the pavement approach the age of the pavement. For example, if a pavement is 7 years old and has seven defects per mile, then there is a high probability that the rate of defect occurrence may be equal to the critical rate. This would provide a practical means for estimating pavement "failure" from condition survey data.

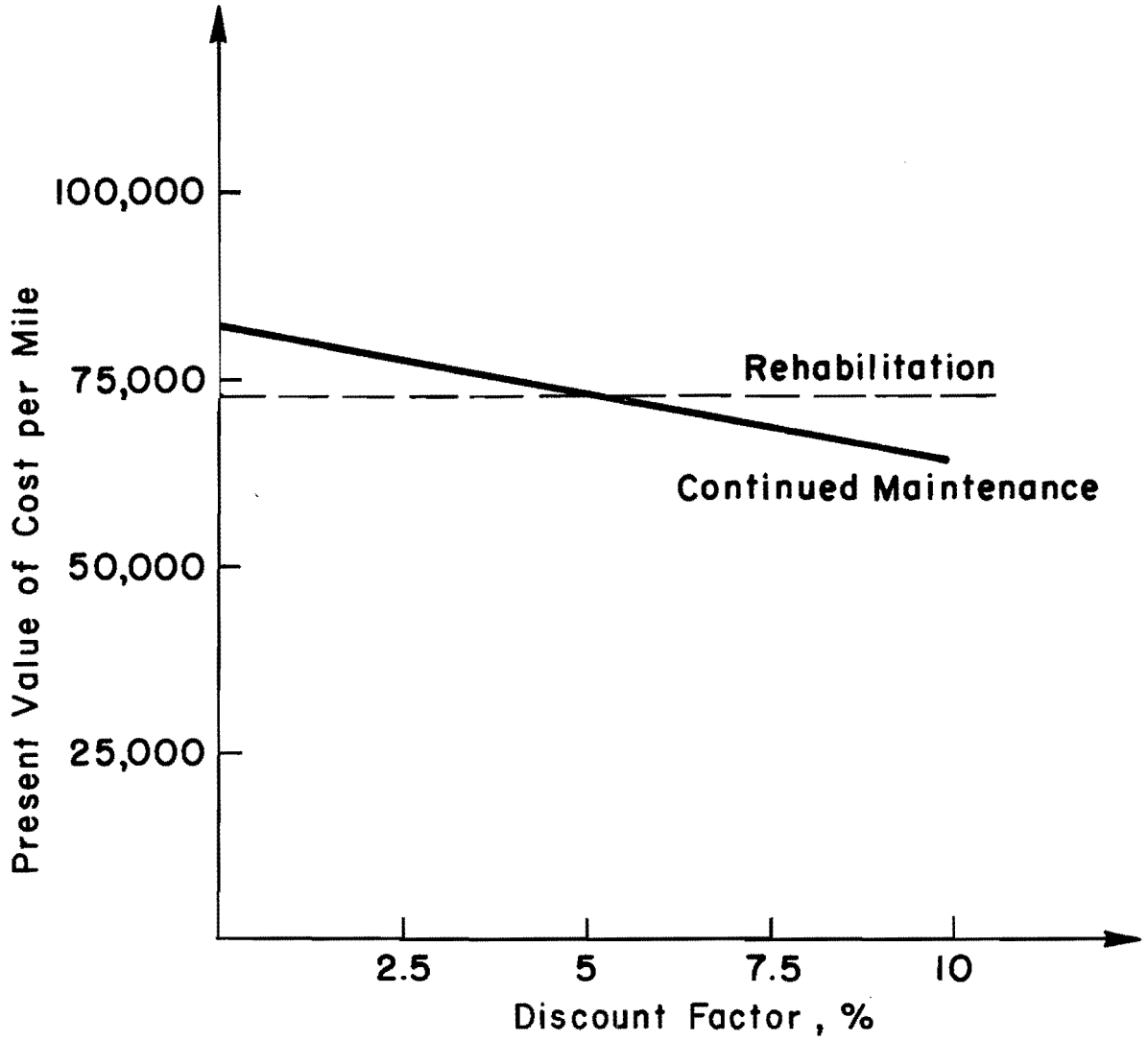

Fig E.5 Comparison between the present value of continued maintenance or rehabilitation for varying discount rates.

APPENDIX F

TRAFFIC TABLES

TRAFFIC CALCULATIONS

CFHR No. 2009

MANUAL COUNT STATION NUMBER: A-26-A

YEAR	18 kips/TRUCK	% TRUCKS	A.A.D.T.	AAD 18-KESAL
1963	1.3	15	7000	1365
1964	1.3	15	7090	1383
1965	1.32	15	7800	1544
1966	1.32	15	8400	1688
1967	1.36	15	10130	2067
1968	1.39	15	11000	2294
1969	1.41	15	11930	2523
1970	1.44	15	10940	2363
1971	1.46	15	12690	2779
1972	1.49	15	13470	3011
1973	1.51	15	14440	3271
1974	1.53	16	14610	3577
1975	1.56	17	14800	3925
1976	1.58	18	16030	4559
1977	1.60	19	17050	5183
1978	1.63	20	18810	6132

TOTAL 47663

X 365 = 17.4×10^6

TOTAL AT 1978 FOR ONE DIRECTION $\div$ 2 = 8.7×10^6 ESAL

TOTAL IN 1974 = 5.1×10^6 ESAL

TRAFFIC CALCULATIONS

CFHR No. 1302

MANUAL COUNT STATION NUMBER: L-10-2, S164

YEAR	18 kips/TRUCK	% TRUCKS	A.A.D.T.	AAD 18-KESAL
1963				
1964	1.3	20	3500	910
1965	1.32	20	3500	910
1966	1.34	20	3510	941
1967	1.36	20	4200	1142
1968	1.39	20	4900	1362
1969	1.41	20	5300	1495
1970	1.44	20	5810	1673
1971	1.46	20	6800	1986
1972	1.49	21	8040	2516
1973	1.51	24	8300	2883
1974	1.53	25	8750	3345
1975	1.56	27	9300	3517
1976	1.58	29	9910	4541
1977	1.60	30	10330	4958
1978	1.63	30	11100	5428

TOTAL 38008

X 365 = 13.9

TOTAL 18-Kip AXLES FOR ONE DIRECTION ÷ 2 = $\underline{6.9 \times 10^6}$ ESAL

TOTAL IN 1974 = 3.5×10^6 ESAL

TRAFFIC CALCULATIONS

CFHR No. 1301

MANUAL COUNT STATION NUMBER: L-10-2, S164

YEAR	18 kips/TRUCK	% TRUCKS	A.A.D.T.	AAD 18-KESAL
1962	1.3	20	4000	1040
1963	1.3	20	4000	1040
1964	1.3	20	4100	1066
1965	1.32	20	4200	1109
1966	1.34	20	4340	1163
1967	1.36	20	5000	1360
1968	1.39	20	5700	1585
1969	1.31	20	6400	1810
1970	1.44	20	7230	2082
1971	1.46	20	8000	2336
1972	1.49	21	9790	3063
1973	1.51	23	11000	3820
1974	1.53	25	12480	4774
1975	1.56	27	13000	5476
1976	1.58	29	14150	6484
1977	1.60	30	14740	7075
1978	1.63	30	16550	8093

TOTAL 53376

X 365 = 19.5×10^6

TOTAL AXLES IN 1978 FOR ONE DIRECTION ÷ 2 = 9.7×10^6 ESAL

TOTAL IN 1974 = 4.8×10^6 ESAL

TRAFFIC CALCULATIONS

CFHR No: 1701

MANUAL COUNT STATION NUMBER: L-45-2

YEAR	18 kips/TRUCK	% TRUCKS	A.A.D.T.	AAD 18--KESAL
1961	1.3	20	7000	1820
1962	1.3	20	7300	1898
1963	1.3	20	7700	2002
1964	1.3	20	8000	2080
1965	1.32	20	9000	2376
1966	1.34	20	9500	2546
1967	1.36	20	10000	2720
1968	1.39	20	10300	2863
1969	1.41	20	10500	2961
1970	1.44	20	11000	3168
1971	1.46	20	12500	3650
1972	1.49	20	14000	4172
1973	1.51	21	15000	5757
1974	1.53	23	14000	4927
1975	1.56	25	15000	5850
1976	1.58	27	16000	6826
1977	1.60	28	17500	7840
1978	1.63	28	18000	8215

TOTAL 71671

X 365 = 26×10^6

TOTAL AT 1978 FOR ONE DIRECTION $\div$ 2 = $\underline{13.0 \times 10^6}$ ESAL

TOTAL IN 1974 = 7.8×10^6 ESAL

TRAFFIC CALCULATIONS

CFHR No. 1303

MANUAL COUNT STATION NUMBER: L-10-2, S164

YEAR	18 kips/TRUCK	% TRUCKS	A.A.D.T.	AAD 18-KESAL
1963	1.3			
1964	1.3			
1965	1.32			
1966	1.34	20	5500	1474
1967	1.36	20	6000	1632
1968	1.39	20	6700	1863
1969	1.41	20	7500	2115
1970	1.44	20	8500	2448
1971	1.46	20	9700	2686
1972	1.49	21	11000	3442
1973	1.51	24	12000	4168
1974	1.53	25	13500	5164
1975	1.56	27	14500	6107
1976	1.58	29	15500	7102
1977	1.60	30	16000	7680
1978	1.63	30	17500	8558

TOTAL 54438

$X\ 365 = 19.9 \times 10^6$

TOTAL AT 1978 FOR ONE DIRECTION $\div$ 2 = 9.9×10^6 ESAL

TOTAL IN 1974 = 4.6×10^6 ESAL

APPENDIX G

SUBGRADE MODULUS UNDER 18-KIP AXLE LOAD

APPENDIX G. CALCULATION OF SUBGRADE MODULUS UNDER AN 18-kip AXLE LOAD

Due to subgrade stress sensitivity the modulus under an 18-kip axle load may be different from that under a Dynaflect load.

Regression equations for calculating the deviator stress at the subbase - subgrade interface:

Variable Ranges: $E_1 = 5 \times 10^6$ psi = constant

E_2 = 100,000 to 1,100,000 psi

E_3 = 2,000 to 30,000 psi

D_1 = 8" to 12"

D_2 = 6" to 10"

Deviator stress under Dynaflect load:

$$D_{dyn} = 10\exp(-2.718 - 0.0226D_2 - 2.387E-7 \times E_2 - 1.61 \log D_1 + 0.8362 \log E_3) \quad (G.1)$$

STD error = 8% $R^2 = 0.99$

Deviator stress under 18-kip axle:

$$D_a = 10\exp(-1.542 - 0.01766D_2 - 1.928E-7 \times E_2 - 1.2972 \log D_1 + 0.6876 \log E_3) \quad (G.2)$$

or

$$\log D_a = K + C \log E_{3_a} \quad (G.2a)$$

STD = 7% $R^2 = 0.99$

If the resilient modulus vs deviator stress plots as a straight line on the log - log plot:

$$\text{Log } M_R = A + B \log \sigma d. \quad (G.3)$$

and

$$B = S_{SG} = \text{slope of this line}$$

Calculate D_{dyn} using equation (G.1) and E_3 as obtained from deflection measurements.

Therefore

$$A = \log E_{3_{dyn}} - S_{SG} \log D_{dyn}$$

and

$$\log M_R = \log E_{3_{dyn}} - S_{SG} \log D_{dyn} + S_{SG} \log \sigma D \qquad (G.4)$$

use (G.2a) in (G.4)

$$\log E_{3_a} = \log E_{3_{dyn}} - S_{SG} \log D_{dyn} + S_{SG} (K + C \log E_{3_a})$$

$$\log E_{3_a} = \frac{\log E_{3_{dyn}} - S_{SG} \log D_{dyn} + K \cdot S_{SG}}{1 - C \cdot S_{SG}}$$

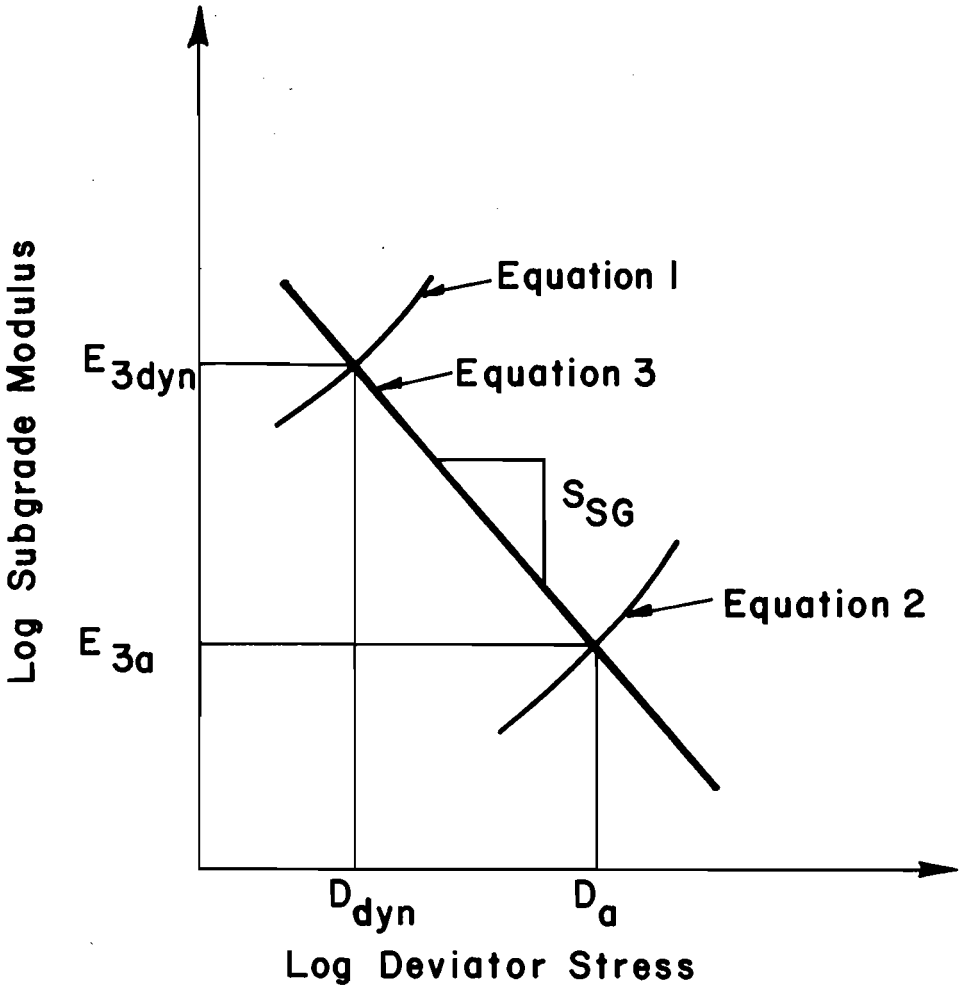

Fig G.1. The different equations used in the calculation of the subgrade modulus.

THE AUTHORS

Arthur Taute received his B.S. degree in Civil Engineering at the University of Stellenbosch, South Africa, in November 1974. He has had several years of experience in Civil Engineering construction in the geotechnical and tunnelling fields and further experience as a consulting engineer in the pavement design field in South Africa. He joined the Center for Transportation Research at The University of Texas at Austin as a Research Assistant, in the Fall of 1978 where he did research on rigid pavement overlay designs and subsequently received his M.S. degree in Engineering in May 1980.

B. Frank McCullough is a Professor of Civil Engineering at The University of Texas at Austin, and is Director of the Center for Transportation Research. He has strong interests in pavements and pavement design and has developed design methods for continuously reinforced concrete pavements currently used by the State Department of Highways and Public Transportation, U. S. Steel Corporation, and others. He has also developed overlay design methods now being used by the FAA, U. S. Air Force, and FHWA. During nine years with the State Department of Highways and Public Transportation he was active in a variety of research and design activities.

He worked for two years with Materials Research and Development, in Oakland, California, and for the past nine years for The University of Texas at Austin. He participates in many national committees and is the author of over 100 publications that have appeared nationally.

W. Ronald Hudson is a Professor of Civil Engineer at The University of Texas at Austin and was technical director of a four-year project sponsored by the Brazilian Government, The United Nations Development Program, and the World Bank to study the road development costs in Brazil. He has had a wide variety of experience as a research engineer with the State Department of Highways and Public Transportation and the Center for Transportation Research at The University of Texas at Austin and was Assistant Chief of the Rigid Pavement Research Branch of the AASHO Road Test. He is the author of numerous publications and was the recipient of the 1967 ASCE J. James R. Croes Medal. He is presently concerned with research in the areas of (1) analysis and design of pavement management systems, (2) measurement of pavement roughness performance, (3) slab analysis and design, and (4) tensile strength of stabilized subbase materials.